

Regulation of digestive tract and progenitor cell homeostasis by intestinal bacteria

in *Drosophila melanogaster*

by David Fast

A thesis submitted in partial fulfilment of the requirements for the degree of

Doctor of Philosophy

in

Immunology

Department of Medical Microbiology and Immunology

University of Alberta

## ABSTRACT

The digestive tract facilitates nutrient uptake in the presence of a heterogeneous cohort of symbiotic microbes. These microbes along with their collective genetic material form the intestinal microbiome and contribute to animal phenotypes. Similar to mammals, the microbiome of insects forms a barrier that rebuffs invasive bacteria and activates the intestinal immune response. In the fruit fly, *Drosophila melanogaster*, intestinal immunity couples the bactericidal action of antimicrobial peptides and reactive oxygen species with epithelial repair programs to effectively eliminate toxic bacteria and regenerate the epithelium. Intestinal renewal is accomplished by the proliferation of multipotent intestinal stem cells (ISCs), which divide and differentiate to generate new epithelial cells. Signalling through a complex network of conserved mitogenic pathways regulates ISC division. Epithelial damage, ingestion of cytotoxic compounds, or the presence of gut bacteria activates these pathways in ISCs to stimulate proliferation. Conventionally reared (CR) flies, which host a normal intestinal microbiome, overtime accumulate a population of mis-differentiated cells that leads to the gradual onset of intestinal tissue dysplasia via activation of ISC proliferation. Removal of the microbiome to generate a germ free (GF) organism slows the frequency of epithelial turnover, preserves tissue organization, and extends adult fly lifespan. To explore the relationship between symbiotic bacteria and *Drosophila* longevity, I examined the contributions of individual symbiotic species to adult fly lifespan. Individual populations of GF flies were re-associated with monocultures of bacteria to repopulate the intestine with a single symbiotic species. Association with the widely reported fly commensal *Lactobacillus plantarum* (*L. plantarum*) shortened the lifespan of GF flies. Contrary to expectations, *L. plantarum* monoassociation did not promote the rapid onset of tissue dysplasia characteristic of aged CR flies. Instead, guts associated with *L. plantarum* had diminished expression of growth promoting ligands and reduced epithelial turnover, characterized by a disruption to posterior midgut architecture.

In addition to symbiotic bacteria, the intestine is frequently exposed to pathogens that compete with the microbiome within the digestive tract. One mechanism employed by enteric pathogens to compete with other bacteria in the niche is the type VI secretion system (T6SS). The T6SS of *V. cholerae* and other Gram-negative bacteria is an injection apparatus that translocates toxic effector molecules into adjacent prokaryotic or eukaryotic cells. As the T6SS is active *in vivo* and mediates interactions with other bacterial cells, I examined the contribution of the T6SS to *V. cholerae* pathogenesis in the guts of CR adult *Drosophila*. I demonstrated that ablation of T6SS function extends the viability of flies infected with *V. cholerae*, relative to infection with T6SS functional *Vibrio*. T6SS mediated reduction in viability was dependent on the microbiome as the T6SS was dispensable for *V. cholerae* pathogenesis in a GF host. The reintroduction of symbionts vulnerable to T6SS mediated competition, sensitized the host to T6SS killing via the activation of putative host secondary responses. Given the effect of T6SS mediated interactions on host viability, I examined how these bacteria-bacteria interactions impact intestinal immune responses.

Loss of damaged epithelial cells is complemented by the proliferation of ISCs. However, despite significant intestinal damage, infection with T6SS functional *V. cholerae* did not activate compensatory ISC growth. Instead, challenge with T6SS functional *V. cholerae* impaired proliferation and downregulated the transcription of signaling components required for epithelial renewal. T6SS-dependent arrest of intestinal repair was the result of interactions between the microbiome and the T6SS, as ablation of the microbiome restored epithelial regeneration in response to T6SS functional *V. cholerae*. This inhibition of renewal was not the result of a bilateral interaction between *V. cholerae* and a single symbiotic species, but required interactions between *V. cholerae* and a multi-species consortium of intestinal symbionts. Together, the findings in this thesis define the impact of individual species on intestinal homeostasis and examine how interactions between bacteria in the digestive tract influence host viability and intestinal regeneration.

## Preface

This thesis is composed of original work by David Fast. Throughout, it contains content co-authored by collaborators and republished with permission from the following sources:

- Fast, D., Duggal, A., & Foley, E. Monoassociation with *Lactobacillus plantarum* disrupts intestinal homeostasis in adult *Drosophila melanogaster*. *MBio* 9, e01114-18 (2018).
- Fast, D., Kostiuk, B., Pukatzki, S., & Foley, E. Commensal pathogen competition impacts host viability. *Proc. Natl. Acad. Sci. U. S. A* 115, 7099-7104 (2018).
- Fast, D., Petkau, K., Ferguson, M., Shin, M., Galenza, A., Kostiuk, B., Pukatzki, S., & Foley, E. *Vibrio*-symbiont interaction inhibit intestinal repair in *Drosophila*. *Cell Reports*, 1088-1100.e5 (2020).

All transcriptional data generated in chapter 5 is available at the NCBI GEO database (GSE136069).



## Dedication

This thesis is dedicated to my loving parents Brian and Terry Fast. Their hard work, support, and value of education has made all this possible.

*"Life before death. Strength before weakness. Journey before destination"* – The Way of Kings

## Acknowledgments

A PhD is a considerable undertaking that requires significant input from a number of people and for those people and their contributions I am immensely grateful. First, I am deeply thankful to my supervisor Dr. Edan Foley. Thank you for your always open door, unwavering optimism, and truly invaluable mentorship. Thank you for your willingness to support the pursuit of a project based simply on scientific curiosity. I appreciate all the opportunities to learn, try new techniques, and travel to present science I was afforded as a member of your lab. I will always value your scientific prowess, guidance, and mentorship. My development as an independent investigator is in no small way thanks to your effort and skill. I wish you nothing but the best in the years to come. Thank you.

To the Foley Lab, past and present: Thank you all for creating such an incredible lab environment, filled with bright ideas and helping hands. The projects in this thesis would not have been possible without all of you, and I will always be grateful for your personal kindness and scientific acuity. Kristina Petkau, Brittany Fraser, Anthony Galenza, Saeideh Davoodi, Meghan Ferguson, Dr. Minjeong Shin, Lena Jones, and Reegan Willims, thank you for your support, friendship, and all the coffee. I wish you all success in wherever life takes you. An additional thank you to all the Foley Lab undergraduate students, it was a pleasure to teach and learn beside you. Kristina and Brittany, thank you for all your support when I was a new graduate student. I am so happy for you both and wish you great joy as you start your own families.

Chapter 4 of this thesis represents some of the most fun I have ever had doing science, thanks to my outstanding collaborators Dr. Benjamin Kostiuk and Dr. Stefan Pukatzki. Thank you, Ben, for being part of this project, for coming in at the break of dawn to count dead flies, and for having the patients to deal with all my T6SS and *V. cholerae* related questions. I am profoundly proud of this project and what we were able to accomplish working together. Thank you, Stefan, for fully supporting this collaboration and for your scientific insight on this project. I hope your new lab in Denver continues to flourish.

Thank you to the *Drosophila* research community for being the world's most supportive group of scientists, sharing reagents, ideas, and flies to improve the quality of science everywhere.

I would also like to thank Dr. Tracy Raivio and Dr. Bart Hazes for their stimulating and valuable discussion as members of my committee. Thank you for all your support and guidance.

Thank you to the MMI department, students, and staff. Throughout my graduate studies I have had the privilege to be surrounded by great minds and kind people. Thank you to the MMI students for being an amazing group of supportive friends that work to lift each other up and celebrate one another's successes. Should I one day be able to help any of you, please reach out.

Finally, I am forever grateful to my family and friends, with special thanks to my parents and my partner Alex. This PhD has taken some time, but it has been made easier with all of you in my life. Thank you all so much. This thesis would not have been possible without you.

Financial support for these projects was provided by the Canadian Institutes of Health Research, Alberta Innovates Technology Futures, and the National Science and Engineering Research Council.

## Table of contents

<b>Chapter 1. Introduction</b>	<b>1</b>
1.1 The digestive tract of <i>Drosophila melanogaster</i>	2
1.1.1 Structure of the adult fly gut	2
1.1.2 Immunity in the fly gut	4
1.1.3 Intestinal regeneration and epithelial repair	6
1.2 The microbiome of <i>Drosophila</i>	8
1.2.1 The <i>Drosophila</i> model for microbiome research	8
1.2.2 Acquisition and maintenance of the microbiome	9
1.2.3 Composition of the fruit fly microbiome	10
1.3 Intestinal bacteria and fruit fly biology	12
1.3.1 Host-symbiont interactions	12
1.3.2 Host pathogen interactions	14
1.3.3 The host-symbiont-pathogen triad and bacteria-bacteria interactions	15
1.4 <i>Vibrio cholerae</i> disease, virulence factors, and the fly model	15
1.4.1 The disease cholera and the pandemic outbreaks	15
1.4.2 The virulence factors of <i>V. cholerae</i>	17
1.4.3 The <i>Drosophila</i> model for <i>Vibrio cholerae</i>	18
1.5 The type VI secretion system of <i>Vibrio cholerae</i>	21
1.5.1 The function, structure, and effectors of the <i>Vibrio cholerae</i> type VI secretion system	21
1.5.2 The type VI secretions systems contributions to <i>Vibrio cholerae</i> biology and pathogenesis	23
1.6 Study objectives	24

<b>Chapter 2. Materials and Methods</b>	<b>26</b>
2.1 <i>Drosophila</i> husbandry	27
2.1.1 <i>Drosophila</i> stocks and handling	27
2.1.2 Generation of germ free, axenic, and gnotobiotic <i>Drosophila</i>	27
2.1.3 Measure of adult Lifespan	29
2.2 Bacterial Culture and Assays	29
2.2.1 Bacterial strains and culture conditions	29
2.2.2 Colony forming units per fly	30
2.2.3 Oral infection	31
2.2.4 T6SS competition assay	31
2.2.5 Fly defecation and bacterial shedding assays	31
2.3 Molecular biology and gut related assays	32
2.3.1 Immunofluorescence and confocal microscopy	32
2.3.2 Transmission electron microscopy	33
2.3.3 Reverse Transcription and quantitative real time polymerase chain reaction	34
2.3.4 Quantification of clones and cells per gut area.	34
2.3.5 Quantification of gut length	35
2.3.6 Progenitor cell isolation and RNA extraction	35
2.4 Bioinformatic analysis	36
2.4.1 Microarray data comparison	36
2.4.2 RNA-seq read processing, alignment, differential expression, and GO analysis	36
2.5 Statistical analysis and figure construction	37
2.5.1 Statistical analysis and data visualization	37
2.5.2 Data availability	37

<b>Chapter 3. Monoassociation with <i>Lactobacillus plantarum</i> disrupts intestinal homeostasis in adult <i>Drosophila melanogaster</i>.</b>	<b>38</b>
3.1 Introduction	39
3.2 Results	40
3.2.1 <i>Lactobacillus plantarum</i> outcompetes <i>Lactobacillus brevis</i> for association with adult <i>Drosophila</i>	40
3.2.2 Host genetic background influences transcriptional responses to intestinal microbes	41
3.2.3 Monoassociation with <i>L. plantarum</i> shortens adult longevity relative to germ-free counterparts	42
3.2.4 <i>L. plantarum</i> does not activate proliferative responses in the host intestine	45
3.2.5 Impaired epithelial renewal in <i>L. plantarum</i> -monoassociated flies	46
3.2.6 <i>L. plantarum</i> -monoassociated flies lack intestinal progenitors	48
3.2.7 <i>L. plantarum</i> disrupts posterior midgut ultrastructure	50
3.3 Significance	52
<b>Chapter 4. Commensal pathogen competition impacts host viability</b>	<b>53</b>
4.1 Introduction	54
4.2 Results	55
4.2.1 The T6SS interacts with commensal bacteria to influence host viability	55
4.2.2 The T6SS contributes to disease symptoms	57
4.2.3 The T6SS promotes intestinal epithelial damage	59
4.2.4 The T6SS influences pathogen-commensal interactions in the intestine	61
4.2.5 The microbiome directly influences T6SS-dependent pathogenesis	64
4.3 Significance	66

<b>Chapter 5. <i>Vibrio cholerae</i>-symbiont interactions inhibit intestinal repair in <i>Drosophila</i></b>	<b>67</b>
5.1 Introduction	68
5.2 Results	69
5.2.1 The T6SS promotes epithelial shedding	69
5.2.2 Disrupted intestinal homeostasis in response to the T6SS	70
5.2.3 The T6SS modifies IPC transcriptional responses to <i>V. cholerae</i>	73
5.2.4 IPCs fail to facilitate epithelial repair upon intestinal challenge with <i>V. cholerae</i>	80
5.2.5 Impaired IPC differentiation in response to the T6SS	83
5.2.6 T6SS-dependent failure in epithelial renewal requires intestinal symbionts	86
5.2.7 T6SS suppression of epithelial renewal requires higher-order microbiome interactions	86
5.8 Significance	90
<b>Chapter 6. Discussion</b>	<b>91</b>
6.1 Summary	92
6.2. <i>Drosophila</i> association with <i>L. plantarum</i>	92
6.2.1 Summary of long-term association of adult <i>Drosophila</i> with <i>Lactobacillus plantarum</i>	92
6.2.2 <i>L. plantarum</i> association with <i>Drosophila melanogaster</i>	93
6.2.3 Symbiotic bacteria and host gene expression	94
6.2.4 Intestinal symbionts control host lifespan	95
6.2.5 Symbiotic <i>L. plantarum</i> and homeostatic growth programs	96
6.2.6 Conclusions from chapter 3	97
6.3 Symbiont pathogen-symbiont interactions and host viability	98
6.3.1 Summary of symbiont-pathogen competition and host viability	98
6.3.2 Classical and El Tor strains and the T6SS influence on host viability	99

6.3.3	The T6SS contributes to cholerae like disease	100
6.3.4	The <i>V. cholerae</i> T6SS and <i>In vivo</i> intestinal pathogenesis	101
6.3.5	Composition of the microbiome determines T6SS mediate infection outcomes	103
6.3.6	Composition of the microbiome, <i>V. cholerae</i> infection, and viability	104
6.3.7	Conclusions from chapter 4	105
6.4	Symbiont-pathogen interactions and intestinal homeostasis	106
6.4.1	Summary symbiont pathogen interactions and the effects on intestinal repair	106
6.4.2	<i>V. cholerae</i> , the IMD pathway, and intestinal homeostasis	107
6.4.3	Intestinal response to <i>V. cholerae</i>	108
6.4.4	Pathogen modification of epithelial repair in the gut of <i>Drosophila melanogaster</i>	109
6.4.5	The fruit fly model of <i>Vibrio cholerae</i> . What we learned from <i>Drosophila</i> modelgaster	111
6.4.6	Conclusions from chapter 5	112
6.5	Concluding remarks	112
	<b>Chapter 7. Literature cited</b>	<b>114</b>

## List of tables

### List of abbreviations and notations

Table 1.0	<i>Drosophila</i> nomenclature	xix
-----------	--------------------------------	-----

### Chapter 1. Introduction

Table 1.1	T6SS effectors of pandemic El Tor <i>V. cholerae</i>	23
-----------	--	----

### Chapter 2. Materials and Methods

Table 2.1	<i>Drosophila melanogaster</i> stocks and strains	27
Table 2.2	Bacterial stocks and strains	29
Table 2.3	Antibodies and dyes	33

### Chapter 5. *Vibrio cholerae*-symbiont interactions inhibit intestinal repair in *Drosophila*

Table 5.1.	The T6SS promotes a unique transcriptional response from the intestine	75
Table 5.2	Infection with <i>V. cholerae</i> promotes the transcription of antimicrobial peptides	78



## List of figures

### Chapter 1. Introduction

Figure 1.1	Structure and cellular composition of the <i>Drosophila</i> digestive tract	3
Figure 1.2	The <i>Drosophila</i> IMD and human TNF- $\alpha$ pathways	5
Figure 1.3	The intestinal immune response	8
Figure 1.4	Comparison of cell types in the <i>Drosophila</i> and human intestine	20
Figure 1.5	Structure of the <i>V. cholerae</i> T6SS	22

### Chapter 3. Monoassociation with *Lactobacillus plantarum* disrupts intestinal homeostasis in adult *Drosophila melanogaster*.

Figure 3.1	<i>L. plantarum</i> outcompetes <i>L. brevis</i> in the adult gut	41
Figure 3.2	Monoassociation with symbiotic <i>L. plantarum</i> reduces GF adult fly lifespan	44
Figure 3.3	<i>L. plantarum</i> does not trigger a proliferative response in adult fly intestines	45
Figure 3.4	A lack of epithelial renewal in the guts of <i>L. plantarum</i> -monoassociated flies	47
Figure 3.5	<i>L. plantarum</i> -monoassociated fly guts have low numbers of intestinal progenitor cells	49
Figure 3.6	<i>L. plantarum</i> disrupts posterior midgut ultrastructure	51

### Chapter 4. Commensal pathogen competition impacts host viability

Figure. 4.1	The T6SS contributes to the pathogenesis of <i>V. cholerae</i> in a commensal dependent manner	56
Figure. 4.2	The T6SS contributes to cholera-like disease	58
Figure. 4.3	The T6SS contributes to <i>V. cholerae</i> intestinal pathogenesis	60
Figure. 4.4	Composition of the microbiome determines T6SS-mediated gut infection	63
Figure. 4.5	Composition of commensal microbes impacts T6SS virulence contributions <i>in vivo</i> .	65

## Chapter 5. *Vibrio cholerae*-symbiont interactions inhibit intestinal repair in *Drosophila*

Figure 5.1	The T6SS promotes epithelial shedding	70
Figure 5.2	Disrupted intestinal homeostasis in response to the T6SS	72
Figure 5.3	The T6SS modifies whole gut transcriptional responses to <i>V. cholerae</i>	74
Figure 5.4	The T6SS modifies IPC transcriptional responses to <i>V. cholerae</i>	77
Figure 5.5	The whole gut transcriptional responses to C6706 $\Delta$ <i>vasK</i>	79
Figure 5.6	IPCs fail to facilitate epithelial repair upon intestinal challenge with <i>V. cholerae</i>	82
Figure 5.7	Impaired IPC differentiation in response to the T6SS	85
Figure 5.8	IPC suppression of growth in response to the T6SS requires intestinal symbionts	87
Figure 5.9.	T6SS suppression of epithelial renewal requires higher-order microbiome interactions	90
<b>Chapter 6.</b>	<b>Discussion</b>	
Figure 6.1	Proposed model of symbiont-pathogen interactions that inhibit intestinal repair	107

### List of abbreviations and notations

$\mu$	micro
$^{\circ}\text{C}$	degrees Celsius
AMP	Antimicrobial Peptide
AP-1	Transcription factor AP-1
<i>Ap</i>	<i>Acetobacter pasteurianus</i>
<i>A. pasteurianus</i>	<i>Acetobacter pasteurianus</i>
Att	Attacin
BMP	Bone morphogenic protein
Cdk2	Cyclin dependent kinase 2
cDNA	Complementary DNA
CR	Conventionally reared
CT	Cholera Toxin
CycB3	CyclinB3
DAP-PGN	Diaminopimelic acid-type peptidoglycan
DI	Delta
DNA	Deoxyribonucleic acid
Dome	Domeless
DPP	Decapentaplegic
Dpt	Diptericin
Dredd	Death related ced-3/Nedd2-like protein
DSS	Dextran Sodium Sulfate
DUOX	Dual oxidase
<i>Ecc15</i>	<i>Erwinia carotovora carotovora</i> , isolate 15

<i>E. coli</i>	<i>Escherichia coli</i>
EGF	Epidermal Growth Factor
EGFR	Epidermal Growth Factor Receptor
Esg	Escargot
E(spl)	Enhancer of split
Fadd	Fas-associated protein with death domain
GF	Germ Free
GFP	Green fluorescent protein
GO	Gene Ontology
Hop	Hopscotch
Iap2	Death-associated inhibitor of apoptosis 2
IMD	Immune Deficiency
IPC	Intestinal progenitor cell
ISC	Intestinal stem cell
IκB	Inhibitor of κB
JAK	Janus activated kinase
JNK	c-Jun N-Terminal Kinase
IKK	IκB Kinase Complex
LB	Lysogeny broth
<i>Lb</i>	<i>Lactobacillus brevis</i>
<i>L. brevis</i>	<i>Lactobacillus brevis</i>
<i>Lp</i>	<i>Lactobacillus plantarum</i>
<i>L. plantarum</i>	<i>Lactobacillus plantarum</i>
MARCM	Mosaic Analysis with a Repressible Cell Marker

MAD	Mother against Dpp
Mkk4	Mitogen activated protein Kinase kinase 4
Mkk7	Mitogen activated protein kinase kinase 7
MRS	De Man, Rogosa and Sharpe
mRNA	Messenger Ribonucleic Acid
NaCl	Sodium chloride
NADPH	Nicotinamide adenine dinucleotide phosphate-oxidase
NF-κB	Nuclear Factor of kappa light polypeptide gene enhancer in B-cells
NGS	normal goat serum
Nm	nanometer
OTU	Operational Taxonomic Unit
PAAR	proline-alanine-alanine-arginine
PBS	Phosphate buffered saline
PCR	Polymerase chain reaction
<i>P. entomophila</i>	<i>Pseudomonas entomophila</i>
PGN	peptidoglycan
PGRP-LC	Peptidoglycan recognition protein LC
PGRP-LE	Peptidoglycan recognition protein LE
Pnt	Pointed
Rho	Rhomboid
RNA-seq	RNA-sequencing
ROS	Reactive oxygen species
Pros	Prospero
Put	Punt

Puc	Puckered
PVR	platelet-derived growth factor and vascular endothelial growth factor-receptor related
Sax	Saxophone
Smox	Smad on X
Socs36E	Suppressor of Cytokine Signaling 36E
Spi	Spitz
STAT	Signal transduced activator of transcription
Stg	String
T6SS	Type VI secretion system
Tab2	Tak1-associated binding protein
Tak1	Tumour necrosis factor-B activated kinase
TCP	Toxin co-regulated pilus
TEM	Transmission electron microscopy
Tkv	Thickveins
TNF	Tumor Necrosis Factor
TOR	Target of Rapamycin
UAS	Upstream Activating Sequence
Upd	Unpaired
<i>V. cholerae</i>	<i>Vibrio cholerae</i>
Wg	Wingless
WT	wild-type

**Table 1.0 *Drosophila* nomenclature**

<b>Class</b>	<b>Notation</b>	<b>Example</b>
Pathway	All capitalized	IMD
Allele	Italicized and superscript	<i>imd</i> <sup>EY08573</sup>
Protein	First letter capitalized	Imd
Gene within a chromosome	comma ( , )	<i>esg-Gal4, tub-Gal80<sup>ts</sup>, UAS-GFP</i>
Genes on homologous chromosomes	forward slash ( / )	<i>neoFRT(40A)/neoFRT(40A), tubGAL80</i>
Genes on heterologous chromosomes	semi colon ( ; )	<i>w; esg-Gal4, tub-Gal80<sup>ts</sup></i>
Wild-type chromosome	plus ( + )	<i>esg-Gal4, tub-Gal80<sup>ts</sup>, UAS-GFP /+</i>
GAL4 UAS transgene expression	greater than ( > )	<i>CB&gt;mCD8::GFP</i>

## Chapter 1.

### Introduction

This chapter contains content from the following sources, republished with permission:

- Fast, D., Duggal, A., & Foley, E. Monoassociation with *Lactobacillus plantarum* disrupts intestinal homeostasis in adult *Drosophila melanogaster*. *MBio* 9, e01114-18 (2018).



## 1.1 The digestive tract of *Drosophila melanogaster*

### 1.1.1 Structure of the adult fly gut

*Gut compartmentalization:* The digestive tract of adult *Drosophila* is a complex organ made up of multiple cell types and compartmentalized into three domains of distinct developmental origin. The digestive tract begins with the ectodermal derived foregut which is composed of the esophagus, crop, and cardia (Fig. 1.1). The foregut conjoins with the midgut at the foregut-midgut junction giving way to the primary region of digestion and nutrient absorption(1). Of endodermal origin, the midgut is the largest section of the digestive tract and is broadly divided into six (R0 to R5) anatomical regions(2). These sections are further compartmentalized by the action of region-specific transcription factors that refine midgut regionalization and allow for the development of specialized cell types(2, 3). In the R3ab subsection, the transcription factor Labial maintains a cell type known as copper cells(4), responsible for the acidification of the digestive tract(5). The midgut ends at the midgut-hindgut transition which marks the beginning of the hindgut and the completion of the intestinal tract (Fig. 1.1).

*Cellular composition of the intestinal epithelium:* The posterior midgut, which spans R5 and extends into the R4 subregion, is functionally analogous to the small intestine of mammals. The epithelia of the fly gut is a pseudo-stratified epithelium that extends an apical microvilli brush boarder into the luminal space to facilitate nutrient uptake. The epithelium is predominantly composed of large columnar enterocytes (Fig 1.1), which undergo several rounds of endoreplication to achieve the characteristic polyploid nuclei and large size(6). Interspersed throughout these absorptive cells are a lineage of secretory enteroendocrine cells that dispatch digestive enzymes and peptide hormone messengers into the lumen and to distal tissues(7–9). Under steady state conditions, the intestinal epithelium is renewed every one to two weeks by the proliferation of multipotent intestinal stem cells (ISCs)(7, 8). These small mitotic cells are scattered across the basal surface of the epithelium and are the principle component responsible for the plasticity of the digestive organ. Intestines depleted of enterocytes by cell specific expression of proapoptotic genes are able to regenerate in a matter of hours via an increase in ISC mitosis(10). Typically, intestinal damage promotes the division of ISCs in a symmetric or asymmetric manner. In asymmetric division, one daughter cell is maintained as an ISC while the other daughter exits the cell cycle to become an immature transitory cell type known as an enteroblast (Fig. 1.1)(1). Enteroblasts then differentiate to generate new enterocytes(7, 8, 11) or an enteroendocrine precursor cell(12). The entire cellular structure of the epithelium is supported by a sheath of lateral and longitudinal striated visceral muscle that signals to the epithelium and mediates peristalsis. Together, the structure of the *Drosophila* adult gut represents a

simplified yet anatomically relevant model to study intestinal biology and the mechanisms that maintain intestinal homeostasis.

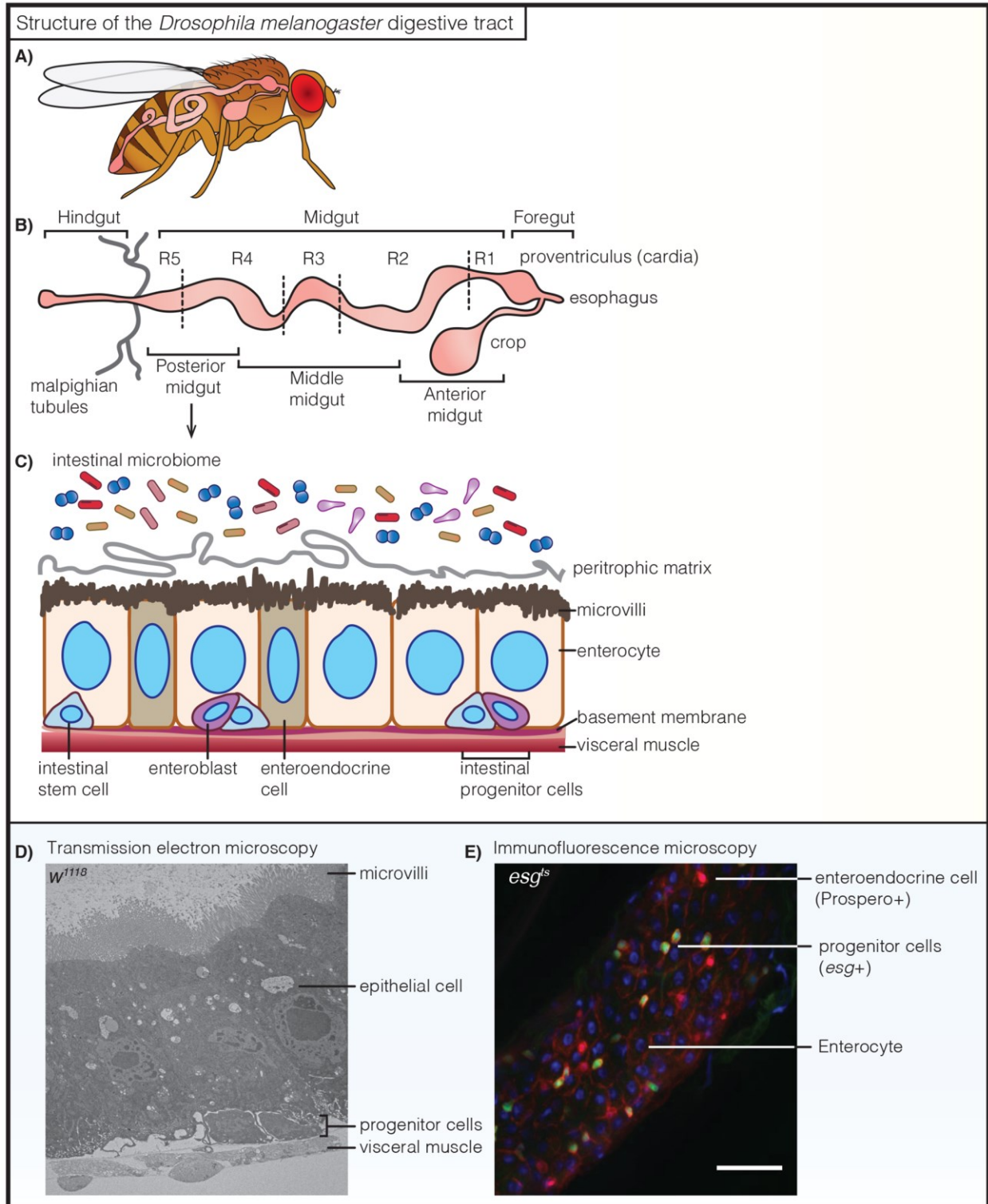


Figure 1.1 Structure and cellular composition of the *Drosophila* digestive tract. (A-C) Schematic representation of A) the digestive tract within the body cavity of an adult fly. B) The three domains of the

digestive tract and the subregions of the midgut. **C)** cellular composition of the midgut. **D)** Transmission electron microscopy of the posterior midgut of an adult *w<sup>1118</sup>* female fly. **E)** Immunofluorescence microscopy of the posterior midgut of an *esg<sup>ts</sup>* adult female fly. Enteroendocrine cells and cell borders were visualized with anti-porspero, anti-armadillo (red) respectively. *esg<sup>ts</sup>>GFP* marks intestinal progenitor cells (green) and Hoechst marks nuclei (blue).

### 1.1.2 Immunity in the fly gut

*The peritrophic matrix:* Like vertebrates, insect intestinal immunity encompasses a series of physical and humoral defenses that protect the epithelium and limit pathogen conquest. In the midgut of *Drosophila melanogaster*, the intestinal epithelium is apically lined by a noncellular chitinous matrix known as the peritrophic matrix (Fig. 1.1)(13). Composed primarily of chitinous fibers held together by chitin binding proteins, the peritrophic matrix forms a physical barrier that shields the midgut from contact with intestinal microbes(1). Loss of function of Drosocrystallin, an integral chitin binding protein, thins the peritrophic matrix, compromises its permeability, and sensitizes the host to infection with entomopathogenic *Pseudomonas entomophila* (*P. entomophila*)(14). Preliminary evidence suggests that the protection afforded to the intestinal epithelium by the peritrophic matrix is complimented by a mucous like layer on the apical surface of midgut cells(2). Although, the role of mucus in the defense of the fly gut has not been properly scrutinized. The peritrophic matrix may also aid in normal gut function. *Drop dead* mutants, the first fly line reported to entirely lack the peritrophic matrix, have a dysregulated pattern of food transit through the digestive tract(15)

*The immune deficiency pathway:* Oral ingestion of toxic bacteria stimulates a rapid antibacterial response that encompasses the production of multiple antimicrobial peptides (AMPs). Systemically, AMPs are controlled by the immune deficiency (IMD) and Toll pathways in response to bacteria and microbially derived molecules. However, the acidity of the intestine prevents the proteolytic cleavage of Spätzle, a necessary step preceding the activation of Toll(16). As a result, the production of AMPs in the gut is regulated by IMD(17, 18), with the exception of the antifungal AMP, Drosomycin, which is produced in the anterior midgut via activation of the JAK/STAT pathway(19). IMD is a cellular transduction cassette, analogous to the mammalian tumor necrosis factor pathway(Fig. 1.2)(20). The IMD response is initiated by diaminopimelic acid (DAP) type peptidoglycan (PGN) from intestinal bacteria sensed by PGN recognition proteins (PGRP) expressed throughout the digestive tract(21–24). In the ectodermal foregut and hindgut regions, PGN is sensed by the transmembrane receptor PGRP-LC, while in the midgut PGN sensing occurs through intracellular PGRP-LE detection of translocated PGN monomers(25, 26). Once bound to PGN, these PGRPs dimerize and recruit the adaptor protein Imd(27, 28). Subsequently, Imd recruits Fas-Associated Death Domain (Fadd)(29) and the caspase 8 homolog Death related ced-3/Nedd2-like caspase (Dredd)(30)

which proteolytically cleaves Imd removing thirty N-terminal amino acids(31). Cleaved Imd initiates a signalling cascade that serves to activate MAPK kinase 4 (MKK4) and MAPK kinase 7 (MKK7) and the *Drosophila* IκB kinase (IKK) complex (Immune response deficient 5 & Kenny)(32). Activation of MKK4 and MKK7 results in the transient phosphorylation of c-Jun N-Terminal Kinase (JNK) which stimulates the transcription of AP-1 target genes(33). IKK-mediated phosphorylation and cleavage by Dredd releases and activates the NF-κB transcription factor, Relish, to initiate the transcription of immune genes(34).

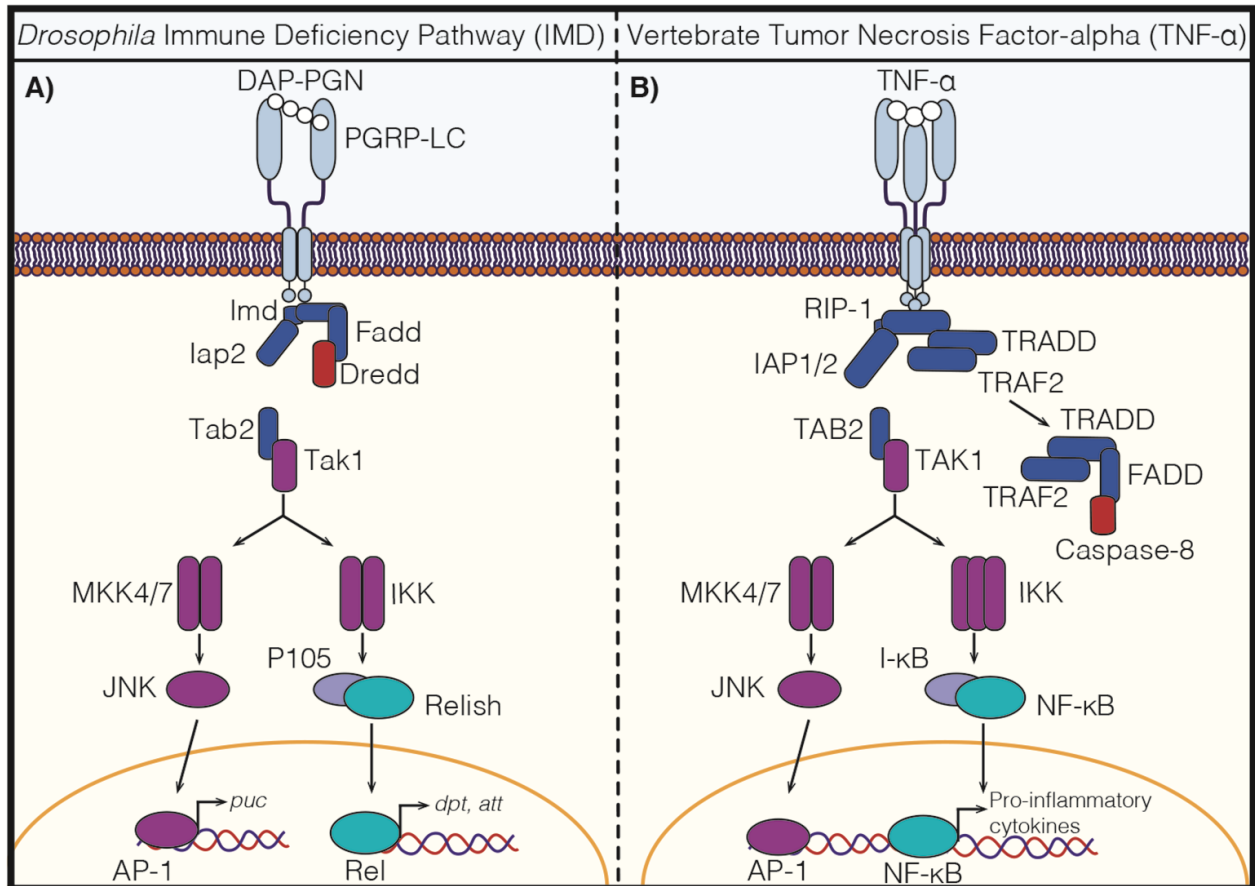


**Figure 1.2 The *Drosophila* IMD and human TNF- $\alpha$  pathways.** Schematic representation of the **A)** *Drosophila* Immune Deficiency Pathway (IMD) and the **B)** human Tumor Necrosis Factor-alpha (TNF- $\alpha$ ). Orthologs are indicated by color.

*Antimicrobial peptides:* Relocation of Relish to the nucleus results in the transcription of a broad spectrum of AMPs, which flood the intestinal lumen to restrict the growth of gut bacteria. AMPs are small cationic peptides that primarily disrupt negatively charged microbial membranes(35). There are seven families of inducible AMPs in *Drosophila* (Attacins, Cecropins, Diptericins, Drosocin, Drosomycin, Metchnikowin and Defensin), that are each associated with resistance to broad categories of microbes. For

example, Attacins and Diptericins primarily exhibit antibacterial activity(36, 37), while Drosomycin and Metchnikowin mediate antifungal defense(38, 39). A recent study found that individual AMPs mediate resistance to certain pathogenic species such that mutation or knockdown of a single AMP is sufficient to sensitize the host to that particular pathogen(40). Knockdown specifically of *dipstericin* rendered adult flies vulnerable to killing by *Providencia rettgeri* in a host background where all other AMPs were intact and functional. The role of IMD in intestinal immunity is most often associated with the control of AMP production. However, recent transcriptomic data demonstrate that IMD activity also controls the expression of a cohort of metabolic related genes(41–43). Consistent with IMD mediated control of host metabolism, mutation of *imd* alters levels of circulating insulin like peptides and significantly increases fly bodyweight(44). Additionally, IMD activation in enterocytes stimulates shedding of stressed epithelial cells as a process to mitigate intestinal injury and replace damaged cells(45).

*Reactive oxygen species:* The second inducible defense factor engaged as a resistance response to intestinal bacteria is the formation of reactive oxygen species (ROS). Dual oxidase (DUOX) catalyzes the synthesis of hypochlorous acid and hydrogen peroxide and NADPH oxidase (Nox) activity forms hydrogen peroxide molecules(46–48). ROS production is governed by the expression of *DUOX* and *Nox* and the subsequent stimulation of their enzymatic activity. At the transcriptional level, *DUOX* expression is regulated by the p38 MAPK pathway, while phospholipase C $\beta$  controls *DUOX* enzymatic activity(48, 49). Metabolically, the production of ROS depends on an enterocyte switch from lipogenesis to lipid catabolism via an inhibition of the target of rapamycin (TOR) signalling pathway(50). ROS production is vital to intestinal immunity as flies with compromised ROS production succumb to oral infection with the nonlethal fly pathogen *Erwinia carotovora carotovora 15 (Ecc15)*(46). However, ROS are far less selective than AMPs and often indiscriminately damage host tissue as a consequence of the intestinal immune response to gut bacteria. The collateral damage inflicted by ROS stimulates intestinal repair programs, boosting epithelial turnover and ISC division.

### 1.1.3 Intestinal regeneration and epithelial repair

*Intestinal stem cell division:* The intestinal immune response is synonymous with the production of offensive effectors aimed at the eradication of foreign agents. However, intestinal immunity encompasses both the responses that eliminate pathogens and the regenerative programs that repair the epithelium and restore tissue homeostasis (Fig. 1.3). The epithelial monolayer is regenerated by a pool of ISCs that are characterized by the expression of *escargot (esg)* and *Delta*(7, 8). These cells are the singular mediators of intestinal repair and loss of ISCs blocks intestinal regrowth(51). When a new epithelial cell is required, ISCs

asymmetrically divide to generate an ISC that retains mitotic capabilities and a transitory post mitotic enteroblast that loses expression of *Delta* and retains *esg*. The subsequent differentiation of enteroblast to enterocyte or enteroendocrine cell is governed by levels of Notch signalling through *Delta* expression by the ISC (Fig. 1.3A)(11, 12, 52). However, new lineage tracing data suggest that enteroendocrine cells do not arise from an enteroblast as previously thought, but instead are generated by committed stem cells expressing the enteroendocrine cell transcription factor *prospero*(12, 53). In contrast to germline stem cells, ISC divisional programs are not asymmetrically committed. In approximately 20% of ISC mitotic events, ISCs symmetrically divide to produce an enteroblast-enteroblast pair or an ISC-ISC pair(54–56). Symmetric vs asymmetric division can be distinguished during mitosis by orientation of the mitotic spindle. Planar spindle orientation indicates symmetric division and rotation of the spindle to form an oblique angle signals an asymmetric event(56). As a whole, the divisional programs of ISCs are capable of expanding the pool of ISCs and generating new terminally differentiated cells that together maintain the epithelial monolayer.

*Regulation of intestinal progenitor cells:* The activity of ISCs is regulated to match the basal rate of cell loss and is accelerated to mediate compensatory growth in response to tissue stress. The regulation of midgut ISCs has been studied in detail and numerous signalling pathways that influence ISC activity have been identified. These pathways include the Epidermal Growth Factor (EGF)(57–60), Janus Kinase and Signal Transduction and Activator of Transcription (JAK/STAT)(10, 61, 62), JNK(63), Wingless (Wg)(64, 65), Notch(11), insulin-like growth factor(54, 66–68), TOR(69, 70), Decapentaplegic (DPP)(71–75), Hippo(76, 77), Hedgehog(78), and platelet-derived growth factor and vascular endothelial growth factor-receptor related (PVR)(79) pathways. The regulation of epithelial renewal by ISCs requires the integration of signals from this network of pathways. Diffusible ligands, such as the cytokine family, Unpaired (Upd) 2 and 3, secreted from enterocytes contact the receptor Domeless on the surface of ISCs to stimulate activation of the JAK/STAT pathway. Binding of Upds to Domeless triggers the dimerization of the tyrosine kinase JAK, Hopscotch. Hopscotch kinases phosphorylate each other and the STAT proteins, which in turn enter the nucleus to activate the transcription of target genes, such as *Suppressor of cytokine signaling 36E* (Socs36E)(80). Activation of the JAK/STAT and additional pathways, such as EGF, in ISCs promotes proliferation. Similarly, activation of the EGF pathway induces ISC mitosis. Together, ISC proliferation is governed by a diverse network of pathways, required for intestinal homeostasis. Additionally, many of these pathways are also engaged in response to exogenous stimuli provided by the presence of symbiotic or pathogenic microbes in the digestive tract(81).

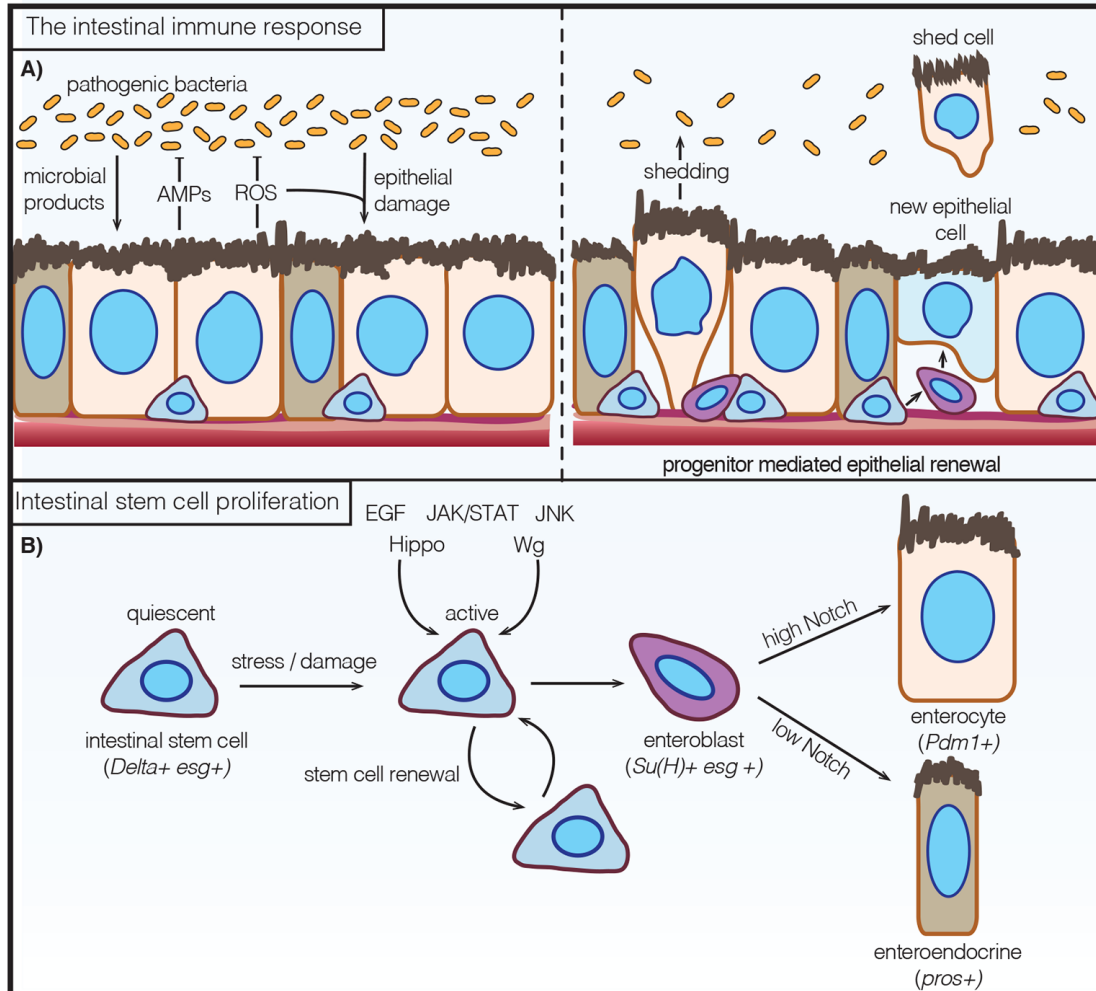


**Figure 1.3 The intestinal immune response. (A,B)** Schematic representation of the **A)** the intestinal immune response of *Drosophila melanogaster*. **(B)** The proliferation of intestinal stem cells. Abbreviations: antimicrobial peptides (AMPs), reactive oxygen species (ROS), *escargot* (*esg*), Epidermal Growth Factor (EGF), Janus Kinase and Signal Transduction and Activator of Transcription (JAK/STAT), c-Jun-N-terminal Kinase (JNK), Wingless (Wg), *Suppressor of hairless* (*Su(H)*), *POU/homeodomain transcription factor* (*Pdm1*), *prospero* (*pros*).

## 1.2 The microbiome of *Drosophila*

### 1.2.1 The *Drosophila* model for microbiome research

*The effects of the microbiome:* Environmental, microbial, and host factors establish an intestinal environment that permits colonization by a variable consortium of bacteria. Extrinsic factors such as pH, oxygen, and nutrient supply influence the biogeography of microbe distribution, while physical barriers contain microbes within the gut lumen. Host-derived bacteriostatic products such as AMPs and ROS limit bacterial numbers and prevent invasion of the host interior. Inside the lumen, microbes compete with each

other for access to nutrients and intestinal attachment sites and release metabolites that influence host processes as diverse as growth(81, 82), immunity(83, 84), and behavior(85).

*Drosophila melanogaster* is a useful model to study interactions between a host and symbiotic bacteria(86–89). The fly microbiome consists of a limited number of bacterial species that are easily cultured and manipulated in isolation(90). Researchers have access to simple protocols for the establishment of gnotobiotic fly cultures(91), and flies lend themselves to manipulation of host gene expression. Of equal importance, there are extensive genetic, developmental, and biochemical similarities between fly and mammalian gut biology(1, 2, 92–94). Thus, discoveries in *Drosophila* provide insights into evolutionarily conserved features of host-bacterium interactions. For example, in flies and mammals, ISCs divide and differentiate at a rate that maintains an intact epithelial barrier(7, 8, 93). A relatively simple “escalator” program times ISC division to match the loss of aged cells, while a more complex, adaptive program activates ISC division to compensate for environmental destruction of host cells(10, 18, 19, 60, 66). This adaptive regulation of growth maintains the integrity of the epithelial barrier and is critical for long-term health of the host. Breaches to the gut barrier permit an invasion by intestinal microbes that activate local immune responses and drive the development of chronic inflammatory illnesses(95, 96).

### 1.2.2 Acquisition and maintenance of the microbiome

*Acquisition of the fly microbiome:* Gut associated microbes of *Drosophila* are acquired from the environment in the immediate hours after larvae emerge from the embryonic chorion(97). In contrast to the endosymbionts *Wolbachia*(98) and *Spiroplasma*(99), which are transmitted directly within the embryo, intestinal commensals are acquired by the ingestion of a bacterial laden meal(100). In the absence of intercellular symbionts, *Drosophila* embryos are devoid of microbial association, while the protective chorion hosts a small population of diverse maternal commensals(87, 101). Accordingly, removal of the chorion and transfer of embryos to a sterile environment is sufficient to obtain an axenic organism(101–104). Conventional larvae immerse themselves in food contaminated by parental symbionts and other environmental species, feeding constantly throughout the larval stages of life. Bacteria density in the gut climbs quickly and reaches its peak at the third-instar stage(101, 105). Following this peak, is a decline in bacterial load during metamorphosis that coincides with a boost in expression of AMPs within the pupal case(106–109). Subsequently, newly eclosed adults harbor a small community of microbes ranging from a few hundred to one thousand colony forming units(18, 101, 105, 110). Similar to larvae, the density of the adult microbiome steadily increases overtime plateauing as the intestinal niche is filled(18, 110–113). Thus, the acquisition and establishment of the microbiome is predicated on maternally transmitted symbionts



on the exterior of the embryonic protective shell and the presence of microbes on the larval and adult food sources.

*Maintenance of the fly microbiome:* In mammals, commensal microbes form long-term symbioses with the host, establishing resident populations that persist throughout life(114). In *Drosophila*, microbes frequently shuttle between food and the digestive tract, raising the possibility that the fly microbiome consists of microbes passively transiting through the gut, rather than an established resident microbial community. This idea is countered by the existence of symbiotic bacteria that are able to persist in the digestive tract without constant resupply(115). However, populational residence or stable colonization is not universal among all fly commensal species, as the abundance of unspecified species of symbiotic *Acetobacter* and *Lactobacillus* is decreased below the limit of detection in the gut when cut off from a microbial reservoir(110). In contrast, particular symbiotic species such as *Lactobacillus plantarum* (*L. plantarum*), remain associated with the gut without consistent replenishment and is stable within the fly upon stochastic challenge(112, 116, 117). Similarly, *Acetobacter thailandicus* forms a stable association with the foregut of wild caught flies, suggesting that endogenous symbionts are capable of establishing a resident state in natural populations of *Drosophila*(115). However, the density of intestinal bacteria in the gut is impacted by the presence of an exogenous pool of food sourced microbes. Frequent food changes, that deplete the number of microbes available for reingestion, significantly reduces the overall bacterial load in the gut(110). Together, the data indicate that the fly microbiome is maintained in density by ingestion of food sourced microbes while residency is achieved by species able to persist within the digestive tract in the absence of environmental sources.

### 1.2.3 Composition of the fruit fly microbiome

*Taxa of the fly microbiome:* The *Drosophila* lifecycle is perpetuated on rotting fruit contaminated by various species of yeast and bacteria(118). Despite this microbially rich environment, the taxonomic makeup of the *Drosophila* microbiome is orders of magnitude less complex than that of higher order vertebrates, ranging from the tens to hundreds vs the thousands found in mammals(87, 88, 119–122). The taxonomic composition of the *Drosophila* microbiota has been analyzed through characterization of culturable species and in greater depth by deep sequencing of 16S rRNA. Laboratory reared flies have relatively low bacterial diversity, consisting of 1-15 individual taxa, and are commonly associated with the *Acetobacter* and *Lactobacillus* genera(87, 103, 111, 119, 123–126). The specific taxonomic composition of the *Drosophila* microbiome is influenced heavily by diet(119, 127). Flies raised on sugar-based mediums favor populations of Proteobacteria, such as *Acetobacter* and *Gluconobacter* species. In contrast, the guts

of flies reared on a complex polysaccharide diet are largely populated by Firmicutes, primarily *Lactobacillus* species (90, 128). In general, laboratory flies are most commonly associated with various species of *Acetobacter* and *Lactobacillus* that often includes *L. plantarum*, *Lactobacillus brevis* (*L. brevis*), *Acetobacter pasteurianus* (*A. pasteurianus*), and *Acetobacter pomorum* (*A. pomorum*). Additionally, some laboratory cultures of *Drosophila* harbor populations of  $\gamma$ -Proteobacteria including *Enterococcus* and *Gluconobacter* species. The pool of bacteria resident in the intestinal tract is more diverse in wild populations of *Drosophila*, expanding up to 80 operational taxonomic units (OTUs) per individual fly(119, 123, 125, 129). This increased diversity is accompanied by an expansion of *Proteobacteria* diversity and a lower abundance of *Lactobacillus*(129, 130). It is yet unclear what proportion of these species represent increased diversity in symbionts or are simply due to an increased flow of transient microbes through the digestive tract. However, consistently wild flies are populated by *Acetobacter* and *Lactobacillus*, suggesting that the low diversity of the *Drosophila* microbiome persists within wild populations(119, 123, 125, 130, 131).

*Variability of the fly microbiome:* The microbiome of *Drosophila* is inconsistent, hallmarked by robust variability. The variability is such that the composition and proportion of bacterial species varies within a single fly line, housed in identical conditions, fed the same diet, and maintained with the same husbandry protocols(88, 119). This variability extends to differences between fly lines(132) and to the individual level, as single isogenic specimens show variability in colonization(112). This between host variation is stable overtime and is likely due, at least in part, to probabilistic events during colonization, whereby each bacterial cell has an equal but independent chance of colonization(112). These stochastic events have also been implicated in the establishment of the microbiome in wild *Drosophila*, indicating that variability in the fly microbiome is probabilistic in nature and persists outside of laboratory culture(130). However, other factors besides these by chance events, such as diet(119, 127) and host genotype(88, 132, 133) shape the symbiotic bacterial community in the gut of *Drosophila*. For example, polymorphisms in the homeobox transcription factor *Caudal*, produce higher levels of AMP expression that modifies microbial density and shifts the proportion of species present(126).

*Symbiotic yeast:* Encompassed within the fly microbiome are a number of species of symbiotic yeast(90). Detected in laboratory and recently captured wild flies, yeasts are vital to fly nutrition, as a source of essential nutrients that are scarce in decaying plant matter. Yeast supplement the diet by serving as a source of amino acids, B vitamins, and fatty acids required for larval growth(134). Axenic larvae, which are devoid of all microbes and raised in their absence, are unable to survive on a sterile carbohydrate diet without the addition of dietary yeast(135). Similarly, symbiotic *Issatchenkia orientalis*, isolated from field caught *Drosophila*, promotes amino acid harvest and extends adult fly lifespan on a protein deficient

diet(136). There is modest diversity in the species of yeast associated with *Drosophila*. These species include *Candida*, *Saccharomyces*, *Hanseniaspora*, and *Pichia* and are most often isolated from the crop(137, 138). Despite the impact of yeast on fruit fly nutrient acquisition, symbiotic yeasts are comparatively understudied members of the microbiome and it is likely that much of their impact on fly biology is yet to be discovered.

Together, the digestive tract of *Drosophila* hosts an eclectic population of commensal yeast and bacteria characterized by simplified diversity and between host variability. These intestinal symbionts form long-term biological associations, or symbioses, existing within a microbial community structure shaped by host inputs. In turn, intestinal microbes facilitate biological changes within the fly that impact various aspects of host fitness.

### 1.3 Intestinal bacteria and fruit fly biology

#### 1.3.1 Host-symbiont interactions

Intestinal symbionts are not required for the survival of *Drosophila* as germ free (GF) flies, devoid of all microbial associations, are viable and have few obvious defects. Superficially, adult GF *Drosophila* are indistinguishable from conventionally reared (CR) flies, which host a full compartment of symbiotic microbes. In actuality, the absence of intestinal bacteria precipitates a number of changes impacting nutritional phenotypes, immune function, and changes to overall fitness.

*Nutritional stability and the microbiome:* The microbiome buffers the host from environmental perturbation, sustaining growth through times of nutritional challenge. Axenic larvae raised on a protein deficient diet are delayed developmentally, spending roughly 48 extra hours as larva(102, 105). This developmental defect is rescued by mutualistic interactions between the host and symbiotic bacteria. *L. plantarum*<sup>WJL</sup> maintains the expression of intestinal peptidases that increase the pool of amino acids to activate the nutrient sensing pathway TOR and sustain larval growth(105, 139). Similarly, *A. pomorum* restores the developmental rate and body size of protein starved larva via insulin-like growth factor signaling(102). Microbes added to axenic fly cultures expand rapidly within the niche and establish a large microbial population. The abundance of the symbiont significantly impacts its effects on host phenotypes(140). For example, *Issatchenkia orientalis* extends the lifespan of adult flies on a protein deficient diet in a dose dependent manner, and reduced availability of the symbiont curtails lifespan extension(116). This raises the possibility that intestinal microbes also complement host metabolism

through dietary supplementation. Consistent with this, thiamine derived from the microbiome is sufficient to sustain larval development when it cannot be acquired directly from the food(141).

*Microbiome activation of intestinal immunity:* The effects of gut bacteria on intestinal homeostasis involve an interplay between metabolism and immunity, whereby immune activity modifies metabolic outputs and immune efficacy requires a coordinated shift in metabolism(142). Symbiotic *L. brevis* provokes the synthesis of ROS through uracil dependent activation of DUOX(143). The production of ROS requires inhibition of TOR to facilitate a shift from lipogenesis to lipolysis necessary for NADPH dependent synthesis of ROS(50). Alternatively, *L. plantarum* stimulates ROS dependent cellular proliferation in the midgut(47) and initiates a cytoprotective response mitigating damage from oxidative insult(144). ROS production in response to the microbiome along with microbially induced AMPs restrict the distribution and density of gut bacteria(41, 126, 143, 145). Accordingly, the expression levels of AMPs are significantly lower in GF flies relative to CR counterparts(18, 111). Intestinal bacteria also directly contribute to defense of the digestive tract. *L. plantarum* colonization protects the host from infection related death when challenged with *Serratia marcescens* or *Pseudomonas aeruginosa*(110).

*Microbial stimulation of intestinal regeneration:* Intestinal symbionts complement host nutrition and safeguard the intestine against invasive pathogens. However, commensal colonization comes at a fitness cost as CR flies have shortened adult lifespans relative to GF organisms(113, 146). Bacterial density increases in the digestive tract with age(18, 41, 111), and this increased burden is associated with age related deterioration of intestinal tissue(18, 63, 147, 148). A gradual erosion of epithelial organization occurs through excessive proliferation of ISCs which leads to an accumulation of miss-differentiated cells, disrupted cellular architecture, and tissue dysplasia(63, 113, 149). This disruption to epithelial structure compromises the integrity of the intestinal barrier and is eventually associated with host mortality(95). Alleviation of bacterial burden slows epithelial dysplasia and reduces markers of age-related homeostatic decline(18, 41, 67). Thus, intestinal bacteria activate ISC divisional programs potentiating a numerical expansion in the pool of intestinal progenitor cells (ISCs and enteroblasts collectively) (IPCs)(18). Accordingly, the intestines of GF flies have fewer mitotic cells and a decreased rate of epithelial renewal. Increased epithelial turnover in response to the microbiome occurs primarily through an increase in basal activity of the JAK/STAT and EGF pathways which regulate IPC proliferation(18, 41). Alternatively, symbiotic *L. brevis* modifies niche cues to increase IPC proliferation, at least in part through changes to integrin expression in IPCs themselves(150). Taken together, the data demonstrate that commensal bacteria have strong effects on IPC proliferation, and symbiont regulation of IPC activity occurs through multiple signalling pathways and mechanisms.

### 1.3.2 Host pathogen interactions

*Intestinal defence against enteric pathogens:* Several different oral bacterial infection models have been used to probe the hosts intestinal response to pathogenic bacteria. These infection models include challenge with sublethal species such as *Ecc15*(18) and highly virulent infections like *Serratia marcescens*(151, 152), *P. entomophila*(153, 154), *Pseudomonas aeruginosa*(155, 156), and *Vibrio cholerae* (*V. cholerae*)(157). Despite distinct mechanisms of pathogenesis, infection with different bacteria typically provokes a generalized response from host tissue, characterized by the production of AMPs, ROS, and the engagement of epithelial repair programs(81, 158). *Serratia marcescens* kills the host through breach of the epithelial barrier and the establishment of a systemic infection(152), while *P. entomophila* secretes the pore-forming toxin Monalysin that contributes to pathogen lethality by damaging intestinal cells(159). Ingestion of either *Serratia marcescens* or *P. entomophila* activates the IMD pathway and ablation of IMD signalling significantly impairs host survivability to either bacteria, suggesting that the *Drosophila* gut immune response is effective against pathogens with different mechanisms of virulence(152, 160). The ability to produce different classes of AMPs with specificity to certain pathogens by IMD, likely contributes to the pathway's ability to defend against diverse bacterial challenge(40). While generally beneficial in times of bacterial infection, IMD has been implicated in the pathogenesis of the enteric bacterium *V. cholerae*. In contrast to challenge with *Serratia marcescens* and *P. entomophila*, IMD pathway mutants infected with *V. cholerae* have extended viability relative to WT *Drosophila*(161), suggesting that similar immune responses to different infections can have different overall effects on the host. Alternatively, pathogen mediated modification of host responses can also dictate infection related outcomes. Flies survive infection with *Ecc15* in part because of the engagement of a robust regenerative response(18), while flies infected with a large dose of *P. entomophila* succumb to infection after a pathogen mediated blockade of IPC proliferation(162).

*Enteric pathogens and intestinal repair:* In absentia of direct inhibitory factors, enteric pathogens activate an escalator program that accelerates epithelial renewal(81). This accelerated regenerative response leads to a rapid expansion of IPCs that generates new epithelial cells. As previously outlined in 1.1.3, a number of mitogenic and stress sensing pathways converge to regulate IPC proliferation. Damaged enterocytes release Upds that activate the JAK/STAT pathway in ISCs(10, 18). Similarly, stressed tissues release diffusible EGF ligands (Spitz, Keren, Vein) that stimulate the EGF pathway to engage ISC mitosis(60). Activation of the EGF pathway is vital in the context of a bacterial infection as inhibition of EGF signalling disables the ability of IPCs to respond to challenge with *Ecc15*(58). Accordingly, deliberate arrest of IPC proliferation renders infection with *Ecc15* lethal(18). Thus, interactions with enteric pathogens provoke a

regulated proliferative response from host tissue. Pathogen mediated disruption to this regulation results in atypical IPC activity and enhanced pathology. Oral infection with *Pseudomonas aeruginosa* causes intestinal hyperplasia through aberrant activation of the conserved stress sensor molecule JNK in enterocytes, which promotes IPC over proliferation(155). Taken together, the data demonstrate that intestinal bacteria induce a proliferative response from IPCs that ultimately orchestrates regeneration of the intestinal monolayer. Upon entry into the digestive tract enteric pathogens encounter the host's natural microbiome which thoroughly occupies the intestinal niche. The density of commensal species resident in the gut necessitates competition between symbiont and pathogen, and the effects of these host-symbiont-pathogen interactions have only just begun to be examined.

### 1.3.3 The host-symbiont-pathogen triad and bacteria-bacteria interactions

*Bacteria-bacteria interactions:* Gut associated microbes moderate intestinal homeostasis. Both symbiotic and pathogenic bacteria elicit a series of responses from the host that alter the luminal environment. However, it is also important to consider how interactions between bacterial species influence intestinal biology. For example, the production of vitamin B<sub>12</sub> by the human microbiome is impacted by the make-up of the bacterial community itself(163). In *Drosophila*, certain aspects of host fitness related to the microbiota cannot be entirely explained by the contributions of the individual symbiotic species present in the digestive tract, demonstrating that interactions between bacteria contribute to host phenotypes(140). These interbacterial interactions have important consequences for intestinal defense. In humans, shifts in symbiotic bacteria diversity characterized by a decrease in abundance of *Firmicutes* and *Bacteroidetes* and an increase the proportion of *Enterobacteriaceae*(164) are associated with an expansion of *Clostridium difficile*(165), suggesting that bacterial community structure shields the host from the expansion of opportunistic pathogens. Alternatively, direct interactions between pathogens and symbiotic bacteria can be detrimental to the host. Interactions with symbiotic *Escherichia coli* (*E. coli*) enhance the disease symptoms of *V. cholerae* in infant mice(166). Therefore, it is important to understand how inputs between bacteria influence the host.

## 1.4 *Vibrio cholerae* disease, virulence factors, and the fly model.

### 1.4.1 The disease cholera and the pandemic outbreaks

*Vibrio cholerae*: A member of the phylum *Proteobacteria*, the intestinal pathogen *V. cholerae* is a diverse bacterial species with over 200 serogroups and a widespread geographic distribution(167, 168). The bacterium is characterized by a distinctive curved rod shape with a polar flagellum that propels the microbe through heterogenous aquatic ecosystems(169). Environmentally, *V. cholerae* is found as a free-living bacterium in estuaries and coastal waters(170). *V. cholerae* in biofilm conformation is often isolated from chitinous detritus or in association with the surfaces of various organisms including algae, copepods, shellfish, fish, and insects(171–173). These organisms exist as natural reservoirs of *V. cholerae* and their prevalence contributes to the spread of the bacteria during seasonal flooding in endemic areas. Endemic to regions in the Caribbean, the Middle East, Asia, and sub-Saharan Africa(174), the disease cholera is caused by ingestion and subsequent colonization of the digestive tract by *V. cholerae*, a process that begins most often with the consumption of contaminated water. In contrast to endemic cholera, outbreaks of epidemic cholera are often initiated by the introduction of *V. cholerae* to naïve populations with an inadequate supply of clean water(175). Sadly, epidemic cholera outbreaks disproportionately affect regions where public health and sanitation measures are compromised by natural disasters, war, or limited resources. For example, through 2016-2018, the civil war in Yemen perpetuated the worst cholera outbreak in modern history, with over one million suspected cases(176).

*The disease cholera*: There are an estimated 1.4-4.3 three million cases of cholera annually that result in approximately one hundred thousand deaths(177). Infection with *V. cholerae* manifests a wide variety of symptoms ranging from asymptomatic inoculation, to a mild illness indistinguishable from gastrointestinal distress, to the debilitating diarrheal disease cholera(167). Cholera itself is hallmarked by rice water diarrheal purges that expel up to 15 liters of pathogen laden fluid per day(178). This rapid fluid loss quickly depletes the host of electrolytes, reduces blood volume, and can result in organ failure(179). Mortality rates associated with *V. cholera* fluctuate from 50-70% without medical intervention. However, simple oral rehydration therapy reduces mortality to under one percent, further emphasizing the critical nature of accessible health infrastructure in combating and preventing the spread of cholera. In instances of serious prolonged outbreaks, new cholera vaccines have been deployed, registering a protection rate of around 50% that persists for approximately 24 months(180).

*Pandemic V. cholerae*: The devastation caused by recent cholera outbreaks is mirrored through the past two hundred years with *V. cholerae* posing a considerable threat to public health through seven

distinct pandemics(181). Despite the diversity of the *V. cholerae* species, only isolates classified as classical strains by the expression of the O1 antigen have been implicated in the cholera pandemics(177, 181). The strains involved in the seven pandemics are further subdivided into two biotypes, classical and El Tor strains that are distinguishable by differences in pathogenesis(182), toxin production(183), phylogenetic analysis(184), and the presence of additional virulence factors(185, 186). Classical strains, responsible for the 1<sup>st</sup>-6<sup>th</sup> pandemics, cause a more severe disease in humans, characterized by production of cholera toxin (CT). In contrast, the ongoing 7<sup>th</sup> pandemic is caused by El Tor strains which produce less CT and trend towards a milder human disease that is regularly asymptomatic in the host(182, 187, 188). Reduced CT production in El Tor strains results from differential activation of the *tcpPH* promoter by the AphB regulator that results in significantly diminished toxin gene expression(183, 189). However, the existence of multiple genotypic divergencies, such as sequence differences in toxin coregulated pilin, indicate that differences in pathogenesis between biotypes cannot be solely attributed to production levels of CT(190, 191). El Tor strains also encode auxiliary factors such as a functional type VI secretion system (T6SS), hemagglutinin, a pore-forming hemolysin, and the multifunctional auto processing RTX toxin, that are absent from classical strains and may contribute to difference in pathology(185, 186, 192). For example, killing of the nematode, *Caenorhabditis elegans*, by the El Tor strain C6706 requires the hemolysin toxin(186). Several virulence factors produced by pandemic *V. cholerae* regulate colonization of the host and the bacteria's overall pathogenesis.

#### 1.4.2 The virulence factors of *V. cholerae*.

*Cholera toxin*: *V. cholerae* encodes a number of virulence factors that negatively impact host health and promote bacterial dissemination back into the environment(193–195). *V. cholerae* is reintroduced to *ex vivo* environs through violent diarrheal purges caused by the enterotoxin CT(196, 197). CT is an AB<sub>5</sub> toxin composed of a single A (active) subunit surrounded by a B (binding) subunit pentamer that facilitates endocytic uptake of the toxin by target cells(198, 199). CT is secreted into the intestinal lumen via a type two secretion system whereby B subunits bind to host GM1 gangliosides on intestinal cells permitting toxin entry. The AB toxin is shuttled to the ER where a misfolded protein response releases the A subunit into the cytoplasm(196). The cytosolic A subunit ADP-ribosylates Gs alpha of adenylate cyclase, securing its active conformation, and increasing cellular levels of 3',5'-cyclic AMP(200, 201). Excess cyclic AMP promotes over activation of protein kinase A which phosphorylates the cystic fibrosis transmembrane conductance regulator channel prompting the unregulated efflux of chloride and sodium ions into the intestinal lumen(201, 202). The resulting ion imbalance results in osmotic flow of water into the lumen,



culminating in profuse watery diarrhea(203). Infection with CT null mutant *V. cholerae* reduces diarrheal symptoms and impairs colonization(197, 204). However, CT mutant *V. cholerae* strains remain infectious and able to cause intestinal disease, suggesting that additional virulence factors contribute to cholera gastroenteritis(205).

*Toxin coregulated pilus: V. cholerae* pathogenesis relies primarily on CT and the toxin co-regulated pilus (TCP)(196, 206). This type IV pilus enables the formation of *V. cholera* microcolonies that support colonization efficiency and mitigate the effects of host digestive processes, promoting resistance to bile(207, 208). In animal models, deletion of TCP significantly impairs intestinal colonization, a phenotype replicated in human volunteers(193, 209). TCP also serves as a receptor for binding and internalization of the CTX $\phi$  bacteriophage(210). Contained within the genome of CTX $\phi$  are the *ctxAB* toxin genes that integrate into the chromosome of *V. cholerae* catalysing a transition from benign to pathogenic microbe. CT and TCP are often described as the quintessential virulence factors of *V. cholerae*. However, the bacteria encodes additional factors like an exopolysaccharide capsule(211) and a T6SS(212) that contribute to *V. cholerae* mediated disease. Given the number of virulence factors, several nonhuman *V. cholerae* models have been developed to study the role of these factors in *Vibrio* infection.

#### 1.4.3 The *Drosophila* model for *Vibrio cholerae*

*Models of V. cholerae disease:* Pandemic *V. cholerae* is transmitted through the fecal oral route. Rapid expulsion of the bacteria from the host into the environmental reservoir perpetuates a cycle of reingestion and expulsion that sustains cholera outbreaks. Since its isolation during the fifth pandemic by Robert Koch, researchers have developed a number of models to study the specifics of *V. cholerae* infection. These models include mammalian hosts, such as guinea pigs(213), rabbits(214, 215), mice(216, 217), and humans(197), the *Danio rerio* fish model(218), and the *Drosophila melanogaster* insect model(157). The use of non-primate animal models, such as the infant mouse and infant rabbit, allowed for the identification of many *V. cholerae* virulence factors and their contribution to disease. An early study in the infant mouse identified TCP and characterized its coordinated regulation with CT(219). Studies of CT in infant rabbits revealed CT toxin impacts the bacteria's pathogenesis beyond causing diarrhea. Specifically, CT depletes mucin from goblet cells and alters the distribution of *V. cholerae* along the brush border of the intestine(209). However, these valuable models are not without shortcomings. *V. cholerae* colonization of Infant rabbits requires the administration of a proton receptor agonist to limit stomach acid production(209) and infant mice have an underdeveloped microbiome that prevents an accurate evaluation of interactions between *V. cholerae* and intestinal symbionts(220).

*The Drosophila V. cholerae model:* The *V. cholerae* fruit fly model was first pioneered with the demonstration that adult *Drosophila* are naturally infectible by *V. cholerae* without the intervention required for many mammalian models(157). Flies supplied with a consistent source of *V. cholerae* in the base of the enclosure quickly develop a lethal intestinal illness causing death in 50-150 hours, depending on the strain of *V. cholerae*(157, 221). The intestine of adult flies is comparatively simplified, yet contains analogous cell types to the mammalian gut and responds to infection in a similar manner (Fig. 1.4)(1). Both intestines exist as a single monolayer of cells renewed by the proliferative action of basal progenitor cells(93). Additionally, adult *Drosophila* infected with *V. cholerae* develop symptoms that closely mimic cholera. Infection promotes the onset of a diarrheal like disease through aberrant activation of the *Drosophila* adenylate cyclase, Rutabaga(157). Furthermore, mutation of CT attenuates but does not abolish *V. cholerae* pathogenicity in flies. However, flies lack a traditional cellular adaptive immune system responsible for the protective immunity acquired by humans after exposure to *V. cholerae*(222, 223). Nonetheless, the physiological similarity to mammals and the natural infectability of the fly make *Drosophila* an excellent model to study *V. cholerae* infection.

To date, several studies in the *Drosophila* model have been conducted to understand how various *V. cholera* virulence factors impact pathogenesis(157, 221, 224). For example, study of CT in the fly gut found that *ctxA* promotes adherence junction defects that results in disrupted cell borders, gaps between epithelial cells, and reduced host viability(225). Separate lines of work in the fly model have also investigated the impacts of *V. cholerae* metabolism on host well-being. A recent study demonstrated that *V. cholera* consumption of acetate modifies intestinal insulin signalling disrupting host metabolism and driving mortality in the fly(224). Additionally, a study of *V. cholerae* biofilm formation uncovered that quorum sensing dependent signalling attenuates the virulence of *V. cholerae in vivo*(221). From a host perspective, *Drosophila* is especially useful as a model, as the fruit fly is particularly amenable to genetic screens for host factors that contribute to disease. This approach was used to demonstrate that IMD activation in response to *V. cholerae* is toxic to the host(161). In summary, *Drosophila* is a physiologically relevant model well suited to the study of *V. cholerae*, its pathogenesis, and *in vivo* interactions. Additionally, the presence of the *Drosophila* microbiome during *V. cholerae* infection makes it possible examine the consequences of interaction between *V. cholerae* and the intestinal microbiome.

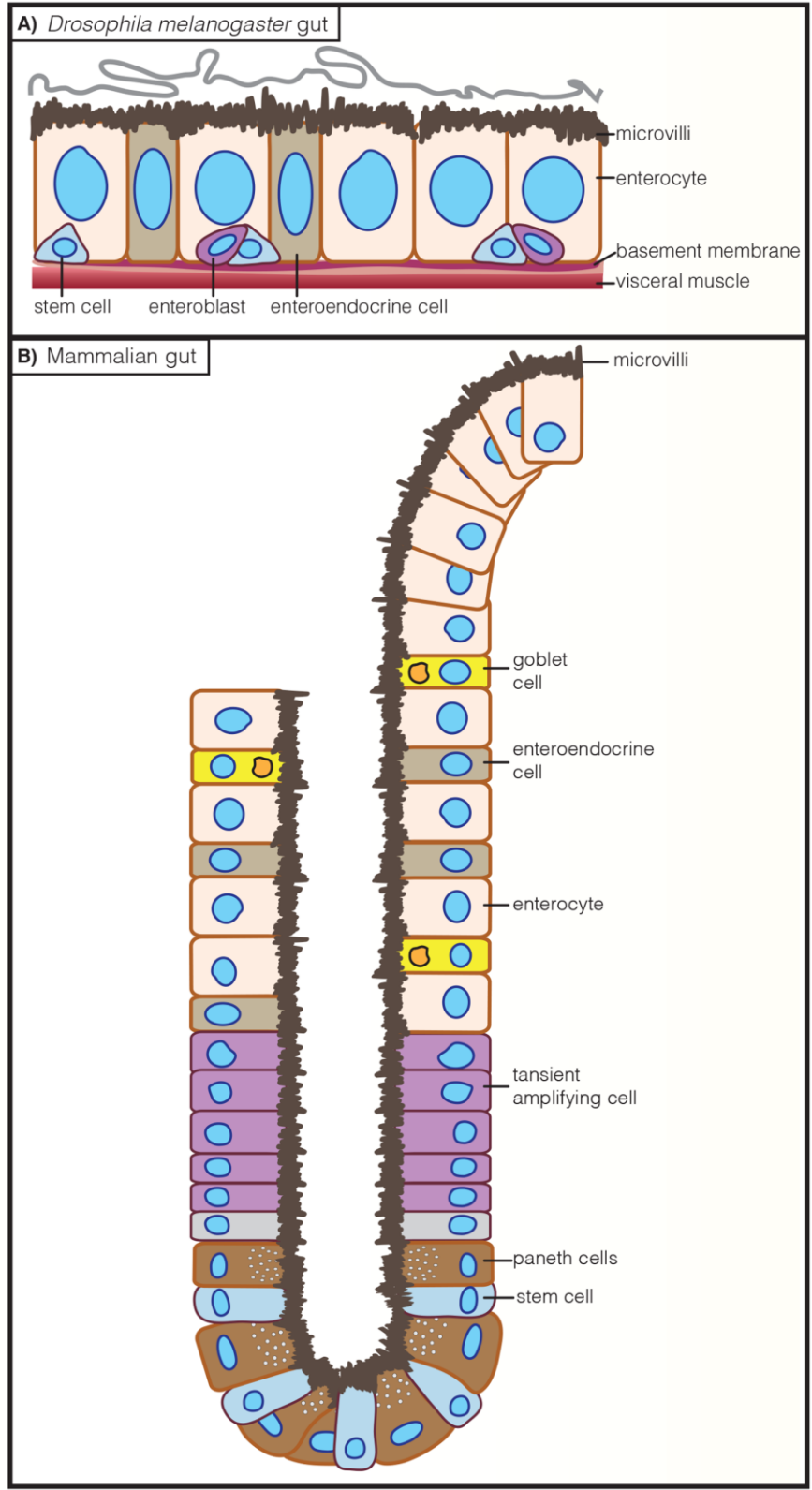


Figure 1.4 Comparison of cell types in the *Drosophila* and human intestine. (A,B) Schematic representation of the A) *Drosophila* and B) human intestine. Functionally orthologous cell types are indicated by color.

## 1.5 The type VI secretion system of *Vibrio cholerae*

### 1.5.1 The function, structure, and effectors of the *Vibrio cholerae* type VI secretion system

*The type VI secretion system:* Principally, *V. cholerae* interacts with competing bacteria in its niche via the action of a molecular injectosome known as the T6SS. The T6SS of *V. cholerae* is a contact-dependent injection apparatus that bears homology to the tail and spike of the T4 bacteriophage (Fig 1.5)(226). This secretion system delivers its lethal payload through the extension of a toxin loaded spike into target cells via the rapid contraction of an outer protein sheath (Fig 1.5)(227, 228). T6SS toxins, or effectors, are lethal to the recipient cell unless the target produces the requisite cognate immunity proteins to bind and sequester the incoming effectors(229, 230). In this regard, the T6SS mediates antagonistic interactions between bacteria and a diverse entourage of eukaryotic and prokaryotic organisms(212, 231, 232). These T6SS interactions allow the bacteria to discourage predation by *Dictyostelium discoideum* and compete for residence within microbially dense environs(166, 212).

*Structure of the T6SS:* The T6SS is a multi-component molecular syringe that bridges the periplasm and spans inner and outer membranes of Gram-negative bacteria (Fig. 1.5). Assembly of the *V. cholerae* T6SS begins with the membrane complex composed of VasD, VasF, and VasK(233). Deletion mutants in the membrane complex prevents the assembly of the T6SS, rendering the secretion system null(231). Next, the baseplate is assembled to anchor the T6SS to the inner membrane and serve as the construction site for the tail complex(233, 234). The tail complex consists of an inner tube composed of hemolysin coregulated protein hexamers encased by an outer contractile sheath made up of the proteins VipA and VipB. The tail complex extends from the baseplate until it makes contact with the far side of the cell, indicating that cell width dictates the length of the tail(235). The inner tube is capped by the VgrG1-3 trimer which contains repeating proline-alanine-alanine-arginine (PAAR) motifs that sharpen the tip of the T6SS spike complex(236, 237). In response to unknown signals, the outer sheath undergoes a contraction event that propels the PAAR tipped spike towards the target cell, punching through the membrane and effectively delivering T6SS toxins(227).

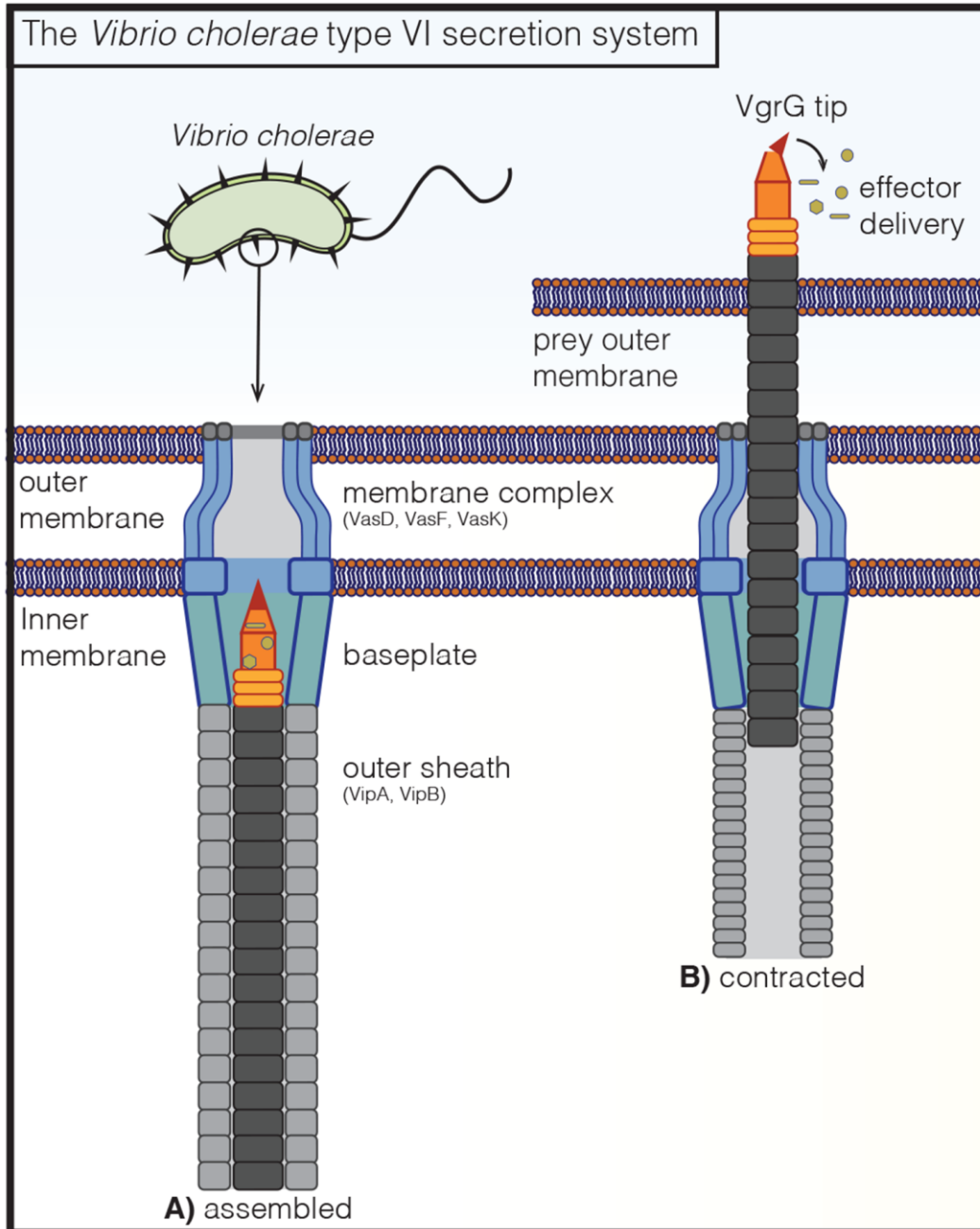


**Figure 1.5 Structure of the *V. cholerae* T6SS. (A,B)** Schematic representation of the **A)** the assembled and **B)** contracted *V. cholerae* T6SS.

*T6SS effectors:* *V. cholerae* T6SS effectors and immunity genes are distributed across the four clusters that encode the T6SS(238). As a species, *V. cholerae* encodes a diverse array of T6SS effectors and corresponding immunity proteins(239). However, pandemic El Tor strains consistently encode five effector proteins that together are capable of intoxicating prokaryotic and eukaryotic cells (Table 1.1). The effectors

are either loaded onto the T6SS as cargo effectors, or exist as components of the spike proteins themselves(240). VgrG-3, TseL, and TseH contribute to T6SS-mediated bacterial killing(230, 241), while VgrG-1 crosslinks actin in the cytoskeleton of eukaryotes(242). VasX, is unique, as it functions against both prokaryotes and eukaryotes. T6SS antibacterial effectors typically act on conserved bacterial components. For example, the T6SS structural component, VgrG-3, and the cargo effector, TseH, contribute to T6SS lethality through degradation of peptidoglycan(229, 243). TseL possesses a putative lipase domain that targets membrane associated lipids(230). The membrane is also targeted by VasX, a pore forming toxin, that disrupts membrane integrity(244). Finally, the eukaryotic effector VgrG-1 cross links actin, promoting cytotoxicity in macrophages and amoeba.(212, 242) Together, the T6SS of pandemic *V. cholerae* secretes a number of effector molecules that are toxic to a variety of cell types.

**Table 1.1 T6SS effectors of pandemic El Tor *V. cholerae***

Effector	Target	Activity	Component
TseL	Prokaryotes	putative lipase	cargo
TseH	Prokaryotes	peptidoglycan degradation	cargo
VgrG-3	Prokaryotes	peptidoglycan degradation	structural
VgrG-1	Eukaryotes	actin crosslinking	structural
VasX	Eukaryotes & Prokaryotes	pore formation	cargo

### 1.5.2 The type VI secretions systems contributions to *Vibrio cholerae* biology and pathogenesis

*T6SS mediated bacterial competition:* Interactions between Gram-negative bacteria and the *V. cholerae* T6SS have two distinct outcomes. Either the target cell is effectively killed or the cell resists T6SS action via the synthesis of requisite immunity proteins. Gram-positive bacteria are naturally immune to T6SS killing, likely due to increased thickness of the cell wall(245). The ability of T6SS positive *V. cholerae* strains to coexist within the same niche is referred to as compatibility. Compatibility is dictated by the sequence of the effector immunity pairs found on the large cluster and the first two auxiliary clusters that encode the T6SS(246). Strains that are compatible, share the same immunity proteins, while those with divergencies are eliminated by T6SS competition. The ability of different strains to co-exist impacts the biology of *V. cholerae* in the environment and in the host. For instance, compatibility determines the ability of strains to acquire genetic elements through horizontal gene transfer. Accordingly, pandemic El Tor strains exist within the same compatibility group and as a result nearly all possess the element Virulence Pathogenicity Island I(246). This is consistent with experimentation demonstrating that *in vivo* plasmid

conjugation between *V. cholerae* strains is inhibited between T6SS positive and negative strains(247). Similarly, compatibility impacts niche occupation(239). The T6SS of most classical strains is disabled and it has been speculated that the emergence of a functional T6SS in El Tor strains contributes to El Tor dominance during the seventh pandemic(248). Compatibility also drives dominance within the host environment, as coinfection with different compatibility groups results in dominance by a single group(246).

*T6SS mediated virulence:* The T6SS of *V. cholerae* been studied in humans(249), mice(250), rabbits(251), and fish(252) for its interactions with eukaryotic host cells and antagonism towards intestinal symbionts(166). The T6SS is active *in vivo*(249, 251), and complements the virulence of *V. cholerae* through a number of different interactions. In the zebrafish model, the actin cross linking domain of the anti-eukaryotic effector VgrG-1 interacts with host tissue to expel intestinal symbionts via the engagement of peristaltic like contractions(252). VgrG-1 also enhances *V. cholerae* colonization in infant mice and provokes disease symptoms via actin cross linking in host cells and increased intestinal immune cell infiltrate(250). T6SS pathology in the infant mouse model also depends on interactions with intestinal symbionts. T6SS dependent elimination of symbiotic *E. coli* promotes *V. cholerae* colonization, exacerbates diarrheal disease, and significantly alters host transcriptional responses(166). Indeed, the T6SS contributes to intestinal disease through interactions with the microbiota and host tissue, forming a host-symbiont-pathogen triad that fundamentally impacts intestinal homeostasis. However, the effects of this triad on host viability, immunity, and intestinal regeneration have yet to be explored.

## 1.6 Study objectives

The digestive tract of metazoan life is in constant association with a diverse population of bacterial taxa that establish specific interactions with the host, ranging from symbiotic colonization to pathogenic invasion. The community of symbiotic bacteria that establish residency in the digestive system, along with various species of commensal yeast, protozoa, and viruses, form the intestinal microbiome. Millions of years of coexistence between host and microbe have established a symbiotic relationship whereby the presence of the microbiome contributes to aspects of host biology. For instance, the microbiota of mammals promotes the development of regulatory immune cells that appropriately dampen acute inflammatory responses to prevent chronic autoimmune disease(253). In insects, the microbiome is tied to many aspects of host fitness and immunity including fecundity(140), developmental rate(102, 105), lifespan(146), AMP production(111), and intestinal regeneration(18). However, the mechanisms by which

intestinal bacteria exert these physiological changes remain uncertain and more research is required to properly understand the effects of intestinal bacteria.

The data in this thesis consist of investigations of host microbe interactions and how these interactions affect mediators of intestinal homeostasis. The three data chapters explore interactions between host and symbiont, host and pathogen, and pathogen and symbiont, to understand the effects of gut bacteria on longevity, viability, and immunity.

1) Although the microbiome insulates the host against pathogenic microbes, flies that contain a full community of symbiotic bacteria have shortened lifespans relative to GF counterparts(113). Furthermore, the intestines of GF flies retain a regular intestinal organizational structure while age matched CR *Drosophila* accumulate miss-differentiated cells and show signs of compromised barrier integrity(95). Notably, data from species specific control of fly lifespan suggests that the presence of individual symbiotic strains are able to regulate host longevity(126). I hypothesize that certain members of the microbiome detract from host longevity via disruptions to mechanisms of intestinal homeostasis and will seek to determine the impact of long-term species-specific association with adult *Drosophila*.

2) Occupation of the intestinal niche by symbiotic microbes aids in host resistance to colonization by toxic bacteria. To compete with this bacterial barrier, enteric pathogens such as *V. cholerae*, encode a T6SS which mediates antagonistic interactions between the bacterium and adjacent cells(212). Although the T6SS of *V. cholerae* is active *in vivo*(249), the role of the T6SS in the pathogenesis of *Vibrio* remains unclear. I propose that antagonistic interactions mediated by the T6SS against intestinal symbionts or host epithelial tissue contributes to *V. cholerae* pathogenesis.

3) Intestinal pathogens and commensal bacteria trigger a series of host responses that restrain bacterial outgrowth and maintain homeostasis in the digestive tract(90). However, the impact of bacteria-bacteria interactions on host intestinal responses has yet to be thoroughly examined. I propose that interactions between intestinal symbionts and the enteric pathogen *V. cholerae* via the T6SS impact the intestinal response to pathogenic bacteria.



## Chapter 2.

### Materials and Methods

This chapter contains content from the following sources, republished with permission:

- Fast, D., Duggal, A., & Foley, E. Monoassociation with *Lactobacillus plantarum* disrupts intestinal homeostasis in adult *Drosophila melanogaster*. *MBio* 9, e01114-18 (2018).
- Fast, D., Kostiuk, B., Pukatzki, S., & Foley, E. Commensal pathogen competition impacts host viability. *Proc. Natl. Acad. Sci. U. S. A* 115, 7099-7104 (2018).
- Fast, D., Petkau, K., Ferguson, M., Shin, M., Galenza, A., Kostiuk, B., Pukatzki, S., & Foley, E. *Vibrio*-symbiont interaction inhibit intestinal repair in *Drosophila*. *Cell Reports*, 1088-1100.e5 (2020).

## 2.1 Drosophila husbandry

### 2.1.1 Drosophila stocks and handling

All fly stocks were maintained at either 18°C or 25°C on standard Bloomington cornmeal medium(254). Standard cornmeal medium: 225g agar, 2850g yellow cornmeal, 675g yeast, 390g soy flour, 3L light corn syrup, 39L water, and 188ml propionic acid. Fresh food was prepared weekly. All experimental flies were adult virgin females. Newly eclosed flies were maintained in an incubator with a 12hour light dark cycle. Fly lines used in this thesis are as follows:

**Table 2.1 Drosophila melanogaster stocks and strains**

Name	Genotype	Source
<i>w</i> <sup>1118</sup> (Wild-type)	<i>w</i> <sup>1118</sup> .	BSC(Stock#5905)
<i>esg</i> <sup>ts</sup> (8)	<i>w; esg-Gal4, tub-Gal80<sup>ts</sup>, UAS-GFP;</i>	Bruce Edgar
<i>imd</i> <sup>-/-</sup> (255, 256)	<i>y,w, P{EPgy2}imd<sup>EY08573</sup></i>	BSC(Stock#17474)
<i>CB&gt;mCD8::GFP</i> (45)	<i>w; upd2_CB-GAL4, UAS-mCD8:: GFP;</i>	Bruno Lemaitre
Oregon-R	wild type	BSC(Stock#25211)
<i>esg</i> <sup>ts</sup> >CFP, <i>Su(H)</i> -GFP (257)	<i>w; esg-Gal4, tub-Gal80<sup>ts</sup>, UAS-his2b::CFP, Su(H)-GFP;</i>	Lucy O'Brien
<i>GFP; FRT40A</i>	<i>y,w, hs-FLP, UAS-mCD8::GFP;neoFRT(40A)/CyO;</i>	Foley Lab
<i>FRT40A; GAL4</i>	<i>w; tubGAL80, neoFRT(40A); tubGAL4/MKRS</i>	Foley Lab

BSC (Bloomington Stock Centre)

Conditional expression of transgenes was performed with temperature sensitive control of the GAL/UAS expression system. GAL4 activation of the UAS gene was prevented by GAL80<sup>TS</sup> at 25°C. A temperature shift to 29°C inactivates GAL80<sup>TS</sup> and permits the expression of the transgene. Flies were raised at 18°C or 25°C and shifted to 29°C for 5 days prior to experimentation to restrict transgene expression to adults. Mitotic clones were generated with flies of the genotype *y, w, hs-FLP, UAS-mCD8::GFP; neoFRT(40A)/neoFRT(40A), tubGAL80; tubGAL4/+*. To obtain isogenic *imd* mutant flies, *y,w, P{EPgy2}imd<sup>EY08573</sup>* flies were backcrossed with *w*<sup>1118</sup> for ten generations.

### 2.1.2 Generation of germ free, axenic, and gnotobiotic Drosophila

*Antibiotics:* To make germ free flies by antibiotic treatment, freshly eclosed adult flies were raised for five days on autoclaved standard medium that was supplemented with an antibiotic solution just prior to pouring sufficiently cooled food into vials (100 g/ml ampicillin (Sigma BCBK5679V), 100 g/ml metronidazole (Sigma SLBG3633V), 50 g/ml vancomycin (Sigma 057M4022V) dissolved in 50% ethanol, and

100 g/ml neomycin (Sigma 071M0117V) dissolved in water) as described in(126). Conventionally reared counterparts were raised on autoclaved standard cornmeal medium.

*Sodium hypochlorite dechorionization:* To generate axenic flies, adult females were placed in acrylic cages and embryos were laid on apple juice plates over a 16-h period and subsequently collected. The following steps were performed in a sterile tissue culture hood. Embryos were rinsed from the plate with sterile phosphate-buffered saline (PBS). Embryos were placed in a 10% solution of household bleach (7.4% sodium hypochlorite)(Clorox 02408961) for 2.5 minutes, then placed into a fresh 10% bleach solution for 2.5 minutes, and then washed with 70% ethanol for 1 minute. Embryos were then rinsed 3 times with sterile water, placed onto sterile food, and maintained at 25°C in a sterilized incubator(91). Prior to infection symbiont association, or GF experimentation microbial elimination from adult flies was confirmed for every vial of axenic or germ-free flies by plating whole-fly homogenates on agar plates permissive for the growth of *Lactobacillus* and *Acetobacter*. Axenic flies were generated in parallel with conventionally reared counterparts that were placed in water at all steps.

*Gnotobiotic flies:* Virgin females were raised on antibiotic-supplemented fly food for 5 days at 25°C with 12/12 hour dark/ light cycles. On day 5 of antibiotic treatment, a fly from each vial was homogenized in MRS broth and plated on MRS and GYC agar plates to ensure eradication of the microbiome. For axenic flies, virgin females were collected and raised for 5 days at 25°C with 12/12 hour dark/ light cycles for 5 days on sterile food. Flies were starved in sterile empty vials for 2hours prior to bacterial association. For mono-associations, the optical density at 600 nm (OD600) of bacterial liquid culture was measured and then the culture was spun down and resuspended in 5% sucrose in PBS to a final OD600 of 50. For poly-associations, bacterial cultures of *A. pasteurianus*, *L. brevis*, and *L. plantarum* were prepared to an OD600 of 50 in 5% sucrose in PBS as described above. The bacterial cultures were then mixed at a 1:1:1 ratio. For longevity of gnotobiotic flies 22 flies/vial were associated with 1 ml of bacterial suspension on autoclaved cotton plugs (Fisher Scientific Canada, 14127106) in sterile fly vials. For infection of gnotobiotic flies with *V. cholerae*, 12flies/vial were associated with 1 ml of bacterial suspension on autoclaved cotton plugs. For all gnotobiotic associations, flies were fed the bacteria-sucrose mixture for 16hours at 25°C and then flipped onto autoclaved food. Conventionally reared control flies were given mock associations of 1 ml of 5% sucrose in sterile PBS for 16 h at 25°C. To ensure bacterial association, a sample fly from every vial was homogenized in MRS broth and plated on MRS periodically throughout adult lifespan studies (Fig. 3.1 – 3.6) or 1 day prior to infection with *V. cholerae* (Fig. 4.5 & 5.10).

### 2.1.3 Measure of adult Lifespan

For analysis of adult lifespan, 100 flies per group were collected at 22 flies/ vial over a 2-3 day period. Once the required number of flies had been collected and microbial association / GF treatment had been completed, flies were flipped to new food and standardized to 20 flies per vial. Flies were flipped to new food every Monday, Wednesday, Friday, and dead flies were quantified before each passage. Survival curves were evaluated in Graph Pad Prism (Version 7.0a) by Log-rank (Mantel-Cox) test

## 2.2 Bacterial Culture and Assays

### 2.2.1 Bacterial strains and culture conditions

Table 2.2 Bacterial stocks and strains

Species	Strain	Abbreviation	Source
<b>Symbiont</b>			
<i>Lactobacillus plantarum</i> (258)	KP	<i>L. plantarum</i>	Foley Lab w <sup>1118</sup> flies
<i>Lactobacillus brevis</i> (258)	EF	<i>L. brevis</i>	Foley Lab w <sup>1118</sup> flies
<i>Acetobacter pasteurianus</i> (258)	AD	<i>A. pasteurianus</i>	Foley Lab w <sup>1118</sup> flies
<i>Lactobacillus plantarum</i> (258) isofemale	DF	<i>L. plantarum</i>	wild <i>Drosophila</i>
<b>Pathogens</b>			
<i>Erwinia carotovora carotovora</i> 15(259)	isolate 15	<i>Ecc15</i>	Nicolas Buchon
<i>Vibrio cholerae</i> (212)	C6706	<i>V. cholerae</i>	Stefan Pukatzki
<i>Vibrio cholerae</i> (212)	C6706Δ <i>vsk</i>	<i>V. cholerae</i>	Stefan Pukatzki
<i>Vibrio cholerae</i> (260)	C6706Δ <i>vipA</i>	<i>V. cholerae</i>	Stefan Pukatzki
<i>Vibrio cholerae</i> (261)	O395	<i>V. cholerae</i>	Stefan Pukatzki
<b>Other</b>			
<i>Escherichia coli</i> K12	MG1655	<i>E. coli</i>	Stefan Pukatzki

*Lactobacillus plantarum* KP (DDBJ/EMBL/GenBank chromosome 1 accession CP013749 and plasmids 1-3 for accession numbers CP013750, CP013751, and CP013752, respectively), *Lactobacillus brevis* EF (DDBJ/EMBL/GeneBank accession LPXV000000000), *Acetobacter pasteurianus* AD (DDBJ/EMBL/GeneBank accession LPWU000000000), and *Lactobacillus plantarum* DF (DDBJ/EMBL/GenBank

chromosome 1 accession CP013753 and plasmids 1-3 accession numbers CP013754, CP013755, and CP013756, respectively).

*Lactobacillus plantarum* was streaked from a glycerol stock onto MRS agar plates and grown at 29°C for 48hours. Single colony isolates were inoculated into MRS broth and grown at 29°C for 24hours. *Lactobacillus brevis* was streaked from glycerol a stock onto MRS agar plates and grown at 29°C for 48hours. Single colony isolates were inoculated into MRS broth and grown at 29°C for 48hours with shaking. *Acetobacter pasteurianus* was streaked from glycerol a stock onto MRS or GYC agar plates and grown at 29°C for 72hours. Single colony isolates were inoculated into MRS broth and grown at 29°C for 48hours with shaking. *Vibrio cholerae* C6706, C6706 $\Delta$ vasK, C6706 $\Delta$ vipA, and O395 have previously been described(212, 260). *Vibrio* strains were grown in Lysogeny Broth (LB) (1% tryptone, 0.5% yeast extract, 0.5% NaCl) at 37°C with shaking in the presence of 100  $\mu$ g/ml streptomycin. *Erwinia carotovora carotovora*15(259) was grown in LB (Difco Luria Broth Base, Miller. BD, DF0414-07-3) medium at 29°C with shaking for 24hours. Specific details and procedures are indicated below.

### 2.2.2 Colony forming units per fly

At indicated time points, 25 flies were collected from an indicated group and placed into successive solutions of 20% bleach, distilled water, 70% ethanol, and distilled water to surface sterilize and rinse flies, respectively. These 25 flies were then randomly divided into groups of 5 and mechanically homogenized in 500 $\mu$ l of MRS broth for evaluation of symbionts or in LB for quantification of *V. cholerae*. The fly homogenate was then serially diluted in a 96-well plate, and 10 $\mu$ l spots were plated onto prewarmed MRS/GYC agar to select for *Lactobacillus* and *Acetobacter* or LB plates in the presence of 100  $\mu$ g/ml streptomycin for *V. cholerae*. Plates were prewarmed inside a 37°C incubator with lids ajar for 1hour. MRS/GYC plates for bacterial growth were incubated for 2 days at 29°C and LB plates were incubated for 16hours at 37°C for bacterial growth. Following incubation, the number of colonies per bacterial species was counted under a dissecting scope. *L. plantarum* colonies were identified on MRS agar as round, solid white, opaque colonies that grew to easily visible colonies after 2 days at 29°C. *L. brevis* colonies were identified as large, round, irregular-edged colonies on MRS agar with an off-white center fading to translucence at the edges of the colony that grew to easily visible colonies in 2 days at 29°C. *A. pasteurianus* colonies were identified on MRS and GYC agar as small, round, beige, translucent colonies that grew to visually identifiable colonies after 3 days at 29°C and began to clear calcium carbonate from the GYC plate in 4 days. *V. cholerae* colonies were identified as circular, flat, undulate, transparent colonies identifiable

as colonies after 12 hours at 37°C. Colonies were then counted by hand under a dissecting microscope and a felt tipped pen was used to mark the lid of the petri dish indicating a counted colony.

### 2.2.3 Oral infection

All infections in this thesis were administered orally. Virgin female flies were separated from male flies after eclosion and placed on autoclaved standard Bloomington food for 5 days at 29°C without flipping. Flies were starved for 2 hours prior to infection. For *Vibrio* infections, *V. cholerae* was grown on LB plates (1% tryptone, 0.5% yeast extract, 0.5% NaCl, 1.5% agar) at 37°C in the presence of 100 µg/ml streptomycin (Sigma SLBK5521V). Colonies were removed from the plate and suspended in LB broth and diluted to a final OD600 of 0.125. For each infection group, groups of 10-12 flies were placed in vials containing one third of a cotton plug soaked with 3ml of sterile LB (Mock) or with LB containing *V. cholerae*. For infection with *Erwinia*, *Ecc15* was grown in medium at 29°C with shaking for 24hours and gathered by centrifugation. The pellet was then re-suspended in the residual LB, and 1ml of the suspension was pipetted onto a thin slice of a cotton plug at the bottom of a sterile fly vial. Flies were kept on their respective infections for the duration of all experiments. For survival analysis, 10 flies per vial for a total of 50 flies per infection group were continuously fed *V. cholerae* and dead flies were counted every 8 h for the first 100hours, and every 24hours thereafter.

### 2.2.4 T6SS competition assay

*V. cholerae* V52 or V52Δ*vasK* were grown overnight in LB without antibiotic supplementation. The commensal (prey) bacteria were grown as described above. Predator and prey bacteria were then mixed at a 1:1 ratio and a 25µl aliquot was spotted on a on a pre-warmed LB agar plates. After a 2hour incubation at 37°C, bacteria were harvested in 1ml of LB and vortexed for 30 seconds. The harvested liquid was then serially diluted and plated onto GYC/MRS/LB agar plates to enumerate surviving bacteria. Colony-forming units were then counted as previously described in 2.2.2.

### 2.2.5 Fly defecation and bacterial shedding assays

*Quantification of fly defecation:* Adult flies were infected as described in 2.2.3, with the addition of Erioglaucline disodium salt (0.1%) to the infection media to visualize fly defecation marks. After 24 hours of infection, flies were placed in a petri dish lined with filter paper. The number of fecal marks (blue spots) was counted every hour four 4 hours. After 4 hours flies were anesthetized, and the filter paper was

removed. The filter paper was imaged, and the size of the spots was calculated with CellProfiler (3.0.0, Broad Institute) by Dr. Steven Ogg at the University of Alberta Imaging Core.

*Shedding of V. cholerae:* Following a 24hour infection, individual flies were placed in a 96 well plate where each well had been lined with filter paper soaked in PBS + 5% sucrose. After 4 hours, individual filter papers were removed and vortexed vigorously for 30 seconds in 1mL of sterile LB. The LB was then serially diluted on LB + 100 µg/ml streptomycin and incubated for 16hours at 37°C. Following incubation, colonies were enumerated.

## **2.3 Molecular biology and gut related assays**

### **2.3.1 Immunofluorescence and confocal microscopy**

Flies were washed in a 9 well galls plates (corning, 7220-85) with 95% ethanol and then submerged in PBS for dissection. The abdomen was separated from the thorax and the genitalia was removed with dissection scissors. Using forceps, the gut was carefully excised from the abdomen and the malpighian tubules were removed. The dissected gut was then stored in ice cold PBS until fixation. Guts were fixed for 1hour at room temperature in 8% formaldehyde in PBS. Guts were rinsed in PBS for 20 minutes at room temperature and blocked overnight in PBT + 3% bovine serum albumin (BSA) (Sigma-Aldrich A3059-10G) (PBS, 0.2% Triton-X) at 4°C. Guts were stained overnight at 4°C in PBT + 3% BSA with appropriate primary antibodies (Listed in table 2.3), washed with PBT and stained for 1 hour at room temperature with appropriate secondary antibodies. Guts were rinsed with PBT and then stained with DNA dye for 10 minutes at room temperature. Guts were then rinsed in PBT and a final wash in PBS. Guts were mounted on slides in Fluoromount (Sigma-Aldrich F4680), and R4/R5 region of the posterior midgut was visualized.

For sagittal sections, the posterior midgut was excised from dissected whole guts and imbedded in clear frozen section compound (VWR, 95057-838). Guts were cryosectioned in 10µm sections at the Alberta Diabetes Institute Histocore at the University of Alberta. Sectioned guts were fixed in 4% formaldehyde for 20 minutes at room temperature, rinsed with PBS, and then blocked overnight at 4°C in 5% normal goat serum, 1% BSA, and 0.1% tween-20. Sections were rinsed in 1% BSA and 0.1% tween-20, and then stained for 1 hour at room temperature with primary antibodies in blocking buffer. Samples were rinsed with blocking buffer and then stained for 1 hour at room temperature with appropriate secondary antibodies and nuclear stain, followed by a final rinse in blocking buffer.

**Table 2.3 Antibodies and dyes****Primary Antibodies**

Target	Species	Type	Concentration	Source
Armadillo	mouse	monoclonal	1:200	DSHB N2 7A1
GFP	rabbit	monoclonal	1:1000	ThermoFisher G10362
Myospheroid	mouse	monoclonal	1:100	DSHB cf.6g11
Phospho-Histone H3	rabbit	polyclonal	1:1000	Milipore Sigma 06-570
Prospero	mouse	monoclonal	1:200	DSHB MR1A

continued...

**Secondary Antibodies and dyes**

Antibody	Fluorophore	Concentration	Source
Goat anti-rabbit IgG	Alexa Fluor 488	1:1000	ThermoFisher A-11008
Goat anti-mouse IgG	Alexa Fluor 568	1:1000	ThermoFisher A-11004
Goat anti-mouse IgG	Alexa Fluor 647	1:1000	ThermoFisher A32728
DRAQ5		1:500	ThermoFisher 62251
Hoechst 33258		1:500	ThermoFisher H3569

DSHB: Developmental Studies Hybridoma Bank

For all intestinal immunofluorescence, guts were visualized with an Olympus IX-81 microscope with a Yokagawa CSU 10 spinning disk confocal scan head. Images were captured with a Hamamatsu EMCCD (C9100-13) camera, while sample acquisition was accomplished with Perkin Elmer's Volocity software. Guts were imaged in the Z plane with an ASI MS-2000 motorised XY stage with a piezo Z insert for 100µm travel. Fluorophores were excited as follows: 405nm for Hoechst and CFP, 488nm for GFP or Alexa Fluor 488, 561nm for Alexa Fluor 568, 652nm for Alexa Fluor 647 and DRAQ5.

**2.3.2 Transmission electron microscopy**

Flies were washed with 95% ethanol and dissected into ice cold PBS as described in 2.3.1. The posterior midguts were immediately excised and placed into fixative (3% paraformaldehyde plus 3% glutaraldehyde, 0.1M Sucrose and 0.1CB). Fixation preparation, contrasting sectioning, sectioning, and visualization were performed at the Faculty of Medicine and Dentistry Imaging Core at the University of Alberta. The midgut sections of 2 separate flies per treatment were visualized with a Hitachi H-7650 transmission electron microscope at 60 kV in high-contrast mode.



### 2.3.3 Reverse Transcription and quantitative real time polymerase chain reaction

The reverse transcription PCR and quantitative real-time PCR protocol used in this study have been described previously(262). RT-PCR was performed on the dissected guts of adult *Drosophila*. Five biological replicates consisting of five guts per replicate were measured in technical triplicate. Guts were dissected and immediately placed into TRizol. The tissue was homogenized and total RNA was isolated using a TRizol-chloroform extraction procedure according to the manufacturer's recommendations. Purified total RNA was treated with DNase I to eliminate DNA contamination. cDNA was generated from 5µg of RNA using BIO-RAD iScript cDNA Synthesis Kit as described in the manufacturer's guidelines. cDNA was synthesized with an Eppendorf Mastercycler thermocycler with the following program 25°C for 5min, 42°C for 30min, 85°C for 5min.

Transcript analysis was performed using the reverse transcribed cDNA. Prepared qRT-PCR mixtures consisted of 2.5µl cDNA, 7.5µl master mix (2.5µl of a 1.6µM primer mix and 5.0µl of PerfeCTa SYBR Green SuperMix(Quantabio 023917). Eppendorf twin.tec real-time PCR 96well PCR plates were sealed with Eppendorf heat sealing film, vortexed, and briefly centrifuged. Transcripts were amplified and monitored with an Eppendorf realplex<sup>2</sup> PCR machine with the following program: 95°C for 10min followed by a 40x repeat of 95°C for 15seconds, 60°C for 1min. Melting curve analysis was also performed. Primers used in this thesis are as follows: *actin* forward 5'-TGCCTCATCGCCGACATAA-3' and *actin* reverse 5'-CACGTCACCAGGGCGTAAT-3'; *spitz* forward 5'-TACCAGGCATCGAAGCTTTC-3', *spitz* reverse 5'-GACCCAGGCTCCAGTCACTA-3'; and *rhomboid* forward 5'-GGATATCGGCCTGCTGAA-3', *rhomboid* reverse 5'-CGGAATCGGAACGGGTAG-3'. Expression values were normalized to actin and quantified using the  $\Delta\Delta C_T$  method.

### 2.3.4 Quantification of clones and cells per gut area.

Mounted whole guts were loaded on a spinning disk confocal microscope (described in 2.3.1) for visualization. The R4-R5 region of the posterior midgut of each sample was located by identifying the midgut hindgut transition and moving 1-2 frames anterior from the attachment site of the malpighian tubules. The top and bottom of the intestine were located and marked. Guts were then imaged as z-slices through the depth of the entire tissue. Images were acquired using Velocity software. All intestines damaged by the dissection process were excluded from quantification. The collected z-slices were split into individual fluorescent channels and compressed into single images with Fiji software (263). To quantify clones, cells per clones, and *esg+* / *Su(H)+* cells, compressed images spanning the width of the intestine

were inverted and cells were counted manually by marking each cell with a colored dot using the brush tool. In cases where multiple cells were in close proximity to one another, the nuclear channel was used to identify the number of nuclei present within the cluster. Area of the gut was measured by tracing the intestinal outline in the nuclear channel. The outlined area was then measured with the measure analysis tool in Fiji, as outlined previously(43). Quantification of cells from Fig. 5.1 and 5.8 were reanalyzed in a double-blinded study to confirm the findings. Ph3 positive cells were quantified by with a manual scan of the indicated area through the eye piece of the an Olympus IX-81 microscope. Ph3 positive cells were identified by bright fluorescence and counted with a FisherScientific laboratory counter.

### **2.3.5 Quantification of gut length**

The guts of aged flies were dissected and immediately mounted on slides. Length was measured with an eyepiece micrometer (Motic B1-220 series system microscopes) at 4X magnification (Motic 4/0.10 160/0.17 lens) by tracing from posterior of the proventriculus along the midgut to just anterior of the midgut-hindgut junction (identified by the branching of the Malpighian tubules).

### **2.3.6 Progenitor cell isolation and RNA extraction**

IPC isolation by fluorescence activated cell sorting (FACS) was adapted from(264). In brief, three biological replicates consisting of 100 fly guts per replicate with the malpighian tubules and crop removed were dissected into diethyl pyrocarbonate (DEPC) PBS and placed on ice. Guts were dissociated with 1mg/ml of elastase at 27°C with gentle shaking and periodic pipetting for 1hour. IPCs were sorted based on GFP fluorescence and size with a BD FACSAria IIIu. All small GFP positive cells were collected into a tube containing DEPC PBS. Cells were pelleted at 500G for 20 minutes and then resuspended in 500µl of Trizol (ThermoFisher 155596026). Samples were stored at -80°C until all samples from each group were collected. RNA was isolated via a standard Trizol chloroform extraction. Purified RNA was sent on dry ice to the Lunenfeld-Tanenbaum Research Institute (Toronto, Canada) for library construction and sequencing. The sample quality was evaluated using Agilent Bioanalyzer 2100. TaKaRa SMART-Seq v4 Ultra Low Input RNA Kit for Sequencing was used to prepare full length cDNA. The quality and quantity of the purified cDNA was measure with Bioanalyzer and Qubit 2.0. Libraries were sequenced on the Illumina HiSeq3000 platform. For RNA-sequencing of whole guts, RNA was extracted in biological triplicate consisting of 10 dissected whole guts per replicate. RNA was purified by standard TRIZOL chloroform protocol. Purified RNA was sent on dry ice to Novogene (California, USA) for poly-A pulling, library construction and sequencing with

Illumina Platform PE150 (NOVaseq 600). The sample quality was evaluated before and after library construction using an Agilent Bioanalyzer 2100.

## 2.4 Bioinformatic analysis

### 2.4.1 Microarray data comparison

Comparisons were performed on genes previously characterized as microbe responsive in the intestines of adult *Drosophila*(41, 43). For this study, we defined genes with greater than 1.5-fold expression changes as differentially regulated. We then used PANTHER(265) to identify gene ontology terms with a minimum of five genes that were enriched in the respective groups. Metadata are available in Data Set S1 in the supplemental material from(266).

### 2.4.2 RNA-seq read processing, alignment, differential expression, and GO analysis

For RNAseq studies, we obtained on average 30 million reads per biological replicate. We used FASTQC (<https://www.bioinformatics.babraham.ac.uk/projects/fastqc/>, version 0.11.3) to evaluate the quality of raw, paired-end reads, and trimmed adaptors and reads of less than 36 base pairs in length from the raw reads using Trimmomatic (version 0.36)(267). HISAT2 ((version 2.1.0)(268) was used to align reads to the *Drosophila* transcriptome- bdgp6 (<https://ccb.jhu.edu/software/hisat2/index.shtml>), and converted the resulting BAM files to SAM files using Samtools (version 1.8) (269). Converted files were counted with Rsubread (version 1.24.2) (270) and loaded into EdgeR(271, 272). In EdgeR, genes with counts less than 1 count per million were filtered and libraries normalized for size. Normalized libraries were used to call genes that were differentially expressed among treatments. For IPC RNA-seq, genes with P-value < 0.05 were defined as differentially expressed genes. For whole gut RNA-seq, Genes with P-value < 0.01 and FDR < 0.01 were defined as differentially expressed genes Principle component analysis was performed on normalized libraries using Factoextra (version 1.0.5)(273), and Gene Ontology enrichment anaLysis and visualiZAtion tool (GORilla) was used to determine Gene Ontology (GO) term enrichment (274). Specifically, differentially expressed genes were compared in a two-list unranked comparison to all genes output from edgeR as a background set. Redundant GO terms were removed.

## **2.5 Statistical analysis and figure construction**

### **2.5.1 Statistical analysis and data visualization**

In chapters 3 and 4, all graphs and plots were constructed using Prism 7 (version 7.0a) for Mac. All statistics were performed using the same program. In chapter 5, all graphs, plots, Venn diagrams, and GO-term lists were constructed using R (version 3.5.1) via R-studio (version 1.1.463) with ggplot2 (version 3.1.1). All statistical analysis was completed with R. Normality of data was determined by Bartlett test for equal variances. For normal data, one-way Analysis of Variance (ANOVA) was used to determine overall statistical difference and a Tukey's test for Honest Significant Differences was used for multiple comparisons. For non-normal data, a Kruskal-Wallis test was used to determine overall statistical difference and pairwise Willcoxon tests with a Bonferroni correction for multiple comparisons was used for multiple comparisons. Details of the specific test used for each data panel can be found in the table below each panel. Statistical significance was set at  $p \leq 0.05$ . For the entire thesis, all figures were assembled using Adobe Illustrator.

### **2.5.2 Data availability**

Gene expression data from chapter 5 has been deposited to the NCBI GEO database (GSE136069).

### Chapter 3.

#### Monoassociation with *Lactobacillus plantarum* disrupts intestinal homeostasis in adult *Drosophila melanogaster*.

This chapter contains content from the following source, republished with permission:

- Fast, D., Duggal, A. & Foley, E. Monoassociation with *Lactobacillus plantarum* disrupts intestinal homeostasis in adult *Drosophila melanogaster*. *MBio* 9, e01114-18 (2018).

Experiments shown in Figure 3.1-3.6 were performed by D.F and A.D and conceived and analyzed by D.F and E.F.

### 3.1 Introduction

Under homeostatic conditions, intestinal microbes contribute to a complex network of metabolic, immune, and growth events that support host fitness. In *Drosophila*, the microbiome sustains systemic growth upon nutritional deprivation(105), improves resistance to enteric challenge(110), and stimulates the regeneration of intestinal tissue(18). However, flies with a full contingent of intestinal bacteria have reduced lifespans relative to GF counterparts(113, 146, 275), suggesting that microbial colonization has a cost. To test if individual symbiotic species contribute to age dependent death of adult *Drosophila*, we investigated the impact of common fly commensals on adult longevity. We found that mono-association with *L. plantarum*, a symbiont identified in populations of wild and lab reared *Drosophila*(87, 258), curtails GF fly lifespan extension. Elimination of the fly microbiome reduces IPC turnover, slows age dependent tissue disorganization, and extends adult longevity. Contrary to our expectations, *L. plantarum* control of adult lifespan was independent of tissue aging. Instead we found that guts monocolonized by *L. plantarum* were characterized by a loss of IPCs, impaired intestinal regeneration, and a gradual erosion of epithelial ultrastructure. Combined, our data demonstrate that long term association of adult *Drosophila* with *L. plantarum* abrades intestinal homeostasis and shortens host lifespan.

## 3.2 Results

### 3.2.1 *Lactobacillus plantarum* outcompetes *Lactobacillus brevis* for association with adult *Drosophila*

Our lab strains of *Drosophila melanogaster* predominantly associate with *L. plantarum*, *L. brevis*, and *A. pasteurianus*(258). Of those strains, *Lactobacilli*, particularly *L. plantarum*, are the dominant symbionts, typically accounting for >75% of all bacterial OTUs in flies that we raise on standard cornmeal medium. As fly symbionts regularly cycle from the intestine to the food(110, 117, 276), we conducted a longitudinal study of the association of *L. plantarum* and *L. brevis* with cultures of virgin female WT *Drosophila*. For this work, we fed freshly emerged adult flies an antibiotic cocktail to eliminate the endogenous bacterial microbiome(126, 146). We then fed antibiotic-treated adult flies equal doses of *L. plantarum* or *L. brevis* for 16 hours, transferred flies to fresh food, and determined bacterial titers in the intestine and on the food at regular intervals thereafter (Fig. 3.1A).

We typically found less than  $1 \times 10^4$  CFU per fly gut 5 days after inoculation with either *L. plantarum* or *L. brevis* (Fig. 3.1B and D). In both cases, intestinal bacterial loads increased over time. However, the effect was more pronounced for *L. plantarum* than *L. brevis*. We detected a mean  $4 \times 10^3$ -fold change in numbers of *L. plantarum* associated with the fly gut between days 16 and 26, rising to approximately  $1 \times 10^7$  CFU per fly gut by day 26. In contrast, we observed only a 2.5-fold increase in *L. brevis* gut association over the same time, yielding less than  $1 \times 10^5$  CFU per fly gut. Likewise, we found that the *L. plantarum* load steadily increased in the food over time (Fig. 3.1C), while the association of *L. brevis* with food remained relatively constant (Fig. 3.1E). These observations suggest that *L. plantarum* has a growth advantage over *L. brevis* when cocultured on fly food with adult *Drosophila*. To determine if *L. plantarum* outcompetes *L. brevis* for association with *Drosophila*, we fed GF adult flies a 1:1:1 mixed culture of *L. plantarum*, *L. brevis*, and *A. pasteurianus* and monitored bacterial association rates over time. We added *A. pasteurianus* to the culture in this experiment to more accurately represent the microbiome of our conventional lab flies. Of this defined bacterial community, we found that *L. plantarum* and *A. pasteurianus* populated the fly intestine (Fig. 3.1F) and food (Fig. 3.1G) with near-equal efficiency. In both cases, the microbial load associated with the gut or food increased over time, reaching approximately  $1 \times 10^6$  CFU per intestine 36 days after inoculation. Intestinal association by *L. plantarum* was an order of magnitude higher in monoassociated flies (Fig. 3.1B) than in polyassociated flies (Fig. 3.1F), suggesting that *A. pasteurianus* partially limits host association with *L. plantarum*. In contrast to *L. plantarum* and *A. pasteurianus*, we found that *L. brevis* gradually disappeared from the food and the intestines of polyassociated adult flies over time (Fig. 3.1F and G). By 36 days, we repeatedly failed to detect *L. brevis* in the intestine or food. Combined, these observations suggest that the *L. plantarum* and *A. pasteurianus* strains used in this study are more

effective at forming persistent, long-term associations with *Drosophila* than the *L. brevis* strain and may explain the predominance of *L. plantarum* and *A. pasteurianus* in fly cultures. However, given the differences in bacterial load on the food, we cannot exclude the possibility that microbial competition on the food increases the availability of a particular species such that it is more likely to be consumed and thereby contribute to enhanced *in vivo* populations.

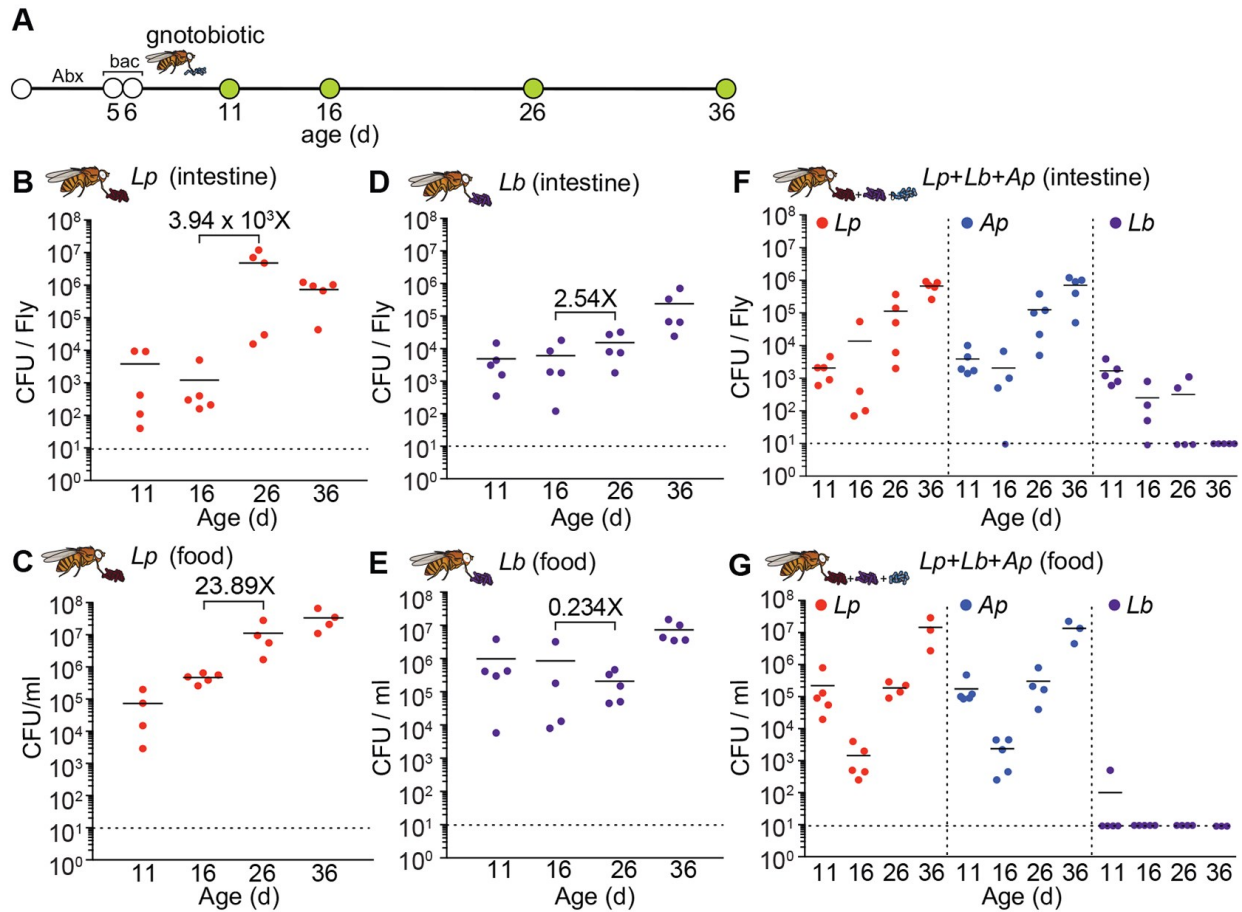


**Figure 3.1.** *L. plantarum* outcompetes *L. brevis* in the adult gut. **(A)** Schematic representation of the experimental timeline and generation of gnotobiotic adult flies. “Abx” indicates duration of antibiotic treatment, and “bac” indicates duration of bacterial feeding. **(B to E)** CFU per fly of *L. plantarum* (*Lp*) and *L. brevis* (*Lb*) in the intestines **(B and D)** and on the food **(C and E)** of *L. plantarum*-monoassociated and *L. brevis*-monoassociated adult flies, respectively, at days 11, 16, 26, and 36 of age. **(F and G)** CFU per fly of *L. plantarum*, *L. brevis*, and *A. pasteurianus* (*Ap*) in the intestines **(F)** and on the food **(G)** of *L. plantarum*-*L. brevis*-*A. pasteurianus*-polyassociated adult flies. Black numbers on graphs denote fold change in the mean between indicated time points.



### 3.2.2 Host genetic background influences transcriptional responses to intestinal microbes

As *L. plantarum* and *A. pasteurianus* form long-term associations with adult *Drosophila*, we tested the effects of the respective strains on adult longevity. This experiment requires the generation of GF flies that we subsequently associated with defined bacterial cultures. For the data in Fig. 3.1, we generated GF adult flies by supplementing the food with antibiotics. In an alternative method, investigators incubate embryos in a bleach solution that removes all associated microbes and establishes an axenic organism that develops in the absence of symbiotic bacteria(91). To determine if the respective methods have distinct impacts on transcription in the gut, we compared microarray data on microbe-dependent gene expression in GF flies derived from bleached embryos or from antibiotic-treated adults. Specifically, we compared microbe-dependent transcriptional changes in the intestines of Oregon R and Canton S flies derived from bleached embryos(41) to microbial responses in the intestines of *w*; *esgGAL4*, *GAL80ts*, *UAS-GFP* (*esg<sup>ts</sup>*) antibiotic-treated adults(43). The *esg<sup>ts</sup>* genotype is a variant of the *Drosophila* TARGET system(277) and is commonly used for temperature-dependent expression of upstream activation sequence (UAS)-bearing transgenes in green fluorescent protein (GFP)-marked ISCs and enteroblasts, collectively referred to as intestinal progenitor cells (IPCs)(18, 255). For this study, we used PANTHER to identify gene ontology (GO) terms that were significantly enriched in CR fly intestines relative to GF guts for all three fly lines.

In this comparison, we did not detect clear distinctions between the effects of bleach and antibiotics on transcriptional outputs from the gut (Fig. 3.2A and B). In each case, removal of the microbiome altered the expression of immune response genes (Fig. 3.2B), a result that matches earlier data linking gut bacteria and intestinal immunity(41).

Further analysis suggested that changes in microbe-dependent gene expression were influenced to a greater extent by fly genotype rather than by the method used to ablate the microbiome. For example, of the remaining microbe-responsive GO terms, we noticed a more pronounced similarity between bleached Oregon R flies and antibiotic-treated *esg<sup>ts</sup>* flies. Of the 21 processes affected by bleach treatment of Oregon-R cultures, 10 were similarly affected by antibiotic treatment of *esg<sup>ts</sup>* flies (Fig. 3.2A and B). In contrast, removal of the microbiome with bleach had a mild effect on gut transcription in Canton S flies. In this case, bleach affected only five GO terms, three of which are unique to Canton S (Fig. 3.2A and B). As a caveat to these interpretations, we note that uncontrolled variables such as differences between the microbiomes of the respective CR flies may impact the differences noted in these comparisons. Nonetheless, these results suggest that host genetic background contributes to the effects of the microbiome on intestinal gene expression.

### 3.2.3 Monoassociation with *L. plantarum* shortens adult longevity relative to germ free counterparts

We then asked if the method of bacterial elimination influences host survival after reassociation with symbiotic bacteria. For this assay, we prepared GF adults from bleached eggs or from CR adults raised on antibiotic-treated food and measured the longevity of flies associated with one of two common fly symbionts. Specifically, we inoculated the respective GF adult flies with *A. pasteurianus* or *L. plantarum* and measured their lifespans relative to CR counterparts. Irrespective of the means used to generate GF flies, we found that *L. plantarum* significantly shortened the lifespan of adult *Drosophila* (Fig. 3.2C and E). These observations match recent reports that GF adults outlive flies monoassociated with *L. plantarum* strains(140, 278). In addition, we found that flies associated with either the *L. plantarum* DF strain isolated from a wild *Drosophila melanogaster* fly(258) or the *L. plantarum* 39 strain, isolated from pickled cabbage(279), also have shorter lifespans than GF controls (Fig. 3.2J). Combined, we found that monoassociation with *Lp* shortened fly lifespan relative to GF *Drosophila* across four independent experiments. Together, these data indicate that monoassociation of adults with *L. plantarum* reverses the lifespan extension afforded by ablation of the microbiome. In contrast, monoassociation of adult *Drosophila* with *A. pasteurianus* had no effect on adult lifespan, regardless of the method used to generate GF flies (Fig. 3.2D and F). As *A. pasteurianus* attenuates gut colonization by *L. plantarum* (Fig. 3.1F) and *A. pasteurianus* does not affect adult lifespan, we tested if *A. pasteurianus* attenuates the impacts of *L. plantarum* on GF lifespan extension. For these assays, we measured the lifespans of GF adults that we cultured with different ratios of *A. pasteurianus* and *L. plantarum*. Here, we observed a clear relationship between *A. pasteurianus* *L. plantarum* input ratios and adult lifespan—the greater the ratio of *A. pasteurianus* to *L. plantarum*, the longer the lifespan of coassociated flies (Fig. 3.2G to I). Together, these data argue that monoassociation with *L. plantarum* reverts the lifespan extension observed in GF flies.

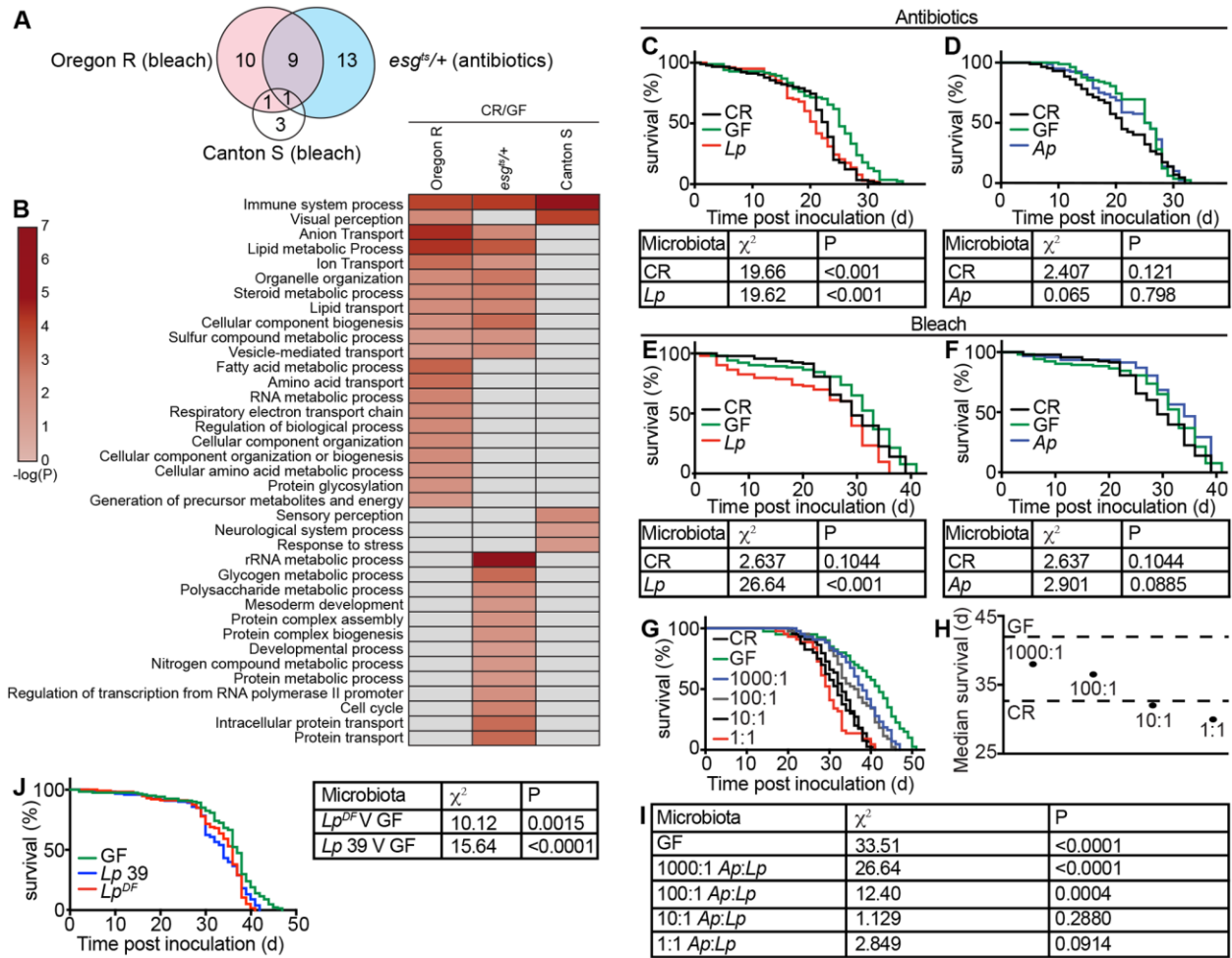


**Figure 3.2. Monoassociation with symbiotic *L. plantarum* reduces GF adult fly lifespan.** (A and B) Microbe-dependent gene expression microarray data from the intestines of Oregon-R and Canton S flies from bleached embryos(41) and from the intestines of *esg[ts]* antibiotic-treated adults(43). The heat map (B) shows gene ontology terms that were significantly enriched in the respective groups, and the Venn diagram (A) shows overlapping gene ontology terms between each group. (C) Survival curve of conventionally reared (CR), germ free (GF), and *L. plantarum*-monoassociated (*Lp*) adult flies from GF adults generated with antibiotics. (D) Survival curve of CR, GF, and *A. pasteurianus*-monoassociated (*Ap*) adult flies from GF adults generated with antibiotics. (E) Survival curve of CR, GF, and *L. plantarum*-monoassociated adult flies generated from bleached embryos. (F) Survival curve of CR, GF, and *A. pasteurianus*-monoassociated adult flies generated from bleached embryos. (G) Survival curves of CR and GF flies and flies coassociated with *A. pasteurianus*/*L. plantarum* at indicated ratios. For each graph (C to G and J), the y axis represents percent survival and the x axis represents time post-bacterial inoculation. (H) Median survival from data represented in panel G. Dashed lines show median survival times for GF and CR flies. (I) Comparisons of survival data for the indicated treatment groups relative to CR flies. (J) Survival curve of monoassociated adult flies associated with one of two different strains of *L. plantarum* (*L. plantarum* DF or *L. plantarum* 39) and comparisons of survival data for GF flies versus flies associated with the indicated *L. plantarum* strains. All  $\chi^2$  and P values are relative to GF flies. Tables are results of log rank (Mantel-Cox) test for panel data.

### 3.2.4 *L. plantarum* does not activate proliferative responses in the host intestine

Symbiotic bacteria provide mitogenic cues that accelerate the growth and aging of intestinal tissues(18), a factor associated with host longevity(67). This prompted us to test if *L. plantarum* activates ISC division. Initially, we quantified expression of the EGF ligand *spitz* and the *spitz*-activating endopeptidase *rhuboid* in dissected intestines. We selected the EGF pathway for this study as EGF activates ISC proliferation in response to symbiotic bacteria(18) and damage to the intestinal epithelium(60). Consistent with a relationship between gut bacteria and ISC proliferation, we detected significantly higher levels of *spitz* (Fig. 3.3B) and *rhuboid* (Fig. 3.3C) in CR flies than in GF counterparts. In contrast, we did not observe expression of EGF pathway activators in the intestines of flies associated with *L. plantarum* (Fig. 3.3B and C). Instead, we found that *spitz* was expressed at significantly lower levels in the midguts of *L. plantarum*-monoassociated flies than in GF flies 15 days after association (Fig. 3.3B). These data suggest that monocolonization of the adult intestine with *L. plantarum* fails to activate EGF-dependent proliferative responses in the host intestine.

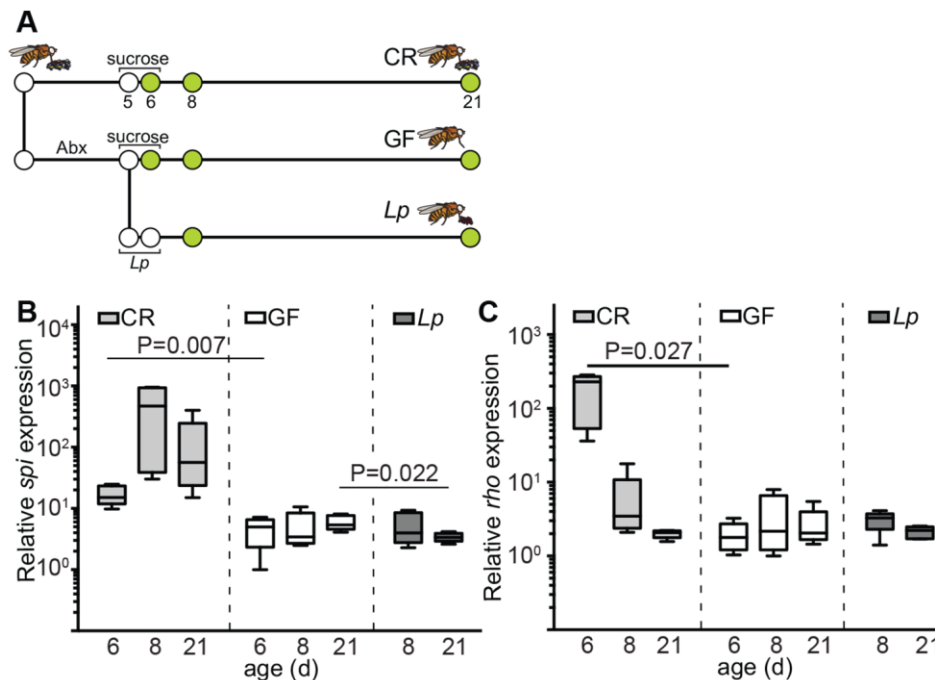


**Figure 3.3. *L. plantarum* does not trigger a proliferative response in adult fly intestines. (A)** Schematic representation of gnotobiotic fly generation and experimental timeline. “Abx” indicates duration of antibiotic treatment. Sucrose and *L. plantarum* (*Lp*) show feeding regimes for the respective groups. Green circles indicate times at which samples were processed. **(B and C)** Quantitative real-time PCR analysis of expression of the EGF-type growth factor *spitz* (*spi*) **(B)** and the *spitz*-activating endopeptidase *rhuboid* (*rho*) **(C)** from the dissected guts of adult CR, GF, and *L. plantarum*-associated flies. Each time point represents five independent measurements. P values are the results of pairwise comparisons from a one-way ANOVA. Conventionally reared (CR), germ free (GF), and *L. plantarum* monoassociated.

### 3.2.5 Impaired epithelial renewal in *L. plantarum* monoassociated flies

To more accurately determine the effects of *L. plantarum* on ISC proliferation, we used the MARCM clonal marking method to assess stem cell proliferation in the intestines of CR, GF, and *L. plantarum*-associated flies. MARCM labels all progeny of an ISC division with GFP(280). As a result, clone number and size provide a simple proxy for total divisions in the midgut. We looked at ISC division in CR flies, GF flies, and flies that we associated with *L. plantarum*. In each case, we counted the total number of mitotic clones per posterior midgut and the number of cells per clone. As expected, we noticed greater mitotic activity in the intestines of CR flies than GF flies. CR flies had significantly more mitotic clones than GF counterparts (Fig. 3.4A, B, and D), and CR clones contained significantly more cells than GF clones (Fig. 3.4E). In contrast to CR flies, monoassociation with *L. plantarum* failed to initiate proliferative responses in the host (Fig. 3.4C). In fact, the midgut contained significantly fewer clones than CR flies, or GF flies (Fig. 3.4D), and the clones that we observed in *L. plantarum*-associated flies invariably had fewer cells than age-matched clones in CR flies (Fig. 3.4E). To determine if impaired epithelial renewal occurs upon monoassociation with different strains of *L. plantarum*, we assessed stem cell proliferation in the intestines of flies that we monoassociated with *L. plantarum* *DF*. We noticed a similar absence of epithelial renewal in flies that we monoassociated with the *L. plantarum* *DF* strain, suggesting that this phenotype is not limited to a single strain of *L. plantarum* (Fig. 3.4F). In contrast, we observed significant levels of epithelial growth in the intestines of adult flies that we associated with *A. pasteurianus* (Fig. 3.4G to I), confirming that GF flies are not impaired in their ability to renew the intestinal epithelium upon reassociation with symbionts. These results, in conjunction with our quantitative measurements of host gene expression (Fig. 3.3), demonstrate a near-complete absence of epithelial renewal in intestines associated exclusively with *L. plantarum*.

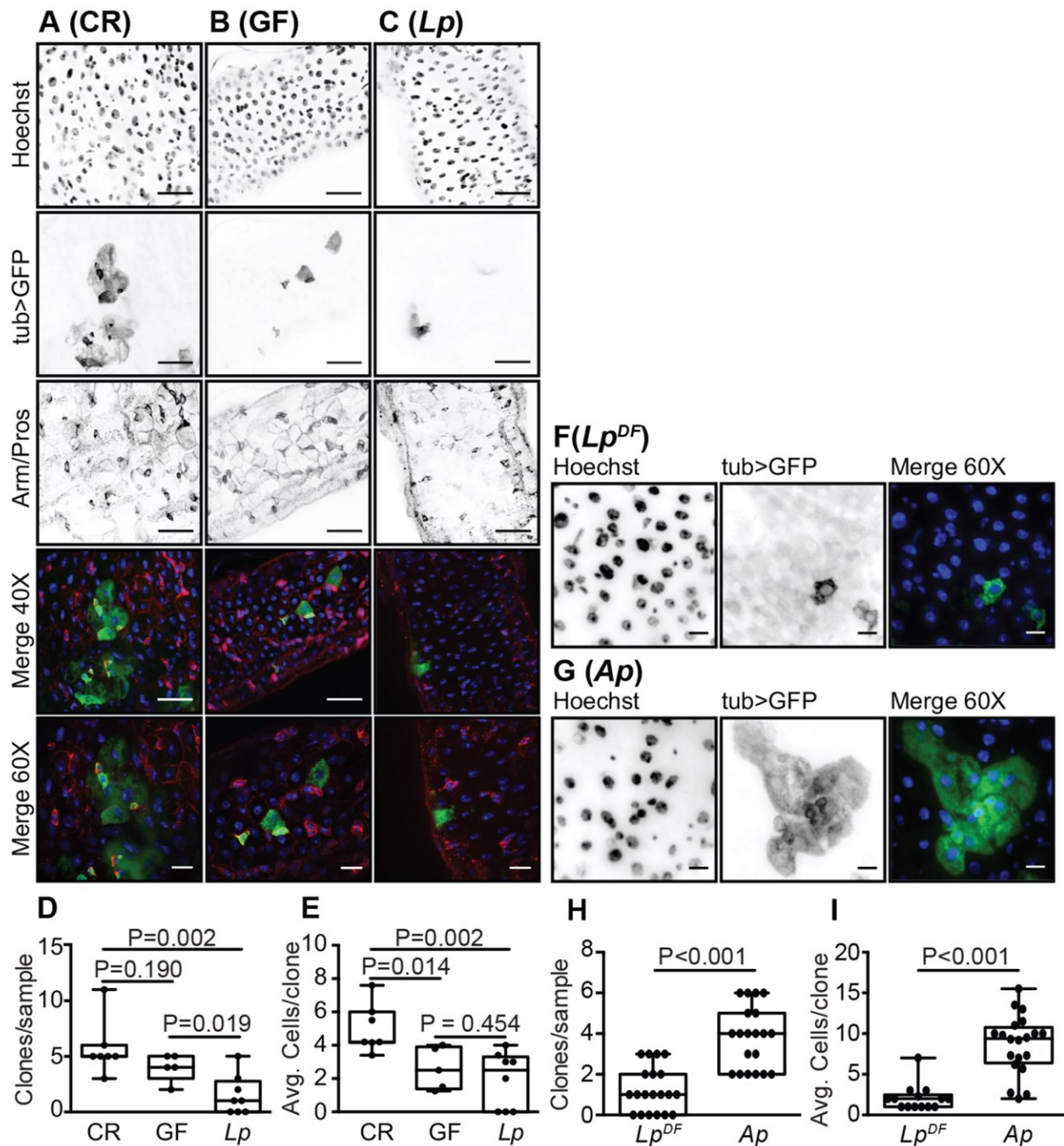


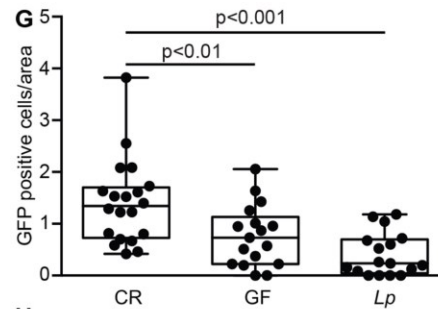
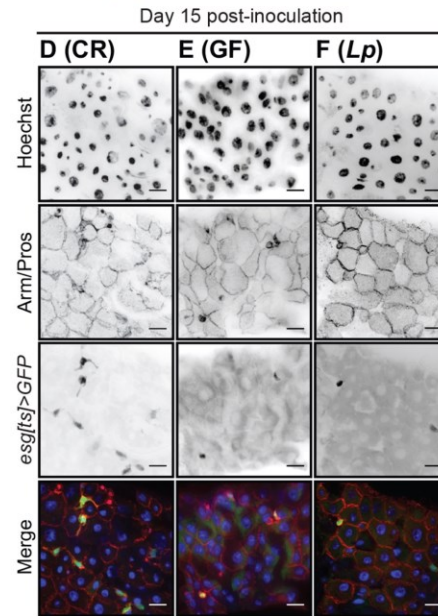
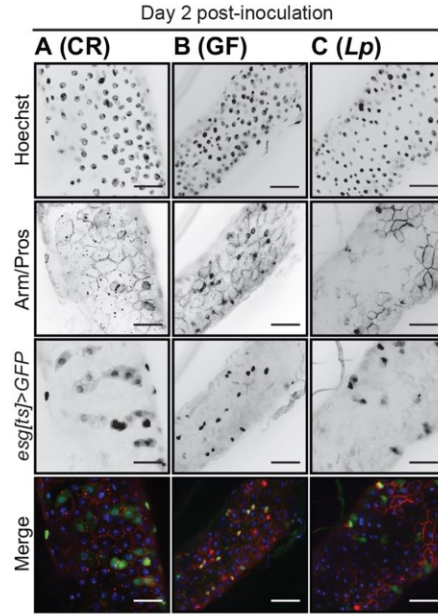
**Figure 3.4. A lack of epithelial renewal in the guts of *L. plantarum*-monoassociated flies.** (A to C) GFP-positive MARCM clones from the posterior midgut of CR (A), GF (B), and *L. plantarum*-monoassociated (C) flies at day 26 of age. Guts were stained with Hoechst stain and anti-Armadillo/Prospero antibodies as indicated. Hoechst stain (blue), GFP (green), and Armadillo/Prospero (red) were merged in the fourth (x40 magnification) and fifth rows. Boxed regions in the fourth row are shown at a higher magnification (x60) in the fifth row. (D and E) Quantification of clones per sample (D) and cells per clone (E) in CR, GF, and *L. plantarum*-monoassociated flies. (F and G) GFP-positive MARCM clones from the posterior midgut of *L. plantarum* *DF*-monoassociated (F) or *A. pasteurianus*-monoassociated (G) flies at day 26 of age. Guts were stained with Hoechst stain. Hoechst stain (blue) and GFP (green) were merged in the third column (x60).

(H and I) Quantification of clones per sample (H) and cells per clone (I) in *L. plantarum* DF- and *A. pasteurianus*-monoassociated flies. For all images, x40 bars are 25  $\mu\text{m}$  and x60 bars are 10  $\mu\text{m}$ . P values are the results of pairwise comparisons from a one-way ANOVA. Conventionally reared (CR), germ free (GF), *L. plantarum* monoassociated (*Lp*), and *A. pasteurianus*-monoassociated (*Ap*).

### 3.2.6 *L. plantarum* monoassociated flies lack intestinal progenitors

Given the absence of ISC proliferation, we used immunofluorescence to determine if prolonged monoassociation with *L. plantarum* affected the cellular organization of posterior midguts. To measure the influence of *L. plantarum* on midgut morphology, we visualized the posterior midguts of CR, GF, and *L. plantarum*-monoassociated *esg<sup>ts</sup>* flies at 2- and 15-days post association. We used *esg<sup>ts</sup>* to specifically mark IPCs with GFP and anti-Armadillo and anti-Prospero to highlight cell borders and identify enteroendocrine cells, respectively. We did not observe differences between the treatment groups at the early time point (Fig. 3.5A to C). In each case, midguts displayed hallmarks of young intestines— evenly spaced nuclei, regular arrangement of GFP-positive progenitors, and neatly organized cell boundaries. As expected, 15 days post inoculation, CR midguts showed signs of age-dependent tissue disorganization (Fig. 3.5D). We no longer observed regular spacing between individual nuclei, Prospero and Armadillo stains revealed mild epithelium disruption, and the population of GFP-positive progenitors had expanded relative to 2-day-old fly guts. Consistent with bacterial contributions to age related dysplasia, we did not see a similar degree of disorganization in GF guts. Instead, GF flies had regularly spaced nuclei, an organized epithelium, and fewer GFP-positive progenitor cells (Fig. 3.5E). We also saw minimal signs of disorganization in the intestines of flies that we associated with *L. plantarum* for 15 days. In this case, we observed regularly spaced nuclei, defined cell borders, and an even distribution of enteroendocrine cells (Fig. 3.5F). However, we noticed that *L. plantarum*-associated guts had approximately half the number of progenitors of GF guts and significantly fewer progenitors than CR guts (Fig. 3.5G). We then examined the impacts of *L. plantarum* on the length of adult posterior midguts as microbial association affects midgut length in adult *Drosophila*(41, 102). Consistent with an earlier report(41), we noticed a similar, albeit milder, effect of microbial removal on the length of the adult intestine. On average, we found that the intestines of GF flies were 5% longer than CR controls (Fig. 3.5H). Similarly, we found that the intestines associated with *L. plantarum* were, on average, 6% longer than CR controls (Fig. 3.5H). However, we did not detect a statistically significant difference in mean gut length between the three treatments. We speculate that the relatively mild effects of bacterial removal on intestinal length noted in our study may be the result of fly strain differences or differences in fly culture methods or may occur as a result of removing the microbiome after completion of juvenile development. Nonetheless, our data suggest a detrimental impact of *L. plantarum* monoassociation on the pool of progenitor cells in adult flies.





**H**

Microbiota	mean midgut length ( $\mu\text{m}$ )	Std. error	% increase	Dunnett's test
CR (n=20)	4974	278		
GF (n=19)	5236	183	+5.3	n.s.
<i>Lp</i> (n=16)	5299	185	+6.5	n.s.



**Figure 3.5. *L. plantarum*-monoassociated fly guts have low numbers of intestinal progenitor cells.** (A to C) Immunofluorescence of posterior midguts of *esg[ts]* CR (A), GF (B), and *L. plantarum*-monoassociated (C) flies at day 11 of age. Bars, 25  $\mu$ m. (D to F) Immunofluorescence of posterior midguts of CR (D), GF (E), and *L. plantarum*-monoassociated (F) flies at day 26 of age. Bars, 10  $\mu$ m. Guts were stained with Hoechst stain and anti-Armadillo/Prospero antibodies as indicated. Progenitor cells were visualized with GFP as indicated. Hoechst stain (blue), GFP (green), and anti-Armadillo/Prospero (red) were merged in the fourth and eighth rows. (G) Quantification of progenitor numbers per unit surface area at day 26 of age. P values are the results of pairwise comparisons from a one-way ANOVA. (H) Mean midgut length of CR, GF, and *L. plantarum*-monoassociated flies at day 15 post-inoculation. n.s., not significant. Conventionally reared (CR), germ free (GF), and *L. plantarum* monoassociated (*Lp*).

### 3.2.7 *L. plantarum* disrupts posterior midgut ultrastructure

As monoassociation with *L. plantarum* results in a loss of intestinal progenitors and a failure of epithelial renewal, we used transmission electron microscopy (TEM) to directly examine the effects of 15 days of monoassociation with *L. plantarum* on posterior midgut ultrastructure. As controls, we visualized the posterior midguts of age-matched CR and GF flies. CR midguts had the anticipated sheath of visceral muscle that surrounds small, basal cells, and large, columnar epithelial cells (Fig. 3.6A to C). As it is not possible to distinguish between ISCs and enteroblasts with TEM of this kind, we refer to the small basal cells as progenitor cells. In many ways, GF flies mirrored CR flies, with an organized visceral musculature (Fig. 3.6D), basal progenitors (Fig. 3.6D and E), and an intact brush border (Fig. 3.6F). Upon examination of midguts associated with *L. plantarum*, we were struck by substantial alterations to intestinal morphology. The epithelium contained an undulating population of cells (Fig. 3.6G and H) with large vacuoles (Fig. 3.6G to I, arrowheads) and poorly discernible nuclei (Fig. 3.6G). We also noticed alterations to the morphology of presumptive progenitor cells. In place of the small, densely stained progenitors intimately associated with the visceral muscle of CR or GF flies, monoassociation with *L. plantarum* resulted in the appearance of misshapen cells that did not associate properly with the muscle and had large, lightly stained nuclei and numerous cytosolic vacuoles (Fig. 3.6G and H). These findings show that monocolonization of a GF adult midgut with *L. plantarum* causes an intestinal phenotype that is characterized by thinning of the epithelium, formation of large cytosolic vacuoles, and a loss of progenitor cells. In summary, monoassociation of adult *Drosophila* with *L. plantarum* results in an intestinal phenotype that is distinct from CR or GF flies. *L. plantarum* forms a persistent association with GF *Drosophila* that impairs epithelial renewal programs, depletes progenitor cell populations, and ultimately shortens host longevity.

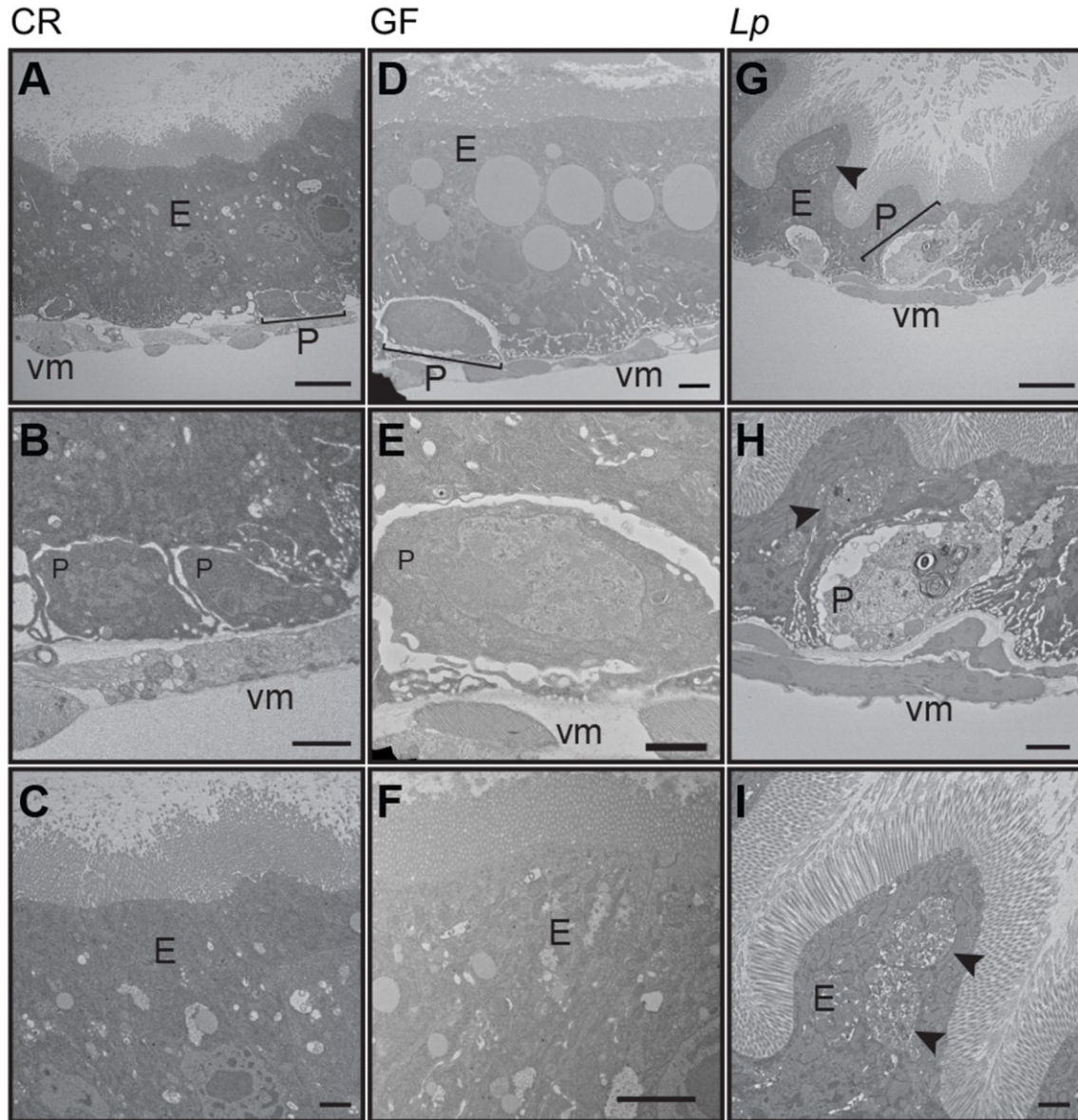


**Figure 3.6. *L. plantarum* disrupts posterior midgut ultrastructure.** Transmission electron microscopy of conventionally reared (CR) (A to C), germ free GF (D to F), and *L. plantarum*-monoassociated (*Lp*) (G to I) fly posterior midguts 15 days after inoculation. Epithelium (E), progenitors (P), and visceral muscle (vm) are labeled. Arrowheads indicate large vacuoles. (A, D, and G) Direct magnification, x1,200. Bars, 5  $\mu$ m. (B, E, and H) Direct magnification, x3,000. Bars, 1  $\mu$ m. (C, F, and I) Direct magnification, x3,500. Bars, 1  $\mu$ m.

### 3.3 Significance

*L. plantarum* is a routinely identified member of the microbiome of laboratory cultures of *Drosophila*(90). The data in this chapter examines the consequence of long-term intestinal association of adult *Drosophila* with symbiotic *L. plantarum*. We found that *L. plantarum* repopulates GF intestines and forms a stable association with adult flies. Flies monoassociated with *L. plantarum* had significantly shorter lifespans than GF counterparts. This shortening of lifespan was accompanied by a gradual loss of IPCs and diminished epithelial renewal that resulted in an abrasion of gut ultrastructure. Together, these results uncover negative effects of *L. plantarum* on the IPC pool and intestinal regeneration. Furthermore, we believe this study provides a valuable step in understanding how individual symbiotic species influence IPC homeostasis.

## Chapter 4.

### Commensal pathogen competition impacts host viability

This chapter contains content from the following source, republished with permission:

- Fast, D\*, Kostiuk, B\*, Foley, E. & Pukatzki, S. Commensal pathogen competition impacts host viability. *Proc. Natl. Acad. Sci. U. S. A.* 115, 7099–7104 (2018).

\*Authors contributes equally

Experiments shown in Figure 4.1-4.6 were conceived and performed by D.F and B.K and analyzed by D.F, B.K, E.F, and S.P.

## 4.1 Introduction

Gut associated microbes have effects on a broad range of host traits with considerable influence on metabolism and intestinal immunity(142). Symbiotic bacteria form a barrier that rebuffs the ingress of intestinal pathogens while actively stimulating transcriptional responses in host tissue. For example, indigenous bacteria trigger the synthesis of reactive oxygen species and the transcription of cytoprotective genes required to survive oxidative stress(144). Previously, interactions of this nature, between host and microbe, have been thought of as binary transactions between individual bacterial species and the host. However, new evidence has emerged to indicate that this view of host microbe interactions is limited, and should consider how interactions between bacterial species influence host phenotypes(140). For instance, interactions between symbiotic species was recently demonstrated to have measurable impacts on aspects of host fitness, such as fecundity and lifespan, indicating that interbacterial interactions indeed influence host biology(140). Despite evidence of the impact of bacteria-bacteria interactions on the host, it remains unclear how interactions between symbiotic species and invading pathogens influence enteric disease.

The T6SS is found in a number of enteric pathogens including *Salmonella typhimurium*(281, 282), *Campylobacter jejuni*(283), and *V. cholerae*(212). This molecular syringe facilitates interactions between bacteria and adjacent cells. Given the T6SS' ability to mediate interactions between bacteria, and its prevalence in disease causing microbes, we asked if interactions between the T6SS of *V. cholerae* and intestinal symbionts impact the progression of intestinal disease. We found that ablation of the T6SS attenuates disease symptoms, reduces intestinal damage, and extends the viability of flies infected with *V. cholerae*. T6SS dependent killing of the host required association of adult flies with the Gram-negative fly symbiont *A. pasteurianus*. Removal of the microbiome abolished T6SS dependent killing of the host and reintroduction of *A. pasteurianus* was sufficient to restore T6SS pathogenesis. Furthermore, inactivation of the IMD pathway extended the viability of flies infected with *V. cholerae*, implicating host responses in *V. cholerae* mediated lethality. Together, the work presented in this chapter demonstrates that interactions between symbiotic bacteria and enteric pathogens contribute to intestinal disease in *Drosophila*.

## 4.2 Results

### 4.2.1 The T6SS interacts with commensal bacteria to influence host viability.

As *Drosophila* is susceptible to infection with *V. cholerae*(157), we reasoned that the fly provides a platform to determine the in vivo function of the T6SS. Pandemic *V. cholerae* strains belong to two biotypes of the O1 serogroup. The classical biotype responsible for the first six pandemics carries multiple nonsense mutations and deletions in T6SS genes, resulting in a disabled T6SS(248). Conversely, the El Tor biotype, responsible for the seventh pandemic, has a functional T6SS that becomes active upon host entry(251, 284). To examine the impact of T6SS on *V. cholerae* pathogenesis, we tracked the survival of flies that we infected orally with either a classical biotype, O395, or an El Tor biotype, C6706. C6706 has been shown to be avirulent in the fly model, due to repression of quorum sensing by the regulator HapR(221). However, our laboratory isolate of C6706 kills adult *Drosophila*, due to decreased *hapR* levels(221, 285). As controls, we measured the viability of adult flies raised on lysogeny broth (LB). Infection with O395 caused a moderate reduction in adult viability compared with controls (Fig. 4.1A). In contrast, the median viability of C6706-infected flies was a third of that observed for controls (50 hours vs. 149hours; Fig. 4.1A), and all C6706-infected flies perished within 72 hours of infection (compared with 170 hours for mock-infected flies).

As C6706 encodes a functional T6SS, we then asked whether disabling the *Vibrio* T6SS affects pathogenesis. We infected adult flies with wild-type C6706, or with C6706 carrying an in-frame deletion of *vasK*, which encodes an inner membrane protein essential for T6SS assembly(231). We found that disabling the T6SS in C6706 significantly impaired pathogenesis (Fig. 4.1B). As variability in fly killing exists from experiment to experiment, likely due to subtle differences between individual cultures of flies, control experiments with C6706 and C6706 $\Delta$ *vasK* were repeated concurrently with each new experiment and plotted accordingly. Mutation of *vasK* consistently extended viability across six independent trials and on average increased median survival by 16%. Deletion of *vipA*, a component that makes up the outer sheath of the T6SS nanomachine(260, 286), had near-identical attenuating effects on host killing (Fig. 4.1C). Combined, these results establish that T6SS contributes to *V. cholerae* pathogenesis *in vivo*. However, inactivation of T6SS does not abolish pathogenesis. This is consistent with earlier reports that *V. cholerae* employs additional virulence factors(157, 221, 224) to kill the host in a T6SS-independent manner.

As the T6SS targets eukaryotic and prokaryotic cells(212, 231, 250), we asked whether T6SS contributes to host killing either by direct effects on the host or by indirect effects on the intestinal microbiota. We examined survival rates of CR and GF flies that we challenged with C6706 or C6706 $\Delta$ *vasK*. If the T6SS acts directly on the fly, we expect that removal of commensal bacteria will not affect T6SS-

dependent killing of the host. Instead, we found that an absence of commensal bacteria impaired C6706-dependent killing to the point that it was no longer distinguishable from C6706 $\Delta vasK$  (Fig. 4.1D), indicating that T6SS-dependent killing of a fly host requires the presence of commensal bacteria.

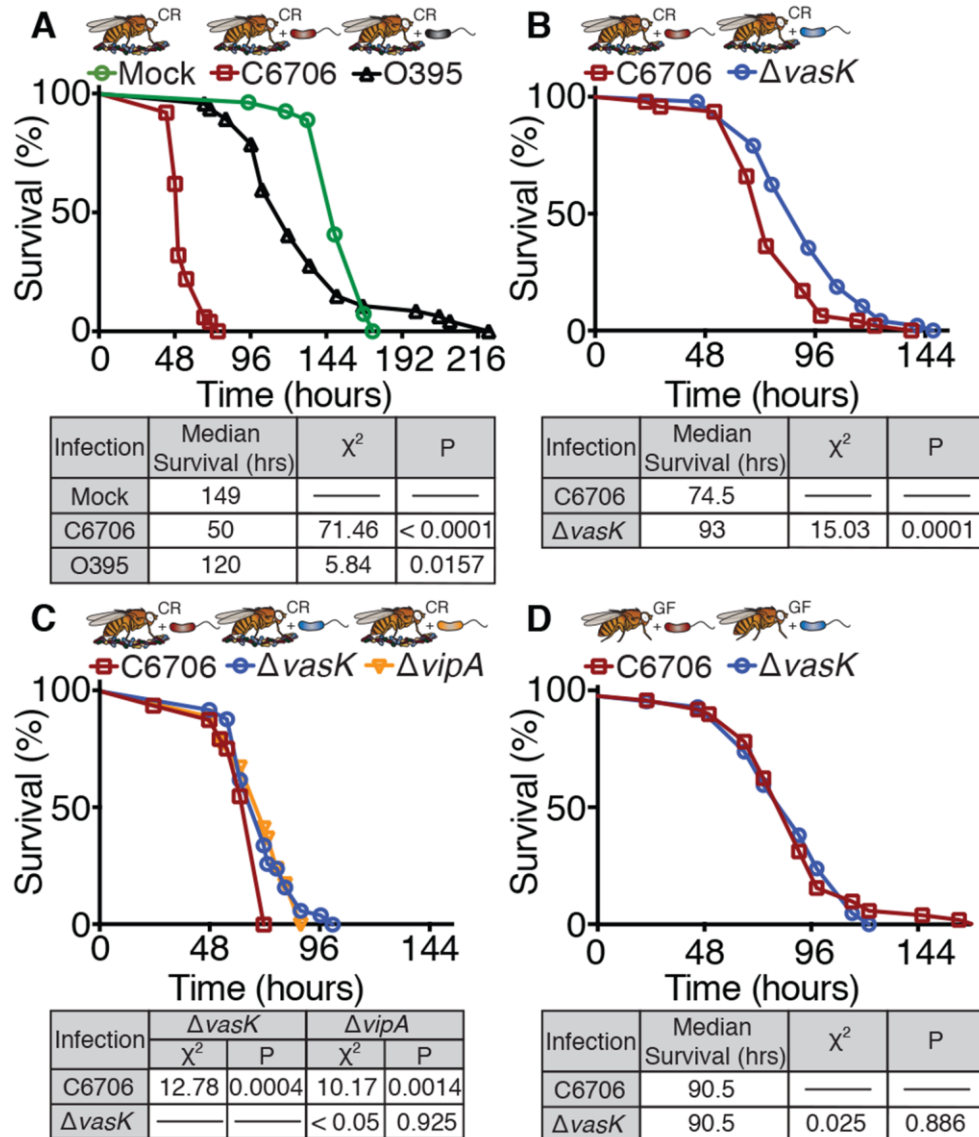


**Figure 4.1.** The T6SS contributes to the pathogenesis of *V. cholerae* in a commensal dependent manner. (A) Survival curves of 5- to 6-d-old conventionally reared (CR) *w<sup>1118</sup>* flies infected with the indicated *V. cholerae* strains. LB alone served as mock infection. (B and C) Survival curve of CR flies infected with T6SS functional (C6706) or T6SS nonfunctional (C6706 $\Delta vasK$  and C6707 $\Delta vipA$ ) mutants. (D) Survival curve of germ free (GF) flies infected with C6706 or C6706 $\Delta vasK$ . (D) was performed at the same time and infected with the same bacterial cultures as (B). The y axis shows percent survival, and x axis shows infection time. Tables show Longrank (Mantel–Cox) tests. In A,  $\chi^2$  and P values are relative to mock infected flies; in B–D,  $\chi^2$  and P values are relative to wild-type C6706 infected flies; n = 50 per group, for all experiments.

#### 4.2.2 The T6SS contributes to disease symptoms.

As T6SS inactivation impairs *V. cholerae* pathogenesis, we monitored how the T6SS impacts the development of pathogen-laden diarrhea, the hallmark symptom of cholera. We supplemented the infection culture with a nontoxic, non-absorbable blue dye(95). We infected flies for 24 hours and placed them in filter paper lined chambers. To determine the defecation frequency of infected flies, we counted individual blue dots hourly for the next 4 hours. As controls, we measured defecation by uninfected flies that we raised on a solid fly culture medium with blue dye, or on bacterial growth medium supplemented with the same dye. We observed no difference in defecation frequency between flies raised on solid or liquid diets, confirming that the bacterial growth medium does not cause diarrhea (Fig. 4.2A). Likewise, O395 had no measurable effects on defecation frequency (Fig. 4.2A). In contrast, we found that C6706 caused an increase in the number of fecal marks per fly (Fig. 4.2A). Similarly, we found an increase in the number of fecal marks per fly from flies infected with C6706 $\Delta$ vasK. However, this increase was less pronounced than that of flies infected with C6706. To better assess the contributions of the T6SS to defecation frequency, we performed a linear regression analysis on the groups indicated in Fig. 4.2A. We noticed a significant increase in the number of fecal marks per fly over time from flies infected with C6706, but not from mock-infected flies. There was a significantly lower increase in the number of fecal marks per fly from C6706 $\Delta$ vasK-infected flies. Furthermore, we found that the relationship between increased fecal marks and time was stronger upon infection with C6706 ( $R=0.66$ ) than infection with C6706 $\Delta$ vasK ( $R=0.50$ ). This difference was reflected in the respective P-values whereby only infection with C6706 reaches significance at the 1% threshold ( $P=0.0015$ ) and infection with C6706 $\Delta$ vasK ( $P=0.02$ ) does not, indicating a more severe change in fecal marks associated with infection with C6706. Although, we acknowledge there is no statistical method to compare significance between P-values. Additionally, T6SS inactivation does not abate diarrheal symptoms likely due to the continued production of CT. Together, these data indicate that the T6SS impacts the severity of diarrheal symptoms in infected flies.

To measure T6SS effects on defecation volume, we calculated the surface area of each dot as a proxy for volume of feces. We observed an increase in the area of fecal spots from mock-infected flies raised on a liquid diet compared with flies raised on a solid diet (Fig. 4.2B). Infection with O395 did not impact defecation volume (Fig. 4.2B). In contrast, both C6706 and C6706 $\Delta$ vasK significantly increased fecal volume relative to mock-infected controls (Fig. 4.2B), confirming enhanced diarrheal disease in flies infected with either strain. Finally, as the shedding of *V. cholerae* in fecal matter accompanies diarrhea, we quantified the number of *V. cholerae* bacteria excreted by flies that we challenged with the different strains of *V. cholerae*. Whereas we only detected *V. cholerae* in the feces of a single fly infected with O395, we



found that 8 out of 10 flies infected with C6706 shed *V. cholerae*. Consistent with contributions of T6SS to disease severity, we only found 5 out of 10 C6706 $\Delta vasK$ -infected flies shed the bacteria. In short, our results establish a role for the T6SS in diarrheal symptoms during a *V. cholerae* infection. Loss of T6SS reduces defecation frequency, and lowers shedding of *V. cholerae* in the feces of infected animals. As O395 has comparatively mild effects on host viability, and to specifically examine the influence of the T6SS on disease progression, O395 was excluded from subsequent experiments.

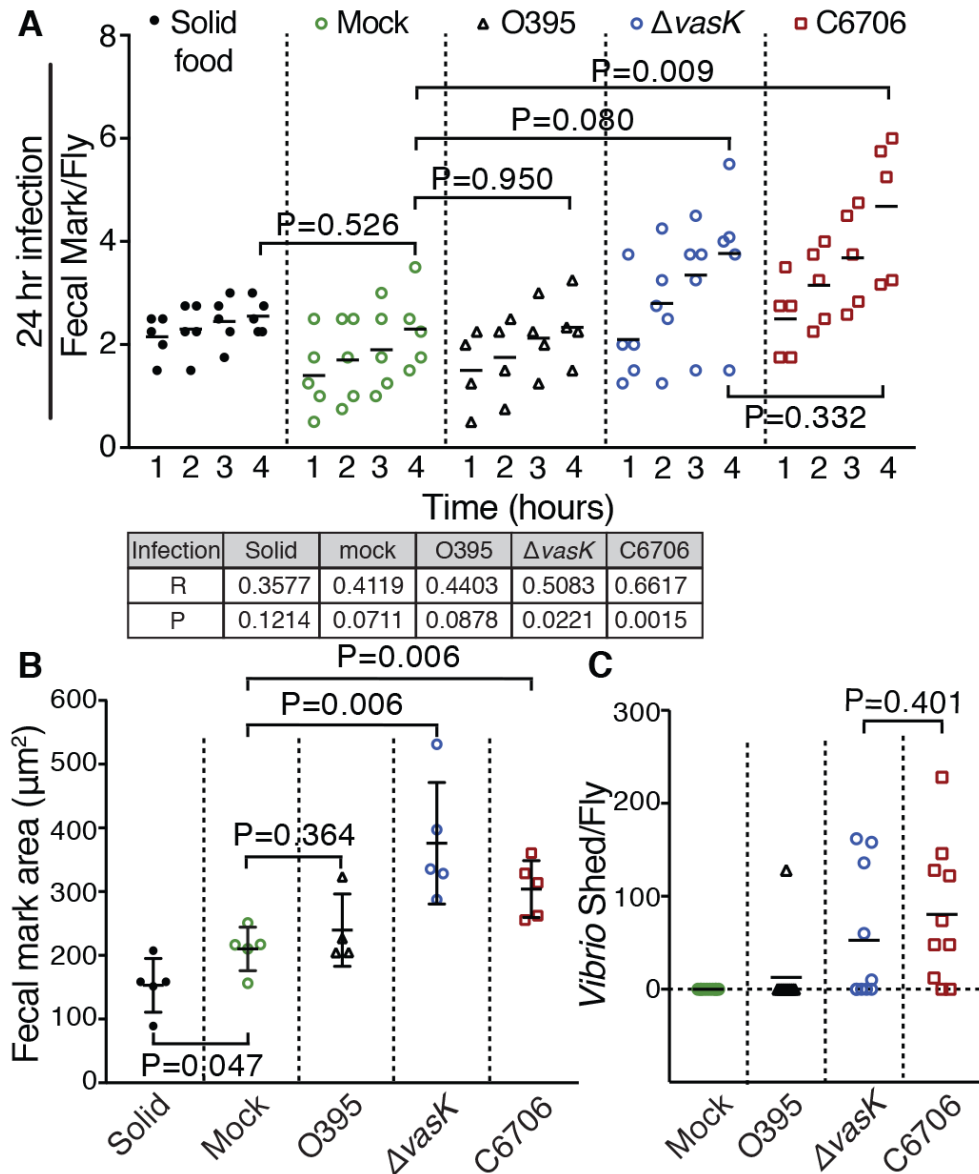


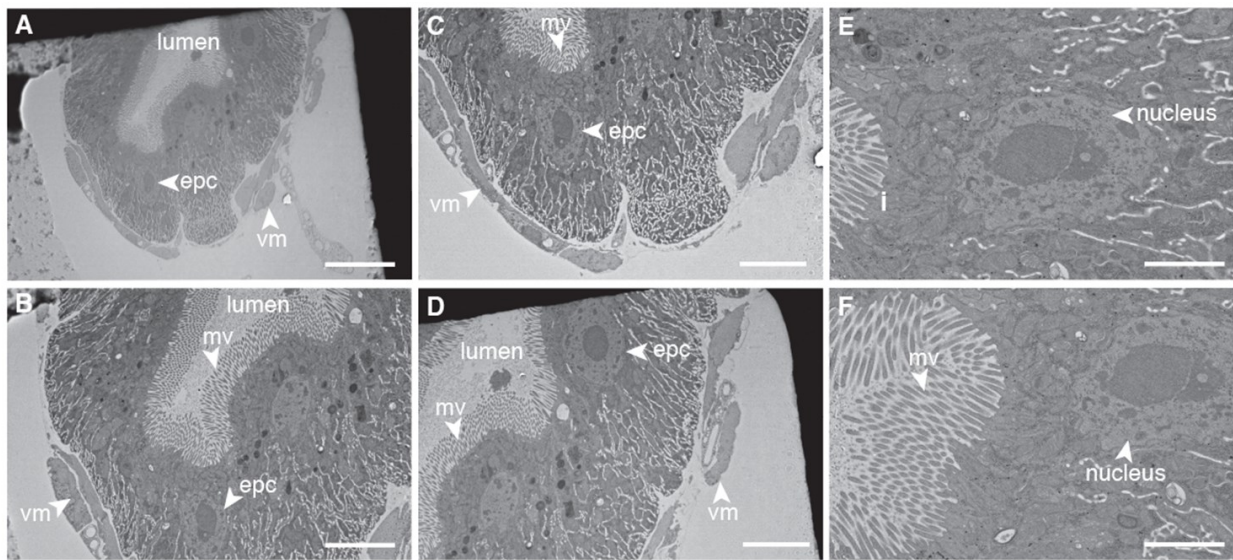
**Figure 4.2. The T6SS contributes to cholera-like disease. (A)** Fecal marks from  $w^{1118}$  flies fed solid fly food or LB broth (mock) supplemented with O395, C6706 $\Delta vasK$ , or C6706 for 24 hours. The table shows a linear regression analysis of each group, and P values are the result of a Student's t test at 4 hours. **(B)** Fecal mark area, in micrometers, of spots counted. Each point is the average area of a given replicate. Statistics show

Student's t tests for each group compared with solid food. (C) *V. cholerae* shed per fly fed LB or infected with *V. cholerae* C6706, C6706 $\Delta$ *vasK*, or O395 for 24 hours. Each point is the number of *Vibrio* isolated from fecal matter of a single fly.

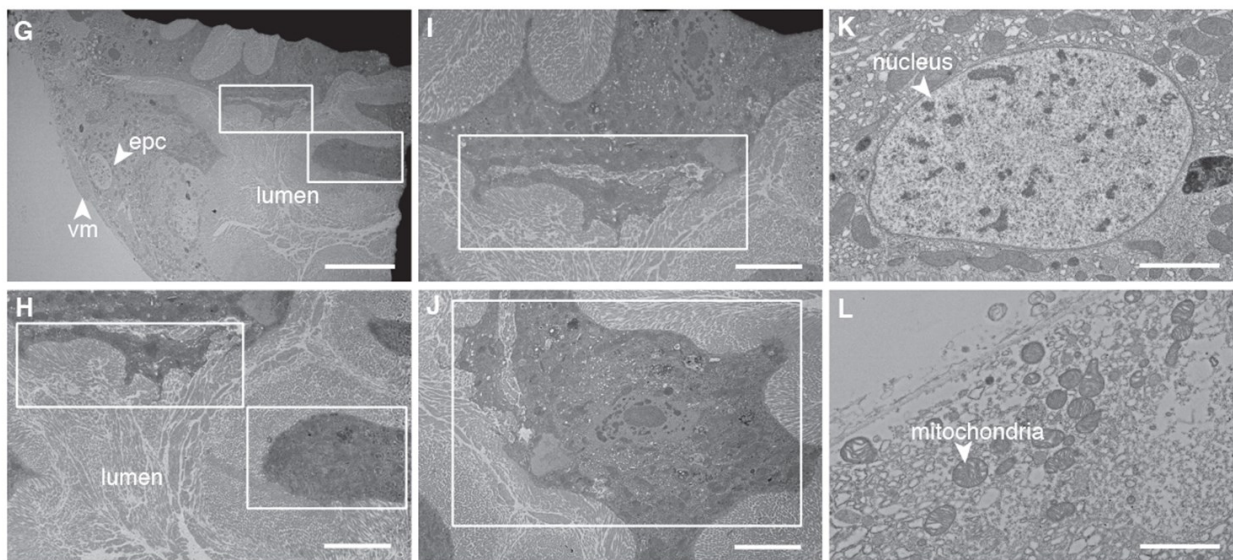
#### 4.2.3 The T6SS promotes intestinal epithelial damage.

During infection with *V. cholerae*, diarrhea is accompanied by ultrastructural changes to the host intestinal epithelium(287). Therefore, we used TEM to examine the ultrastructure of the small intestine analog, the posterior midgut, of mock-infected flies, or flies challenged with C6706 or C6706 $\Delta$ *vasK* for 50 hours. Intestines from mock-infected flies had a readily identifiable lumen, an epithelium of evenly spaced columnar cells with extensive brush borders, and morphologically normal nuclei and mitochondria (Fig. 4.3A–F). In contrast, we could not discern an intact intestine in flies challenged with C6706 (Fig. 4.3G–I). The gut consisted of a disorganized mass of cells that lacked apical brush borders, and completely engulfed the lumen. We observed extensive shedding of epithelial structures into the presumptive lumen (boxes, Fig. 4.3G–J), and high magnification images revealed characteristics of cell death, such as nuclear decondensation, and swollen mitochondria (Fig. 4.3K and L). Infection with C6706 $\Delta$ *vasK* caused a phenotype that was intermediate between mock-infected controls and C6706-infected adults. Guts infected with C6706 $\Delta$ *vasK* retained elements of intestinal organization, such as identifiable epithelial cells with brush borders, a recognizable lumen (Fig. 4.3M–P), and intact nuclear and mitochondrial organization (Fig. 4.3Q and R). However, we noticed that infection with C6706 $\Delta$ *vasK* caused an extrusion of epithelial cell matter into the lumen (boxes, Fig. 4.3M), a phenotype consistent with pathogen-mediated destruction of the host epithelium(153). In summary, these results uncover a role for the T6SS in the severity of disease in adult *Drosophila*. Inactivation of the T6SS diminishes damage to the intestinal epithelium, lowers the severity of diarrhea, and extends host mortality times.

Mock



C6706



$\Delta$ vasK

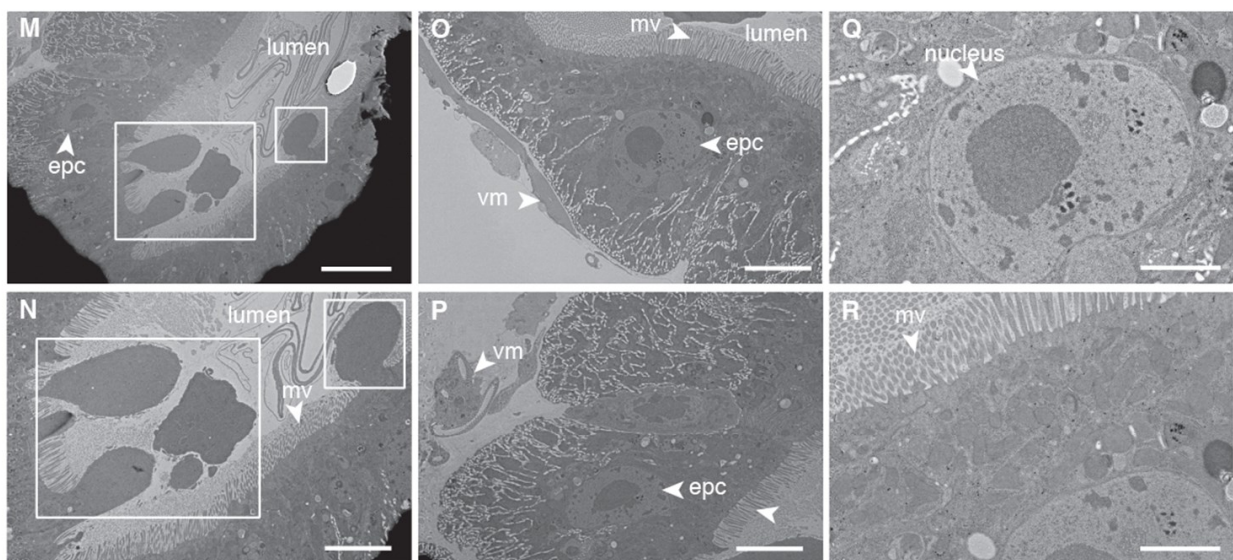


**Figure. 4.3. The T6SS contributes to *V. cholerae* intestinal pathogenesis.** TEM of the posterior midguts of flies, (A–F) mock-infected or (G–L) infected with C6706 or (M–R) C6706 $\Delta$ *vasK* after 50 hours of infection. Cells protruding into the lumen are indicated with boxes. (Large scale bars, 10  $\mu$ m; small scale bars, 5  $\mu$ m.) Epithelial cells, epc; microvilli, mv; visceral muscle, vm.

#### 4.2.4 The T6SS influences pathogen-commensal interactions in the intestine.

As T6SS-assisted pathogenesis requires the microbiota (Fig. 4.1D), we asked whether intestinal bacteria influence colonization by *V. cholerae*. The gut microbiota of laboratory-reared *Drosophila* is of modest diversity(87, 90). In our laboratory, fly intestines are dominated by the Gram-negative *A. pasteurianus*, and the Gram-positive *Lactobacillus* species *L. brevis* and *L. plantarum*(258). To determine whether *A. pasteurianus* or *Lactobacilli* influence host colonization by *V. cholerae*, we established populations of GF adult flies, and adults that we associated exclusively with *A. pasteurianus* or *L. brevis* (Fig. 4.4A). We challenged the populations with C6706 or C6706 $\Delta$ *vasK* and measured the colony-forming units per fly (CFU/Fly) of *V. cholerae* as a function of time. We found that C6706 and C6706 $\Delta$ *vasK* were equally effective at colonizing GF intestines, or intestines that exclusively carry *L. brevis* (Fig. 4.4B and C). In each case, the numbers of C6706 and C6706 $\Delta$ *vasK* increased over time and reached nearly identical levels at 24 hours of infection (Fig. 4.4B). These data indicate that the T6SS is dispensable for the colonization of a GF gut, or a gut that houses the Gram-positive bacteria *L. brevis*. In contrast, removal of the T6SS significantly impaired the ability of *V. cholerae* to colonize an adult intestine that we preassociated with the Gram-negative commensal, *A. pasteurianus*. In this scenario, C6706 titers increased significantly from 6 hours to 24 hours of infection in the intestines of *A. pasteurianus*-colonized adults. In contrast, there was no increase in the load of C6706 $\Delta$ *vasK* from 6 hours to 24 hours (Fig. 4.4D). By 24 hours, we found an appreciable difference in CFU/Fly between C6706 and C6706 $\Delta$ *vasK* (Fig. 4.4D). These data indicate that the T6SS supports colonization of intestines inhabited exclusively by *A. pasteurianus*.

As the T6SS assists colonization of a gut associated with *A. pasteurianus*, we asked whether the T6SS is able to kill *A. pasteurianus* in a standard competition assay(231). For these *in vitro* assays, we used V52, a strain of *V. cholerae* that does not require *in vivo* stimulation to activate the T6SS, and employs the same T6SS effector molecules as C6706(246). Consistent with an earlier study(231), *V. cholerae* effectively killed the T6SS susceptible prey *E. coli* K12 strain MG1655 (Fig. 4.4E). Furthermore, we saw no evidence of T6SS-dependent killing of either *L. plantarum* or *L. brevis* (Fig. 4.4E). This is consistent with previous observations that Gram-positive bacteria are naturally refractory to T6SS activity (6, 28). In contrast, we noticed substantial T6SS-dependent killing of *A. pasteurianus* by *V. cholerae* (Fig. 4.4E). These data raise the possibility that T6SS facilitates host colonization through eradication of *A. pasteurianus*. To test this

hypothesis, we measured total *A. pasteurianus* numbers in the intestines of flies that we monoassociated with *A. pasteurianus* and challenged with C6706 or C6706 $\Delta$ *vasK*. We did not detect obvious impacts of T6SS-positive C6706 on the numbers of intestinal *A. pasteurianus* (Fig. 4.4F). As colonization of the intestinal tract is hallmarked by fly-to-fly variability, it is possible that our assay failed to detect subtle changes in *A. pasteurianus* numbers. However, we cannot exclude the possibility that infection with C6706 leads to relocalization of *A. pasteurianus* within the intestine, thereby exacerbating disease. Nonetheless, our data suggest that *V. cholerae* infection does not substantially alter total *A. pasteurianus* numbers. As we did not detect a change in *A. pasteurianus* numbers, we tested the alternate possibility that T6SS-mediated interactions with a subset of intestinal *A. pasteurianus* induce secondary responses in the host that accelerate death. For example, mutations in the IMD antibacterial pathway attenuate *V. cholerae*-dependent killing of the host(161). IMD contributes to antibacterial responses in the fly gut(19), and is similar to the mammalian TNF pathway, a regulator of intestinal inflammation in mammals(18, 288). To determine whether T6SS-mediated interactions with the host involve pathological activation of immune responses, wild-type *w<sup>1118</sup>* or isogenic *imd* mutant flies were infected with with C6706 or C6706 $\Delta$ *vasK*. Mutation of either *vasK* or *imd* prolonged host viability to near-equal extents (Fig. 4.4G). Ablation of T6SS in combination with an *imd* mutation extended host viability further (Fig. 4.4G). These data suggest that additive effects from the T6SS of *V. cholerae* and the IMD pathway of *Drosophila* synergistically control host viability.



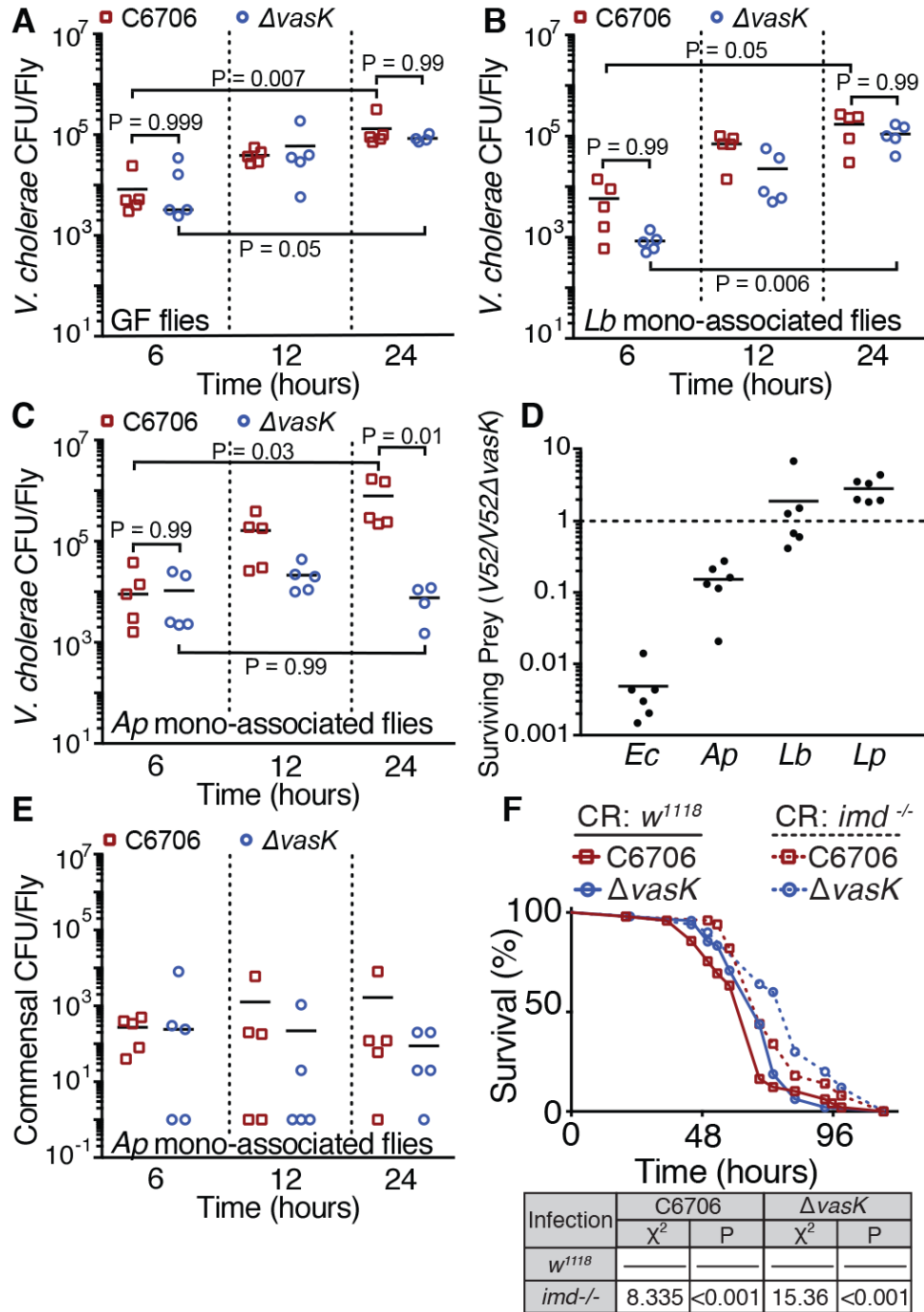


**Figure 4.4. Composition of the microbiome determines T6SS-mediated gut infection.** (A) Generation of monoassociated flies. (B–D) CFU/Fly of *V. cholerae* strains C6706 and C6706 $\Delta vasK$  of surface-sterilized (B) GF, (C) *L. brevis* monoassociated flies, and (D) *A. pasteurianus* monoassociated flies at indicated times. Each point represents a replicate of five randomly selected flies. P values are the result of Willcoxon multiple comparisons with Bonferroni correction. (E) An in vitro competitive assay between *V. cholerae* V52 and V52 $\Delta vasK$  against *E. coli* as a positive control and *A. pasteurianus*, *L. brevis*, and *L. plantarum*. Bacteria were coincubated for 4 hours at 37 °C. Surviving prey bacteria in the presence of T6SS were divided by the surviving prey in the absence of T6SS ( $\Delta vasK$ ). (F) CFU/Fly of *Ap* from flies infected with C6706 or

C6706 $\Delta$ vasK. Each point represents a biological replicate of five flies. **(G)** Survival of 5- to 6-d-old female CR *w*<sup>1118</sup> or *imd* flies infected with C6706 or C6706 $\Delta$ vasK. Tables show Long-rank (Mantel–Cox) test;  $\chi^2$  and P values are relative to *w*<sup>1118</sup> infected flies. Conventionally reared (CR), Germ free (GF), and *L. brevis* monoassociated (*Lb*), and *A. pasteurianus* monoassociated (*Ap*).

#### 4.2.5 The microbiome directly influences T6SS-dependent pathogenesis.

The T6SS contributes to the killing of *Drosophila* by *V. cholerae* (Fig. 4.1 B, C), T6SS-assisted killing of *Drosophila* requires an intestinal microbiome (Fig. 4.1D), and the T6SS specifically targets the Gram-negative symbiont *A. pasteurianus*. These observations led us to ask whether interactions between the T6SS and *A. pasteurianus* are a prerequisite for T6SS-mediated killing of the host. To test this hypothesis, we examined host viability in adult flies that we associated exclusively with *A. pasteurianus*, or *L. brevis*, and subsequently infected with C6706 or C6706 $\Delta$ vasK. For each study, we ran a parallel infection in CR flies with the same cultures of *V. cholerae*. Loss of the T6SS significantly impaired pathogenesis in each test with control, CR flies (Fig. 4.5 D–F). However, loss of the T6SS did not diminish *Vibrio* pathogenesis in adult flies that we associated exclusively with *L. brevis* (Fig. 4.5A). As *L. brevis* also fails to block host colonization by a T6SS defective C6706 strain (Fig. 4.5C), our data suggest that interactions between T6SS and *L. brevis* have minimal relevance for host viability. In contrast, we detected significant involvement of T6SS in the extermination of adults that we monoassociated with *A. pasteurianus* (Fig. 4.5B), indicating that *A. pasteurianus* is sufficient for T6SS-mediated killing of the host. We then asked whether Gram-positive commensals can protect *Drosophila* from T6SS-dependent killing of *A. pasteurianus*-associated flies. Here, we associated adult *Drosophila* with a 1:1:1 mixture of *A. pasteurianus*, *L. brevis*, and *L. plantarum*. We then challenged the flies with C6706 or C6706 $\Delta$ vasK, and measured survival rates. In this experiment, we found that Gram-positive commensals do not impact T6SS-dependent killing of the host, suggesting that the presence of the common fly commensal *A. pasteurianus* renders *Drosophila* sensitive to T6SS-dependent killing of the host irrespective of the presence of additional commensals.

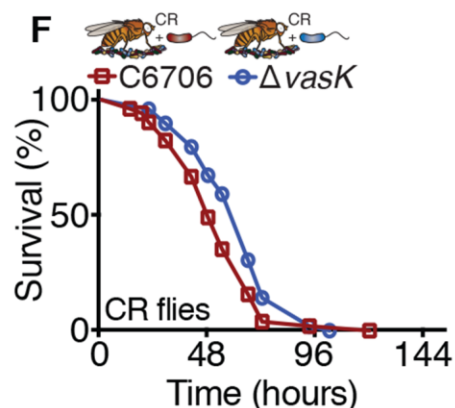
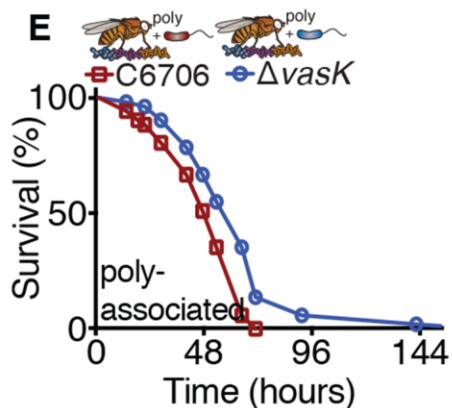
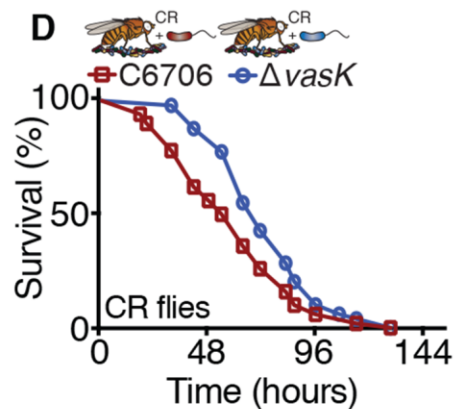
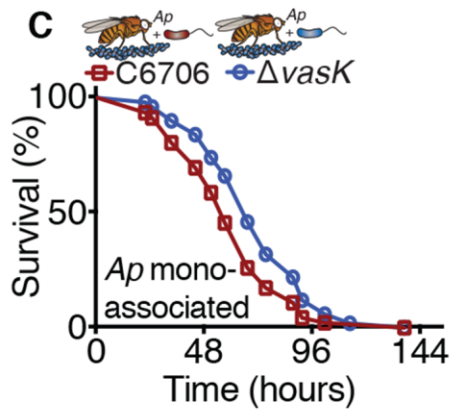
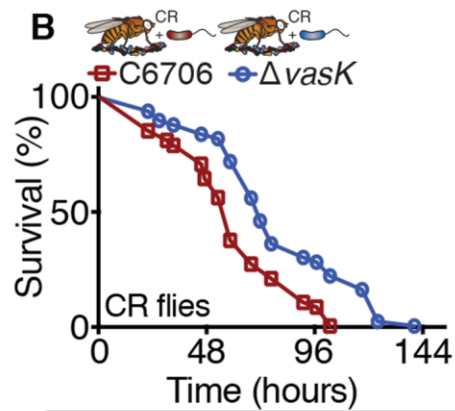
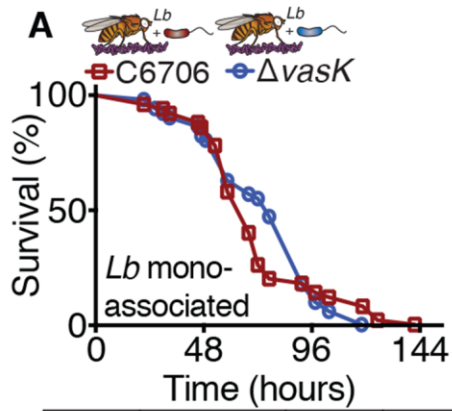




**Figure. 4.5. Composition of commensal microbes impacts T6SS virulence contributions *in vivo*.** (A) Survival curves for adult *L. brevis* monoassociated (*Lb*) flies. (B) Survival curves for adult flies monoassociated with *A. pasteurianus* (*Ap*). (C) Survival curves for adult flies polyassociated with *L. brevis*, *A. pasteurianus*, and *L. plantarum*. (D–F) Survival curves for parallel infection studies performed on conventionally reared (CR) flies. The y axis represents percent survival, and the x axis represents infection time in hours. Tables show Log-rank (Mantel–Cox) test.

### 4.3 Significance

Once ingested, enteric pathogens travel through the upper digestive system to the small intestine where they encounter the host's endogenous microbiome. This dense poly-microbial shield protects the host from colonization by harmful microbes. For example, *L. plantarum* protects the fly from *Serratia marcescens*(110) and in the mouse intestine, *E. coli* outcompetes and reduces the colonization of *Salmonella typhimurium*(289). However, despite numeric inferiority, intestinal pathogens like *V. cholerae* are able to penetrate or displace the commensal barrier. To accomplish this, *V. cholerae* and other bacteria encode a T6SS to interact with and destroy competing bacteria within its niche(231). In this chapter, we examined the consequence of interactions between the *V. cholerae* T6SS and symbiotic bacteria of *Drosophila*. We found that in the absence of the T6SS, the symbiont *A. pasteurianus* was able to limit the expansion of *V. cholerae*. However, *V. cholerae* with a fully functional T6SS was able to expand within the host and establish a more lethal infection relative to T6SS null infected counterparts. We found that the lethality of the T6SS required the presence of *A. pasteurianus* in the microbiome. Furthermore, we identified mutation of the IMD pathway extended the viability of flies infected with *V. cholerae*, implicating host secondary responses in *V. cholerae* dependent killing of the host. Collectively, the data presented in this chapter demonstrate that interactions between symbiotic bacteria and *V. cholerae* significantly impact intestinal pathogenesis, indicating that interactions between bacteria in the gut have important consequences for host health.

## Chapter 5.

### *Vibrio cholerae*-symbiont interactions inhibit intestinal repair in *Drosophila*

This chapter contains content from the following source, republished with permission:

- Fast, D., Petkau, K., Ferguson, M., Shin, M., Galenza, A., Kostiuik, B., Pukatzki, S., & Foley, E. *Vibrio*-symbiont interaction inhibit intestinal repair in *Drosophila*. *Cell Reports*, 1088-1100.e5 (2020).

Experiments shown in Figure 5.1-5.9 and Tables 5.1 & 5.2 were conceived, performed, by D.F and analyzed by D.F and E.F. Gut dissections for RNA-sequencing were performed by D.F, K.P, M.F, M.S, and A.G.

All transcriptional data generated in this chapter is available at the NCBI GEO database (GSE136069).

## 5.1 Introduction

The arrival of bacteria in the digestive tract triggers a well-defined series of defensive and regenerative responses to limit bacterial dissemination and maintain tissue homeostasis(1). Epithelial cells damaged by moribific bacteria or cytotoxic compounds are replaced through the proliferation and differentiation of intestinal progenitor cells (IPCs)(81). Despite the importance of IPC growth to intestinal homeostasis and the impact of intestinal wellbeing on host health, little is known about how interactions between bacteria influence epithelial repair programs.

To understand how bacterial interactions influence intestinal immunity, we examined the impact of the T6SS on mediators of digestive tract homeostasis. We found that despite pervasive intestinal damage, *V. cholerae* blocks critical growth and differentiation pathways in *Drosophila* IPCs. Failure to engage epithelial renewal required interactions between the *V. cholerae* T6SS and the host's endogenous microbiome, and ablation of symbiotic bacteria restored IPC proliferation in response to *Vibrio*. Finally, we show that inhibition of intestinal repair, is not the product of specific interaction between *Vibrio* and a particular symbiotic species, but instead required a complex community of intestinal symbionts. Together, the data in this chapter further highlight the contributions of the T6SS to *Vibrio* pathogenesis and demonstrate the impact of symbiont-pathogen interactions on intestinal immune responses.

## 5.2 Results

### 5.2.1 The T6SS promotes epithelial shedding.

In *Drosophila*, enteric infection results in the delamination and expulsion of damaged epithelial cells (45, 58). To test the effect of the T6SS on epithelial delamination, we measured epithelial shedding in the guts of adult *CB>mCD8::GFP* flies infected with WT *V. cholerae* (C6706) or an isogenic C6706 $\Delta$ *vasK* mutant, that carries an in-frame deletion in the essential T6SS gene that encodes the VasK protein(212). In this fly line, delaminating cells are marked with the induction of GFP(45). In chapter 4, we found that the T6SS contributes to the intestinal pathogenesis of *V. cholerae*. Based on this work, we examined epithelial cell shedding in the guts of flies infected with *V. cholerae* for 24 hours as flies have been robustly colonized by *V. cholerae* at this time point, developed disease symptoms, but remain viable. In mock-infected control flies, we observed few delaminating cells in the posterior midgut (Fig. 5.1Aa-c). In these flies, we mostly detected instances of one or two delaminating cells per gut with 90% of guts containing ten or fewer shedding cells (Fig. 5.1B). Infection with C6706 $\Delta$ *vasK* prompted an increase in shedding. Specifically, we observed clusters of GFP-positive cells that typically contained fewer than ten cells per cluster, with 40% of guts containing more than ten shedding cells (Fig 5.1Ad-f, Fig. 5.1B). Infection with C6706 caused a more severe delamination phenotype that was readily visible throughout the posterior midgut (Fig. 5.1Ag-i). In this challenge, infected guts had multiple patches of large numbers of delaminating cells. For example, whereas 5% of samples infected with C6706 $\Delta$ *vasK* had greater than 20 shedding cells in the posterior midgut, 45% of all samples infected with C6706 contained 20 or more shedding cells (Fig. 5.1B). Furthermore, challenge with C6706 caused greater than 40 shedding cells per posterior midgut in 10% of infected samples, a phenotype that was absent from intestines infected with C6706 $\Delta$ *vasK* (Fig. 5.1B). Comparisons between treatment groups confirmed that infection with C6706 not only greatly increased the number of shedding cells per area relative to unchallenged guts ( $P = 4.0 \times 10^{-6}$ ), but also increased the number of shedding cells compared to C6706 $\Delta$ *vasK* ( $P=0.007$ , Fig. 5.1C). Together, these data demonstrate that the *V. cholerae* T6SS significantly enhances epithelial shedding in infected *Drosophila* hosts.

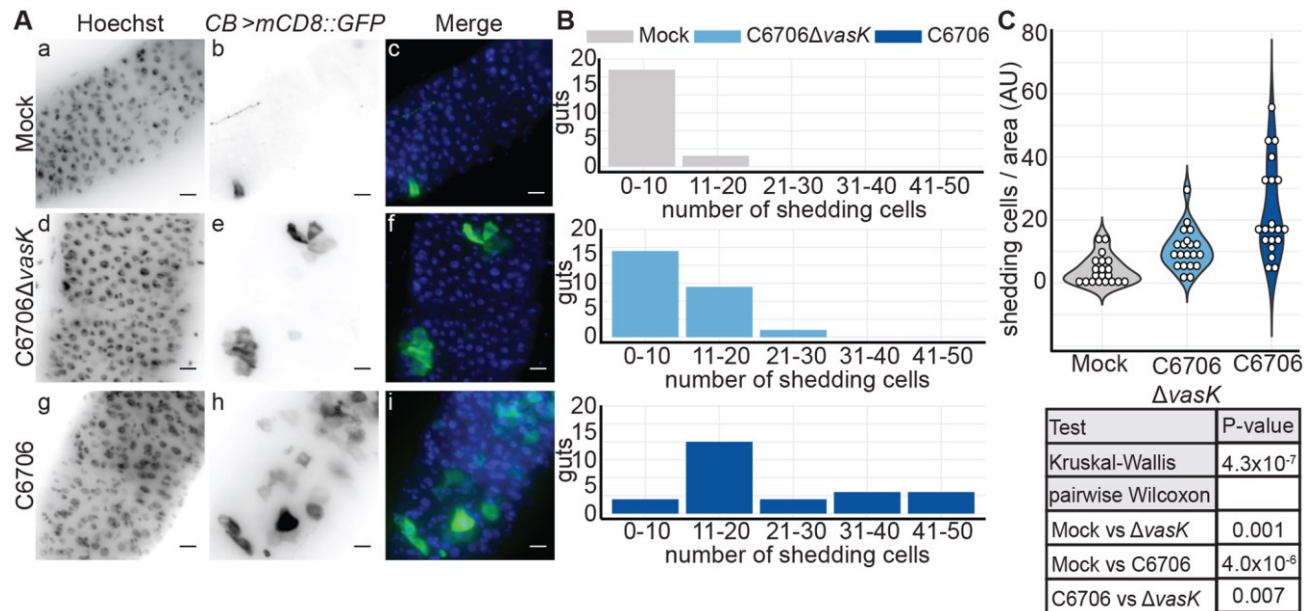


**Figure 5.1. The T6SS promotes epithelial shedding.** (A) Immunofluorescence images of the posterior midguts of *CB>mCD8::GFP* flies mock infected or infected with C6706 $\Delta vasK$ , or C6706. Hoechst marks DNA (blue) and GFP marks shedding intestinal cells (green). Scale bars are 10 $\mu$ m. (B) Histogram of the number of shedding cells in the posterior midguts from (A). (C) Quantification of shedding cells per unit surface area from (A). Each dot represents a measurement from a single fly gut.

### 5.2.2 Disrupted intestinal homeostasis in response to the T6SS.

Intestinal damage and epithelial shedding promotes compensatory growth of IPCs to maintain the epithelial barrier(81). As there was extensive T6SS-dependent sloughing of epithelial cells, we tested if the T6SS promotes homeostatic growth of IPCs. To address this, we used the *esg<sup>ts</sup>>GFP* fly line to visualize GFP-positive IPCs in sagittal sections prepared from the posterior midguts of flies infected with C6706 or C6706 $\Delta vasK$ . The midguts of control flies had a clear intestinal lumen surrounded by an intact epithelium (Fig. 5.2Aa-d). Consistent with Fig. 5.1, infection with C6706 $\Delta vasK$  stimulated a modest shedding of cellular material (asterisks) into the intestinal lumen without an apparent loss of barrier integrity (Fig. 5.2Ae-h). Challenge with C6706 once again promoted extensive shedding of epithelial cells and cellular debris into the lumen (Fig. 5.2Ai-l), as well as the appearance of numerous breaks along the basement membrane (arrowheads), suggesting pathogen-dependent damage to the epithelial barrier.

As we observed epithelial damage and shedding cells in *V. cholerae*-infected intestines, we determined if *V. cholerae* promoted compensatory growth of IPCs. In mock-infected flies, we observed the regular distribution of small GFP-positive IPCs along the basement membrane of the midgut (Fig 2Ba-d). Infection with C6706 $\Delta vasK$  caused an accumulation of GFP-positive IPCs, consistent with enhanced epithelial renewal in response to infection (Fig. 5.2B e-h). In contrast, despite extensive shedding of cellular material

(Fig 5.1) and obvious epithelial damage (Fig. 5.2A), guts challenged with C6706 did not appear to have elevated numbers of IPCs (Fig. 5.2B i-l). Instead, these cells were similar to the basal GFP-positive cells of mock infected flies (Fig 5.2Ca-d), despite an immediate proximity of luminal bacteria to the epithelium (dotted outline). Together, these results demonstrate that C6706 $\Delta$ vasK provokes shedding of intestinal cells along with the accumulation of *esg* positive IPCs in a manner consistent with a conventional intestinal immune response to pathogenic bacteria. In contrast, we did not observe signs of epithelial renewal in flies infected with C6706, despite widespread intestinal damage, raising the possibility that the *V. cholerae* T6SS uncouples epithelial shedding from intestinal regeneration.

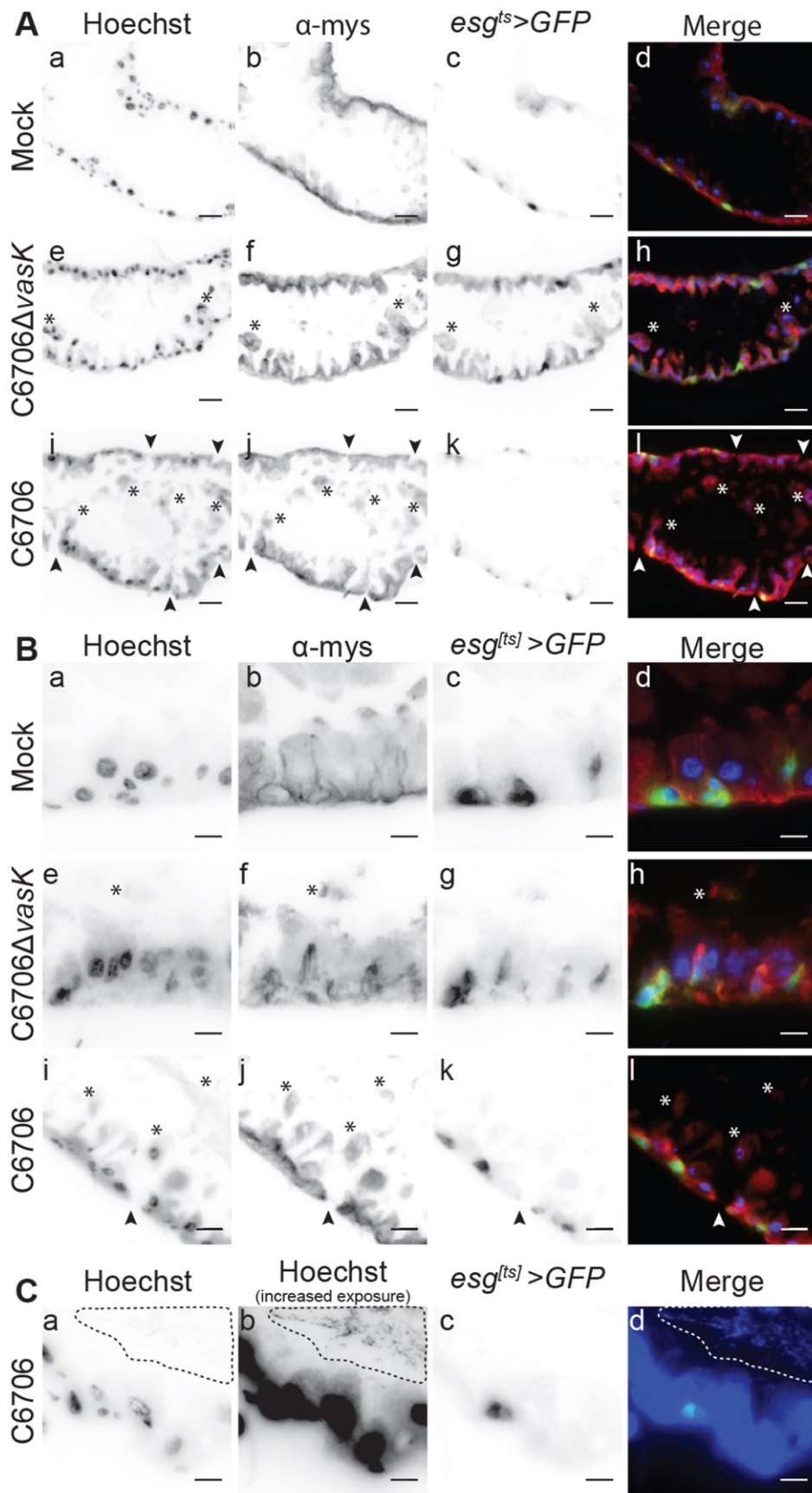


**Figure 5.2. Disrupted intestinal homeostasis in response to the T6SS. (A-C)** Immunofluorescence of sagittal sections prepared from the posterior midgut of *esg<sup>ts</sup>>GFP* flies mock infected or infected with C6706 $\Delta$ *vasK*, or C6706. Hoechst marks DNA (blue), GFP marks IPCs (green), and  $\alpha$ -mys marks the  $\beta$ -integrin, myospheroid (mys, red). Arrowheads indicate damage to the intestinal epithelium and asterisks denote cellular matter in the lumen. **(C)** Visualization of intestinal bacteria via increased exposure of Hoechst stain. The dotted line circles bacteria in the lumen. Scale bars are **(A)** 25 $\mu$ m and **(B & C)** 10 $\mu$ m.

### 5.2.3 The T6SS modifies IPC transcriptional responses to *V. cholerae*.

Given the apparent absence of IPC growth in C6706-infected flies, we used RNA sequencing (RNA-seq) analysis to identify the intestinal response to infection with C6706 (Fig. 5.3). We found that the host response to C6706 is characterized by the activation of antibacterial defenses, re-programming of metabolic pathways, and the expression of a large cohort of genes required for the generation and assembly of mature ribosomes. Many of these responses match our understanding of the fly transcriptional response to pathogenic bacteria (Fig. 5.3, Table 5.1)(19, 290, 291). However, and in contrast to classical responses to enteric challenge, we did not detect changes in mRNA levels characteristic of JAK-STAT or EGF responses, two pathways that are intimately linked with homeostatic renewal of a damaged epithelium.



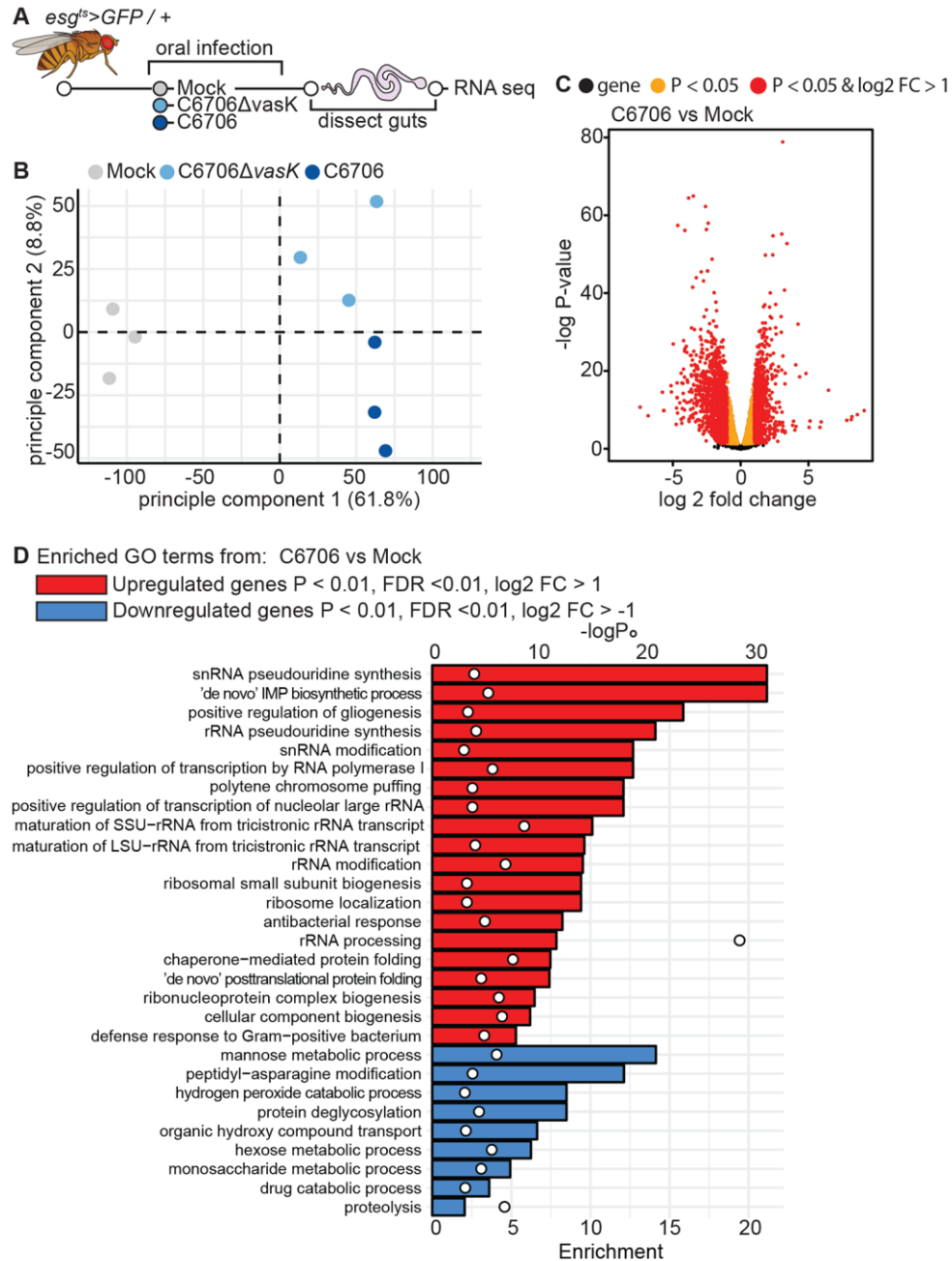


**Figure 5.3. The T6SS modifies whole gut transcriptional responses to *V. cholerae*.** (A) Schematic representation of the RNA-sequencing of *V. cholerae* infected guts. (B) Principle component analysis from the counts per million obtained from RNA-sequencing of guts dissected from mock infected flies or flies infected with C6706 or C6706ΔvasK. (C) Volcano plot of differentially expressed genes from comparison of C6706 to Mock. Each dot represents a single gene. Yellow indicates a P<0.05 and red indicates P<0.05 and log<sub>2</sub> fold change >1 or <-1. (D) Gene Ontology (GO) analysis from the top 500 up or down regulated differentially expressed genes (P<0.01, false discovery rate (FDR) <0.01, and log<sub>2</sub> fold change >1 or <-1) from comparisons of C6706 to Mock. Bars (bottom X-axis) represent enrichment scores and circles (top X-axis) represent -logP values for each enriched GO term.

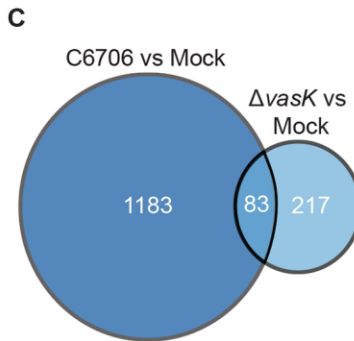
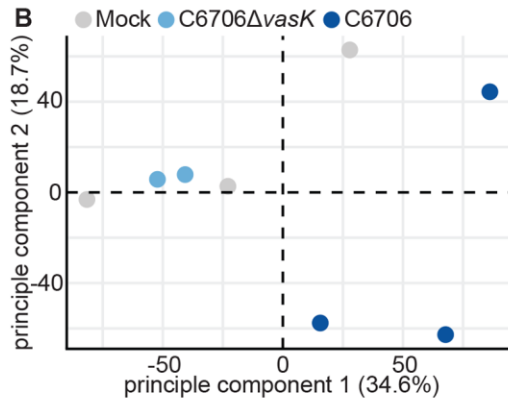
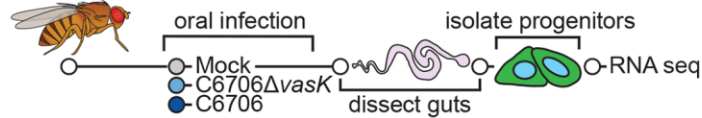
gene	log2 fold change	function	annotation	gene	log2 fold change	function	annotation
<i>wech</i>	1.03	adhesion	intergrin	<i>bbg</i>	-1.10	adhesion	septate junction
<i>pasi2</i>	1.03	adhesion	septate junction	<i>Cad89D</i>	-3.28	adhesion	cadherin
<i>cold</i>	1.04	adhesion	septate junction	<i>ItgaPS4</i>	-1.01	adhesion	intergrin
<i>ruX</i>	1.08	cell cycle	CDK inhibitor	<i>Tsp42Ef</i>	-1.04	adhesion	septate junction
<i>Atg13</i>	1.07	metabolism	autophagy	<i>Cdk1</i>	-2.24	cell cycle	M phase
<i>Atg6</i>	1.00	metabolism	autophagy	<i>Cdk4</i>	-1.13	cell cycle	S phase
<i>Atg8a</i>	1.04	metabolism	autophagy	<i>cort</i>	-1.64	cell cycle	APC/C
<i>cbt</i>	1.17	signaling	dpp	<i>PCNA2</i>	-1.55	cell cycle	S phase
<i>dpp</i>	1.01	signaling	dpp	<i>insc</i>	-1.39	cell division	asymmetric
<i>lilli</i>	1.11	signaling	dpp	<i>msd1</i>	-1.99	cell division	spindle assembly
<i>salm</i>	1.09	signaling	dpp	<i>Nnf1b</i>	-1.18	cell division	kinetochore
<i>salr</i>	1.21	signaling	dpp	<i>pav</i>	-2.67	cell division	cytokinesis
<i>tkv</i>	1.06	signaling	dpp	<i>tum</i>	-1.97	cell division	cytokinesis
<i>ebd1</i>	1.09	signaling	Wnt	<i>brk</i>	-1.32	signaling	dpp
<i>Hsp22</i>	2.73	stress response	heat shock protein	<i>Dh31</i>	-1.26	signaling	diuretic hormone
<i>Hsp23</i>	2.00	stress response	heat shock protein	<i>Pvr</i>	-1.14	signaling	RTK
<i>Hsp26</i>	2.44	stress response	heat shock protein	<i>Ror</i>	-2.08	signaling	RTK
<i>Hsp27</i>	2.05	stress response	heat shock protein	<i>tor</i>	-1.51	signaling	RTK
<i>Hsp67Bc</i>	1.97	stress response	heat shock protein				
<i>Hsp68</i>	4.08	stress response	heat shock protein				
<i>Hsp70Aa</i>	3.08	stress response	heat shock protein				
<i>Hsp70Ab</i>	3.07	stress response	heat shock protein				
<i>Hsp70Ba</i>	3.93	stress response	heat shock protein				
<i>Hsp70Bb</i>	3.26	stress response	heat shock protein				
<i>Hsp70Bbb</i>	3.26	stress response	heat shock protein				
<i>Hsp70Bbc</i>	3.28	stress response	heat shock protein				
<i>GATAe</i>	1.02	transcription	intestinal homeostasis				

**Table 5.1. The T6SS promotes a unique transcriptional response from the intestine.** Representative genes involved in intestinal homeostasis, growth, and stress responses differentially regulated in response to C6706 relative to C6706 $\Delta$ *vasK* from RNA-seq of *Drosophila* whole guts.

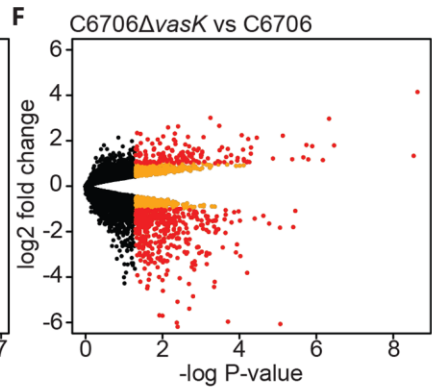
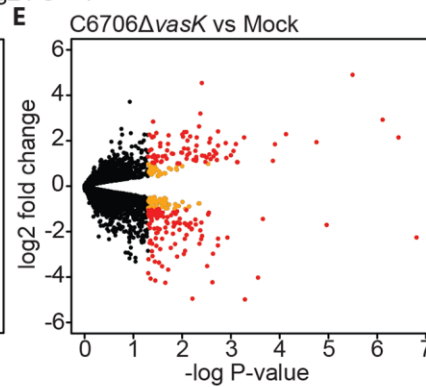
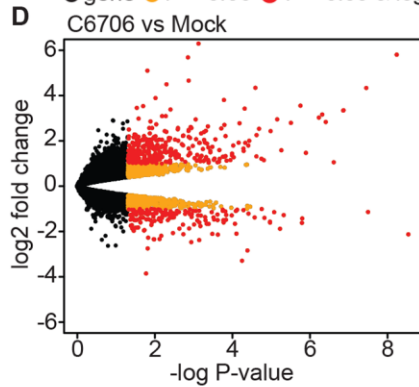
The apparent absence of homeostatic growth signals in C6706-infected intestines prompted us to directly determine the transcriptional response of IPCs to *V. cholerae* infection. For this experiment, we performed RNA-seq on IPCs purified from the guts of adult *esg<sup>ts</sup>/+* flies that we challenged with C6706 or C6706 $\Delta$ *vasK* (Fig. 5.4). As a control, we sequenced the transcriptome of purified IPCs from uninfected *esg<sup>ts</sup>/+* flies. Principle component analysis showed that samples from uninfected flies and those from flies infected with C6706 $\Delta$ *vasK* grouped relatively closely. In contrast, samples from C6706-infected flies grouped away from both uninfected and C6706 $\Delta$ *vasK*-infected flies (Fig. 5.4B). Differential gene expression analysis confirmed minimal overlaps between the transcriptomes of C6706 and C6706 $\Delta$ *vasK*-infected flies relative to uninfected controls (Fig. 5.4C). From there, we examined Gene Ontology (GO) term enrichment among the differentially upregulated and downregulated genes. Here, we also compared C6706 $\Delta$ *vasK* to C6706 to identify changes in IPC transcriptional responses specific to the T6SS (Fig. 5.4F). Of note, comparison of the transcription profile of C6706-challenged IPCs relative to uninfected IPCs revealed a downregulation of biological processes involved in growth and mitosis. This included a significant downregulation of processes such as cell proliferation and nuclear division (Fig. 5.4G). In contrast, this downregulation of growth processes was absent when we compared the transcriptional profile of

C6706 $\Delta$ *vasK*-infected IPCs to that of uninfected IPCs (Fig. 5.4H). Instead, we detected a significant enrichment of mitotic processes in flies infected with C6706 $\Delta$ *vasK* relative to flies challenged with C6706 (Fig. 5.4I). Together, these data suggest that IPCs have distinct transcriptional responses to wildtype and T6SS-deficient *V. cholerae*. In particular, we found that the T6SS inhibits the expression of genes required for growth and renewal of the epithelium.

**A** *esg<sup>ts>GFP/+</sup>*

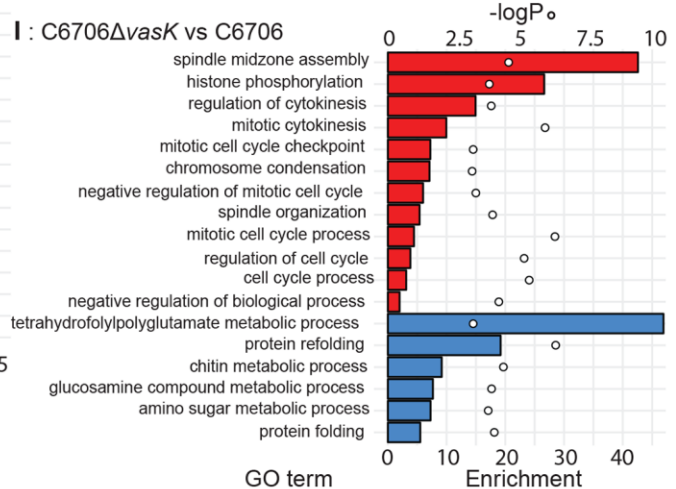
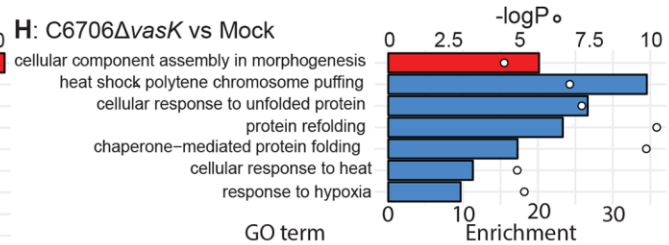
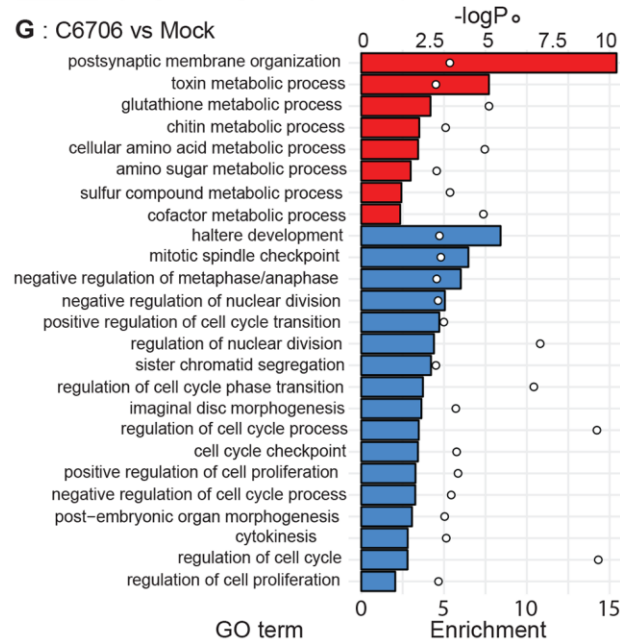


● gene ● P < 0.05 ● P < 0.05 & log<sub>2</sub> FC > 1



Enriched GO terms from:

■ Upregulated genes (P < 0.05) ■ Downregulated genes (P < 0.05)





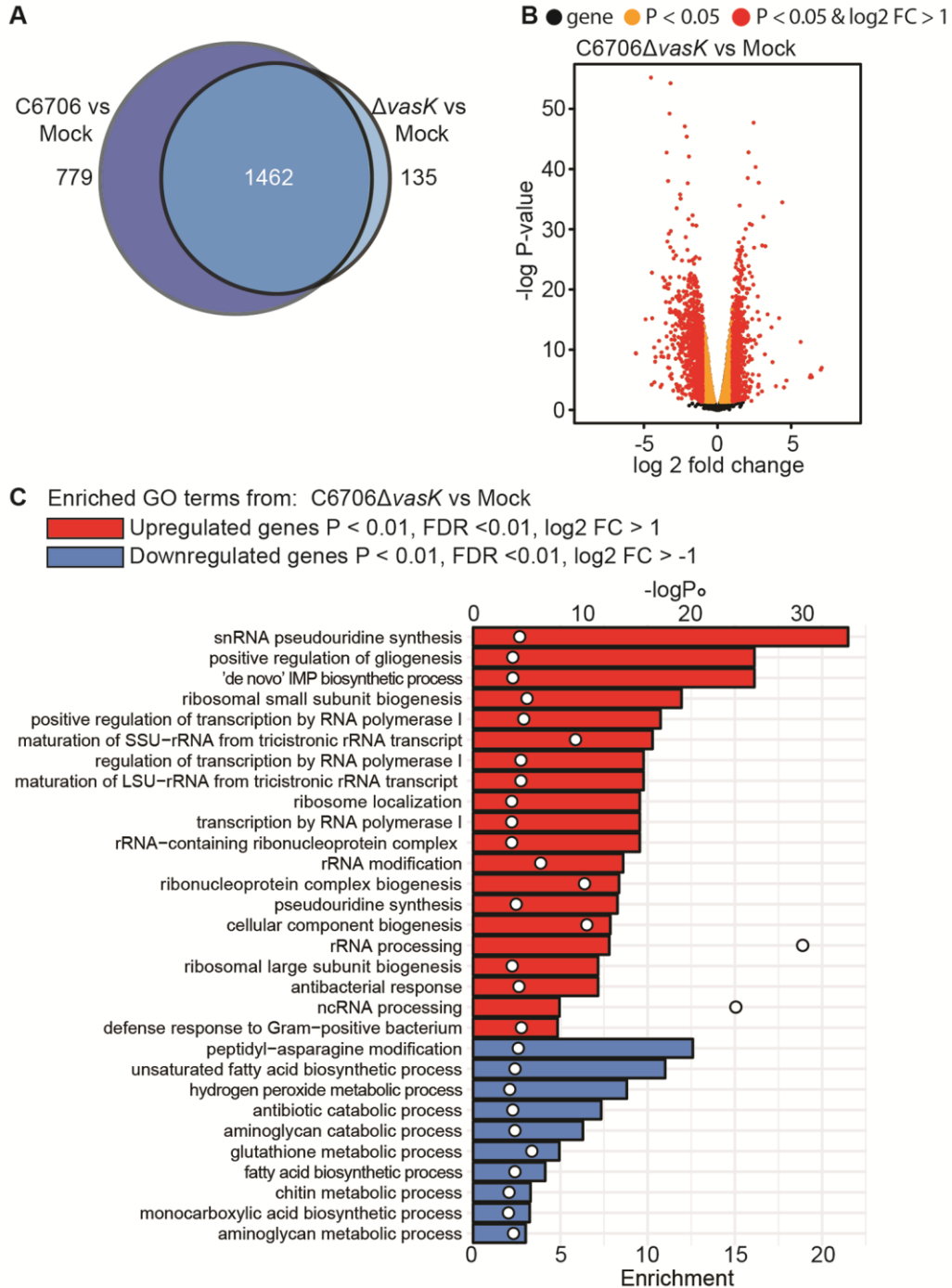


**Figure 5.5. The whole gut transcriptional responses to C6706 $\Delta vasK$ .** (A) Venn diagram of differentially expressed genes ( $P < 0.01$ ,  $FDR < 0.01$ , and  $\log_2$  fold change  $> 1$  or  $< -1$ ) from comparisons of C6706 to Mock and C6706 $\Delta vasK$  to Mock. (B) Volcano plot of differentially expressed genes from comparison of C6706 $\Delta vasK$  to Mock. Each dot represents a gene. Yellow indicates a  $P < 0.05$  and red indicates  $P < 0.05$  and  $\log_2$  fold change  $> 1$  or  $< -1$ . (C) Gene Ontology (GO) analysis from the top 500 up or down regulated differentially expressed genes ( $P < 0.01$ ,  $FDR < 0.01$ , and  $\log_2$  fold change  $> 1$  or  $< -1$ ) from comparisons of C6706 $\Delta vasK$  to Mock. Bars (bottom X-axis) represent enrichment scores and circles (top X-axis) represent  $-\log P$  values for each enriched GO term.

#### 5.2.4 IPCs fail to facilitate epithelial repair upon intestinal challenge with *V. cholerae*.

Epithelial damage activates the JAK/STAT and EGF pathways to stimulate epithelial repair. We observed increased levels of mRNA of several genes indicative of JAK/STAT and EGF pathway activation in IPCs from C6706 $\Delta$ *vasK*-infected flies compared to those from C6706-infected counterparts (Fig. 5.6A). Furthermore, infection with C6706 $\Delta$ *vasK* led to an increase in the expression of cell cycle activators in the IPC population (Figure 5.6A). These data suggest enhanced IPC growth in progenitors of flies challenged with C6706 $\Delta$ *vasK* relative to C6706. Indeed, we observed the transcription signature of diminished EGF and JAK/STAT activity in IPCs purified from flies infected with C6706 relative to IPCs purified from uninfected controls. Specifically, we noted diminished expression of the EGF pathway transcription factor *pointed* (*pnt*) and the EGF receptor (*EGFR*) itself in IPCs from flies infected with C6706 compared to IPCs from uninfected controls (Fig. 5.6A). Similarly, we noted a reduction in the relative proportions of mRNAs that encode central components of the JAK/STAT pathway. In the JAK/STAT pathway, binding of interleukin-like ligands to the receptor Domeless (*dome*) induces signaling through the kinase Hopscotch (*hop*), and results in the transcription of *Socs36E(80)*. We observed diminished mRNA levels of all three of these signaling components in IPCs from C6706-challenged flies relative to uninfected controls. Furthermore, we detected significant drops in mRNA that encode prominent cell cycle genes, such as the CDC25 ortholog, *string*, the S-phase *cyclin dependent kinase 2* (*Cdk2*), and the essential M phase cyclin *CyclinB3* (*CycB3*) (Fig. 5.6A). In summary, we detected T6SS-dependent decreases in mRNA of genes in pathways responsible for epithelial renewal alongside diminished levels of cell cycle genes, consistent with a failure of intestinal renewal in flies infected with WT *V. cholerae*.

To directly test this hypothesis, we examined IPC growth in guts infected with C6706, or with C6706 $\Delta$ *vasK*, in two different functional assays. First, we quantified the number of IPCs per area in guts of infected flies as a measure of IPC expansion. As a control, we quantified the number of IPCs in guts of flies infected with the Gram-negative fly pathogen *Ecc15*, a known activator of IPC growth(18). In agreement with previous reports, infection with *Ecc15* promoted a significant increase in the number of IPCs per area ( $P=0.04$ , Fig. 5.6B, C). Similarly, guts infected with C6706 $\Delta$ *vasK* had greater numbers of IPCs per area than uninfected controls ( $P=0.004$ , Fig. 5.6B, C). This phenotype was not specific to the *vasK* T6SS mutation, as we observed a near-identical expansion of IPCs in intestines challenged with *V. cholerae* with a null mutation in the *vipA* gene, an essential component of the T6SS outer sheath ( $P=0.013$ , Fig. 5.6B, C)(260). In contrast, guts infected with C6706 had significantly fewer IPCs per area than guts infected with either C6706 $\Delta$ *vasK* or C6706 $\Delta$ *vipA* ( $P<0.001$  and  $P<0.003$  respectively, Fig. 5.6B, C). Furthermore, there was no difference in the number of IPCs per area between uninfected flies and those infected with C6706 ( $P=0.985$ ,


Fig. 5.6B, C), indicating a failure of renewal that requires the T6SS. Next, we quantified mitotic PH3 positive cells in the posterior midguts of two different wildtype fly strains, *w<sup>1118</sup>*, and Oregon R, that we infected with C6706 $\Delta$ *vasK* or C6706. In both fly backgrounds, infection with C6706 $\Delta$ *vasK* prompted an increase in the number of mitotic cells in the posterior midgut. In contrast, both wildtype fly strains had significantly fewer mitotic cells in C6706-infected guts compared to C6706 $\Delta$ *vasK*-challenged counterparts (P=0.04 and P=0.002, Fig. 5.6D, E).

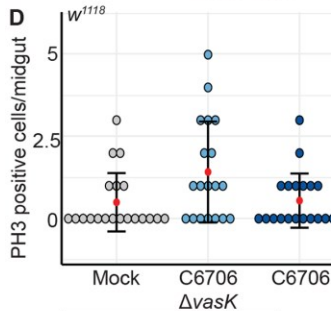
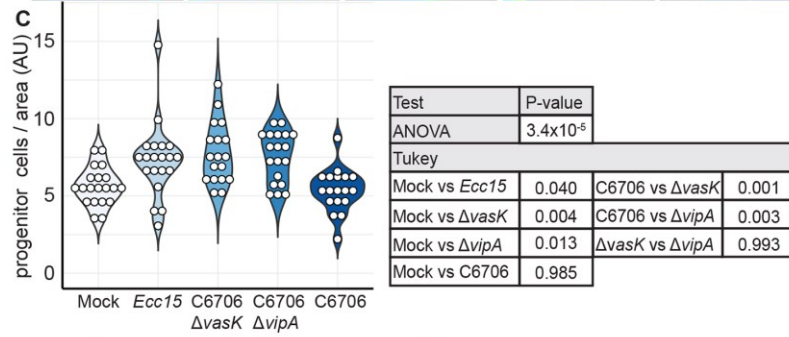
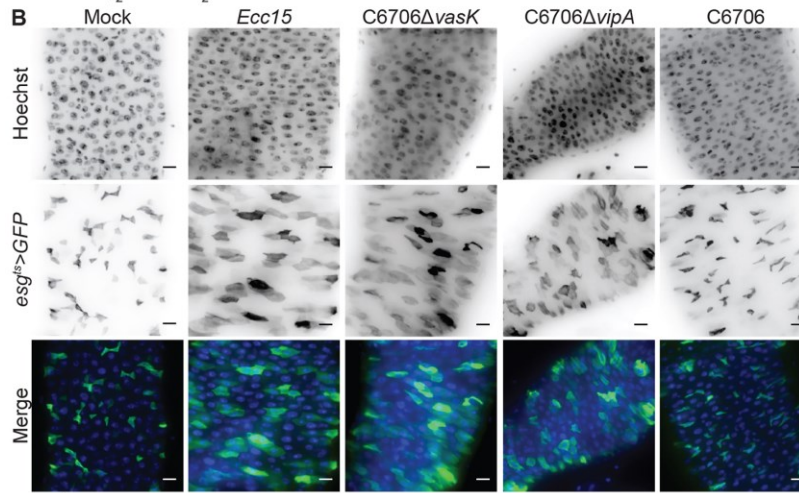
Collectively, these data demonstrate that the transcriptional response of IPCs to *V. cholerae* is significantly altered by the presence of a functional T6SS. This difference in response to the T6SS is highlighted by a significant downregulation of pathways critical for intestinal renewal, diminished IPC proliferation, and failed epithelial regeneration.



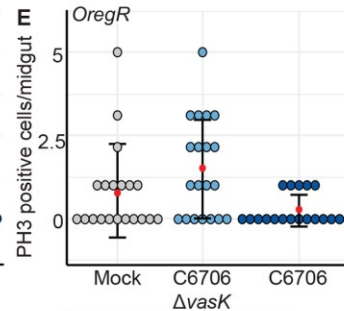
**A**

gene name	function	C6706 vs Mock	C6706ΔvasK vs Mock	C6706ΔvasK vs C6706	gene name	function	C6706 vs Mock	C6706ΔvasK vs Mock	C6706ΔvasK vs C6706
<b>EGF</b>					<b>regulation of cell cycle</b>				
<i>aos</i>	signaling	-1.29	---	1.22	<i>borr</i>	mitosis	-1.87	---	1.49
<i>rau</i>	signaling	-1.14	---	1.28	<i>stg</i>	cell cycle	-1.60	---	1.35
<i>pnt</i>	transcription	-1.02	---	0.95	<i>CycB3</i>	cell cycle	-1.45	---	---
<i>EGFR</i>	signaling	-0.95	---	---	<i>pav</i>	mitosis	-1.43	---	1.24
<i>mkp3</i>	signaling	-0.91	---	0.84	<i>Mcm7</i>	DNA replication	-1.39	---	---
<i>sty</i>	signaling	-0.77	---	0.71	<i>Cdk2</i>	cell cycle	-1.19	---	---
<i>cic</i>	transcription	-0.55	---	---	<i>BubR1</i>	cell cycle	-1.05	---	1.12
<i>cbl</i>	signaling	-0.47	---	---	<i>polo</i>	mitosis	-1.00	---	0.95
<b>JAK/STAT</b>					<i>fzr</i>	cell cycle	-0.72	---	0.72
<i>hop</i>	signaling	-0.79	---	0.69	<i>Mcm2</i>	DNA replication	-0.70	---	0.73
<i>Socs36E</i>	signaling	-0.65	---	0.63	<i>CycD</i>	cell cycle	-0.47	---	0.54
<i>dome</i>	signaling	-0.62	---	0.68					

log2 fold change 



Test	P-value
ANOVA	0.02
Tukey	
Mock vs <i>ΔvasK</i>	0.03
Mock vs C6706	0.98
C6706 vs <i>ΔvasK</i>	0.04



Test	P-value
Kruskal-Wallis	0.007
pairwise Wilcoxon	
Mock vs <i>ΔvasK</i>	0.09
Mock vs C6706	0.13
C6706 vs <i>ΔvasK</i>	0.002

**Figure 5.6. IPCs fail to facilitate epithelial repair upon intestinal challenge with *V. cholerae*.** (A) Genes that regulate IPC growth and cell cycle from RNA-seq of IPCs of flies mock infected or infected with C6706 or C6706 $\Delta$ *vasK*. (B) Immunofluorescence of the posterior midguts of *esg<sup>ts</sup>>GFP* flies mock infected or infected with *Ecc15*, C6706 $\Delta$ *vasK*, C6706 $\Delta$ *vipA*, or C6706. Hoechst marks DNA (blue) and GFP marks *esg* positive IPCs (green). Scale bars are 10 $\mu$ m. (C) Quantification of the number of IPCs per unit surface area from (B). Each dot represents a measurement from a single fly gut. (D-E) Quantification of the number of PH3 positive cells in the posterior midguts of (D) *w<sup>1118</sup>* or (E) *OregR* flies that were mock infected or infected with C6706 $\Delta$ *vasK*, or C6706.

### 5.2.5 Impaired IPC differentiation in response to the T6SS

IPC proliferation is accompanied by signals through the Notch-Delta axis that direct the generation and differentiation of transitory enteroblasts(7, 8, 11). Our analysis of the RNA-seq data suggested T6SS-dependent effects on Notch pathway activity. For example, we detected an increase in the levels of mRNA of the Notch-response gene, *Enhancer of split (E(spl))*, as well as *Delta (Dl)* itself in IPCs from C6706 $\Delta$ *vasK*-infected guts relative to C6706-infected guts (Fig. 5.7A). Furthermore, we noticed a suppression of *E(spl)* genes and *Dl* in IPCs from flies infected with C6706 compared to uninfected controls (Fig. 5.7A). As genes in the *E(spl)* complex are primary transcriptional targets of the Notch pathway, these data suggest a potential impairment of IPC differentiation programs by the T6SS(293).

To test if IPC differentiation responds differently to the presence of a T6SS, we quantified the number of enteroblasts and stem cells in the posterior midguts of *esgGAL4, UAS-CFP; Su(H)-GFP* flies that we infected with C6706 or C6706 $\Delta$ *vasK*. In the absence of infection, we detected approximately equal numbers of intestinal stem cells (CFP-positive, GFP-negative) and enteroblasts (EB) (CFP-positive, GFP-positive) in the posterior midgut (Fig. 5.7B, D, E). Consistent with Figure 4, infection with C6706 $\Delta$ *vasK* stimulated an expansion of IPCs (Fig. 5.7B, C). This expansion of IPCs was the result of an increased population of enteroblasts ( $P = 0.0004$ , Fig. 5.7E), not stem cells (Fig. 5.7D), consistent with the generation of undifferentiated enteroblasts required to renew the intestinal epithelium. In contrast, guts infected with C6706 contained significantly fewer IPCs per area than their C6706 $\Delta$ *vasK*-infected counterparts ( $P = 0.0003$ , Fig. 5.7B, C). There was no difference in the number of intestinal stem cells between C6706 or C6706 $\Delta$ *vasK* infected guts (Fig. 5.7D). Instead, there was a significant drop in the number of enteroblasts per unit area in guts challenged with C6706 relative to those infected with C6706 $\Delta$ *vasK* ( $P = 0.005$ , Fig. 5.7B, E), indicating that the T6SS likely prevents the generation of enteroblasts.

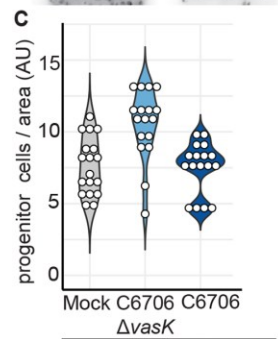
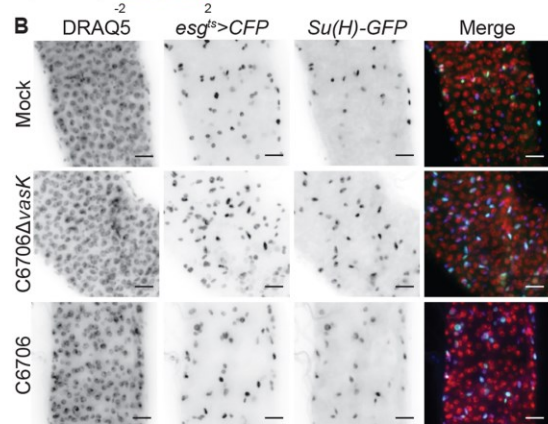
Together, the data presented here uncover a T6SS-dependent failure of epithelial renewal in *V. cholerae*-infected flies. We find that flies activate conventional growth and differentiation programs in response to C6706 $\Delta$ *vasK*. This response is absent from intestines challenged with pathogenic *V. cholerae* with a functional T6SS. Instead, we find that despite extensive damage and increased epithelial shedding,

IPCs fail to induce genes required for IPC proliferation. This failure of gene expression was accompanied by a lack of ISC proliferation along with an absence of enteroblast differentiation, culminating in impaired epithelial regeneration.

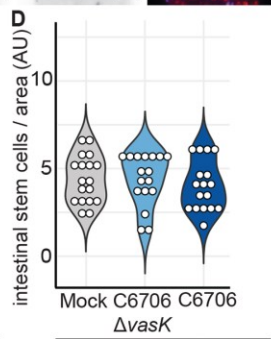
**A**

gene name	function	C6706 vs Mock	C6706 $\Delta$ vasK vs Mock	C6706 $\Delta$ vasK vs C6706
<b>Notch</b>				
<i>Dl</i>	signaling	-1.56	—	1.13
<i>E(spl)m6-BMF</i>	protein binding	-1.51	—	1.57
<i>pon</i>	cell fate	-1.48	—	1.70
<i>ct</i>	transcription	-1.41	—	—
<i>E(spl)m5-HLH</i>	DNA binding	-1.25	—	1.46
<i>E(spl)m7-HLH</i>	DNA binding	-0.95	—	1.39
<i>E(spl)m3-HLH</i>	DNA binding	-0.90	—	—
<i>E(spl)mY-HLH</i>	DNA binding	—	—	0.73

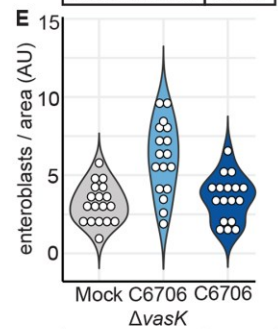
log<sub>2</sub> fold change



Test	P-value
ANOVA	$8.7 \times 10^{-6}$
Tukey	
Mock vs $\Delta$ vasK	0.0004
Mock vs C6706	0.992
C6706 vs $\Delta$ vasK	0.0003



Test	P-value
ANOVA	0.632
Tukey	
Mock vs $\Delta$ vasK	0.990
Mock vs C6706	0.680
C6706 vs $\Delta$ vasK	0.669



Test	P-value
Kruskal-Wallis	0.07
pairwise Wilcoxon	
Mock vs $\Delta$ vasK	0.0005
Mock vs C6706	1.00
C6706 vs $\Delta$ vasK	0.005

**Figure 5.7. Impaired IPC differentiation in response to the T6SS. (A)** Differentially regulated genes in the Notch signaling pathway, from RNA-sequencing of IPCs from flies mock infected or infected with C6706 $\Delta vasK$  or C6706 **(B)** Immunofluorescence of the posterior midguts of *esg<sup>ts</sup>>CFP*, *Su(H)-GFP* flies mock infected or infected with C6706 $\Delta vasK$ , or C6706. DRAQ5 marks DNA (red), CFP marks *esg* positive IPCs (blue), and GFP marks *Su(H)* positive enteroblasts. Scale bars are 10 $\mu$ m. **(C)** Quantification of the number of IPCs (CFP-positive), per unit surface area from **(B)**. Each dot represents a measurement from a single fly gut. **(D)** Quantification of the number of intestinal stem cells (CFP-positive, GFP-negative) per unit surface area from **(B)**. **(E)** Quantification of the number of enteroblasts (CFP-positive, GFP-positive) per unit surface area from **(B)**.

### 5.2.6 T6SS-dependent failure in epithelial renewal requires intestinal symbionts.

T6SS effectors are toxic to eukaryotic and prokaryotic cells(238). For example, interactions between the *V. cholerae* T6SS and eukaryotic cells have been implicated in intestinal inflammation, and interactions between the T6SS and the endogenous microbiome are linked to the virulence of *V. cholerae* (166, 250). This prompted us to ask if the IPC response to the T6SS is a function of direct interactions between the T6SS and host cells, or instead requires interactions between the T6SS and the intestinal microbiota.

To test this, we measured epithelial renewal in the guts of GF flies that were infected with C6706 or C6706 $\Delta vasK$ . Flies were considered GF if commensal load was eliminated below the limit of detection such that no microbial colonies were visible upon plating whole fly homogenates on agar permissive for the growth of *Drosophila* symbiotic species. Similar to CR flies, infection of GF flies with C6706 $\Delta vasK$  stimulated an expansion of IPCs relative to uninfected controls ( $P < 0.01$ , Fig. 5.8A, B). Enteric infection of GF flies with C6706 resulted in an expansion of IPCs in a manner nearly identical to that of C6706 $\Delta vasK$ -infected intestines. Indeed, we found no significant difference in the number of IPCs per area between C6706 and C6706 $\Delta vasK$ -infected GF flies ( $P = 0.658$ , Fig. 5.8A, B). To test if interactions between the T6SS and the gut microbiota prevent infection-dependent induction of epithelial renewal, we generated germ-free flies by two different methods and measured epithelial regeneration in guts infected with C6706. Specifically, we measured the number of IPCs per area in adult germ-free flies that we generated either by administration of antibiotics to adult flies, or by hypochlorite dechoriation and sterilization of embryos. Here, we found that infection with C6706 promoted a significant expansion of IPCs, regardless of the method used to generate germ-free flies ( $P=0.0004$ ,  $P=0.001$ , Fig. 5.8C), and there was no significant difference in the number of IPCs per area between antibiotic-treated or axenic flies infected with C6706 ( $P = 0.950$ , Fig. 5.8C). Together these results indicate that interactions between the T6SS of *V. cholerae*, and the endogenous microbiome of *Drosophila*, prevent the activation of conventional epithelial repair pathways.

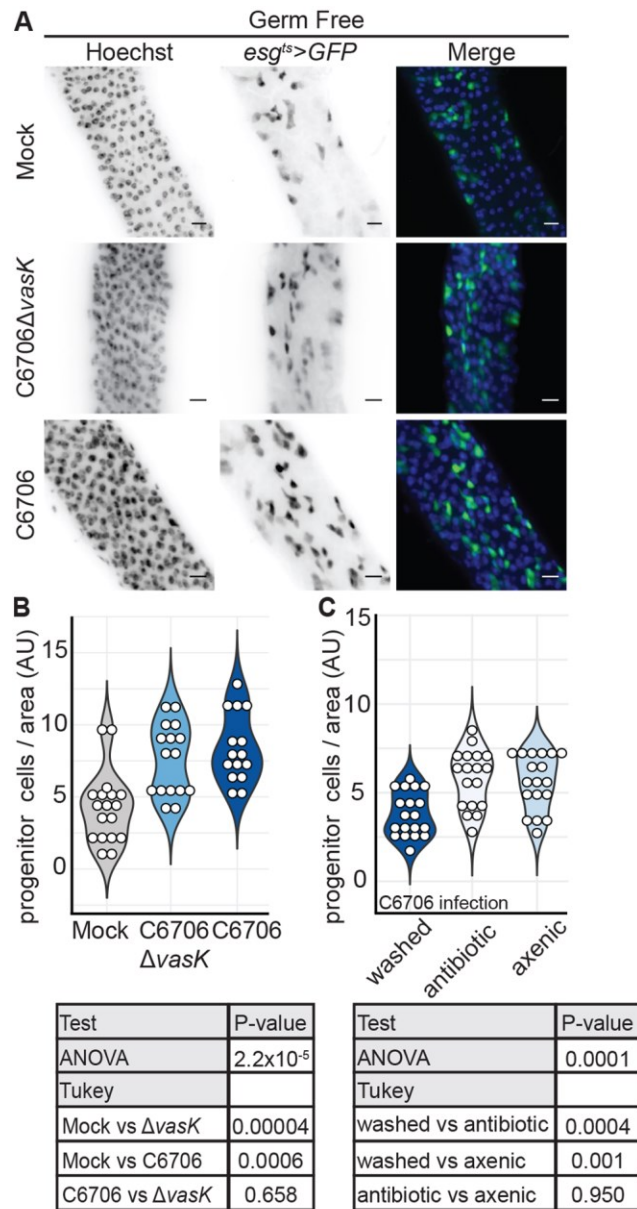


**Figure 5.8. IPC suppression of growth in response to the T6SS requires intestinal symbionts.** (A) Immunofluorescence of the posterior midguts of germ free *esg<sup>ts</sup>>GFP* flies mock infected or infected with C6706 $\Delta vasK$ , or C6706. Hoechst marks DNA (blue) and GFP marks *esg* positive IPCs (green). Scale bars are 10 $\mu$ m. (B) Quantification of the number of IPCs per unit surface area from (A). Each dot represents a measurement from a single fly gut. (C) Quantification of the number of IPCs per unit surface area in *esg<sup>ts</sup>>GFP* flies infected with C6706. Flies were made germ-free either by the administration of antibiotics to adults (antibiotic) or by bleaching of embryos (axenic).

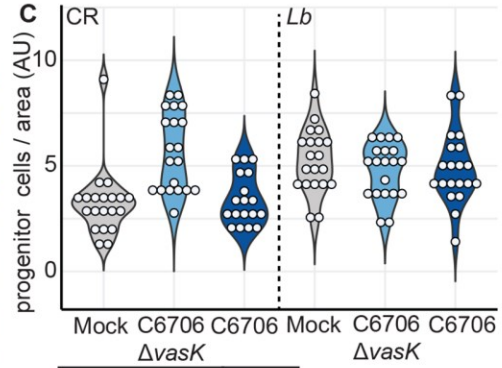
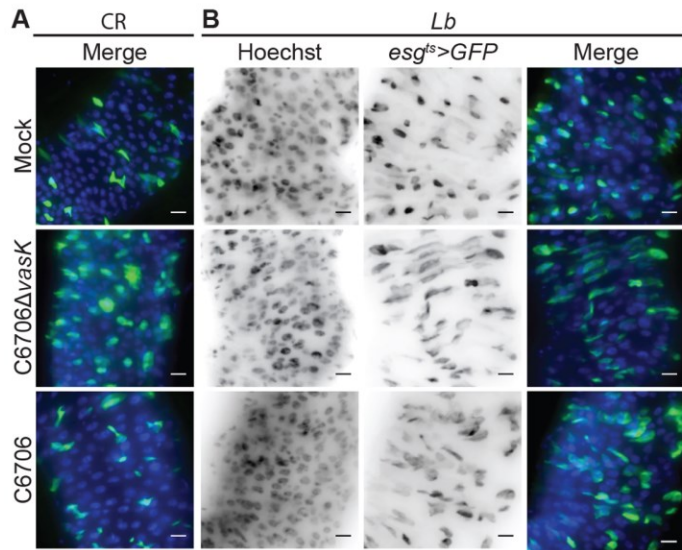
### 5.2.7 T6SS suppression of epithelial renewal requires higher-order microbiome interactions.

As the failure of epithelial renewal in response to the T6SS requires gut microbes, we asked if interactions with specific members of the *Drosophila* microbiome were responsible for T6SS-mediated loss of epithelial regeneration. We previously showed that the T6SS of *V. cholerae* targets the Gram-negative

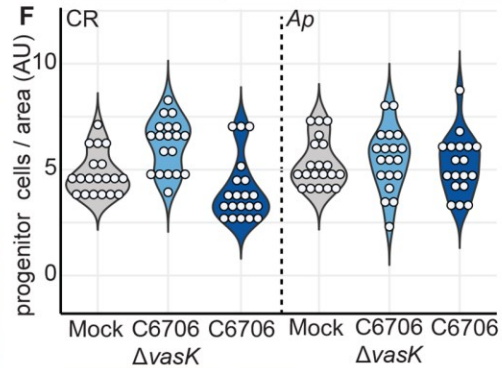
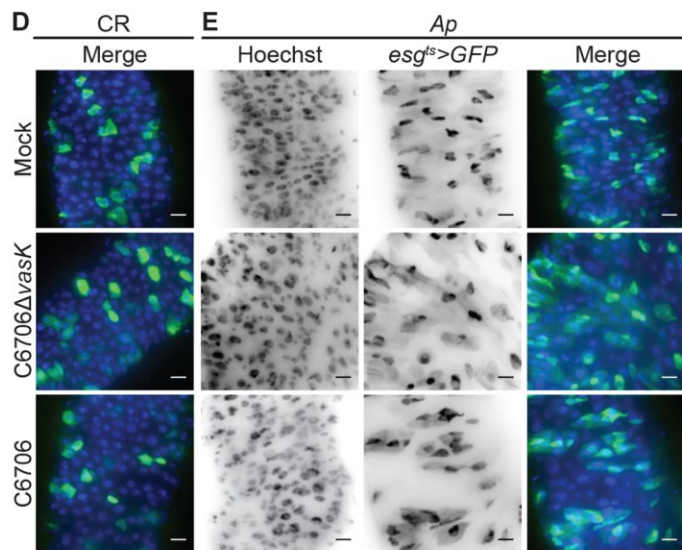
fly symbiont *A. pasteurianus* for destruction, while the Gram-positive symbiont *L. brevis* is refractory to T6SS-mediated elimination. As *L. brevis* is insensitive to the T6SS, we hypothesized that interactions between C6706 and *L. brevis* would fail to prevent epithelial repair. To test this hypothesis, we measured the number of IPCs in the guts of infected adult flies that we associated exclusively with *L. brevis*. For each bacterial association, we performed a parallel control infection of CR flies with the same cultures of C6706 and C6706 $\Delta$ vasK. In each control infection, C6706 $\Delta$ vasK promoted a regenerative response that significantly increased the number of IPCs. In contrast, challenge with C6706 consistently impaired IPC proliferation (Fig. 5.9A,C,D,F, G, I). We observed similar amounts of epithelial renewal in the intestines of *L. brevis* mono-associated flies infected with C6706 or C6706 $\Delta$ vasK (Fig. 5.9B, C P=0.999), indicating that interactions between *V. cholerae* and *Lb* alone do not affect epithelial renewal. We then tested the ability of *A. pasteurianus* to modify renewal. Given the sensitivity of *A. pasteurianus* to T6SS-dependent killing, we expected diminished epithelial regeneration in *A. pasteurianus*-associated flies challenged with C6706. However, contrary to our prediction, we did not detect a difference in the number of IPCs between *A. pasteurianus*-associated guts infected with C6706 or C6706 $\Delta$ vasK (P=0.996, Fig. 5.9E, F). Instead, we found that C6706 promoted IPC proliferation when confronted with an intestine populated exclusively by *A. pasteurianus*, indicating that T6SS- *A. pasteurianus* alone does not impact epithelial renewal.

Recently, higher-order interactions among polymicrobial communities have been demonstrated to significantly influence host phenotypes in response to bacteria(140). This led us to ask if T6SS-dependent interruption of renewal requires a more complex community of symbiotic bacteria. To test this, we associated adult *Drosophila* with a 1:1:1 mixture of three common fly symbionts, *A. pasteurianus*, *L. brevis*, and *L. plantarum*, and quantified IPC numbers in the guts of flies that we infected with C6706 or C6706 $\Delta$ vasK. Similar to what we observed in CR flies, guts infected with C6706 $\Delta$ vasK had increased numbers of IPCs per area, indicating that poly-association with *A. pasteurianus*, *L. brevis*, and *L. plantarum*, is sufficient to reproduce physiologically relevant intestinal growth phenotypes in response to infection. In contrast, we did not see a difference in the number of IPCs between guts infected with C6706 and uninfected controls in poly-associated flies (Fig. 5.9H,I). Furthermore, we found an appreciable, although not statistically significant, difference in the number of IPCs between poly-associated guts infected with C6706 and C6706 $\Delta$ vasK. These data suggest that interactions between the T6SS and individual symbiotic species are not sufficient to modify IPC repair responses to *V. cholerae*. Instead, a failure of epithelial renewal in response to the T6SS is a function of interactions between the T6SS and a consortium of intestinal symbionts. These results uncover negative effect of the T6SS on epithelial regeneration programs, mediated by complex interactions between the T6SS and the intestinal microbiome.

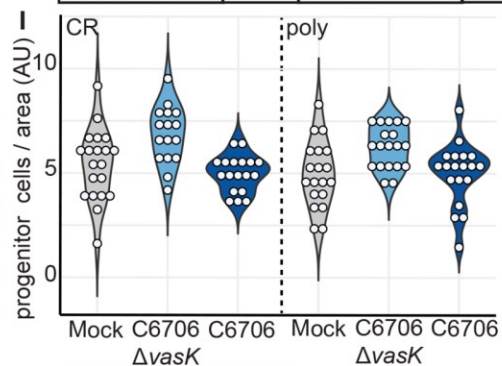
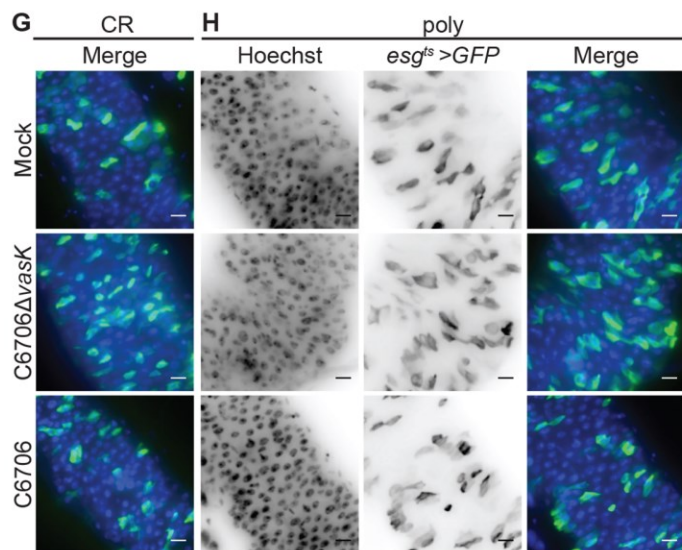




Test	P-value
ANOVA	0.0001
Tukey (CR)	
Mock vs ΔvasK	0.00003
Mock vs C6706	0.999
C6706 vs ΔvasK	0.0002
Tukey ( <i>Lb</i> )	
Mock vs ΔvasK	0.922
Mock vs C6706	0.967
C6706 vs ΔvasK	0.999



Test	P-value
ANOVA	0.004
Tukey (CR)	
Mock vs ΔvasK	0.01
Mock vs C6706	0.397
C6706 vs ΔvasK	0.00001
Tukey ( <i>Ap</i> )	
Mock vs ΔvasK	0.991
Mock vs C6706	0.999
C6706 vs ΔvasK	0.996



Test	P-value
ANOVA	$9.8 \times 10^{-6}$
Tukey (CR)	
Mock vs ΔvasK	0.02
Mock vs C6706	0.945
C6706 vs ΔvasK	0.002
Tukey ( <i>poly</i> )	
Mock vs ΔvasK	0.06
Mock vs C6706	0.999
C6706 vs ΔvasK	0.07



**Figure 5.9. T6SS suppression of epithelial renewal requires higher-order microbiome interactions.** Immunofluorescence of posterior midguts of **(A,D,G)** CR, **(B)** *L. brevis* (*Lb*) mono-associated, **(E)** *A. pasteurianus* (*Ap*) mono-associated, or **(H)** poly-associated *esg<sup>ts</sup>>GFP* flies mock infected or infected with C6706 $\Delta$ *vasK*, or C6706. Hoechst marks DNA (blue) and GFP marks *esg* positive IPCs (green). Scale bars are 10 $\mu$ m. Quantification of the number of IPCs per unit surface area in the guts of **(C,F,I)** CR, **(C)** *L. brevis* mono-associated, **(F)** *A. pasteurianus* mono-associated, or **(I)** poly-associated flies. 2-3 day old virgin female flies were raised on antibiotics 5 day at 25°C to eliminate the microbiome.

## 5.8 Significance

The ability of the digestive tract to consistently withstand physical, chemical, and bacterial insult stems from the capacity of IPCs to rapidly generate new epithelial cells. Failure to renew the epithelium in times of stress is often lethal, as inhibition of IPC growth is sufficient to render an otherwise survivable infection fatal(18). Given that enteric pathogens enter a densely populated bacterial environment, and that interactions between bacteria influence host physiology, it is important to understand how these bacterial interactions influence key mediators of intestinal repair. Here, we found that interactions between the *V. cholerae* T6SS and intestinal symbionts block key growth and differentiation pathways in *Drosophila* IPCs. Our data shows, that this inhibition of IPC growth is not the product of singular species interactions but requires a complex community of bacterial species. Together, the findings in this chapter uncover a previously undescribed effect of the T6SS and highlight the impact of bacterial interactions on intestinal immune responses.

## Chapter 6.

### Discussion

This chapter contains content from the following sources, republished with permission:

- Fast, D., Duggal, A., & Foley, E. Monoassociation with *Lactobacillus plantarum* disrupts intestinal homeostasis in adult *Drosophila melanogaster*. *MBio* 9, e01114-18 (2018).
- Fast, D., Kostiuk, B., Pukatzki, S., & Foley, E. Commensal pathogen competition impacts host viability. *Proc. Natl. Acad. Sci. U. S. A* 115, 7099-7104 (2018).
- Fast, D., Petkau, K., Ferguson, M., Shin, M., Galenza, A., Kostiuk, B., Pukatzki, S., & Foley, E. *Vibrio*-symbiont interaction inhibit intestinal repair in *Drosophila*. *Cell Reports*, 1088-1100.e5 (2020).

## 6.1 Summary

Intestinal symbionts are ubiquitous, found in the digestive tract of virtually all surveyed animals(294). The effects of the microbiome are diverse, yet the molecular basis of these effects are only just beginning to be understood. The data in this thesis examine interactions between host and symbiont, and symbiont and pathogen at the phenotypic and molecular level to understand how microbes impact host biology. Many of the findings from these studies were drawn from the intestines of previously GF flies that were repopulated with a defined bacterial culture. In particular, reconstitution of the microbiota with monocultures of individual symbiotic species identified *L. plantarum* specific effects on intestinal homeostasis. Under homeostatic conditions, the intestine of adult *Drosophila* is populated by a heterogeneous community of microbes. As interactions between these intestinal bacteria impact host fitness(140), it is important to understand how bacteria-bacteria interactions influence mediators of intestinal homeostasis and immunity. In chapters 4 and 5, I explored how interactions between the enteric pathogen *V. cholerae* and the microbiome of *Drosophila* via the T6SS contribute to bacterial pathogenesis and intestinal regeneration. Together, the data in this thesis study interactions between host and microbe, and microbe and microbe. I uncover previously uncharacterized effects of symbiotic species and highlight the influence of bacterial interactions on the intestinal immune response.

## 6.2. *Drosophila* association with *L. plantarum*

### 6.2.1 Summary of long-term association of adult *Drosophila* with *Lactobacillus plantarum*

Gut bacteria activate homeostatic IPC divisional programs that contribute to the maintenance of a healthy digestive tract(18). Failure to regulate stem cell division exposes the host to microbial invasion and potentiates the development of chronic inflammatory illnesses(18, 95). In chapter 3, I used *Drosophila* to examine the effects of symbiotic bacteria on adult longevity and epithelial renewal programs. Specifically, I asked how symbiotic *L. plantarum* affects adult longevity and homeostatic repair. I found that monoassociation with *L. plantarum* shortens adult lifespan relative to GF flies without accelerating IPC divisions. Instead, monoassociation with *L. plantarum* depletes ISC pools, blocks epithelial renewal, and damages the intestinal epithelium. A previous study showed that *Gluconobacter morbifer* causes disease in adult *Drosophila* if allowed to expand within the digestive tract(126). However, *Gluconobacter* is a comparatively rare symbiont of *Drosophila*, and disease onset requires impaired immunity within the host. In contrast, the work in chapter 3 identifies an intestinal phenotype associated with monoassociation of a

common fly symbiont with a GF host. I believe that these findings represent a valuable model to define the mechanistic basis for symbiont-dependent epithelial damage.

### 6.2.2 *L. plantarum* association with *Drosophila melanogaster*.

Symbiotic bacteria form long-term associations with *Drosophila* that persist throughout adult lifespan(90). Newly hatched larvae acquire the microbiome through the consumption of bacterially laden food, contaminated by the activities of previous generations of flies and the deposition of eggs coated by maternal symbionts(100, 110). This is supported by evidence that embryos subjected to a regime of ethanol/hypochlorite sterilization and subsequently housed in a sterile habitat, do not develop microbial associations(91, 101). In our work, I identified association of two symbiotic *Lactobacillus* species with adult *Drosophila* (Fig. 3.1). Both *L. brevis* and *L. plantarum* successfully colonized the fly intestine and established environmental populations on the food of the enclosure (Fig. 3.1). This is consistent with previous findings that the microbiome is maintained by a microbial reservoir on the food, and that depletion of this reservoir by frequent food changes reduces bacterial burden in the gut(110). There is also evidence to suggest that while the microbiome as a whole requires frequent maintenance via bacterial reingestion, there are certain members of the microbiota that are capable of establishing a resident population. For example, frequent food changes have minimal impact on the load of *L. plantarum* in the adult flies(116). However, a separate study found that frequent food changes did indeed significantly reduce the intestinal abundance of *L. plantarum* in the larval gut(117). Although, *L. plantarum* was never eliminated from the digestive tract in either study. The difference between these two studies has many possible explanations. First, the two studies are conducted at different stages in the fly lifecycle, suggesting a possible difference in population dynamics between stages of insect life. Additionally, the two studies were completed with different strains of *L. plantarum*. This is critical as strain specific experiments have demonstrated that different strains of symbiotic species, including *L. plantarum*, have distinct impacts on the observed phenotype(105, 125, 295). For example, an examination of *L. plantarum* colonization showed that three different strains of *L. plantarum* had three distinct colonization efficiencies and that each were differently able to persist within the gut upon stochastic challenge(112). Taken together, the data indicate that *L. plantarum* is able to establish a resident population in the gut of *Drosophila*. Thus, the data in chapter 3 is consistent with existing literature demonstrating that *L. plantarum* is able to form a stable long-term association with *Drosophila melanogaster*.

### 6.2.3 Symbiotic bacteria and host gene expression.

The analyses of the microbiomes influence on gene expression have principally focused on changes in the transcriptome that result from removal of the microbiome(41–43). *Drosophila* raised axenically display altered gene expression throughout the body, with the majority of changes occurring in the digestive tract(128). Consistently, across studies the data show that the microbiome has effects on growth(18, 41, 144), immune(17, 18, 126), and metabolic (42, 43, 124, 296) related genes. In agreement with this, I found that ablation of the microbiome through the administration of antibiotics or via the generation of axenic embryos significantly impacted immune and metabolic related processes (Fig. 3.2). Based on several sequencing data sets, it can be concluded that the presence of gut bacteria in the lumen of *Drosophila* induces a higher level of immune signalling, attributed to activation of the IMD pathway(17, 18, 126). In accordance with this, the IMD pathway has been shown to regulate the gut response to the microbiota. Mutation of the NF- $\kappa$ B transcription factor *Relish* (Fig 1.2), impacts the expression of more than 50% of microbiota induced genes(41). Similarly, specific activation of the IMD pathway in the gut not only increases the expression of expected immune genes, but also differentially regulates the expression of a cohort of metabolic genes(43). It is also important to consider that the microbiome enhances the co-expression of groups of genes or gene modules within the transcriptome, suggesting that intestinal symbionts also modify host transcriptional networks(297). Thus, it is clear that the microbiome has significant impacts on host gene expression. However, it remains in question if specific symbiotic species or taxonomic composition of the microbiome have targeted effects on individual host genes.

Evidence exists to suggest that specific species indeed have unique effects on host gene expression. This data is garnered from studies of gnotobiotic flies that are associated with a single symbiotic species. A recent study from our group demonstrated that in IPCs, monocolonization with *L. brevis* promoted transcriptional changes to integrins which coordinate cell adhesion and polarity, while these changes were absent from flies associated with the closely related *L. plantarum*(150). Similarly, under chronic protein deficiency *L. plantarum*<sup>WJL</sup> was shown to boost the expression of insulin and TOR related genes to promote larval growth(105). A phenotype that was not replicated by association of protein starved larvae with commensal *Enterococcus faecalis* or other symbiotic strains of *L. plantarum*, such as *L. plantarum*<sup>IBDM1L</sup>. Together, these studies indicate that individual species of the microbiome have unique effects on host gene expression.

Contrary to this idea are a series of large transcriptional data sets that found that the transcriptional response of the host was not affected by the taxonomic composition of bacteria resident in the digestive tract(298, 299). Additionally, a curious phenomenon exists in the literature surrounding the microbiome

and its effects on gene expression in *Drosophila*. Research has demonstrated that the microbiome is compositionally variable between individual flies and is inconsistent between cultures from different laboratories(88). Despite these dissimilarities, consistently across studies, the microbiome impacts the expression of immune, metabolic, and growth-related genes(90). This suggests that the gut is transcriptionally sensitive to the presence of intestinal bacteria rather than initiating responses to particular symbiotic species. One possible explanation for this phenomenon, is that different bacterial species have redundant effects on the host. This is supported by data from two independent studies that found recolonization of axenic larvae with commensal *L. plantarum* or *Acetobacter pomorum* activated insulin signalling(102, 105). However, other factors such as symbiotic yeast(298), diet(300), sex(299, 301), and age(302, 303) of the organism influence transcriptional responses. Therefore, when evaluating the effects of the microbiome on gene expression it is important to consider how the environment and host status contribute to the results.

#### **6.2.4 Intestinal symbionts control host lifespan.**

My work began with a consideration of reports from our group and others that GF adult flies outlive CR counterparts(113, 146). This commensal mediated shortening of lifespan is not restricted to *Drosophila* as axenically raised *Caenorhabditis elegans* have a nearly doubled lifespan compared to that of control worms(304). Furthermore, age related mortality of flies is associated with distinct taxonomic shifts in the microbiome(113). Given the association between composition of the microbiome and longevity, and as our cultures of *Drosophila* are dominated by *Lactobacillus* and *Acetobacter*(43, 305), I tested the impacts of *L. plantarum* and *A. pasteurianus* on adult fly lifespan. I found that monoassociation of GF adult flies with *L. plantarum* curtailed GF lifespan extension, while colonization with *A. pasteurianus* had no effect (Fig. 3.2). These results are consistent with other studies that found monoassociation with *L. plantarum* reduces lifespan relative to GF flies(140, 278). However, other reports have found variable effects of microbiome removal on adult lifespan(103, 111). Given that composition of the microbiome has impacts on host longevity, it is possible that these discrepancies in the microbial control of lifespan is due to different taxonomic make ups of the respective microbiomes. For example, a rare strain of cytolysin producing commensal *Enterococcus faecalis* negatively impacts the lifespan of adult flies, while other studies have found *Enterococcus faecalis* to be benign(125). We believe that the differences between the individual reports reflect the intricate nature of interactions within a host-microbe-environment triad. Research groups typically raise their flies on an incompletely defined diet that exerts uncharacterized influences on the metabolic outputs of intestinal bacteria and the transcriptional outputs of the host.

Studies of fly lifespan show that dietary modification impacts the effects of a microbial species on host longevity. Inoculation with the symbiotic yeast *Issatchenkia orientalis* extends lifespan by nearly 150% on a protein deficient diet(0.1% yeast extract)(116, 136). In contrast, *Issatchenkia orientalis* negatively impacts fly lifespan on a high nutrition diet that contains 5.0% yeast extract(306). In a similar manner, *L. plantarum* monoassociation had minimal effects on axenic fly lifespan on a nutritionally replete medium but extended adult longevity on a sucrose only diet(116). Additionally, the ability of a symbiotic species to buffer nutritional challenge and extend lifespan was dependent on microbial abundance as decreased microbial load minimized the influence of a symbiotic species on host longevity. Given this data, I believe that a complete evaluation of the relationship between microbes and their hosts requires consideration of environmental inputs, diet, and bacterial strain. Overall, the observation that *L. plantarum* diminishes GF lifespan extension fits with a broader body of literature showing that colonization of adult flies with *L. plantarum* shortens lifespan.

#### 6.2.5 Symbiotic *L. plantarum* and homeostatic growth programs

The replacement of lost or damaged intestinal tissue by IPCs is vital to the maintenance of homeostasis in the digestive tract. The proliferation of IPCs is regulated by multiple converging pathways and is influenced by host nutrition(307) and the presence of intestinal bacteria(81). Microbial stimulation of IPC proliferation is evident, as GF intestines are less proliferative and show fewer signs of mis-differentiation than age matched CR controls(18, 41). This is reflected in the lifespans of flies with different microbial contents, as GF flies are longer lived than CR counterparts. Given the relationship between IPC proliferation and fly lifespan, I expected the guts of *L. plantarum* monoassociated flies to phenotypically resemble CR intestines. Contrary to our expectations, the organization of intestines monoassociated with *L. plantarum* more closely resembled GF intestines, despite a significantly shorter lifespan (Fig. 3.4 & 3.5). An examination of EGF ligand expression revealed that both GF and *L. plantarum* monoassociated intestines had significantly lower expression levels of *spitz* than CR flies, suggesting limited growth in intestines colonized exclusively by *L. plantarum*. This was substantiated by a recent study from our group that found the expression profile of IPCs isolated from *L. plantarum* monoassociated guts closely resembled that of GF flies despite the presence of intestinal bacteria(150). However, high resolution imaging of the epithelium revealed that flies monoassociated with *L. plantarum* did not display intestinal architecture similar to GF flies but instead, was characterized by a disrupted epithelium and distressed IPCs (Fig. 3.6). At present, I do not know how monoassociation with *L. plantarum* causes an intestinal pathology within the host. It is possible that this phenotype arises from collateral damage through chronic expression and synthesis of

toxic ROS. This hypothesis is supported by the observation that *L. plantarum* activates NADPH-oxidase in the *Drosophila* intestine(47). Alternatively, errant intestinal immune responses through the IMD pathway may account for *L. plantarum*-dependent pathologies. In this context, it is important to consider that several transcriptional studies demonstrated that a relatively small fraction of IMD-responsive transcripts are categorized as bacteriostatic or immunomodulatory(41, 308). In fact, it seems that intestinal IMD activity primarily modifies metabolic gene expression(41–43). As intestinal microbes are known to control nutrition and metabolism in their *Drosophila* host(42, 82, 102, 124), I consider it possible that the *L. plantarum*-dependent pathologies described in this study reflect an underlying imbalance in IMD-dependent regulation of host metabolism.

Consistent with possible links between *L. plantarum*, IMD, and host metabolism, it is noteworthy that a recent study established a link between *L. plantarum* and the IMD-dependent expression of intestinal peptidases(139). Our data show that intestinal colonization by *L. plantarum* is much greater in monoassociated flies than in polyassociated flies. I speculate that the elevated levels of *L. plantarum*, combined with the absence of additional symbionts, alter metabolic responses in the host, leading to impaired intestinal function. This hypothesis includes the possibility that *L. plantarum* directly affects host diet as proposed for other *Drosophila*-associated microbes(136, 309, 310). This is supported by findings that incubation of conventional fly food with *L. plantarum* depletes macronutrients, such as the carbohydrates sucrose, trehalose, fructose, and glucose, as well as a number of amino acids including leucine, tryptophan, phenylalanine, and tyrosine(117). In our TEM analysis of *L. plantarum* associated guts (Fig. 3.6), we identified the presence of large vacuolar structures that appeared to have a double membrane, indicative of autophagy(311). Given that autophagy is used as a mechanism to scavenge amino acids, it is possible that depletion of vital macronutrients from the food by *L. plantarum* contributes to intestinal pathologies via nutritional starvation of the host. However, these observations are speculative, and in-depth testing would be required to thoroughly examine this hypothesis.

### 6.2.6 Conclusions from chapter 3

A variety of phenotypes have been associated with the presence and composition of *Lactobacillus* species in the gut of *Drosophila*. These phenotypes include effects on development(105), nutrition(296, 309), cell growth(47), immunity(143, 144), gene expression(41), and overall host fitness(140). Given the range of effects of *Lactobacilli* on *Drosophila*, it is important to consider that individual species may be associated with multiple phenotypes in the host. For example, release of uracil from *L. brevis* promotes chronic generation of ROS that leads to an increase in intestinal apoptosis and decreased longevity(143),



while *L. brevis* acts in association with *Acetobacter* to regulate triglyceride levels in the fly(296). Likewise, it is important to consider genotypic inputs from species or strains associated with a given phenotype. For instance, the beneficial contributions of *L. plantarum* to mouse and larval nutrition display strain-specific effects(105, 139). Our study adds to this body of work through an examination of the impact of *L. plantarum* monoassociation with adult *Drosophila* on intestinal health and longevity. In summary, this chapter uncovers long-term negative effects of *L. plantarum* on the maintenance and growth of the intestinal stem cell pool. Given the experimental accessibility of *Drosophila* and *Lactobacillus*, I believe that these findings represent a valuable tool for the definition of the mechanisms by which individual symbionts influence intestinal homeostasis.

### 6.3 Symbiont pathogen-symbiont interactions and host viability

#### 6.3.1 Summary of symbiont pathogen competition and host viability

Commensal bacteria form a protective barrier that shields the host from microbial invaders(96). To subvert this barrier, enteric pathogens such as *Salmonella*(282, 312, 313) and *V. cholerae*(212, 231, 246) encode a T6SS to remove commensals and establish colonization of the digestive tract. However, it is unclear how interactions between bacteria impact disease progression and host survival. In chapter 4, I used the fruit fly *V. cholera* model to ask whether T6SS-mediated pathogen-commensal interactions impact the host. I found that the T6SS contributes to *V. cholerae* pathogenesis, and that the T6SS accelerates host death by interactions with symbiotic *A. pasteurianus*. Removal of either the T6SS or *A. pasteurianus* extended the viability of infected adult flies, and inoculation of GF adult flies with *A. pasteurianus* was sufficient to restore T6SS-dependent killing of the host. These results demonstrate an *in vivo* contribution of the T6SS to *V. cholerae* pathogenesis. Removal of all intestinal bacteria did not enhance host killing by T6SS-deficient *V. cholerae*, arguing against a simple replacement model where *V. cholerae* expands into a vacant niche left behind after T6SS-mediated killing of *A. pasteurianus*. Furthermore, there was not a substantial drop in *A. pasteurianus* titers in flies challenged with *V. cholerae*, indicating that *A. pasteurianus* persists during infection. This suggests that complete eradication of commensals is not a critical step in T6SS-mediated pathogenesis of *V. cholerae*. Instead, removal of commensal bacteria attenuated host killing by WT *V. cholerae*, suggesting that the presence of commensal bacteria is essential for T6SS-dependent killing of the host. Finally, I found that inoculation of GF adults with *A. pasteurianus*, either alone or in combination with *Lactobacilli*, was sufficient to restore T6SS-dependent killing of the host. These observations are in line with a model where T6SS mediated killing of a proportion of intestinal *A.*

*pasteurianus* initiates secondary events that enhance host destruction by *V. cholerae*. This work shows that additive effects between IMD and T6SS dependent interactions with *A. pasteurianus* program the intestinal environment in a manner that supports *V. cholerae* pathogenesis. This model is supported by recent work in the infant mouse, which found that the T6SS of *V. cholerae* activates the immune system to a greater extent when commensals are present(166). Together, the system described in this chapter presents a simple *in vivo* model to define host–microbe–pathogen interactions and the impacts of these interactions on the host.

### 6.3.2 Classical and El Tor strains and the T6SS influence on host viability

This work was initially inspired by a dichotomy that exists between the classical and El Tor biotypes of *V. cholerae*. Classical strains, responsible for the 1<sup>st</sup> (1817) to the 6<sup>th</sup> (1950) *V. cholerae* pandemics, harbour multiple disabling mutations in T6SS gene clusters(181, 248, 314). In contrast, 7<sup>th</sup> pandemic (on going) El Tor strains, such as C6706, have an intact T6SS that is active *in vivo*(251, 284). I asked if the T6SS impacts the disease progression of *V. cholerae*. I found that El Tor C6706 was able to rapidly kill the host, while the classical O395 strain was far less lethal, killing the host in almost double the time of C6706 (Fig. 4.1). This is consistent with clinical studies describing differences in virulence between classical and El Tor strains of *V. cholerae*(187, 315, 316). However, these studies find that El Tor strains are more likely to be asymptomatic and result in fewer human hospitalizations compared to infection with classical biotypes(182, 188). This difference in virulence between *Drosophila* and humans has many possible explanations, including divergences in host evolution and immunology. Alternatively, there are genetic and regulatory differences between classical and El Tor strains, aside from mutations in T6SS gene clusters, that could account for this pathological inversion(189, 190). For example, El Tor strains encode axillary toxins such as the metalloprotease hemagglutinin which degrades mammalian occludin, that are absent from classical *V. cholerae* strains(192). Therefore, it is possible that these auxiliary toxins play a more prominent role in *V. cholerae* pathogenesis in an arthropod host and are dispensable in a human environment.

To focus on the contributions of the T6SS to host disease, and exclude confounding variables presented by genetic divergencies between biotypes, I infected flies with an isogenic mutant of C6706 with a null mutation in the T6SS essential gene, *vasK*(231), and compared fly survival to that of C6706 infected counterparts. I found that mutation of the T6SS significantly extended the survival of flies infected with *V. cholerae* (Fig. 4.1). This is consistent with an earlier study in the wax moth, *Galleria mellonella*, that found that mutation of *tssM* in the T6SS of *Acinetobacter baumannii* abolished T6SS activity and extended the survival of infected moths(317). Given the ability of the T6SS to interact with and effect both eukaryotic

and prokaryotic cells, I next questioned if the T6SS' influence on host viability required interactions with intestinal symbionts. Interestingly, the T6SS had no effect on host viability in the absence of the microbiome, demonstrating that symbiont-pathogen interactions have measurable impacts on host viability. Similarly, interactions between commensal *E. coli* and *V. cholerae* via the T6SS exacerbate the virulence of *V. cholerae* by promoting intestinal inflammation in infant mice(166). Thus, these data are in line with research demonstrating that the T6SS negatively impacts host viability and potentiates *V. cholerae* pathogenesis through microbial interactions.

### 6.3.3 The T6SS contributes to cholerae like disease

Infection with *V. cholerae* causes a wide range of symptoms, from asymptomatic infection to severe dehydration, heart failure, and death(167). Likewise, we found that infection with different biotypes of *V. cholerae* had a range of effects on host viability and disease severity. Infection with O395 had modest effects on host viability (Fig. 4.1) and a similarly mild impact on the development of cholera like symptoms (Fig. 4.2). In contrast, C6706 established a lethal infection and promoted a significant increase in the frequency and volume of fly defecation, indicative of cholera like disease. Ablation of the T6SS extends fly survival and partially attenuates diarrheal disease, indicating that the T6SS contributes to disease symptoms (Fig. 4.2). The finding that the T6SS contributes to cholera symptoms is perhaps surprising as the principle factor known to cause diarrhea during a *V. cholerae* infection is CT. However, the T6SS was also shown to contribute to diarrheal symptoms in infant mice. In the mouse model, this was perpetuated through an increase in the expression of CT and the toxin coregulated pilus(166). In *Drosophila*, it remains unclear how the T6SS is able to influence the onset of diarrheal disease. One possible explanation is that T6SS dependent killing of susceptible prey activates virulence factor expression during the early stages of infection in a manner similar to infected mice. This is supported by findings that CT is known to contribute to the killing of adult flies infected with the O139 serogroup *V. cholerae* strain MO10(157).

In mammals, CT enters intestinal cells through endocytosis by binding to GM1 gangliosides on epithelial cells(318, 319). Gangliosides are glycosphingolipids conserved in mammals, but absent from insects including fruit flies. *Drosophila* specifically lacks the GalT6/5 and SAT1 enzymes required for ganglioside synthesis(320). Despite missing the canonical receptor, flies infected with *V. cholerae* appear to develop diarrhea by the same mechanism as mammals(157). Accumulation of 3',5'-cyclic AMP, through aberrant activation of adenylate cyclase activates cystic fibrosis transmembrane conductance regulator chloride ion channels which results in ion imbalance and the efflux of water into the intestinal lumen(201, 202). *Rutabaga* mutant flies, the fly homolog of adenylyl cyclase responsible for the synthesis of cyclic AMP,

infected with *V. cholerae* have extended survival times relative to WT infected controls(157). As mutation of CT significantly attenuates the virulence of *V. cholerae* in the fly host, together these data suggest that CT has similar functions in *Drosophila* and mammalian intestinal cells. However, viability of *V. cholerae* infected *rutabaga* mutants was used as a proxy for severity of disease without a direct measure of fecal output. In the future, it may be valuable to assess these mutants for diarrheal symptoms to ensure the mechanism of extended survivability is indeed do to less severe symptoms and not via other extraneous factors caused by *rutabaga* mutation.

#### 6.3.4 The *V. cholerae* T6SS and *In vivo* intestinal pathogenesis

A large body of literature derived from different model organisms has shaped our understanding of the effects of *V. cholerae* on the intestinal epithelium. In adult human volunteers, infection with an O1 *V. cholerae* strain promoted ultrastructural changes to the upper small intestine(287). Patients infected with *V. cholerae* manifested abnormalities in apical intercellular junctions and blebbing of cellular material from enterocytes in intestinal crypts. Similarly, I found that infection of adult *Drosophila* with the O1 pandemic strain, C6706, induced ultrastructural changes to the epithelium characterized by the displacement of cell debris and significant damage to the posterior midgut (Fig. 4.3). Mutation of the T6SS reduced epithelial damage and minimized changes to gut structure. However, ablation of T6SS function did not entirely abolish *Vibrio* induced ultrastructural changes, suggesting that *V. cholerae* deploys other virulence factors that damage the intestinal lining. Likewise, sagittal sectioning of the posterior midgut confirmed that removal of the T6SS attenuates intestinal damage (Fig. 5.2). In both assays, infection with C6706 $\Delta$ *vasK* caused a noticeably less severe intestinal pathology than WT infected counterparts. Guts infected with C6706 $\Delta$ *vasK* showed signs of delaminating cells and cellular debris in the luminal space, while as a whole the epithelium appeared largely intact (Fig. 4.3 & 5.2). In contrast, intestines infected with C6706 were characterized by a thinning of the epithelium, disorganized structure, and the presence of large masses of cellular material in the lumen (Fig. 4.3 & Fig. 5.2). Together, these data are consistent with growing evidence demonstrating the effect of the T6SS on the intestinal epithelium.

The means by which the T6SS acts on host intestinal tissue is variable and may be unique to the infected organism. For example, in the zebrafish model, the actin cross linking domain of VgrG-1 stimulates peristaltic movements along the epithelium that purge commensal bacteria from the digestive tract(252). Removal of commensals by T6SS action is a common theme accompanying *in vivo* studies of the T6SS of *V. cholerae* and other bacteria. The antibacterial activity of the *Salmonella* Typhimurium T6SS directly outcompetes commensal *Klebsiella oxytoca* to establish residence in the mouse gut(313). Interactions like

this, between the T6SS and prokaryotic cells also impact host epithelial tissue. T6SS destruction of symbiotic *E. coli* by *V. cholerae* in the murine intestine stimulates inflammatory responses from gut tissue(166). Furthermore, the T6SS interacts directly with mouse intestinal tissue through the anti-eukaryotic VgrG-1 effector(250). Together, the data demonstrate that the T6SS is capable of impacting the epithelium directly or through interactions with commensal bacteria. Therefore, the possibility that both types of interactions may occur as part of a single infection cannot be excluded. It is conceivable that a similar combination of interactions may be responsible for the changes to the epithelium observed in *V. cholerae* infection of the *Drosophila* posterior midgut (discussed in 6.4.2 & 6.4.4).

Studies of T6SS effects on the digestive tract are typically organized to compare results of infection plus and minus the T6SS. Differences in pathology, gene expression, or viability are then ascribed to the T6SS. This approach is largely accepted and has been used to discover much of what is known about the T6SS *in vivo*. There is preliminary data to suggest that activation of the T6SS may in part influence the regulation of other virulence factors, such as CT and the toxin coregulated pilus(166). Therefore, it is possible that inhibition of the T6SS attenuates virulence through ablation of T6SS activity and through the abrogation of virulence factor expression. To understand how the T6SS impacts the intestinal epithelium, I propose a dual RNA-seq experiment, that simultaneously sequences the transcriptome of intestinal bacteria and that of the infected host(321). This experimental paradigm permits the *in vivo* identification of differences in bacterial transcription plus and minus the T6SS while subsequently monitoring host responses. This design can be further modified to include the presence or absence of the microbiome to detail how symbionts factor into T6SS dependent pathologies. Although technically challenging, dual RNA-seq has been used to analyze the transcriptional profile of many bacterial pathogens including *Salmonella* Typhimurium(322), uropathogenic *E. coli*(323), and *Chlamydia trachomatis*(324). In the case of uropathogenic *E. coli*, the authors identified *phage shock protein A* as a factor important for bacterial survival inside murine macrophages(323). Despite the success of dual RNA-seq studies, these experiments are primarily carried out in purified cell culture systems. This is likely because the bacterial RNA is a small fraction of genetic material amongst the overwhelming transcriptional mass of the host(325). A promising alternative to purified cells that moves closer to an *in vivo* setting, is the development of organoid systems. Organoids are 3D cell culture systems that more closely mimic the function and characteristics of an organ. Thus, it may be more feasible to conduct a dual RNA-seq experiment plus and minus the T6SS in this simpler and more controlled system. It is also noteworthy that previous studies were able to successfully sequence the transcriptome of *V. cholerae* derived from the guts of rabbits and mice(326). Therefore, it is possible to obtain transcriptional data from *V. cholerae* inside a model organism. I believe a thorough examination of

host and bacterial gene expression would be a powerful tool to understand how the T6SS promotes changes to the structure of the fly gut.

### 6.3.5 Composition of the microbiome determines T6SS mediated infection outcomes

The T6SS destroys Gram-negative bacteria through a contact dependent delivery of toxic effectors while Gram positives are naturally immune to T6SS assault(238). This is attributed to a thickness of peptidoglycan that the T6SS is unable to span. This is supported by a recent study that found that T6SS competition is also rebuffed by an exopolysaccharide capsule(327). Consistent with this, the Gram-positive symbionts *L. brevis* and *L. plantarum* were refractory to T6SS mediated destruction, while *A. pasteurianus* was effectively killed (Fig. 4.4). The capacity of the fly's symbiotic bacteria to resist T6SS competition was mirrored in their ability to mitigate *V. cholerae* expansion in the host. Only when the fly was associated with the T6SS sensitive *A. pasteurianus* was there a difference in the CFU of *V. cholerae* plus and minus the T6SS (Fig. 4.4). This suggests that the T6SS is able to aid in colonization when T6SS sensitive bacteria inhabit the host digestive tract. However, there was no difference in the CFU of *A. pasteurianus* in monoassociated flies infected with C6706 or C6706 $\Delta$ vasK. The microbiome of *Drosophila* is inconsistent, stratified by taxonomic differences between geographic cultures of flies and fly to fly variability(88, 112, 119). We specifically measured bacterial CFU in pools of five organisms per replicate to reduce noise and measure the bacterial population as a whole. Given the degree of fly to fly variability in the microbiota, it is possible that the method used to measure the CFU of *A. pasteurianus* masked any subtle changes in the population of *A. pasteurianus* signaling T6SS activity. It is possible that a repeat of this experiment that measured the CFU of *A. pasteurianus* from individual flies and subsequently binned the data according to CFU would provide clarity on the nature of the T6SS's influence on intestinal populations of *A. pasteurianus*. It is also possible that small localized destruction of symbionts by *V. cholerae* microcolonies triggers aberrant activation of the immune response resulting in a pathology that requires secondary host responses. This is supported by findings from us and others that inactivation of IMD extends the viability of adult flies infected with *V. cholerae*(161, 328).

A previous study found that infection with *V. cholerae* activates IMD and induces expression of AMPs(161, 329). Consistent with this, I found that *V. cholerae* stimulated the transcription of AMPs in intestinal tissue (Table 5.2). Inactivation of the IMD pathway through mutation of either signaling components, such as *imd* and *kenny* (IKK) , or through inhibition of the transcription factor *relish* (Fig. 1.2) extends viability upon *V. cholerae* infection(161). Thus, secondary responses in the fly host contribute to *V. cholerae* mediated death. While the precise mechanism is unclear, the consideration of IMD as a mediator

of toxic secondary responses can be explored by an examination of the different functions of the IMD pathway. Activation of IMD stimulates the production of AMPs, alters metabolic gene expression, and controls the delamination of enterocytes(45). In line with this, RNA-seq of whole intestines infected with C6706 and C6706 $\Delta$ *vasK* revealed an upregulation of IMD response genes (AMPs). The mRNA levels for all detected AMPs sequences was enhanced in guts infected with C6706 compared to those challenged with C6706 $\Delta$ *vasK*, suggesting increased activation of IMD in flies infected with *V. cholerae* with a functional T6SS. In addition to AMPs, activation of IMD promotes the transcription of negative regulators that dampen IMD activity(330). For example, newly synthesized PGRP-LB is secreted into the lumen where its amidase activity cleaves the amide bond of N-acetylmuramic acid to the alanine of the peptidoglycan peptide dampening its immunostimulatory activity preventing further IMD signaling(331, 332). However, negative regulators of this kind were absent from the RNA-seq of whole guts. Furthermore, oral challenge with *V. cholerae* promoted the sloughing of epithelial cells, with C6706 stimulating more shedding than C6706 $\Delta$ *vasK* (Fig. 5.1). It is therefore possible that *V. cholerae* stimulates an overactivation of IMD that results in a heightened shedding of epithelial cells that dysregulates and damages the digestive tract. This is supported by a recent cell specific study from our group that found that expression of dominant negative *imd* specifically in enterocytes extended fly lifespan upon challenge with C6706(305). However, ablation of IMD signalling extended the longevity of both C6706 and C6706 $\Delta$ *vasK* infected flies, suggesting that extended viability of IMD pathway mutants may be unrelated to the T6SS. In this scenario, it is possible that loss of IMD signalling allows for the mitigation or delay of *V. cholerae* related pathologies that would otherwise kill the host. Specifically, mutation of IMD may attenuate intestinal damage and thus preserve an intact epithelial barrier, which is known to extend fly longevity. Alternatively, inactivation of IMD may prevent the onset of an intestinal metabolic state that is beneficial to growth and virulence of *V. cholerae*. This is consistent with recent findings demonstrating that the insulin pathway, a key mediator of metabolic homeostasis, has close ties to the IMD pathway and improves resistance to oral *V. cholerae* infection(44, 224). As studies have implicated host metabolites in the pathogenesis of *V. cholerae*(224, 333), and as IMD is a regulator of metabolic genes, I believe this represents a valuable avenue of exploration.

### 6.3.6 Composition of the microbiome, *V. cholerae* infection, and viability.

Given the differential ability of Gram-negative and Gram-positive fly symbionts to resist T6SS assault and mitigate the *in vivo* expansion of *V. cholerae*, I tested if monoassociation with different commensal species impacted T6SS control of host viability. I found that the presence of the Gram-negative *A. pasteurianus* was uniquely able to sensitize the host to the T6SS (Fig. 4.5). These data suggest that

specific symbiont pathogen interactions have consequences for host viability. At present, it is unclear how interactions between *A. pasteurianus* and *V. cholerae* shorten host viability. It is possible that T6SS mediated interactions destroy small populations of *A. pasteurianus* releasing peptidoglycan and bacterial products that exacerbate secondary responses perpetuating increased pathology. Here, the release of bacterial products may promote an increase in the synthesis of ROS and AMPs that together reduce the symbiotic population to the benefit of a pathogen able to resist increased concentration of bactericidal products. This is consistent with previous work that found that *V. cholerae* was resistant to elevated concentrations of hydrogen peroxide(334) and data from the study of *Salmonella* Typhimurium that found that *Salmonella* benefited from an inflammatory response that effectively reduced symbiont density(335). It is also possible that interactions with specific species, such as *A. pasteurianus*, stimulate an increase in T6SS activity. Bacterial specific regulation of the T6SS is an intriguing line of study with much to consider. Despite T6SS activation *in vivo*, C6706 does not express T6SS genes under laboratory conditions. High resolution sequencing of individual *V. cholerae* cells isolated from an *in vivo* environment monoclonized with a single symbiotic species may provide a resolution to this question. In this scenario, I speculate that single cell sequencing of fluorescently labeled bacteria, isolated by flow cytometry from infected flies constitutes a viable avenue of study. Single cell sequencing of prokaryotes is at present possible, but still undergoing development. A recent study was able to successfully distinguish single bacterial cells within an isogenic population as in stationary or exponential phases of growth based on single cell transcriptomes. Furthermore, the resolution of this assay was such that the authors were able to identify a rare population of *Staphylococcus aureus* undergoing prophage induction(336). Thus, there are established protocols for single cell sequencing of bacterial cells. Therefore, with careful optimization I hypothesize that it would be possible to sequence the transcriptome of *V. cholerae* in association with T6SS sensitive and resistant symbionts to understand the impacts of specific bacterial interactions on *V. cholerae* gene expression. This project combined with the dual seq experiments proposed in section 6.4.4 together represent an unbiased approach to the exploration of T6SS mediated virulence.

### 6.3.7 Conclusions from chapter 4

Symbiotic colonization of the digestive tract establishes a barrier that guards the host against the ingress of enteric pathogens(96). However, intestinal invaders have evolved effective strategies to displace or outcompete resident microbes. The T6SS is deployed by competing bacteria within microbially dense environments to remove cells that occupy a shared niche. In zebrafish, the T6SS activates peristaltic like movements in the digestive tract that expel commensal *Aeromonas veronii*(252). In chapter 4, I explored



the role the T6SS in the gut of *Drosophila melanogaster*. This study found that the T6SS acts through the endogenous microbiome to restrict the viability of orally infected flies. Similarly, a study of the *V. cholerae* T6SS in mice found T6SS removal of symbiotic *E. coli* to be toxic. Thus, this work adds to growing evidence that interactions between bacteria in the gut have significant consequences for the host. In summary this chapter identifies a negative effect of the T6SS on the viability of adult *Drosophila* colonized with T6SS sensitive commensals.

## 6.4 Symbiont-pathogen interactions and intestinal homeostasis

### 6.4.1 Summary symbiont pathogen interactions and the effects on intestinal repair

Enteric infection initiates a series of host measures that halt the expansion and dissemination of pathogenic bacteria. Renewal of the epithelium is achieved by the coordinated expulsion of damaged cells and accelerated proliferation of IPCs(1). However, it is unclear how interactions among gut-resident bacteria influence this response. Chapter 5 explored how host responses are impacted by interactions between an enteric pathogen and intestinal symbionts via the T6SS. We found that T6SS-deficient *V. cholerae* activates classical defense and repair responses in the host. Specifically, C6706 $\Delta$ vasK promoted transcription of AMPs, shedding of epithelial cells, and IPC proliferation and differentiation. In contrast, infection with C6706, which encodes a fully operational T6SS, significantly altered host responses to infection. Challenge with C6706 caused extensive epithelial shedding but prevented the activation of regenerative pathways that regulate intestinal repair. I found that interactions between the T6SS and the microbiome were responsible for impaired epithelial regeneration as infection of a GF host with C6706 promoted normal IPC proliferation. Furthermore, inhibition of IPC proliferation required interactions with a consortium of symbiotic bacteria rather than a simple interaction between *V. cholerae* and a particular symbiotic species (Fig. 6.1). In chapter 4, I demonstrated that interactions between symbiotic *A. pasteurianus* and the T6SS of *V. cholerae* diminished host viability. However, interactions between *A. pasteurianus* and *V. cholerae* alone do not prevent induction of intestinal regeneration, suggesting that host killing, and the impairment of IPC proliferation in response to the T6SS are independent consequences of infection with *V. cholerae*. Together, the data in chapter 5 highlight the impact of symbiont-pathogen interactions on epithelial regeneration and outline a framework to explore the consequences of bacteria-bacteria interactions on intestinal immunity.

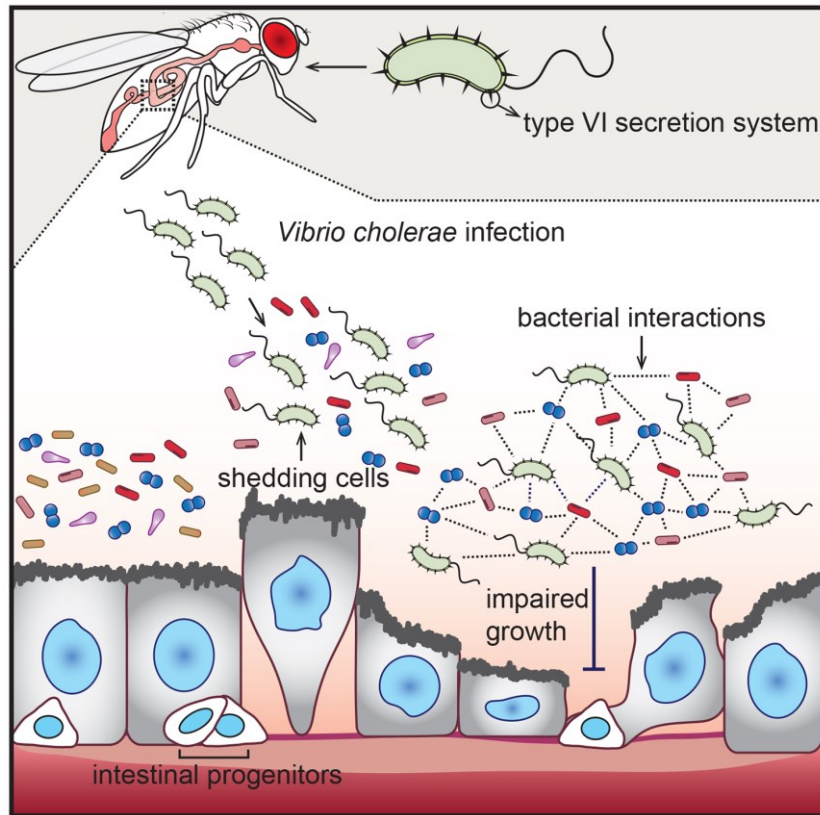


Figure 6.1 Proposed model of symbiont-pathogen interactions that inhibit intestinal repair

#### 6.4.2 *V. cholerae*, the IMD pathway, and intestinal homeostasis.

*V. cholerae* triggers the activation of the IMD pathway in the digestive tract of *Drosophila melanogaster*(161). Typically, activation of IMD in response to the ingestion of toxic bacteria is protective and is required to survive infection with pathogens like entomopathogenic *P. entomophila*(160). In contrast, IMD is detrimental in the context of a *V. cholerae* infection, as IMD pathway mutants outlive WT flies challenged with *V. cholerae*(157). The precise mechanism that mediates extended viability of IMD mutants remains to be clarified. In chapter 5, I found that *V. cholerae* promoted the transcription of AMPs and stimulated delamination of epithelial cells (Fig. 5.4 & Fig. 5.1), processes controlled by IMD(45). Infection with T6SS competent C6706 increased shedding compared to T6SS null mutant counterparts. IMD is activated by detection of microbial products such as DAP type peptidoglycan by peptidoglycan recognition proteins (PGRP), PGRP-LC and PGRP-LE. Both *Lactobacillus* and *Acetobacter* contain DAP-PGN(332). As *A. pasteurianus* is sensitive to T6SS competition (Fig. 4.4), it is possible that T6SS destruction of small populations of *A. pasteurianus* release DAP-type PGN enhancing an IMD response that elevates shedding

of epithelial cells promoting putative epithelial damage. This is supported by our findings that GF flies infected with C6706 outlive similarly infected flies with a full contingent of symbiotic microbes. Furthermore, sloughing of intestinal cells appears to contribute to intestinal damage as we simultaneously observed delaminated cells in association with epithelial disorganization (Fig. 4.3) and thinning of the intestinal lining (Fig. 5.2). Additionally, expression of dominant negative *imd* specifically in epithelial cells extends the viability of C6706 infected flies(305). In this scenario I hypothesize that inhibition of IMD prevents the shedding of epithelial cells preserving integrity of the intestinal barrier. The disrupted nature of the epithelium raises the possibility of impaired intestinal barrier function. Breach of the intestinal barrier by pathogens is lethal. For example, the human opportunistic pathogen, *Pseudomonas aeruginosa*, crosses the gut epithelium of *Drosophila* to reach the hemolymph where bacteremia facilitates death of the infected host(156). Similarly, *V. cholerae* inoculation of the hemolymph is fatal, causing death in approximately 10 hours(44, 337). However, in mammals *V. cholerae* is generally considered to be non-invasive and retained in the intestinal tract throughout the duration of infection. Future studies should consider intestinal permeability in *V. cholerae* infected guts and if shedding of intestinal cells in response to *V. cholerae* is impacted by the presence of commensal bacteria.

#### 6.4.3 Intestinal response to *V. cholerae*

The establishment of intestinal homeostasis is coordinated by a tightly regulated signaling network that integrates cues from luminal bacteria, intestinal cells, and adjacent tissues(1). These signals are transmitted by several cytokine and growth factor pathways, including Transforming Growth Factor  $\beta$ s, such as decapentaplegic (DPP)(81). I found that infection with *V. cholerae* negatively impacted gut homeostasis and prevented the engagement of intestinal repair programs. This inhibition of repair was characterized by a downregulation of genes in pathways that regulate IPC proliferation and differentiation (Fig. 5.7). Given the coverage of this response, which spans several genes in a given pathway across multiple pathways, it is possible that this regulation is coordinated by the host in response to *V. cholerae* mediated damage. For example, modulation of DPP signaling impacts the activation of other mitotic pathways in the intestine of adult *Drosophila*. Loss of DPP signaling specifically in IPCs results in the expression of the JAK/STAT ligand Upd3 and phosphorylation of the mitogen activated protein kinase ERK (*rolled*)(292).

Signalling through DPP, a bone morphogenic protein (BMP) homologue and member of the Transforming growth factor  $\beta$  superfamily of ligands, is initiated by ligand binding to a transmembrane receptor complex. The receptor tetramer complex is composed of two type I and two type II receptors. In the fly gut, the type I receptors are Thickveins (Tkv) and Saxophone (Sax), while Punt (Put) is the type II

receptor(338). The activated complex phosphorylates the downstream transcription factor Mother against Dpp (MAD) which associates with the co-Smad Medea, accumulates in the nucleus, and mediates transcription. DPP has complex roles in the regulation of IPCs. The complexity is such that the function of DPP is described differently between studies. One study found that knockdown of *put* prevented IPC proliferation in response to bleomycin and DSS(72). This work also demonstrated that BMP signaling is required for homeostatic IPC maintenance. In contrast, a series of other studies found that *Drosophila* DPP inhibits IPC proliferation(75, 292). In the context of infection, loss of DPP through knockdown of *Mad* in IPCs resulted in intestinal hyperproliferation(292). Similarly, a separate study found that loss of BMP signaling in response to intestinal injury results in IPC hyperproliferation(75), consistent with DPP mediated inhibition of IPC activity. Similarly, BMP signalling in the pseudostratified lung epithelium of mice blocks the proliferation of airway basal stem cells, demonstrating a functional evolutionary conservation of BMP activity(339, 340). Evidence exists to suggest that DPP signaling in *Drosophila* is more complex than a simple activation inactivation paradigm. In the same 2014 study that found loss of DPP inhibited IPC proliferation, the authors demonstrate that hypomorphic *Mad* results in IPC hyperproliferation instead of an expected partial loss of IPC division(72). This suggests that levels of BMP signaling significantly alter DPP's effects on IPCs. Additionally, it seems likely that the function of DPP is regulated by the make-up of the receptor complex and responding signaling proteins. A recent study found that a receptor complex of Sax and Put signaling through SMOX (dSMAD2) promotes proliferation, while DPP signaling via a Tkv-Put complex that is transduced through *Mad* results in IPC quiescence(73). Consistent with this, we found that guts infected with C6706 had an upregulation of *dpp* and *Tkv* (Fig. 5.3) while also failing to engage reparative programs (Fig. 5.6 & 5.7). I speculate that the tissue injury by infection with T6SS functional C6706 promotes the activation of DPP which contributes to lack of epithelial repair. However, more testing is required to thoroughly examine this hypothesis.

In addition to differential regulation of pathways that promote IPC proliferation, I also detected a down regulation of components of the Notch signalling pathway, which governs the differentiation of new epithelial cells. Specifically, I measured a significant downregulation in the Notch response gene complex, *E(spl)*, in IPCs isolated from guts infected with C6706 (Fig. 5.7). This change to Notch signalling was accompanied by significantly fewer enteroblasts in guts infected with C6706 relative to C6706 $\Delta$ *vasK* infected counterparts, suggesting impaired enteroblast generation in response to C6706. Together, these data are consistent with activation of Notch as a requirement for enteroblast formation, and it is likely that impaired IPC proliferation prevents enteroblast synthesis. Alternatively, new formed enteroblasts maybe lost or harmed during generation, due to the disrupted nature of the epithelium being unable to provide

an appropriate niche. It is also possible that infection with C6706 favors IPC generation of enteroendocrine cells. As new evidence suggests that enteroendocrine cells arise from cells negative for the enteroblast marker Su(H)(12), it is possible that the change in enteroblast numbers in response to C6706, as measured by the number of Su(H) positive cells, is a function of increased generation of enteroendocrine cells. Nonetheless, the data demonstrate the infection with C6706 impacts the regulation of key epithelial repair pathways and disrupts intestinal regeneration.

#### 6.4.4 Pathogen modification of epithelial repair in the gut of *Drosophila melanogaster*

Toxic invaders set off a cascade of intestinal responses that limit pathogen dispersal and accelerate IPC activity to repair epithelial injury(81). During infection, IPC proliferation is required to mitigate damage by the pathogen or host ROS. In the case of the EGF pathway, disabled signalling prevents IPC proliferation in response to damaging chemicals like paraquat(59) or infection with *Ecc15*(58). RNA-sequencing detected a down regulation of many key regulators and signalling components of both the EGF and JAK/STAT pathways in IPCs from guts infected with C6706 (Fig. 5.6). Subsequently, infection with *V. cholerae* with a functional T6SS did not result in IPC proliferation, while mutation of the T6SS restored normal epithelial regeneration. Microbial modification of IPC activity is most commonly associated with the increase in epithelial turnover that accompanies colonization by symbiotic bacteria(90). However, enteric pathogens aside from *V. cholerae* have been demonstrated to negatively affect the proliferative homeostasis of *Drosophila* IPCs. *Pseudomonas aeruginosa* damages the midgut by activation of JNK to stimulate IPC hyperproliferation(155). Alternatively, oral infection of *Drosophila* with large doses of *P. entomophila* induces a translational blockade that diminishes intestinal repair(162). In contrast to *P. entomophila*, *V. cholerae*-mediated inhibition of epithelial renewal requires interactions between the T6SS and the gut microbiota (Fig. 6.1). As of yet, it is unclear how interactions between C6706, and the microbiome diminish IPC-mediated repair, although there are several possible explanations for this effect. For example, the gut is sensitive to growth cues received or generated through host-microbe interactions(18, 41, 47, 102), raising the possibility that *V. cholerae* prevents IPC proliferation by modifying microbiota-derived pro-growth cues. Consistent with this hypothesis, other studies have documented the effects of *V. cholerae* on the availability of microbial metabolites with downstream effects on epithelial renewal(221, 333). Specifically, expression of the *V. cholerae* glycine cleavage system promotes the consumption of methionine-sulfoxide by the bacteria in the fly gut. Consumption of methionine-sulfoxide by *V. cholerae* disrupts host metabolic signalling resulting in a depletion of lipids from the fat body (an insect organ similar to the vertebrate liver and adipose tissue) and an accumulation of lipids in the midgut. These changes are

accompanied by a depression of insulin signalling and a suppression of IPC proliferation(333). Mutation of the *V. cholerae* glycine cleavage system impairs bacterial consumption of methionine-sulfoxide, restores lipid homeostasis, and rescues IPC proliferation. Additionally, dietary supplementation with methionine-sulfoxide was sufficient to maintain IPC proliferation in response to *V. cholerae*, indicating that *V. cholerae* induced shifts in metabolite availability impact epithelial renewal.

Interactions between symbionts and *V. cholerae* may also support the anti-eukaryotic function of the T6SS. In this scenario, *V. cholerae* may be required for microbiota-dependent shedding of differentiated epithelial cells, exposing underlying IPCs to intoxication by T6SS effectors such as the actin crosslinker, VgrG-1(212, 242). Putative links between shedding of enterocytes and IPC access are consistent with a role for the IMD pathway in the shedding of damaged epithelial cells(45). Flies that express dominant negative *imd* specifically in enterocytes outlive WT flies when infected with C6706(161). Thus, it is possible that null mutations in the IMD pathway prevent excess epithelial shedding, and thereby maintain a barrier that protects IPCs from exposure to *V. cholerae* toxins. Alternatively, T6SS symbiont interactions may only be required to expose IPCs while other pathogenic factors act on IPCs to prevent proliferation. Factors such as the auxiliary multifunctional auto processing toxin, which inactivates the eukaryotic transcription factor Rho(341) and suppresses innate immune responses(342), could diffuse through the luminal space to make contact with underlying IPCs. One possible way to test the effect of bacterial toxins directly on IPCs is through transgenic induced expression. This approach was recently used to express the *Helicobacter pylori* toxin *cagA* in *Drosophila* IPCs. The authors found that CagA promotes pathological IPC proliferation and that this proliferation was mediated through a shift in the microbiome that required interspecies interaction between bacteria(343). Similarly, the work in chapter 5 uncovered links between bacterial components, the microbiome, and IPC proliferation. However, interactions between the *V. cholerae* T6SS and intestinal symbionts resulted in failed intestinal repair rather than the onset of hyperproliferative disease. Taken together, the data here are in line with growing evidence demonstrating bacterial modification of intestinal repair and the influence of bacterial interactions on these modifications.

#### **6.4.5 The fruit fly model of *Vibrio cholerae*. What we learned from *Drosophila modelgaster*.**

There is no single model for *V. cholerae* that can properly account for all aspects of disease and meet the requirements for malleability needed to study molecular mechanisms of pathogenesis. Previous studies have used healthy human participants to examine the role of CT in the development of diarrhea(197). However, there are many drawbacks to this system. Aside from ethical and financial difficulties, the molecular biology, invasive assays, and genetic manipulations required to properly study

molecular mechanisms of disease are simply not possible. To study *V. cholerae*, researchers have pioneered insect(157), fish(218), and non-human mammalian models(214–216). Together, the collective findings from these different organisms have shaped our understanding of the pathogen by identifying specifics that are unique to particular models and trends that persist across different systems.

The *Drosophila* model of *V. cholerae* offers many advantages over its mammalian counterparts. Primarily, the fruit fly is naturally susceptible to infection by *V. cholerae* without depletion of the microbiome or modification to the acidity of the digestive tract, required in adult mice(344) or infant rabbits(209) respectively. Furthermore, flies infected with *V. cholerae* develop diarrhea symptoms(157) akin to cholera unlike other popular models like the suckling mouse(216). Therefore, this insect, that has been established as a model for other human disease, can be used to dissect the nuances of *V. cholerae* infection.

Since the establishment of *Drosophila* as a model for oral infection with *V. cholerae*(157) researchers have identified a network of immune, metabolic, and growth-regulatory events that influence disease progression. For example, *V. cholerae* activates the antibacterial IMD pathway in infected flies(161) and IMD pathway mutants have extended viability after infection with *V. cholerae*. At the same time, studies of the effect of infection with *V. cholerae* on host metabolism demonstrated that *V. cholerae* challenge impacts intestinal levels of acetate(224), succinate(221), and methionine sulfoxide(333) with consequences for host insulin signaling, lipid homeostasis, and epithelial renewal. For instance, consumption of the short chain fatty acid, acetate, by *V. cholerae* via the expression of *acetyl-CoA synthase*, disrupts insulin signalling and results in a relocalization of lipids from the fat body to the gut. Removal of lipids from the fly diet prevented lipid relocalization and extended the viability of adult flies infected with *V. cholerae*, implicating lipid metabolism as a mediator of *V. cholerae* pathogenesis(224). Additionally, *V. cholerae* consumption of the metabolite, methionine sulfoxide, impaired epithelial regeneration(333). Interestingly, the ability of *V. cholerae* to suppress epithelial renewal is reverted by mutational inactivation of IMD(334), suggesting functional links between immune activity and IPC growth in infected flies. In contrast to this study of C6706, some strains of C6706 cause limited disease in flies and fail to block epithelial renewal(221). It is likely that this is a function of differences in quorum sensing between the C6706 strains used in the respective studies, as the strain of C6706 used in this work has low expression of the quorum-sensing master regulator, HapR(285, 328). HapR suppresses the expression of virulence factors such as CT and TCP(345), and deletions of HapR convert non-pathogenic strains to lethal strains that have the ability to block IPC growth(221). Together, studies of *V. cholerae* in the fly model have identified IMD and disruptions to metabolic signalling as important contributors to *V. cholerae* pathogenesis.

#### **6.4.6 Conclusions from chapter 5**

In summary, the work presented in chapter 5 demonstrates that complex interactions between intestinal symbionts and enteric invaders combine to influence critical components of the intestinal immune response (Fig. 6.1). While the effects of pathogenic bacteria on epithelial repair have been previously described, this work takes into consideration how interactions between bacterial species within a complex community structure affects this process. Given the diversity of intestinal microbial communities, I believe these findings represent a valuable contribution to the understanding of the effects of the microbiome on host immunity.

#### **6.5 Concluding remarks**

The digestive tract is an ancestral organ to most animals and intestinal homeostatic regulators have been conserved throughout evolution. The works presented in this dissertation highlight the value of model organisms in studying the microbiome's influence on fundamental mechanisms of immune and tissue homeostasis. I dissect the molecular transactions between host tissue and microbial symbiont in the intestine by means of high-resolution sequencing and modification of microbial contents to better understand the impact of the microbiome on host biology. In closing, the data in this thesis contribute to the understanding of the complex relationship that exists between host and microbe.



## Chapter 7.

### Literature Cited

1. Miguel-Aliaga, I., H. Jasper, and B. Lemaitre. 2018. Anatomy and physiology of the digestive tract of *Drosophila melanogaster*. *Genetics* 210: 357–396.
2. Buchon, N., D. Osman, F. P. A. David, H. Yu Fang, J.-P. Boquete, B. Deplancke, and B. Lemaitre. 2013. Morphological and molecular characterization of adult midgut compartmentalization in *Drosophila*. *Cell Rep.* 3: 1725–1738.
3. Marianes, A., and A. C. Spradling. 2013. Physiological and stem cell compartmentalization within the *Drosophila* midgut. *Elife* 2013.
4. Hoppler, S., and M. Bienz. 1994. Specification of a single cell type by a *Drosophila* homeotic gene. *Cell* 76: 689–702.
5. Shanbhag, S., and S. Tripathi. 2009. Epithelial ultrastructure and cellular mechanisms of acid and base transport in the *Drosophila* midgut. *J. Exp. Biol.* 212: 1731–1744.
6. Xiang, J., J. Bandura, P. Zhang, Y. Jin, H. Reuter, and B. A. Edgar. 2017. EGFR-dependent TOR-independent endocycles support *Drosophila* gut epithelial regeneration. *Nat. Commun.* 8: 1–13.
7. Ohlstein, B., and A. Spradling. 2006. The adult *Drosophila* posterior midgut is maintained by pluripotent stem cells. *Nature* 439: 470–474.
8. Micchelli, C. A., and N. Perrimon. 2006. Evidence that stem cells reside in the adult *Drosophila* midgut epithelium. *Nature* 439: 475–479.
9. Takashima, S., K. L. Adams, P. A. Ortiz, C. T. Ying, R. Moridzadeh, A. Younossi-Hartenstein, and V. Hartenstein. 2011. Development of the *Drosophila* entero-endocrine lineage and its specification by the Notch signaling pathway. *Dev. Biol.* 353: 161–72.
10. Jiang, H., P. H. Patel, A. Kohlmaier, M. O. Grenley, D. G. McEwen, and B. A. Edgar. 2009. Cytokine/Jak/Stat signaling mediates regeneration and homeostasis in the *Drosophila* midgut. *Cell* 137:

1343–1355.

11. Ohlstein, B., and A. Spradling. 2007. Multipotent *Drosophila* intestinal stem cells specify daughter cell fates by differential Notch signaling. *Science* (80- ). 315: 988–992.

12. Biteau, B., and H. Jasper. 2014. Slit/Robo signaling regulates cell fate decisions in the intestinal stem cell lineage of *Drosophila*. *Cell Rep.* 7: 1867–1875.

13. Hegedus, D., M. Erlandson, C. Gillott, and U. Toprak. 2009. New insights into peritrophic matrix synthesis, architecture, and function. *Annu. Rev. Entomol.* 54: 285–302.

14. Kuraishi, T., O. Binggeli, O. Opota, N. Buchon, and B. Lemaitre. 2011. Genetic evidence for a protective role of the peritrophic matrix against intestinal bacterial infection in *Drosophila melanogaster*. *Proc. Natl. Acad. Sci. U. S. A.* 108: 15966–71.

15. Conway, S., C. L. Sansone, A. Benske, K. Kentala, J. Billen, J. Vanden Broeck, and E. M. Blumenthal. 2018. Pleiotropic and novel phenotypes in the *Drosophila* gut caused by mutation of drop-dead. *J. Insect Physiol.* 105: 76–84.

16. Weber, A. N. R., S. Tauszig-Delamasure, J. A. Hoffmann, E. Lelièvre, H. Gascan, K. P. Ray, M. A. Morse, J. L. Imler, and N. J. Gay. 2003. Binding of the *Drosophila* cytokine Spätzle to Toll is direct and establishes signaling. *Nat. Immunol.* 4: 794–800.

17. Lhocine, N., P. S. Ribeiro, N. Buchon, A. Wepf, R. Wilson, T. Tenev, B. Lemaitre, M. Gstaiger, P. Meier, and F. Leulier. 2008. PIMS modulates immune tolerance by negatively regulating *Drosophila* innate immune signaling. *Cell Host Microbe* 4: 147–158.

18. Buchon, N., N. Broderick, S. Chakrabarti, and B. Lemaitre. 2009. Invasive and indigenous microbiota impact intestinal stem cell activity through multiple pathways in *Drosophila*. *Genes Dev.* 23: 2333–2344.

19. Buchon, N., N. A. Broderick, M. Poidevin, S. Pradervand, and B. Lemaitre. 2009. *Drosophila* intestinal response to bacterial infection: activation of host defense and stem cell proliferation. *Cell Host Microbe* 5: 200–211.

20. Buchon, N., N. Silverman, and S. Cherry. 2014. Immunity in *Drosophila melanogaster* — from microbial recognition to whole-organism physiology. *Nat. Rev. Immunol.* 14: 796–810.
21. Kaneko, T., W. E. Goldman, P. Mellroth, H. Steiner, K. Fukase, S. Kusumoto, W. Harley, A. Fox, D. Golenbock, and N. Silverman. 2004. Monomeric and polymeric gram-negative peptidoglycan but not purified LPS stimulate the *Drosophila* IMD pathway. *Immunity* 20: 637–49.
22. Leulier, F., C. Parquet, S. Pili-Floury, J.-H. Ryu, M. Caroff, W.-J. Lee, D. Mengin-Lecreux, and B. Lemaitre. 2003. The *Drosophila* immune system detects bacteria through specific peptidoglycan recognition. *Nat. Immunol.* 4: 478–484.
23. Stenbak, C. R., J.-H. Ryu, F. Leulier, S. Pili-Floury, C. Parquet, M. Hervé, C. Chaput, I. G. Boneca, W.-J. Lee, B. Lemaitre, and D. Mengin-Lecreux. 2004. Peptidoglycan molecular requirements allowing detection by the *Drosophila* immune deficiency pathway. *J. Immunol.* 173: 7339–7348.
24. Werner, T., K. Borge-Renberg, P. Mellroth, H. Steiner, and D. Hultmark. 2003. Functional diversity of the *Drosophila* PGRP-LC gene cluster in the response to lipopolysaccharide and peptidoglycan. *J. Biol. Chem.* 278: 26319–26322.
25. Neyen, C., M. Poidevin, A. Roussel, and B. Lemaitre. 2012. Tissue- and ligand-specific sensing of Gram-negative infection in *Drosophila* by PGRP-LC isoforms and PGRP-LE. *J. Immunol.* 189: 1886–1897.
26. Bosco-Drayon, V., M. Poidevin, I. G. Boneca, K. Narbonne-Reveau, J. Royet, and B. Charroux. 2012. Peptidoglycan sensing by the receptor PGRP-LE in the *Drosophila* gut induces immune responses to infectious bacteria and tolerance to microbiota. *Cell Host Microbe* 12: 153–165.
27. Choe, K. M., H. Lee, and K. V. Anderson. 2005. *Drosophila* peptidoglycan recognition protein LC (PGRP-LC) acts as a signal-transducing innate immune receptor. *Proc. Natl. Acad. Sci. U. S. A.* 102: 1122–1126.
28. Kleino, A., N. F. Ramia, G. Bozkurt, Y. Shen, H. Nailwal, J. Huang, J. Napetschnig, M. Gangloff, F. K. M. Chan, H. Wu, J. Li, and N. Silverman. 2017. Peptidoglycan-sensing receptors trigger the formation of functional amyloids of the adaptor protein Imd to initiate *Drosophila* NF- $\kappa$ B signaling. *Immunity* 47: 635–

647.e6.

29. Leulier, F., S. Vidal, K. Saigo, R. Ueda, and B. Lemaitre. 2002. Inducible expression of double-stranded RNA reveals a role for dFADD in the regulation of the antibacterial response in *Drosophila* adults. *Curr. Biol.* 12: 996–1000.
30. Leulier, F., A. Rodriguez, R. S. Khush, J. M. Abrams, and B. Lemaitre. 2000. The *Drosophila* caspase Dredd is required to resist Gram-negative bacterial infection. *EMBO Rep.* 1: 353–358.
31. Paquette, N., M. Broemer, K. Aggarwal, L. Chen, M. Husson, D. Ertürk-Hasdemir, J.-M. Reichhart, P. Meier, and N. Silverman. 2010. Caspase-Mediated Cleavage, IAP Binding, and Ubiquitination: Linking Three Mechanisms Crucial for *Drosophila* NF- $\kappa$ B Signaling. *Mol. Cell* 37: 172–182.
32. Silverman, N., R. Zhou, S. Stöven, N. Pandey, D. Hultmark, and T. Maniatis. 2000. A *Drosophila* IkappaB kinase complex required for Relish cleavage and antibacterial immunity. *Genes Dev.* 14: 2461–71.
33. Chen, W., M. A. White, and M. H. Cobb. 2002. Stimulus-specific requirements for MAP3 kinases in activating the JNK pathway. *J. Biol. Chem.* 277: 49105–49110.
34. Dushay, M. S., B. Asling, and D. Hultmark. 1996. Origins of immunity: Relish, a compound Rel-like gene in the antibacterial defense of *Drosophila*. 93: 10343–10347.
35. Imler, J. L., and P. Bulet. 2005. Antimicrobial peptides in *Drosophila*: Structures, activities and gene regulation. *Chem. Immunol. Allergy* 86: 1–21.
36. Cudic, M., P. Bulet, R. Hoffmann, D. J. Craik, and L. Otvos. 1999. Chemical synthesis, antibacterial activity and conformation of diptericin, an 82-mer peptide originally isolated from insects. *Eur. J. Biochem.* 266: 549–558.
37. Hedengren, M., K. Borge, and D. Hultmark. 2000. Expression and evolution of the *Drosophila* Attacin/Diptericin gene family. *Biochem. Biophys. Res. Commun.* 279: 574–581.
38. Fehlbaum, P., P. Bulet, L. Michaut, M. Lagueux, W. F. Broekaert, C. Hetru, and J. A. Hoffmann. 1994. Insect immunity: Septic injury of *drosophila* induces the synthesis of a potent antifungal peptide with

- sequence homology to plant antifungal peptides. *J. Biol. Chem.* 269: 33159–33163.
39. Levashina, E. A., S. Ohresser, P. Bulet, J. -M Reichhart, C. Hetru, and J. A. Hoffmann. 1995. Metchnikowin, a novel immune-inducible proline-rich peptide from *Drosophila* with antibacterial and antifungal properties. *Eur. J. Biochem.* 233: 694–700.
40. Hanson, M. A., A. Dostálová, C. Ceroni, M. Poidevin, S. Kondo, and B. Lemaitre. 2019. Synergy and remarkable specificity of antimicrobial peptides in vivo using a systematic knockout approach. *Elife* 8.
41. Broderick, N. A., N. Buchon, and B. Lemaitre. 2014. Microbiota-induced changes in *Drosophila melanogaster* host gene expression and gut morphology. *MBio* 5: 1–13.
42. Combe, B. E., A. Defaye, N. Bozonnet, D. Puthier, J. Royet, and F. Leulier. 2014. *Drosophila* microbiota modulates host metabolic gene expression via IMD/NF- $\kappa$ B signaling. *PLoS One* 9: e94729.
43. Petkau, K., M. Ferguson, S. Guntermann, and E. Foley. 2017. Constitutive immune activity promotes tumorigenesis in *Drosophila* intestinal progenitor cells. *Cell Rep.* 20: 1784–1793.
44. Davoodi, S., A. Galenza, A. Panteluk, R. Deshpande, M. Ferguson, S. Grewal, and E. Foley. 2019. The immune deficiency pathway regulates metabolic homeostasis in *Drosophila*. *J. Immunol.* 202: 2747–2759.
45. Zhai, Z., J.-P. Boquete, and B. Lemaitre. 2018. Cell-specific Imd-NF- $\kappa$ B responses enable simultaneous antibacterial immunity and intestinal epithelial cell shedding upon bacterial infection. *Immunity* 48: 897–910.
46. Ha, E.-M., C.-T. Oh, Y. S. Bae, and W.-J. Lee. 2005. A direct role for dual oxidase in *Drosophila* gut immunity. *Science (80- )*. 310: 847–850.
47. Jones, R. M., L. Luo, C. S. Ardita, A. N. Richardson, Y. M. Kwon, J. W. Mercante, A. Alam, C. L. Gates, H. Wu, P. A. Swanson, J. D. Lambeth, P. W. Denning, and A. S. Neish. 2013. Symbiotic Lactobacilli stimulate gut epithelial proliferation via Nox-mediated generation of reactive oxygen species. *EMBO J.* 32: 3017–28.
48. Ha, E. M., K. A. Lee, Y. Y. Seo, S. H. Kim, J. H. Lim, B. H. Oh, J. Kim, and W. J. Lee. 2009. Coordination of

multiple dual oxidase-regulatory pathways in responses to commensal and infectious microbes in *Drosophila* gut. *Nat. Immunol.* 10: 949–957.

49. Ha, E. M., K. A. Lee, S. H. Park, S. H. Kim, H. J. Nam, H. Y. Lee, D. Kang, and W. J. Lee. 2009. Regulation of DUOX by the  $G\alpha_q$ -phospholipase  $C\beta$ - $Ca^{2+}$  pathway in *Drosophila* gut immunity. *Dev. Cell* 16: 386–397.

50. Lee, K. A., K. C. Cho, B. Kim, I. H. Jang, K. Nam, Y. E. Kwon, M. Kim, D. Y. Hyeon, D. Hwang, J. H. Seol, and W. J. Lee. 2018. Inflammation-modulated metabolic reprogramming is required for DUOX-dependent gut immunity in *Drosophila*. *Cell Host Microbe* 23: 338-352.e5.

51. Lu, Y., and Z. Li. 2015. No intestinal stem cell regeneration after complete progenitor ablation in *Drosophila* adult midgut. *J. Genet. Genomics* 42: 83–86.

52. Guo, Z., and B. Ohlstein. 2015. Bidirectional Notch signaling regulates *Drosophila* intestinal stem cell multipotency. *Science (80-. )*. 350.

53. Zeng, X., and S. X. Hou. 2015. Enteroendocrine cells are generated from stem cells through a distinct progenitor in the adult *Drosophila* posterior midgut. *Dev.* 142: 644–653.

54. O'Brien, L. E., S. S. Soliman, X. Li, and D. Bilder. 2011. Altered modes of stem cell division drive adaptive intestinal growth. *Cell* 147: 603–614.

55. Jin, Y., P. H. Patel, A. Kohlmaier, B. Pavlovic, C. Zhang, and B. A. Edgar. 2017. Intestinal stem cell pool regulation in *Drosophila*. *Stem Cell Reports* 8: 1479–1487.

56. Hu, D. J. K., and H. Jasper. 2019. Control of intestinal cell fate by dynamic mitotic spindle repositioning influences epithelial homeostasis and longevity. *Cell Rep.* 28: 2807-2823.e5.

57. Jiang, H., and B. A. Edgar. 2009. EGFR signaling regulates the proliferation of *Drosophila* adult midgut progenitors. *Development* 136: 483–493.

58. Buchon, N., N. A. Broderick, T. Kuraishi, and B. Lemaitre. 2010. *Drosophila* EGFR pathway coordinates stem cell proliferation and gut remodeling following infection. *BMC Biol.* 8: 1–19.

59. Biteau, B., and H. Jasper. 2011. EGF signaling regulates the proliferation of intestinal stem cells in

*Drosophila. Development* 138: 1045–1055.

60. Jiang, H., M. O. Grenley, M.-J. Bravo, R. Z. Blumhagen, and B. A. Edgar. 2011. EGFR/Ras/MAPK signaling mediates adult midgut epithelial homeostasis and regeneration in *Drosophila*. *Cell Stem Cell* 8: 84–95.

61. Beebe, K., W. C. Lee, and C. A. Micchelli. 2010. JAK/STAT signaling coordinates stem cell proliferation and multilineage differentiation in the *Drosophila* intestinal stem cell lineage. *Dev. Biol.* 338: 28–37.

62. Lin, G., N. Xu, and R. Xi. 2010. Paracrine Unpaired signaling through the JAK/STAT pathway controls self-renewal and lineage differentiation of *Drosophila* intestinal stem cells. *J. Mol. Cell Biol.* 2: 37–49.

63. Biteau, B., C. E. Hochmuth, and H. Jasper. 2008. JNK activity in somatic stem cells causes loss of tissue homeostasis in the aging *Drosophila* gut. *Cell Stem Cell* 3: 442–55.

64. Lin, G., N. Xu, and R. Xi. 2008. Paracrine Wingless signalling controls self-renewal of *Drosophila* intestinal stem cells. *Nature* 455: 1119–1123.

65. Lee, W.-C., K. Beebe, L. Sudmeier, and C. A. Micchelli. 2009. Adenomatous polyposis coli regulates *Drosophila* intestinal stem cell proliferation. *Development* 136.

66. Amcheslavsky, A., J. Jiang, and Y. T. Ip. 2009. Tissue damage-induced Intestinal stem cell division in *Drosophila*. *Cell Stem Cell* 4: 49–61.

67. Biteau, B., J. Karpac, S. Supoyo, M. DeGennaro, R. Lehmann, and H. Jasper. 2010. Lifespan extension by preserving proliferative homeostasis in *Drosophila*. *PLoS Genet.* 6: e1001159.

68. Choi, N. H., E. Lucchetta, and B. Ohlstein. 2011. Nonautonomous regulation of *Drosophila* midgut stem cell proliferation by the insulin-signaling pathway. *Proc. Natl. Acad. Sci. U. S. A.* 108: 18702–7.

69. Kapuria, S., J. Karpac, B. Biteau, D. Hwangbo, and H. Jasper. 2012. Notch-mediated suppression of TSC2 expression regulates cell differentiation in the *Drosophila* intestinal stem cell lineage. *PLoS Genet.* 8: e1003045.

70. Quan, Z., P. Sun, G. Lin, and R. Xi. 2013. TSC1/2 regulates intestinal stem cell maintenance and lineage

- differentiation through Rheb-TORC1-S6K but independently of nutritional status or notch regulation. *J. Cell Sci.* 126: 3884–3892.
71. Tian, A., B. Wang, and J. Jiang. 2017. Injury-stimulated and self-restrained BMP signaling dynamically regulates stem cell pool size during *Drosophila* midgut regeneration. *Proc. Natl. Acad. Sci. U. S. A.* 114: E2699–E2708.
72. Tian, A., and J. Jiang. 2014. Intestinal epithelium-derived BMP controls stem cell self-renewal in *Drosophila* adult midgut. *Elife* 3: e01857.
73. Ayyaz, A., H. Li, and H. Jasper. 2015. Haemocytes control stem cell activity in the *Drosophila* intestine. *Nat. Cell Biol.* 17: 736–748.
74. Li, H., Y. Qi, and H. Jasper. 2013. Dpp signaling determines regional stem cell identity in the regenerating adult *Drosophila* gastrointestinal tract. *Cell Rep.* 4: 10–18.
75. Guo, Z., I. Driver, and B. Ohlstein. 2013. Injury-induced BMP signaling negatively regulates *Drosophila* midgut homeostasis. *J. Cell Biol.* 201: 945–61.
76. Karpowicz, P., J. Perez, and N. Perrimon. 2010. The Hippo tumor suppressor pathway regulates intestinal stem cell regeneration. *Development* 137: 4135–4145.
77. Shaw, R. L., A. Kohlmaier, C. Polesello, C. Veelken, B. A. Edgar, and N. Tapon. 2010. The Hippo pathway regulates intestinal stem cell proliferation during *Drosophila* adult midgut regeneration. *Development* 137: 4147–4158.
78. Tian, A., Q. Shi, A. Jiang, S. Li, B. Wang, and J. Jiang. 2015. Injury-stimulated Hedgehog signaling promotes regenerative proliferation of *Drosophila* intestinal stem cells. *J. Cell Biol.* 208: 807–819.
79. Bond, D., and E. Foley. 2012. Autocrine platelet-derived growth factor-vascular endothelial growth factor receptor-related (Pvr) pathway activity controls intestinal stem cell proliferation in the adult *Drosophila* midgut. *J. Biol. Chem.* 287: 27359–70.
80. Zeidler, M. P., and N. Bausek. 2013. The *Drosophila* JAK-STAT pathway. *JAK-STAT* 2: e25353.



81. Bonfini, A., X. Liu, and N. Buchon. 2016. From pathogens to microbiota: How *Drosophila* intestinal stem cells react to gut microbes. *Dev. Comp. Immunol.* 64: 22–38.
82. Wong, A. C.-N., A. J. Dobson, and A. E. Douglas. 2014. Gut microbiota dictates the metabolic response of *Drosophila* to diet. *J. Exp. Biol.* 217: 1894–901.
83. Hooper, L. V., D. R. Littman, and A. J. Macpherson. 2012. Interactions between the microbiota and the immune system. *Science* 336: 1268–73.
84. Kamada, N., S.-U. Seo, G. Y. Chen, and G. Núñez. 2013. Role of the gut microbiota in immunity and inflammatory disease. *Nat. Rev. Immunol.* 13: 321–335.
85. Hsiao, E. Y., S. W. McBride, S. Hsien, G. Sharon, E. R. Hyde, T. McCue, J. A. Codelli, J. Chow, S. E. Reisman, J. F. Petrosino, P. H. Patterson, and S. K. Mazmanian. 2013. Microbiota modulate behavioral and physiological abnormalities associated with neurodevelopmental disorders. *Cell* 155: 1451–1463.
86. Ma, D., G. Storelli, M. Mitchell, and F. Leulier. 2015. Studying host–microbiota mutualism in *Drosophila*: Harnessing the power of gnotobiotic flies. *Biomed. J.* 38: 285–293.
87. Wong, C. N. A., P. Ng, and A. E. Douglas. 2011. Low-diversity bacterial community in the gut of the fruitfly *Drosophila melanogaster*. *Environ. Microbiol.* 13: 1889–1900.
88. Wong, A. C.-N., J. M. Chaston, and A. E. Douglas. 2013. The inconstant gut microbiota of *Drosophila* species revealed by 16S rRNA gene analysis. *ISME J.* 7: 1922–1932.
89. Adair, K. L., and A. E. Douglas. 2017. Making a microbiome: the many determinants of host-associated microbial community composition. *Curr. Opin. Microbiol.* 35: 23–29.
90. Broderick, N. A., and B. Lemaitre. 2012. Gut-associated microbes of *Drosophila melanogaster*. *Gut Microbes* 3: 307–321.
91. Koyle, M. L., M. Veloz, A. M. Judd, A. C.-N. Wong, P. D. Newell, A. E. Douglas, and J. M. Chaston. 2016. Rearing the fruit fly *Drosophila melanogaster* under axenic and gnotobiotic conditions. *J. Vis. Exp.* 113: e54219.

92. Lemaitre, B., and I. Miguel-Aliaga. 2013. The digestive tract of *Drosophila melanogaster*. *Annu. Rev. Genet.* 47: 377–404.
93. Jiang, H., and B. A. Edgar. 2012. Intestinal stem cell function in *Drosophila* and mice. *Curr. Opin. Genet. Dev.* 22: 354–360.
94. Cheng, H., and C. P. Leblond. 1974. Origin, differentiation and renewal of the four main epithelial cell types in the mouse small intestine V. Unitarian theory of the origin of the four epithelial cell types. *Am. J. Anat.* 141: 537–561.
95. Rera, M., R. I. Clark, and D. W. Walker. 2012. Intestinal barrier dysfunction links metabolic and inflammatory markers of aging to death in *Drosophila*. *Proc. Natl. Acad. Sci. U. S. A.* 109: 21528–33.
96. Belkaid, Y., and T. W. Hand. 2014. Role of the microbiota in immunity and inflammation. *Cell* 157: 121–141.
97. Harris, H. L., L. J. Brennan, B. A. Keddie, and H. R. Braig. 2010. Bacterial symbionts in insects: Balancing life and death. *Symbiosis* 51: 37–53.
98. Werren, J. H., L. Baldo, and M. E. Clark. 2008. Wolbachia: Master manipulators of invertebrate biology. *Nat. Rev. Microbiol.* 6: 741–751.
99. Haselkorn, T. S. 2010. The spiroplasma heritable bacterial endosymbiont of *Drosophila*. *Fly (Austin)*. 4: 80–87.
100. Bakula, M. 1967. The ecogenetics of a *Drosophila*-bacteria association. .
101. Bakula, M. 1969. The persistence of a microbial flora during postembryogenesis of *Drosophila melanogaster*. *J. Invertebr. Pathol.* 14: 365–374.
102. Shin, S. C., S.-H. Kim, H. You, B. Kim, A. C. Kim, K.-A. Lee, J.-H. Yoon, J.-H. Ryu, and W.-J. Lee. 2011. *Drosophila* microbiome modulates host developmental and metabolic homeostasis via insulin signaling. *Science (80- )*. 334: 670–674.
103. Brummel, T., A. Ching, L. Seroude, A. F. Simon, and S. Benzer. 2004. *Drosophila* lifespan

- enhancement by exogenous bacteria. *Proc. Natl. Acad. Sci. U. S. A.* 101: 12974–9.
104. Ridley, E. V, A. C. N. Wong, and A. E. Douglas. 2013. Microbe-dependent and nonspecific effects of procedures to eliminate the resident microbiota from *Drosophila melanogaster*. *Appl. Environ. Microbiol.* 79: 3209–14.
105. Storelli, G., A. Defaye, B. Erkosar, P. Hols, J. Royet, and F. Leulier. 2011. *Lactobacillus plantarum* promotes *Drosophila* systemic growth by modulating hormonal signals through TOR-dependent nutrient sensing. *Cell Metab.* 14: 403–414.
106. Tryselius, Y., C. Samakovlis, D. A. Kimbrell, and D. Hultmark. 1992. CecC, a cecropin gene expressed during metamorphosis in *Drosophila* pupae. *Eur. J. Biochem.* 204: 395–399.
107. Russell, V., and P. E. Dunn. 1996. Antibacterial proteins in the midgut of *Manduca sexta* during metamorphosis. *J. Insect Physiol.* 42: 65–71.
108. Samakovlis, C., D. A. Kimbrell, P. Kylsten, A. Engström, and D. Hultmark. 1990. The immune response in *Drosophila*: pattern of cecropin expression and biological activity. *EMBO J.* 9: 2969–2976.
109. Tzou, P., S. Ohresser, D. Ferrandon, M. Capovilla, J.-M. Reichhart, B. Lemaitre, J. A. Hoffmann, and J.-L. Imler. 2000. Tissue-specific inducible expression of antimicrobial peptide genes in *Drosophila* surface epithelia. *Immunity* 13: 737–748.
110. Blum, J. E., C. N. Fischer, J. Miles, and J. Handelsman. 2013. Frequent replenishment sustains the beneficial microbiome of *Drosophila melanogaster*. *MBio* 4: e00860-13.
111. Ren, C., P. Webster, S. E. Finkel, and J. Tower. 2007. Increased internal and external bacterial load during *Drosophila* aging without life-span trade-off. *Cell Metab.* 6: 144–152.
112. Obadia, B., Z. T. Güvener, V. Zhang, J. A. Ceja-Navarro, E. L. Brodie, W. W. Ja, and W. B. Ludington. 2017. Probabilistic invasion underlies natural gut microbiome stability. *Curr. Biol.* 27: 1999-2006.e8.
113. Clark, R. I., A. Salazar, R. Yamada, S. Fitz-Gibbon, M. Morselli, J. Alcaraz, A. Rana, M. Rera, M. Pellegrini, W. W. Ja, and D. W. Walker. 2015. Distinct shifts in microbiota composition during *Drosophila*

- aging impair intestinal function and drive mortality. *Cell Rep.* 12: 1656–67.
114. Chow, J., S. M. Lee, Y. Shen, A. Khosravi, and S. K. Mazmanian. 2010. Host-bacterial symbiosis in health and disease. In *Advances in Immunology* vol. 107. Academic Press Inc. 243–274.
115. Pais, I. S., R. S. Valente, M. Sporniak, and L. Teixeira. 2018. *Drosophila melanogaster* establishes a species-specific mutualistic interaction with stable gut-colonizing bacteria. *PLoS Biol.* 16.
116. Keebaugh, E. S., R. Yamada, B. Obadia, W. B. Ludington, and W. W. Ja. 2018. Microbial quantity impacts *Drosophila* nutrition, development, and lifespan. *iScience* 4: 247–259.
117. Storelli, G., M. Strigini, T. Grenier, L. Bozonnet, M. Schwarzer, C. Daniel, R. Matos, and F. Leulier. 2018. *Drosophila* perpetuates nutritional mutualism by promoting the fitness of its intestinal symbiont *Lactobacillus plantarum*. *Cell Metab.* 27: 362–377.e8.
118. Reaume, C. J., and M. B. Sokolowski. 2006. The nature of *Drosophila melanogaster*. *Curr. Biol.* 16.
119. Chandler, J. A., J. Morgan Lang, S. Bhatnagar, J. A. Eisen, and A. Kopp. 2011. Bacterial communities of diverse *Drosophila* species: ecological context of a host–microbe model system. *PLoS Genet.* 7: e1002272.
120. Robinson, C. J., B. J. M. Bohannan, and V. B. Young. 2010. From structure to function: the ecology of host-associated microbial communities. *Microbiol. Mol. Biol. Rev.* 74: 453–476.
121. Sender, R., S. Fuchs, and R. Milo. 2016. Revised estimates for the number of human and bacteria cells in the body. *PLoS Biol.* 14: e1002533.
122. Ley, R. E., C. A. Lozupone, M. Hamady, R. Knight, and J. I. Gordon. 2008. Worlds within worlds: Evolution of the vertebrate gut microbiota. *Nat. Rev. Microbiol.* 6: 776–788.
123. Staubach, F., J. F. Baines, S. Künzel, E. M. Bik, and D. A. Petrov. 2013. Host species and environmental effects on bacterial communities associated with *Drosophila* in the laboratory and in the natural environment. *PLoS One* 8: e70749.
124. Ridley, E. V., A. C.-N. Wong, S. Westmiller, and A. E. Douglas. 2012. Impact of the resident microbiota on the nutritional phenotype of *Drosophila melanogaster*. *PLoS One* 7: e36765.

125. Cox, C. R., and M. S. Gilmore. 2007. Native microbial colonization of *Drosophila melanogaster* and its use as a model of *Enterococcus faecalis* pathogenesis. *Infect. Immun.* 75: 1565–1576.
126. Ryu, J.-H., S.-H. Kim, H.-Y. Lee, J. Y. Bai, Y.-D. Nam, J.-W. Bae, D. G. Lee, S. C. Shin, E.-M. Ha, and W.-J. Lee. 2008. Innate immune homeostasis by the homeobox gene *caudal* and commensal-gut mutualism in *Drosophila*. *Science* 319: 777–782.
127. Sharon, G., D. Segal, J. M. Ringo, A. Hefetz, I. Zilber-Rosenberg, and E. Rosenberg. 2010. Commensal bacteria play a role in mating preference of *Drosophila melanogaster*. *Proc. Natl. Acad. Sci. U. S. A.* 107: 20051–20056.
128. Douglas, A. E. 2018. The *Drosophila* model for microbiome research. *Lab Anim. (NY)*. 47: 157–164.
129. Corby-Harris, V., A. C. Pontaroli, L. J. Shimkets, J. L. Bennetzen, K. E. Habel, and D. E. L. Promislow. 2007. Geographical distribution and diversity of bacteria associated with natural populations of *Drosophila melanogaster*. *Appl. Environ. Microbiol.* 73: 3470–3479.
130. Adair, K. L., M. Wilson, A. Bost, and A. E. Douglas. 2018. Microbial community assembly in wild populations of the fruit fly *Drosophila melanogaster*. *ISME J.* 12: 959–972.
131. Shehata, A. M. E. T., E. M. Mrak, and H. J. Phaff. 1955. Yeasts isolated from *Drosophila* and from their suspected feeding places in southern and central California. *Mycologia* 47: 799–811.
132. Chaplinska, M., S. Gerritsma, F. Dini-Andreote, J. Falcao Salles, and B. Wertheim. 2016. Bacterial communities differ among *Drosophila melanogaster* populations and affect host resistance against parasitoids. *PLoS One* 11: e0167726.
133. Early, A. M., N. Shanmugarajah, N. Buchon, and A. G. Clark. 2017. *Drosophila* genotype influences commensal bacterial levels. *PLoS One* 12: e0170332.
134. Sang, J. 1956. The quantitative nutritional requirements of *Drosophila melanogaster*. *J. Exp. Biol.* 33.
135. Anagnostou, C., M. Dorsch, and M. Rohlf. 2010. Influence of dietary yeasts on *Drosophila melanogaster* life-history traits. *Entomol. Exp. Appl.* 136: 1–11.

136. Yamada, R., S. A. Deshpande, K. D. Bruce, E. M. Mak, and W. W. Ja. 2015. Microbes promote amino acid harvest to rescue undernutrition in *Drosophila*. *Cell Rep.* 10: 865–872.
137. Chandler, J. A., J. A. Eisen, and A. Kopp. 2012. Yeast communities of diverse *Drosophila* species: Comparison of two symbiont groups in the same hosts. *Appl. Environ. Microbiol.* 78: 7327–7336.
138. Lam, S. S. T. H., and K. S. Howell. 2015. *Drosophila*-associated yeast species in vineyard ecosystems. *FEMS Microbiol. Lett.* 362.
139. Erkosar, B., G. Storelli, M. Mitchell, L. Bozonnet, N. Bozonnet, and F. Leulier. 2015. Pathogen virulence impedes mutualist-mediated enhancement of host juvenile growth via inhibition of protein digestion. *Cell Host Microbe* 18: 445–455.
140. Gould, A. L., V. Zhang, L. Lamberti, E. W. Jones, B. Obadia, N. Korasidis, A. Gavryushkin, J. M. Carlson, N. Beerenwinkel, and W. B. Ludington. 2018. Microbiome interactions shape host fitness. *Proc. Natl. Acad. Sci.* 115: E11951–E11960.
141. Sannino, D. R., A. J. Dobson, K. Edwards, E. R. Angert, and N. Buchon. 2018. The *Drosophila melanogaster* gut microbiota provisions thiamine to its host. *MBio* 9.
142. Galenza, A., and E. Foley. 2019. Immunometabolism: Insights from the *Drosophila* model. *Dev. Comp. Immunol.* 94: 22–34.
143. Lee, K.-A., S.-H. Kim, E.-K. Kim, E.-M. Ha, H. You, B. Kim, M.-J. Kim, Y. Kwon, J.-H. Ryu, and W.-J. Lee. 2013. Bacterial-derived uracil as a modulator of mucosal immunity and gut-microbe homeostasis in *Drosophila*. *Cell* 153: 797–811.
144. Jones, R. M., C. Desai, T. M. Darby, L. Luo, A. A. Wolfarth, C. D. Scharer, C. S. Ardita, A. R. Reedy, E. S. Keebaugh, and A. S. Neish. 2015. Lactobacilli modulate epithelial cytoprotection through the Nrf2 pathway. *Cell Rep.* 12: 1217–1225.
145. Guo, L., J. Karpac, S. L. Tran, and H. Jasper. 2014. PGRP-SC2 promotes gut immune homeostasis to limit commensal dysbiosis and extend lifespan. *Cell* 156: 109–122.

146. Petkau, K., B. D. Parsons, A. Duggal, and E. Foley. 2014. A deregulated intestinal cell cycle program disrupts tissue homeostasis without affecting longevity in *Drosophila*. *J. Biol. Chem.* 289: 28719–29.
147. Choi, N.-H., J.-G. Kim, D.-J. Yang, Y.-S. Kim, and M.-A. Yoo. 2008. Age-related changes in *Drosophila* midgut are associated with PVF2, a PDGF/VEGF-like growth factor. *Aging Cell* 7: 318–334.
148. Li, H., Y. Qi, and H. Jasper. 2016. Preventing age-related decline of gut compartmentalization limits microbiota dysbiosis and extends lifespan. *Cell Host Microbe* 19: 240–253.
149. Park, J. S., Y. S. Kim, and M. A. Yoo. 2009. The role of p38b MAPK in age-related modulation of intestinal stem cell proliferation and differentiation in *Drosophila*. *Aging (Albany, NY)*. 1: 637–651.
150. Ferguson, M., K. Petkau, M. Shin, A. Galenza, D. Fast, and E. Foley. 2019. Symbiotic *Lactobacillus brevis* promote stem cell expansion and tumorigenesis in the *Drosophila* intestine. *bioRxiv* 799981.
151. Kurz, C. L. 2003. Virulence factors of the human opportunistic pathogen *Serratia marcescens* identified by in vivo screening. *EMBO J.* 22: 1451–1460.
152. Nehme, N. T., S. Liégeois, B. Kele, P. Giammarinaro, E. Pradel, J. A. Hoffmann, J. J. Ewbank, and D. Ferrandon. 2007. A model of bacterial intestinal infections in *Drosophila melanogaster*. *PLoS Pathog.* 3: e173.
153. Vodovar, N., M. Vinals, P. Liehl, A. Basset, J. Degrouard, P. Spellman, F. Boccard, and B. Lemaître. 2005. *Drosophila* host defense after oral infection by an entomopathogenic *Pseudomonas* species. *Proc. Natl. Acad. Sci.* 102: 11414–11419.
154. Vallet-Gely, I., O. Opota, A. Boniface, A. Novikov, and B. Lemaître. 2010. A secondary metabolite acting as a signalling molecule controls *Pseudomonas entomophila* virulence. *Cell. Microbiol.* 12: 1666–1679.
155. Apidianakis, Y., C. Pitsouli, N. Perrimon, and L. Rahme. 2009. Synergy between bacterial infection and genetic predisposition in intestinal dysplasia. *Proc. Natl. Acad. Sci. U. S. A.* 106: 20883–20888.
156. Limmer, S., S. Haller, E. Drenkard, J. Lee, S. Yu, C. Kocks, F. M. Ausubel, and D. Ferrandon. 2011.

- Pseudomonas aeruginosa* RhIR is required to neutralize the cellular immune response in a *Drosophila melanogaster* oral infection model. *Proc. Natl. Acad. Sci. U. S. A.* 108: 17378–17383.
157. Blow, N. S., R. N. Salomon, K. Garrity, I. Reveillaud, A. Kopin, F. R. Jackson, and P. I. Watnick. 2005. *Vibrio cholerae* infection of *Drosophila melanogaster* mimics the human disease cholera. *PLoS Pathog.* 1: 0092–0098.
158. Buchon, N., N. A. Broderick, and B. Lemaitre. 2013. Gut homeostasis in a microbial world: insights from *Drosophila melanogaster*. *Nat. Rev. Microbiol.* 11: 615–626.
159. Opota, O., I. Vallet-Gély, R. Vincentelli, C. Kellenberger, I. Iacovache, M. R. Gonzalez, A. Roussel, F.-G. van der Goot, and B. Lemaitre. 2011. Monalysin, a novel  $\beta$ -pore-forming toxin from the *Drosophila* pathogen *Pseudomonas entomophila*, contributes to host intestinal damage and lethality. *PLoS Pathog.* 7: e1002259.
160. Liehl, P., M. Blight, N. Vodovar, F. Bocard, and B. Lemaitre. 2006. Prevalence of Local Immune Response against Oral Infection in a *Drosophila/Pseudomonas* Infection Model. *PLoS Pathog.* 2: e56.
161. Berkey, C. D., N. Blow, and P. I. Watnick. 2009. Genetic analysis of *Drosophila melanogaster* susceptibility to intestinal *Vibrio cholerae* infection. *Cell. Microbiol.* 11: 461–474.
162. Chakrabarti, S., P. Liehl, N. Buchon, and B. Lemaitre. 2012. Infection-induced host translational blockage inhibits immune responses and epithelial renewal in the *Drosophila* gut. *Cell Host Microbe* 12: 60–70.
163. Degnan, P. H., M. E. Taga, and A. L. Goodman. 2014. Vitamin B12 as a modulator of gut microbial ecology. *Cell Metab.* 20: 769–778.
164. Peterfreund, G. L., L. E. Vandivier, R. Sinha, A. J. Marozsan, W. C. Olson, J. Zhu, and F. D. Bushman. 2012. Succession in the gut microbiome following antibiotic and antibody therapies for *Clostridium difficile*. *PLoS One* 7: e46966.
165. Samarkos, M., E. Mastrogianni, and O. Kampouroupolou. 2018. The role of gut microbiota in



- Clostridium difficile infection. *Eur. J. Intern. Med.* 50: 28–32.
166. Zhao, W., F. Caro, W. Robins, and J. J. Mekalanos. 2018. Antagonism toward the intestinal microbiota and its effect on *Vibrio cholerae* virulence. *Science* 359: 210–213.
167. Harris, J. B., R. C. LaRocque, F. Qadri, E. T. Ryan, and S. B. Calderwood. 2012. Cholera. In *The Lancet* vol. 379. Lancet Publishing Group. 2466–2476.
168. Ali, M., A. R. Nelson, A. L. Lopez, and D. A. Sack. 2015. Updated global burden of cholera in endemic countries. *PLoS Negl. Trop. Dis.* 9.
169. Utada, A. S., R. R. Bennett, J. C. N. Fong, M. L. Gibiansky, F. H. Yildiz, R. Golestanian, and G. C. L. Wong. 2014. *Vibrio cholerae* use pili and flagella synergistically to effect motility switching and conditional surface attachment. *Nat. Commun.* 5: 1–8.
170. Conner, J. G., J. K. Teschler, C. J. Jones, and F. H. Yildiz. 2016. Staying Alive: *Vibrio cholerae*'s cycle of environmental survival, transmission, and dissemination. *Microbiol. Spectr.* 4.
171. Almagro-Moreno, S., and R. K. Taylor. 2013. Cholera: environmental reservoirs and impact on disease transmission. *Microbiol. Spectr.* 1.
172. Echeverria, P., B. A. Harrison, C. Tirapat, and A. McFarland. 1983. Flies as a source of enteric pathogens in a rural village in Thailand. *Appl. Environ. Microbiol.* 46: 32–36.
173. Halpern, M., Y. B. Broza, S. Mittler, E. Arakawa, and M. Broza. 2004. Chironomid egg masses as a natural reservoir of *Vibrio cholerae* non-O1 and non-O139 in freshwater habitats. *Microb. Ecol.* 47: 341–349.
174. Mintz, E. 2018. Taking aim at cholera. *Lancet* 391: 1868–1870.
175. Legros, D. 2018. Global cholera epidemiology: Opportunities to reduce the burden of cholera by 2030. *J. Infect. Dis.* 218: S137–S140.
176. Al Yusfi, R., M. Bouhenia, and S. Al-Wesabi. 2018. *Cholera response. Weekly epidemiology bulletin, June–1 July 2018,*

177. Charles, R. C., and E. T. Ryan. 2011. Cholera in the 21st century. *Curr. Opin. Infect. Dis.* 24: 472–477.
178. Alexakis, L. C. 2017. Cholera -“rice water stools.” *Pan Afr. Med. J.* 26.
179. Sharifi-Mood, B., and M. Metanat. 2014. Diagnosis, clinical management, prevention, and control of cholera; a review study. *Int. J. Infect.* 1.
180. World Health Organization. 2018. Cholera vaccine: WHO position paper, August 2017 – Recommendations. *Vaccine* 36: 3418–3420.
181. Barua, D. 1992. *History of Cholera*,. Springer, Boston.
182. Bart, K. J., Z. Huq, M. Khan, W. H. Mosley, Nuruzzaman, and A. K. M. G. Kibriya. 1970. Seroepidemiologic studies during a simultaneous epidemic of infection with El Tor ogawa and classical inaba vibrio cholerae. *J. Infect. Dis.* 121: S17–S24.
183. Kovacikova, G., and K. Skorupski. 2000. Differential activation of the tcpPH promoter by AphB determines biotype specificity of virulence gene expression in *Vibrio cholerae*. *J. Bacteriol.* 182: 3228–3238.
184. Beyhan, S., A. D. Tischler, A. Camilli, and F. H. Yildiz. 2006. Differences in gene expression between the classical and El Tor biotypes of *Vibrio cholerae* O1. *Infect. Immun.* 74: 3633–3642.
185. Cordero, C. L., S. Sozhamannan, and K. J. Fullner Satchell. 2007. RTX toxin actin cross-linking activity in clinical and environmental isolates of *Vibrio cholerae*. *J. Clin. Microbiol.* 45: 2289–2292.
186. Vaitkevicius, K., B. Lindmark, G. Ou, T. Song, C. Toma, M. Iwanaga, J. Zhu, A. Andersson, M. L. Hammarström, S. Tuck, and S. N. Wai. 2006. A *Vibrio cholerae* protease needed for killing of *Caenorhabditis elegans* has a role in protection from natural predator grazing. *Proc. Natl. Acad. Sci. U. S. A.* 103: 9280–9285.
187. Sack, R. B., A. K. Siddique, I. M. L. Jr., A. Nizam, M. Yunus, M. S. Islam, J. G. Morris, Jr., A. Ali, A. Huq, G. B. Nair, F. Qadri, S. M. Faruque, D. A. Sack, and R. R. Colwell. 2003. A 4-Year Study of the epidemiology of *Vibrio cholerae* in four rural areas of Bangladesh. *J. Infect. Dis.* 187: 96–101.

188. Khan, M., and M. Shahidullah. 1980. Cholera due to the E1 Tor biotype equals the classical biotype in severity and attack rates. *J. Trop. Med. Hyg.* 83: 35–9.
189. Murley, Y. M., J. Behari, R. Griffin, and S. B. Calderwood. 2000. Classical and El Tor biotypes of *Vibrio cholerae* differ in timing of transcription of *tcpPH* during growth in inducing conditions. *Infect. Immun.* 68: 3010–3014.
190. Heidelberg, J. F., J. A. Elsen, W. C. Nelson, R. A. Clayton, M. L. Gwinn, R. J. Dodson, D. H. Haft, E. K. Hickey, J. D. Peterson, L. Umayam, S. R. Gill, K. E. Nelson, T. D. Read, H. Tettelin, D. Richardson, M. D. Ermolaeva, J. Vamathevan, S. Bass, Q. Halving, I. Dragol, P. Sellers, L. McDonald, T. Utterback, R. D. Fleishmann, W. C. Nierman, O. White, S. L. Saizberg, H. O. Smith, R. R. Colwell, J. J. Mekalanos, C. J. Venter, and C. M. Fraser. 2000. DNA sequence of both chromosomes of the cholera pathogen *Vibrio cholerae*. *Nature* 406: 477–483.
191. Shaw, C. E., and R. K. Taylor. 1990. *Vibrio cholerae* O395 *tcpA* pilin gene sequence and comparison of predicted protein structural features to those of type 4 pilins. *Infect. Immun.* 58: 3042–3049.
192. Benitez, J. A., and A. J. Silva. 2016. *Vibrio cholerae* hemagglutinin(HA)/protease: An extracellular metalloprotease with multiple pathogenic activities. *Toxicon* 115: 55–62.
193. Herrington, D. A., R. H. Hall, G. Losonsky, J. J. Mekalanos, R. K. Taylor, and M. M. Levine. 1988. Toxin, toxin-coregulated pili, and the *toxR* regulon are essential for *Vibrio Cholerae* pathogenesis in humans. *J. Exp. Med.* 168: 1487–1492.
194. Tacket, C. O., R. K. Taylor, G. Losonsky, Y. U. Lim, J. P. Nataro, J. B. Kaper, and M. M. Levine. 1998. Investigation of the roles of toxin-coregulated pili and mannose-sensitive hemagglutinin pili in the pathogenesis of *Vibrio cholerae* O139 infection. *Infect. Immun.* 66: 692–695.
195. Karaolis, D. K. R., J. A. Johnson, C. C. Bailey, E. C. Boedeker, J. B. Kaper, and P. R. Reeves. 1998. A *Vibrio cholerae* pathogenicity island associated with epidemic and pandemic strains. *Proc. Natl. Acad. Sci. U. S. A.* 95: 3134–3139.

196. Holmgren, J. 1981. Actions of cholera toxin and the prevention and treatment of cholera. *Nature* 292: 413–417.
197. Levine, M. M., J. B. Kaper, D. Herrington, G. Losonsky, J. G. Morris, M. L. Clements, R. E. Black, B. Tall, and R. Hall. 1988. Volunteer studies of deletion mutants of *Vibrio cholerae* O1 prepared by recombinant techniques. *Infect. Immun.* 56: 161–7.
198. Moss, J., S. J. Stanley, M. Vaughan, and T. Tsuji. 1993. Interaction of ADP-ribosylation factor with *Escherichia coli* enterotoxin that contains an inactivating lysine 112 substitution. *J. Biol. Chem.* 268: 6383–7.
199. Yamamoto, S., Y. Takeda, M. Yamamoto, H. Kurazono, K. Imaoka, M. Yamamoto, K. Fujihashi, M. Noda, H. Kiyono, and J. R. McGhee. 1997. Mutants in the ADP-ribosyltransferase cleft of cholera toxin lack diarrheagenicity but retain adjuvanticity. *J. Exp. Med.* 185: 1203–1210.
200. Cassel, D., and Z. Selinger. 1977. Mechanism of adenylate cyclase activation by cholera toxin: Inhibition of GTP hydrolysis at the regulatory site. *Proc. Natl. Acad. Sci. U. S. A.* 74: 3307–3311.
201. Schafer, D. E., W. D. Lust, B. Sircar, and N. D. Goldberg. 1970. Elevated concentration of adenosine 3':5'-cyclic monophosphate in intestinal mucosa after treatment with cholera toxin. *Proc. Natl. Acad. Sci. U. S. A.* 67: 851–6.
202. Cheng, S. H., D. P. Rich, J. Marshall, R. J. Gregory, M. J. Welsh, and A. E. Smith. 1991. Phosphorylation of the R domain by cAMP-dependent protein kinase regulates the CFTR chloride channel. *Cell* 66: 1027–1036.
203. Chowdhury, F., A. I. Khan, A. S. G. Faruque, and E. T. Ryan. 2010. Severe, acute watery diarrhea in an adult. *PLoS Negl. Trop. Dis.* 4: e898.
204. Marsh, J. W., and R. K. Taylor. 1998. Identification of the *Vibrio cholerae* type 4 prepilin peptidase required for cholera toxin secretion and pilus formation. *Mol. Microbiol.* 29: 1481–1492.
205. Anderson, A. M. L., J. B. Varkey, C. A. Petti, R. A. Liddle, R. Frothingham, and C. W. Woods. 2004.

- Non-O1 Vibrio cholerae septicemia: Case report, discussion of literature, and relevance to bioterrorism. *Diagn. Microbiol. Infect. Dis.* 49: 295–297.
206. Krebs, S. J., and R. K. Taylor. 2011. Protection and attachment of Vibrio cholerae mediated by the toxin-coregulated pilus in the infant mouse model. *J. Bacteriol.* 193: 5260–5270.
207. Silva, A. J., and J. A. Benitez. 2016. Vibrio cholerae biofilms and cholera pathogenesis. *PLoS Negl. Trop. Dis.* 10: e0004330.
208. Jude, B. A., and R. K. Taylor. 2011. The physical basis of type 4 pilus-mediated microcolony formation by Vibrio cholerae O1. *J. Struct. Biol.* 175: 1–9.
209. Ritchie, J. M., H. Rui, R. T. Bronson, and M. K. Waldor. 2010. Back to the future: studying cholera pathogenesis using infant rabbits. *MBio* 1.
210. Waldor, M. K., and J. J. Mekalanos. 1996. Lysogenic Conversion by a Filamentous Phage Encoding Cholera Toxin. *Science (80- )*. 272: 1910–1914.
211. Purdy, A. E., and P. I. Watnick. 2011. Spatially selective colonization of the arthropod intestine through activation of Vibrio cholerae biofilm formation. *Proc. Natl. Acad. Sci. U. S. A.* 108: 19737–19742.
212. Pukatzki, S., A. T. Ma, D. Sturtevant, B. Krastins, D. Sarracino, W. C. Nelson, J. F. Heidelberg, and J. J. Mekalanos. 2006. Identification of a conserved bacterial protein secretion system in Vibrio cholerae using the Dictyostelium host model system. *Proc. Natl. Acad. Sci. U. S. A.* 103: 1528–1533.
213. Ritchie, J. M., and M. K. Waldor. 2009. Vibrio cholerae Interactions with the gastrointestinal tract: Lessons from animal studies. In 37–59.
214. Spira, W. M., R. B. Sack, and J. L. Froehlich. 1981. Simple adult rabbit model for Vibrio cholerae and enterotoxigenic Escherichia coli diarrhea. *Infect. Immun.* 32: 739–747.
215. Abel, S., and M. K. Waldor. 2015. Infant rabbit model for diarrheal diseases. *Curr. Protoc. Microbiol.* 2015: 6A.6.1-6A.6.15.
216. Klose, K. E. 2000. The suckling mouse model of cholera. *Trends Microbiol.* 8: 189–191.

217. Olivier, V., N. H. Salzman, and K. J. Fullner Satchell. 2007. Prolonged colonization of mice by *Vibrio cholerae* El Tor O1 depends on accessory toxins. *Infect. Immun.* 75: 5043–5051.
218. Runft, D. L., K. C. Mitchell, B. H. Abuaita, J. P. Allen, S. Bajer, K. Ginsburg, M. N. Neely, and J. H. Withey. 2014. Zebrafish as a natural host model for *Vibrio cholerae* colonization and transmission. *Appl. Environ. Microbiol.* 80: 1710–1717.
219. Taylor, R. K., V. L. Miller, D. B. Furlong, and J. J. Mekalanos. 1987. Use of *phoA* gene fusions to identify a pilus colonization factor coordinately regulated with cholera toxin. *Proc. Natl. Acad. Sci. U. S. A.* 84: 2833–2837.
220. Tanaka, M., and J. Nakayama. 2017. Development of the gut microbiota in infancy and its impact on health in later life. *Allergol. Int.* 66: 515–522.
221. Kamareddine, L., A. C. N. Wong, A. S. Vanhove, S. Hang, A. E. Purdy, K. Kierek-Pearson, J. M. Asara, A. Ali, J. G. Morris Jr, and P. I. Watnick. 2018. Activation of *Vibrio cholerae* quorum sensing promotes survival of an arthropod host. *Nat. Microbiol.* 3: 243–252.
222. Cash, R. A., S. I. Music, J. P. Libonati, M. J. Snyder, R. P. Wenzel, and R. B. Hornick. 1974. Response of man to infection with *Vibrio cholerae*. I. Clinical, serologic, and bacteriologic responses to a known inoculum. *J. Infect. Dis.* 129: 45–52.
223. Cash, R. A., S. I. Music, J. P. Libonati, J. P. Craig, N. F. Pierce, and R. B. Hornick. 1974. Response of man to infection with *Vibrio cholerae*. II. Protection from illness afforded by previous disease and vaccine. *J. Infect. Dis.* 130: 325–333.
224. Hang, S., A. E. Purdy, W. P. Robins, Z. Wang, M. Mandal, S. Chang, J. J. Mekalanos, and P. I. Watnick. 2014. The acetate switch of an intestinal pathogen disrupts host insulin signaling and lipid metabolism. *Cell Host Microbe* 16: 592–604.
225. Guichard, A., B. Cruz-Moreno, B. Aguilar, N. M. van Sorge, J. Kuang, A. A. Kurkciyan, Z. Wang, S. Hang, G. P. Pineton de Chambrun, D. F. McCole, P. Watnick, V. Nizet, and E. Bier. 2013. Cholera toxin disrupts

barrier function by inhibiting exocyst-mediated trafficking of host proteins to intestinal cell junctions. *Cell Host Microbe* 14: 294–305.

226. Leiman, P. G., M. Basler, U. A. Ramagopal, J. B. Bonanno, J. M. Sauder, S. Pukatzki, S. K. Burley, S. C. Almo, and J. J. Mekalanos. 2009. Type VI secretion apparatus and phage tail-associated protein complexes share a common evolutionary origin. *Proc. Natl. Acad. Sci.* 106: 4154–4159.

227. Basler, M., M. Pilhofer, G. P. Henderson, G. J. Jensen, and J. J. Mekalanos. 2012. Type VI secretion requires a dynamic contractile phage tail-like structure. *Nature* 483: 182–186.

228. Basler, M., and J. J. Mekalanos. 2012. Type 6 secretion dynamics within and between bacterial cells. *Science (80-. )*. 337: 815.

229. Miyata, S. T., D. Unterweger, S. P. Rudko, and S. Pukatzki. 2013. Dual expression profile of Type VI secretion system immunity genes protects pandemic *Vibrio cholerae*. *PLoS Pathog.* 9: e1003752.

230. Dong, T. G., B. T. Ho, D. R. Yoder-Himes, and J. J. Mekalanos. 2013. Identification of T6SS-dependent effector and immunity proteins by Tn-seq in *Vibrio cholerae*. *Proc. Natl. Acad. Sci. U. S. A.* 110: 2623–2628.

231. MacIntyre, D. L., S. T. Miyata, M. Kitaoka, and S. Pukatzki. 2010. The *Vibrio cholerae* type VI secretion system displays antimicrobial properties. *Proc. Natl. Acad. Sci. U. S. A.* 107: 19520–19524.

232. Hood, R. D., P. Singh, F. S. Hsu, T. Güvener, M. A. Carl, R. R. S. Trinidad, J. M. Silverman, B. B. Ohlson, K. G. Hicks, R. L. Plemel, M. Li, S. Schwarz, W. Y. Wang, A. J. Merz, D. R. Goodlett, and J. D. Mougous. 2010. A Type VI secretion system of *Pseudomonas aeruginosa* targets a toxin to bacteria. *Cell Host Microbe* 7: 25–37.

233. Brunet, Y. R., A. Zoued, F. Boyer, B. Douzi, and E. Cascales. 2015. The type VI secretion TssEFGK-VgrG phage-like baseplate is recruited to the TssJLM membrane complex via multiple contacts and serves as assembly platform for tail tube/sheath polymerization. *PLOS Genet.* 11: e1005545.

234. Zoued, A., E. Durand, C. Bebeacua, Y. R. Brunet, B. Douzi, C. Cambillau, E. Cascales, and L. Journet.

2013. TssK is a trimeric cytoplasmic protein interacting with components of both phage-like and membrane anchoring complexes of the type VI secretion system. *J. Biol. Chem.* 288: 27031–27041.
235. Santin, Y. G., T. Doan, L. Journet, and E. Cascales. 2019. Cell width dictates type VI secretion tail length. *Curr. Biol.* 29: 3707-3713.e3.
236. Shneider, M. M., S. A. Buth, B. T. Ho, M. Basler, J. J. Mekalanos, and P. G. Leiman. 2013. PAAR-repeat proteins sharpen and diversify the type VI secretion system spike. *Nature* 500: 350–353.
237. Spínola-Amilibia, M., I. Davó-Siguero, F. M. Ruiz, E. Santillana, F. J. Medrano, and A. Romero. 2016. The structure of VgrG1 from *Pseudomonas aeruginosa*, the needle tip of the bacterial type VI secretion system. *Acta Crystallogr. Sect. D Struct. Biol.* 72: 22–33.
238. Joshi, A., B. Kostiuik, A. Rogers, J. Teschler, S. Pukatzki, and F. H. Yildiz. 2017. Rules of engagement: the type VI secretion system in *Vibrio cholerae*. *Trends Microbiol.* 25: 267–279.
239. Kirchberger, P. C., D. Unterweger, D. Provenzano, S. Pukatzki, and Y. Boucher. 2017. Sequential displacement of Type VI Secretion System effector genes leads to evolution of diverse immunity gene arrays in *Vibrio cholerae*. *Sci. Rep.* 7.
240. Unterweger, D., B. Kostiuik, and S. Pukatzki. 2017. Adaptor proteins of type VI secretion system effectors. *Trends Microbiol.* 25: 8–10.
241. Altindis, E., T. Dong, C. Catalano, and J. Mekalanos. 2015. Secretome analysis of *Vibrio cholerae* type VI secretion system reveals a new effector-immunity pair. *MBio* 6.
242. Pukatzki, S., A. T. Ma, A. T. Revel, D. Sturtevant, and J. J. Mekalanos. 2007. Type VI secretion system translocates a phage tail spike-like protein into target cells where it cross-links actin. *Proc. Natl. Acad. Sci. U. S. A.* 104: 15508–15513.
243. Brooks, T. M., D. Unterweger, V. Bachmann, B. Kostiuik, and S. Pukatzki. 2013. Lytic activity of the *Vibrio cholerae* type VI secretion toxin VgrG-3 is inhibited by the antitoxin TsaB. *J. Biol. Chem.* 288: 7618–7625.



244. Miyata, S. T., M. Kitaoka, T. M. Brooks, S. B. McAuley, and S. Pukatzki. 2011. *Vibrio cholerae* requires the type VI secretion system virulence factor VasX to kill *Dictyostelium discoideum*. *Infect. Immun.* 79: 2941–2949.
245. Chou, S., N. K. Bui, A. B. Russell, K. W. Lexa, T. E. Gardiner, M. LeRoux, W. Vollmer, and J. D. Mougous. 2012. Structure of a peptidoglycan amidase effector targeted to Gram-negative bacteria by the type VI secretion system. *Cell Rep.* 1: 656–664.
246. Unterweger, D., S. T. Miyata, V. Bachmann, T. M. Brooks, T. Mullins, B. Kostiuik, D. Provenzano, and S. Pukatzki. 2014. The *Vibrio cholerae* type VI secretion system employs diverse effector modules for intraspecific competition. *Nat. Commun.* 5.
247. Fu, Y., B. T. Ho, and J. J. Mekalanos. 2018. Tracking *Vibrio cholerae* cell-cell interactions during infection reveals bacterial population dynamics within intestinal microenvironments. *Cell Host Microbe* 23: 274-281.e2.
248. Miyata, S. T., M. Kitaoka, L. Wieteska, C. Frech, N. Chen, and S. Pukatzki. 2010. The *Vibrio cholerae* type VI secretion system: evaluating its role in the human disease cholera. *Front. Microbiol.* 1: 117.
249. Lombardo, M. J., J. Michalski, H. Martinez-Wilson, C. Morin, T. Hilton, C. G. Osorio, J. P. Nataro, C. O. Tacket, A. Camilli, and J. B. Kaper. 2007. An in vivo expression technology screen for *Vibrio cholerae* genes expressed in human volunteers. *Proc. Natl. Acad. Sci. U. S. A.* 104: 18229–18234.
250. Ma, A. T., and J. J. Mekalanos. 2010. In vivo actin cross-linking induced by *Vibrio cholerae* type VI secretion system is associated with intestinal inflammation. *Proc. Natl. Acad. Sci. U. S. A.* 107: 4365–4370.
251. Fu, Y., M. K. Waldor, and J. J. Mekalanos. 2013. Tn-Seq analysis of *Vibrio cholerae* intestinal colonization reveals a role for T6SS-mediated antibacterial activity in the host. *Cell Host Microbe* 14: 652–663.
252. Logan, S. L., J. Thomas, J. Yan, R. P. Baker, D. S. Shields, J. B. Xavier, B. K. Hammer, and R. Parthasarathy. 2018. The *Vibrio cholerae* type VI secretion system can modulate host intestinal

- mechanics to displace gut bacterial symbionts. *Proc. Natl. Acad. Sci.* 115: E3779–E3787.
253. Ladinsky, M. S., L. P. Araujo, X. Zhang, J. Veltri, M. Galan-Diez, S. Soualhi, C. Lee, K. Irie, E. Y. Pinker, S. Narushima, S. Bandyopadhyay, M. Nagayama, W. Elhenawy, B. K. Coombes, R. P. Ferraris, K. Honda, I. D. Iliev, N. Gao, P. J. Bjorkman, and I. I. Ivanov. 2019. Endocytosis of commensal antigens by intestinal epithelial cells regulates mucosal T cell homeostasis. *Science* (80-. ). 363.
254. Lakovaara, S. 1969. Malt as a culture medium for *Drosophila* species. *Drosoph. Inf. Serv.* 44: 128.
255. Avadhanula, V., B. P. Weasner, G. G. Hardy, J. P. Kumar, and R. W. Hardy. 2009. A novel system for the launch of alphavirus RNA synthesis reveals a role for the imd pathway in arthropod antiviral response. *PLoS Pathog.* 5: e1000582.
256. Bellen, H. J., R. W. Levis, G. Liao, Y. He, J. W. Carlson, G. Tsang, M. Evans-Holm, P. R. Hiesinger, K. L. Schulze, G. M. Rubin, R. A. Hoskins, and A. C. Spradling. 2004. The BDGP gene disruption project: Single transposon insertions associated with 40% of *Drosophila* genes. *Genetics* 167: 761–781.
257. Martin, J. L., E. N. Sanders, P. Moreno-Roman, L. A. Jaramillo Koyama, S. Balachandra, X. Du, and L. E. O'Brien. 2018. Long-term live imaging of the *Drosophila* adult midgut reveals real-time dynamics of division, differentiation and loss. *Elife* 7.
258. Petkau, K., D. Fast, A. Duggal, and E. Foley. 2016. Comparative evaluation of the genomes of three common *Drosophila*-associated bacteria. *Biol. Open* 5: 1305–1316.
259. Basset, A., R. S. Khush, A. Braun, L. Gardan, F. Boccard, J. A. Hoffmann, and B. Lemaitre. 2000. The phytopathogenic bacteria *Erwinia carotovora* infects *Drosophila* and activates an immune response. *Proc. Natl. Acad. Sci.* 97: 3376–3381.
260. Zheng, J., B. Ho, and J. J. Mekalanos. 2011. Genetic analysis of anti-amoebae and anti-bacterial activities of the type VI secretion system in *Vibrio cholerae*. *PLoS One* 6: e23876.
261. Das, S., A. Chakraborty, R. Banerjee, and K. Chaudhuri. 2002. Involvement of in vivo induced icmF gene of *Vibrio cholerae* in motility, adherence to epithelial cells, and conjugation frequency. *Biochem.*

*Biophys. Res. Commun.* 295: 922–928.

262. Guntermann, S., and E. Foley. 2011. The protein Dredd is an essential component of the c-Jun N-terminal kinase pathway in the *Drosophila* immune response. *J. Biol. Chem.* 286: 30284–94.

263. Schindelin, J., I. Arganda-Carreras, E. Frise, V. Kaynig, M. Longair, T. Pietzsch, S. Preibisch, C. Rueden, S. Saalfeld, B. Schmid, J.-Y. Tinevez, D. J. White, V. Hartenstein, K. Eliceiri, P. Tomancak, and A. Cardona.

2012. Fiji: an open-source platform for biological-image analysis. *Nat. Methods* 9: 676–682.

264. Dutta, D., J. Xiang, B. A. Edgar, D. Dutta, J. Xiang, and B. A. Edgar. 2013. RNA Expression Profiling from FACS-Isolated Cells of the *Drosophila Intestine*. In *Current Protocols in Stem Cell Biology* John Wiley & Sons, Inc., Hoboken, NJ, USA. 2F.2.1-2F.2.12.

265. Ashburner, M., C. A. Ball, J. A. Blake, D. Botstein, H. Butler, J. M. Cherry, A. P. Davis, K. Dolinski, S. S. Dwight, J. T. Eppig, M. A. Harris, D. P. Hill, L. Issel-Tarver, A. Kasarskis, S. Lewis, J. C. Matese, J. E.

Richardson, M. Ringwald, G. M. Rubin, and G. Sherlock. 2000. Gene Ontology: tool for the unification of biology. *Nat. Genet.* 25: 25–29.

266. Fast, D., A. Duggal, and E. Foley. 2018. Monoassociation with *Lactobacillus plantarum* disrupts intestinal homeostasis in adult *Drosophila melanogaster*. *MBio* 9: e01114-18.

267. Bolger, A. M., M. Lohse, and B. Usadel. 2014. Trimmomatic: a flexible trimmer for Illumina sequence data. *Bioinformatics* 30: 2114–2120.

268. Kim, D., B. Langmead, and S. L. Salzberg. 2015. HISAT: a fast spliced aligner with low memory requirements. *Nat. Methods* 12: 357–360.

269. Li, H., B. Handsaker, A. Wysoker, T. Fennell, J. Ruan, N. Homer, G. Marth, G. Abecasis, and R. Durbin. 2009. The Sequence Alignment/Map format and SAMtools. *Bioinformatics* 25: 2078–2079.

270. Liao, Y., G. K. Smyth, and W. Shi. 2013. The Subread aligner: fast, accurate and scalable read mapping by seed-and-vote. *Nucleic Acids Res.* 41: e108–e108.

271. Robinson, M. D., D. J. McCarthy, and G. K. Smyth. 2010. edgeR: a Bioconductor package for

- differential expression analysis of digital gene expression data. *Bioinformatics* 26: 139–140.
272. McCarthy, D. J., Y. Chen, and G. K. Smyth. 2012. Differential expression analysis of multifactor RNA-Seq experiments with respect to biological variation. *Nucleic Acids Res.* 40: 4288–4297.
273. Alboukadel, K., and F. Mundt. 2017. factoextra: Extract and Visualize the Results of Multivariate Data Analyses. .
274. Eden, E., R. Navon, I. Steinfeld, D. Lipson, and Z. Yakhini. 2009. GOrilla: a tool for discovery and visualization of enriched GO terms in ranked gene lists. *BMC Bioinformatics* 10: 1–7.
275. Steinfeld, H. M. 1928. Length of life of *Drosophila melanogaster* under aseptic conditions. .
276. Inamine, H., S. P. Ellner, P. D. Newell, Y. Luo, N. Buchon, and A. E. Douglas. 2018. Spatiotemporally heterogeneous population dynamics of gut bacteria inferred from fecal time series data. *MBio* 9: e01453-17.
277. McGuire, S. E., Z. Mao, and R. L. Davis. 2004. Spatiotemporal gene expression targeting with the TARGET and gene-switch systems in *Drosophila*. *Sci. STKE* 2004: pl6.
278. Téfit, M. A., and F. Leulier. 2017. *Lactobacillus plantarum* favors the early emergence of fit and fertile adult *Drosophila* upon chronic undernutrition. *J. Exp. Biol.* 220: 900–907.
279. Pederson, C. S. 1936. A study of the species *Lactobacillus plantarum* (Orla-Jensen) Bergey et al. *J. Bacteriol.* 31: 217–24.
280. Wu, J. S., and L. Luo. 2007. A protocol for mosaic analysis with a repressible cell marker (MARCM) in *Drosophila*. *Nat. Protoc.* 1: 2583–2589.
281. Folkesson, A., S. Löfdahl, and S. Normark. 2002. The *Salmonella enterica* subspecies I specific centisome 7 genomic island encodes novel protein families present in bacteria living in close contact with eukaryotic cells. *Res. Microbiol.* 153: 537–545.
282. Blondel, C. J., J. C. Jiménez, I. Contreras, and C. A. Santiviago. 2009. Comparative genomic analysis uncovers 3 novel loci encoding type six secretion systems differentially distributed in *Salmonella*

serotypes. *BMC Genomics* 10.

283. Lertpiriyapong, K., E. R. Gamazon, Y. Feng, D. S. Park, J. Pang, G. Botka, M. E. Graffam, Z. Ge, and J. G.

Fox. 2012. *Campylobacter jejuni* type VI secretion system: roles in adaptation to deoxycholic acid, host cell adherence, invasion, and in vivo colonization. *PLoS One* 7: e42842.

284. Bachmann, V., B. Kostiuk, D. Unterweger, L. Diaz-Satizabal, S. Ogg, and S. Pukatzki. 2015. Bile salts modulate the mucin-activated type VI secretion system of pandemic *Vibrio cholerae*. *PLoS Negl. Trop. Dis.* 9: e0004031.

285. Stutzmann, S., and M. Blokesch. 2016. Circulation of a quorum-sensing-impaired variant of *Vibrio cholerae* strain C6706 masks important phenotypes. *mSphere* 1: e00098-16.

286. Bönemann, G., A. Pietrosiuk, A. Diemand, H. Zentgraf, and A. Mogk. 2009. Remodelling of VipA/VipB tubules by ClpV-mediated threading is crucial for type VI protein secretion. *EMBO J.* 28: 315–325.

287. Mathan, M. M., G. Chandy, and V. I. Mathan. 1995. Ultrastructural changes in the upper small intestinal mucosa in patients with cholera. *Gastroenterology* 109: 422–430.

288. Varfolomeev, E., and D. Vucic. 2018. Intracellular regulation of TNF activity in health and disease. *Cytokine* 101: 26–32.

289. Deriu, E., J. Z. Liu, M. Pezeshki, R. A. Edwards, R. J. Ochoa, H. Contreras, S. J. Libby, F. C. Fang, and M. Raffatellu. 2013. Probiotic bacteria reduce *Salmonella typhimurium* intestinal colonization by competing for iron. *Cell Host Microbe* 14: 26–37.

290. Troha, K., J. H. Im, J. Revah, B. P. Lazzaro, and N. Buchon. 2018. Comparative transcriptomics reveals CrebA as a novel regulator of infection tolerance in *D. melanogaster*. *PLOS Pathog.* 14: e1006847.

291. Dutta, D., A. J. Dobson, P. L. Houtz, C. Gläßer, J. Revah, J. Korzelius, P. H. Patel, B. A. Edgar, and N. Buchon. 2015. Regional Cell-Specific Transcriptome Mapping Reveals Regulatory Complexity in the Adult *Drosophila* Midgut. *Cell Rep.* 12: 346–358.

292. Zhou, J., S. Florescu, A.-L. Boettcher, L. Luo, D. Dutta, G. Kerr, Y. Cai, B. A. Edgar, and M. Boutros.

2015. Dpp/Gbb signaling is required for normal intestinal regeneration during infection. *Dev. Biol.* 399: 189–203.
293. Bailey, A. M., and J. W. Posakony. 1995. Suppressor of hairless directly activates transcription of enhancer of split complex genes in response to Notch receptor activity. *Genes Dev.* 9: 2609–2622.
294. McFall-Ngai, M., M. G. Hadfield, T. C. G. Bosch, H. V. Carey, T. Domazet-Lošo, A. E. Douglas, N. Dubilier, G. Eberl, T. Fukami, S. F. Gilbert, U. Hentschel, N. King, S. Kjelleberg, A. H. Knoll, N. Kremer, S. K. Mazmanian, J. L. Metcalf, K. Neelson, N. E. Pierce, J. F. Rawls, A. Reid, E. G. Ruby, M. Rumpho, J. G. Sanders, D. Tautz, and J. J. Wernegreen. 2013. Animals in a bacterial world, a new imperative for the life sciences. *Proc. Natl. Acad. Sci. U. S. A.* 110: 3229–3236.
295. Schwarzer, M., K. Makki, G. Storelli, I. Machuca-Gayet, D. Srutkova, P. Hermanova, M. E. Martino, S. Balmand, T. Hudcovic, A. Heddi, J. Rieusset, H. Kozakova, H. Vidal, and F. Leulier. 2016. *Lactobacillus plantarum* strain maintains growth of infant mice during chronic undernutrition. *Science* 351: 854–7.
296. Newell, P. D., and A. E. Douglas. 2014. Interspecies interactions determine the impact of the gut microbiota on nutrient allocation in *Drosophila melanogaster*. *Appl. Environ. Microbiol.* 80: 788–96.
297. Dobson, A. J., J. M. Chaston, and A. E. Douglas. 2016. The *Drosophila* transcriptional network is structured by microbiota. *BMC Genomics* 17.
298. Elya, C., V. Zhang, W. B. Ludington, and M. B. Eisen. 2016. Stable host gene expression in the gut of adult *Drosophila melanogaster* with different bacterial mono-associations. *PLoS One* 11: e0167357.
299. Bost, A., S. Franzenburg, K. L. Adair, V. G. Martinson, G. Loeb, and A. E. Douglas. 2018. How gut transcriptional function of *Drosophila melanogaster* varies with the presence and composition of the gut microbiota. *Mol. Ecol.* 27: 1848–1859.
300. Heinrichsen, E. T., H. Zhang, J. E. Robinson, J. Ngo, S. Diop, R. Bodmer, W. J. Joiner, C. M. Metallo, and G. G. Haddad. 2014. Metabolic and transcriptional response to a high-fat diet in *Drosophila melanogaster*. *Mol. Metab.* 3: 42–54.

301. Chang, P. L., J. P. Dunham, S. V. Nuzhdin, and M. N. Arbeitman. 2011. Somatic sex-specific transcriptome differences in *Drosophila* revealed by whole transcriptome sequencing. *BMC Genomics* 12.
302. Jin, W., R. M. Riley, R. D. Wolfinger, K. P. White, G. Passador-Gurgell, and G. Gibson. 2001. The contributions of sex, genotype and age to transcriptional variance in *Drosophila melanogaster*. *Nat. Genet.* 29: 389–395.
303. Zhan, M., H. Yamaza, Y. Sun, J. Sinclair, H. Li, and S. Zou. 2007. Temporal and spatial transcriptional profiles of aging in *Drosophila melanogaster*. *Genome Res.* 17: 1236–1243.
304. Houthoofd, K., B. P. Braeckman, I. Lenaerts, K. Brys, A. De Vreese, S. Van Eygen, and J. R. Vanfleteren. 2002. Axenic growth up-regulates mass-specific metabolic rate, stress resistance, and extends life span in *Caenorhabditis elegans*. *Exp. Gerontol.* 37: 1371–1378.
305. Shin, M., L. O. Jones, A. Panteluk, and E. Foley. 2019. Cell-specific regulation of intestinal immunity in *Drosophila*. *bioRxiv* .
306. Keebaugh, E. S., R. Yamada, and W. W. Ja. 2019. The nutritional environment influences the impact of microbes on *Drosophila melanogaster* life span. *MBio* 10.
307. Dobson, A. J., J. M. Chaston, P. D. Newell, L. Donahue, S. L. Hermann, D. R. Sannino, S. Westmiller, A. C.-N. Wong, A. G. Clark, B. P. Lazzaro, and A. E. Douglas. 2015. Host genetic determinants of microbiota-dependent nutrition revealed by genome-wide analysis of *Drosophila melanogaster*. *Nat. Commun.* 6: 6312.
308. De Gregorio, E., P. T. Spellman, P. Tzou, G. M. Rubin, and B. Lemaitre. 2002. The Toll and Imd pathways are the major regulators of the immune response in *Drosophila*. *EMBO J.* 21: 2568–79.
309. Chaston, J. M., P. D. Newell, and A. E. Douglas. 2014. Metagenome-wide association of microbial determinants of host phenotype in *Drosophila melanogaster*. *MBio* 5: e01631-14.
310. Huang, J.-H., and A. E. Douglas. 2015. Consumption of dietary sugar by gut bacteria determines *Drosophila* lipid content. *Biol. Lett.* 11: 20150469.

311. Lőrincz, P., C. Mauvezin, and G. Juhász. 2017. Exploring autophagy in *Drosophila*. *Cells* 6: 22.
312. Brunet, Y. R., A. Khodr, L. Logger, L. Aussel, T. Mignot, S. Rimsky, and E. Cascales. 2015. H-NS silencing of the salmonella pathogenicity island 6-encoded type VI secretion system limits *Salmonella enterica* Serovar Typhimurium interbacterial killing. *Infect. Immun.* 83: 2738–50.
313. Sana, T. G., N. Flaugnatti, K. A. Lugo, L. H. Lam, A. Jacobson, V. Baylot, E. Durand, L. Journet, E. Cascales, and D. M. Monack. 2016. *Salmonella* Typhimurium utilizes a T6SS-mediated antibacterial weapon to establish in the host gut. *Proc. Natl. Acad. Sci. U. S. A.* 113: E5044–E5051.
314. Deen, J., M. A. Mengel, and J. D. Clemens. 2019. Epidemiology of cholera. *Vaccine* .
315. Woodward, W. E., and W. H. Mosley. 1972. The spectrum of cholera in rural Bangladesh. II. Comparison of El Tor Ogawa and classical Inaba infection. *Am. J. Epidemiol.* 96: 342–51.
316. Narkevich, M. I., G. G. Onischenko, J. M. Lomov, E. A. Moskvitina, L. S. Podosinnikova, and G. M. Medinsky. 1993. The seventh pandemic of cholera in the USSR, 1961-89. *Bull. World Health Organ.* 71: 189–96.
317. Repizo, G. D., S. Gagné, M.-L. Foucault-Grunenwald, V. Borges, X. Charpentier, A. S. Limansky, J. P. Gomes, A. M. Viale, and S. P. Salcedo. 2015. Differential role of the T6SS in *Acinetobacter baumannii* virulence. *PLoS One* 10: e0138265.
318. Walia, K., S. Ghosh, H. Singh, G. B. Nair, A. Ghosh, G. Sahni, H. Vohra, and N. K. Ganguly. 1999. Purification and characterization of novel toxin produced by *Vibrio cholerae* O1. *Infect. Immun.* 67: 5215–22.
319. Fujinaga, Y., A. A. Wolf, C. Rodighiero, H. Wheeler, B. Tsai, L. Allen, M. G. Jobling, T. Rapoport, R. K. Holmes, and W. I. Lencer. 2003. Gangliosides that associate with lipid rafts mediate transport of cholera and related toxins from the plasma membrane to endoplasmic reticulum. *Mol. Biol. Cell* 14: 4783–4793.
320. Yamasaki, Y., L. Tsuda, A. Suzuki, and K. Yanagisawa. 2018. Induction of ganglioside synthesis in *Drosophila* brain accelerates assembly of amyloid  $\beta$  protein. *Sci. Rep.* 8: 8345.



321. Westermann, A. J., L. Barquist, and J. Vogel. 2017. Resolving host–pathogen interactions by dual RNA-seq. *PLoS Pathog.* 13: e1006033.
322. Avraham, R., N. Haseley, D. Brown, C. Penaranda, H. B. Jijon, J. J. Trombetta, R. Satija, A. K. Shalek, R. J. Xavier, A. Regev, and D. T. Hung. 2015. Pathogen cell-to-cell variability drives heterogeneity in host immune responses. *Cell* 162: 1309–1321.
323. Mavromatis, C. (Harris), N. J. Bokil, M. Totsika, A. Kakkanat, K. Schaale, C. V. Cannistraci, T. Ryu, S. A. Beatson, G. C. Ulett, M. A. Schembri, M. J. Sweet, and T. Ravasi. 2015. The co-transcriptome of uropathogenic *Escherichia coli*-infected mouse macrophages reveals new insights into host-pathogen interactions. *Cell. Microbiol.* 17: 730–746.
324. Humphrys, M. S., T. Creasy, Y. Sun, A. C. Shetty, M. C. Chibucos, E. F. Drabek, C. M. Fraser, U. Farooq, N. Sengamalay, S. Ott, H. Shou, P. M. Bavoil, A. Mahurkar, and G. S. A. Myers. 2013. Simultaneous transcriptional profiling of bacteria and their host cells. *PLoS One* 8: e80597.
325. Westermann, A. J., S. A. Gorski, and J. Vogel. 2012. Dual RNA-seq of pathogen and host. *Nat. Rev. Microbiol.* 10: 618–630.
326. Mandlik, A., J. Livny, W. P. Robins, J. M. Ritchie, J. J. Mekalanos, and M. K. Waldor. 2011. RNA-seq-based monitoring of infection-linked changes in *Vibrio cholerae* gene expression. *Cell Host Microbe* 10: 165–174.
327. Toska, J., B. T. Ho, and J. J. Mekalanos. 2018. Exopolysaccharide protects *Vibrio cholerae* from exogenous attacks by the type 6 secretion system. *Proc. Natl. Acad. Sci. U. S. A.* 115: 7997–8002.
328. Fast, D., B. Kostiuik, E. Foley, and S. Pukatzki. 2018. Commensal pathogen competition impacts host viability. *Proc. Natl. Acad. Sci. U. S. A.* 115: 7099–7104.
329. Wang, Z., C. D. Berkey, and P. I. Watnick. 2012. The *Drosophila* protein mustard tailors the innate immune response activated by the immune deficiency pathway. *J. Immunol.* 188: 3993–4000.
330. Myllymäki, H., S. Valanne, and M. Rämet. 2014. The *Drosophila* imd signaling pathway. *J. Immunol.*

192: 3455–3462.

331. Mellroth, P., J. Karlsson, and H. Steiner. 2003. A scavenger function for a *Drosophila* peptidoglycan recognition protein. *J. Biol. Chem.* 278: 7059–7064.

332. Zaidman-Rémy, A., M. Hervé, M. Poidevin, S. Pili-Floury, M.-S. Kim, D. Blanot, B.-H. Oh, R. Ueda, D. Mengin-Lecreulx, and B. Lemaitre. 2006. The *Drosophila* amidase PGRP-LB modulates the immune response to bacterial infection. *Immunity* 24: 463–473.

333. Vanhove, A. S., S. Hang, V. Vijayakumar, A. C. Wong, J. M. Asara, and P. I. Watnick. 2017. *Vibrio cholerae* ensures function of host proteins required for virulence through consumption of luminal methionine sulfoxide. *PLoS Pathog.* 13: e1006428.

334. Wang, Z., S. Hang, A. E. Purdy, and P. I. Watnick. 2013. Mutations in the IMD pathway and mustard counter *Vibrio cholerae* suppression of intestinal stem cell division in *Drosophila*. *MBio* 4: e00337-13.

335. Wotzka, S. Y., B. D. Nguyen, and W. D. Hardt. 2017. *Salmonella Typhimurium* Diarrhea Reveals Basic Principles of Enteropathogen Infection and Disease-Promoted DNA Exchange. *Cell Host Microbe* 21: 443–454.

336. Blattman, S. B., W. Jiang, P. Oikonomou, and S. Tavazoie. 2019. Prokaryotic single-cell RNA sequencing by in situ combinatorial indexing. *bioRxiv* 866244.

337. Park, S. Y., Y. J. Heo, K. S. Kim, and Y. H. Cho. 2005. *Drosophila melanogaster* is susceptible to *Vibrio cholerae* infection. *Mol. Cells* 20: 409–415.

338. Hamaratoglu, F., M. Affolter, and G. Pyrowolakis. 2014. Dpp/BMP signaling in flies: From molecules to biology. *Semin. Cell Dev. Biol.* 32: 128–136.

339. Tadokoro, T., X. Gao, C. C. Hong, D. Hotten, and B. L. M. Hogan. 2016. BMP signaling and cellular dynamics during regeneration of airway epithelium from basal progenitors. *Dev.* 143: 764–773.

340. Cibois, M., G. Luxardi, B. Chevalier, V. Thomé, O. Mercey, L. E. Zaragosi, P. Barbry, A. Pasini, B. Marcet, and L. Kodjabachian. 2015. BMP signalling controls the construction of vertebrate mucociliary

epithelia. *Dev.* 142: 2352–2363.

341. Sheahan, K. L., and K. J. Fullner Satchell. 2007. Inactivation of small Rho GTPases by the multifunctional RTX toxin from *Vibrio cholerae*. *Cell. Microbiol.* 9: 1324–1335.

342. Woida, P. J., and K. J. F. Satchell. 2019. The *Vibrio cholerae* MARTX toxin simultaneously induces actin collapse while silencing the inflammatory response to cytoskeletal damage. *bioRxiv* 526616.

343. Jones, T. A., D. Z. Hernandez, Z. C. Wong, A. M. Wandler, and K. Guillemin. 2017. The bacterial virulence factor CagA induces microbial dysbiosis that contributes to excessive epithelial cell proliferation in the *Drosophila* gut. *PLoS Pathog.* 13.

344. Butterton, J. R., E. T. Ryan, R. A. Shahin, and S. B. Calderwood. 1996. Development of a germfree mouse model of *Vibrio cholerae* infection. *Infect. Immun.* 64: 4373–4377.

345. Zhu, J., M. B. Miller, R. E. Vance, M. Dziejman, B. L. Bassler, and J. J. Mekalanos. 2002. Quorum-sensing regulators control virulence gene expression in *Vibrio cholerae*. *Proc. Natl. Acad. Sci. U. S. A.* 99: 3129–3134.